Design, synthesis, characterization, and evaluation of potential dual-action antimalarials

Detection of antibody response against malaria

Homology modeling and docking studies against a malaria-like disease

Malaria chemotherapy and prevention: towards the development of dual action drugs and the understanding of vaccine-induced antibody responses against *P. falciparum*

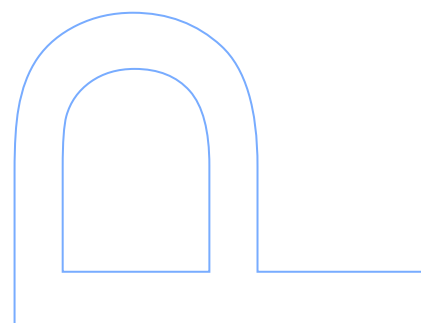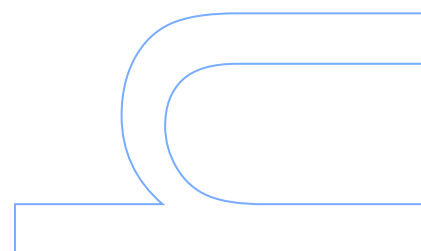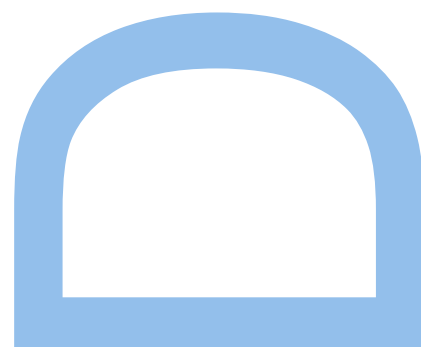## Bianca Celidet Pérez de Lucani
PhD in Chemistry
Departamento de Química e Bioquímica
2013

Adviser
Paula Alexandra de Carvalho Gomes, Assistant Professor, Departamento de Química e Bioquímica, Faculdade de Ciências da Universidade do Porto

Co-adviser
Cátia Andreia Silva Teixeira, Centro de Investigação em Cerâmicas e Materiais Compósitos, Universidade de Aveiro

Acknowledgements

Abstract

Malaria is an infectious tropical disease which mostly affects the world's poorest populations and causes above a half million deaths per year. Its eradication is yet an unmet goal, mostly, due to the emergence of parasite resistance to classical antimalarials and the lack of a commercially available malaria vaccine to prevent the disease. In this context, the doctoral project herein reported comprised two main research lines for malaria eradication. The first and major work of the project centered on the development of dual-action antimalarial drugs. The second research line was dedicated to the study of the influence of vaccination with RTS,S, the most clinically advanced malaria vaccine candidate, on the immune response of African children exposed to the disease.

This doctoral project initially focused on the development of dual-action drugs potentially capable of inhibiting two processes related to the host's hemoglobin degradation by the intraerythrocytic malaria parasite: i) globin degradation by parasite's cysteine proteases, falcipains (FP), and ii) heme detoxification through hemozoin formation (H-f). First generation of compounds, *HEDICIN*s, included a cinnamoyl moiety linked to the 4-amino-7-chloroquinolyl group, the chloroquine (CQ) core, through a dipeptide chain. *HEDICIN*s resulted active in the micromolar range (IC_{50} = 0.83-11 μM) against intraerythrocytic CQ-resistant strain W2 of *Plasmodium falciparum* (*Pf*), but such activity did not correlate with inhibition of FP or H-f. Removal of the hydrophobic dipeptide spacer or substitution of the chloroquinoline core by a non-aromatic ring was detrimental for the antiplasmodial activity. *HEDICIN*s were further evaluated against another protozoal cysteine protease, babesipain-1 (bbspn-1) from *Babesia bigemina*, whose three-dimensional (3D) structure is yet unavailable. Hence, *in silico* studies were carried to build the corresponding 3D structure by homology modeling in order to evaluate the interaction of the *HEDICIN*s with bbspn-1. For rationalizing *in vitro* data at the molecular level, a comparative analysis of the compounds' behavior against FP and bbspn-1 was also performed as *HEDICIN*s demonstrated to be more efficient inhibitors of bbspn-1.

Second generation of compounds, *HEFLECIN*s, were designed as *HEDICIN*s analogues where the dipeptide spacer was replaced by a more flexible hydrophobic spacer, an alkyl chain. Compounds displayed activities in the nanomolar range (IC_{50} = 11.0-46.6 nM) better than CQ (IC_{50} = 138 nM), the reference drug against blood-stage *Pf* CQ-resistant strain W2. These compounds were also highly potent (IC_{50} = 1.1-4.1 μM) *in vitro* against liver-stage *P. berghei* malaria parasites, and superior to primaquine (IC_{50} = 7.5 μM), the reference drug against the latter stage, thus representing dual-stage antimalarial leads. Furthermore, CQ core was respectively replaced by others heteroaromatic core from

known antimalarials. Analysis of the structure-activity relationships demonstrated the relevance of i) the butyl chain, ii) the CQ core, and iii) the amide functionality, for optimal dual-stage antimalarial activity. Two *HEFLECIN*s were further confirmed to be active *in vivo* against blood stage malaria in rodents. Moreover, *HEFLECIN*s were evaluated *in vitro* against the promastigote and amastigote forms of *Leishmania infantum*, and consequently, established as promising anti-leishmanial agents. The mechanism of action of these second-generation compounds is yet to be elucidated, as their antiplasmodial activities did not correlate with the inhibition of H-f or FP.

The second part of this doctoral project consisted in the measurement of the antibody responses to pre-erythrocytic and erythrocytic *Pf* antigens in African children vaccinated with RTS,S or control vaccine and naturally exposed to malaria, and subsequent analysis of the data. According to the results obtained, there seems to be a difference in IgG levels, between the RTS,S and vaccine control groups, that drops over time. The results of this study contribute to the understanding of a pre-erythrocytic malaria vaccine intervention in children.

Keywords: Acridine, antimalarial, babesiosis, chloroquine, cinnamic acid, dual-action, leishmaniasis, malaria, Plasmodium, primaquine, vaccine, RTS,S.

Resumo

A malária é uma doença infeciosa que afecta maioritariamente as populações mais pobres do mundo e causa mais de meio milhão de mortes por ano. Embora a malária já tenha sido erradicada em diversos países, a doença continua presente em cerca de cem países, principalmente devido ao aparecimento de estirpes do parasita resistentes aos antimaláricos clássicos e, à falta de uma vacina contra a malária comercialmente disponível. Neste contexto, o projeto de doutoramento aqui apresentado engloba duas linhas de investigação principais contribuindo para a erradicação da malária. O primeiro, e principal trabalho do projeto, centrou-se no desenvolvimento de antimaláricos de ação dual. O segundo trabalho de investigação dedicou-se ao estudo da influência da vacinação com RTS,S, o candidato a vacina da malária clinicamente mais avançado, na resposta imune de crianças africanas expostas à doença.

A primeira parte do projeto iniciou-se com o desenvolvimento de fármacos potencialmente capazes de atuar contra dois processos intra-eritrocitários, relacionados com a degradação da hemoglobina do hospedeiro pelo parasita da malária: i) degradação de globlina pelas falcipaínas (FP), proteases de cisteína do parasita, e ii) desintoxicação do heme por formação de hemozoína (H-f). A primeira geração de compostos, *HEDICIN*s, consistiu num grupo cinamoílo ligado ao grupo 4-amino-7-cloroquinolinoílo, o núcleo da cloroquina (CQ), através de uma cadeia dipeptídica. Estes compostos resultaram ativos, no ordem do micromolar (IC_{50} = 0.83-11 μM), contra a estirpe resistente à CQ de *Plasmodium falciparum* (*Pf*) W2, mas não se verificou qualquer correlação entre a atividade antiplasmodial e a inibição de H-f ou FP. A remoção do espaçador dipeptídico ou a substituição do núcleo cloroquinolina por um anel não aromático demonstrou ser prejudicial à atividade antiplasmodial. Adicionalmente, os compostos *HEDICIN*s foram avaliados contra a babesipaína-1 (bbspn-1), uma protease de cisteína do protozoário *Babesia bigemina*, cuja estrutura tridimensional (3D) não está disponível. Assim, usaram-se técnicas de modelação por homologia para construir um modelo 3D da bbspn-1, a fim de avaliar a sua interação com os *HEDICIN*s. Com o objetivo de se avançar com uma explicação a nível molecular dos resultados *in vitro*, comparou-se a interação dos compostos com a FP e bbspn-1, respectivamente, já que os *HEDICIN*s mostraram ser inibidores mais eficazes da bbspn-1.

A segunda geração de compostos, *HEFLECIN*s, corresponde a análogos dos *HEDICIN*s, em que a cadeia dipeptídica foi substituída por um espaçador mais flexível e hidrofóbico, uma cadeia alquílica. Os compostos apresentaram atividade antiplasmodial contra a estirpe de *Pf* resistente à CQ, W2, na ordem do nanomolar (IC_{50} = 11.0-

46.6 nM), atividades superiores às da CQ (IC$_{50}$ = 138 nM), o farmáco de referência contra a fase sanguínea do parasita *Pf*. Adicionalmente, estes compostos revelaram-se mais ativos *in vitro* (IC$_{50}$ = 1.1-4.1 μM), contra o parasita *P. berghei* da fase hepática da malária, quando comparados com a primaquina (IC$_{50}$ = 7.5 μM), o farmáco de referência contra esta fase, demonstrando o potencial dos *HEFLECINs* como antimaláricos de ação dual. Posteriormente, substituiu-se o núcleo da CQ por outros núcleos heteroaromáticos de antimaláricos conhecidos e investigou-se a influência da natureza do espaçador. Este estudo de relação estrutura-atividade demonstrou a relevância i) da cadeia de butilica, ii) do núcleo da CQ, e iii) da funcionalidade amida para as ótimas atividades dos composto contra ambas fases da malária acima indicadas. Além disso, dois *HEFLECIN*s foram confirmados ativos contra a infecção da malária na fase sanguínea em roedores. Os *HEFLECIN*s foram ainda testados em culturas de promastigotas e amastigotas de *Leishmania infantum*, revelando-se agentes promissores contra da leishmaniose visceral. Uma vez que a atividade antiplasmodial dos *HEFLECIN*s não se correlacionou com a inibição de H-F ou FP, o mecanismo de ação dos compostos permanece por elucidar.

A segunda parte do projeto de doutoramento consistiu na medição da resposta de anticorpos a antígenos pré-eritrocitários e eritrocitários do *Pf* em crianças africanas vacinados com a vacina RTS,S ou controle e naturalmente expostos à malária, e subsequente análise dos dados. Com base nos resultados obtidos, observou-se uma diferença nos níveis de IgG, entre o grupo da vacina controle e do RTS,S, que diminui ao longo do tempo. Os resultados deste estudo contribuem para a compreensão da intervenção da vacinação pré-eritrocitária contra a malária em crianças.

Palavras-chave: Ácido cinâmico, ação dual, acridina, antimalárico, babesiose, cloroquina, leishmaniose, malária, Plasmódio, primaquina, vacina, RTS,S.

Table of content

List of schemes

List of figures

List of tables

Abbreviations

ab	antibody
ACT	Artemisinin-combination therapies
AMA-1	Apical membrane antigen 1
AQ	Acridine
AMBER	Assisted Model Building with Energy Refinement
ART	Artemisinin
B.	*Babesia*
β-H	β-hematin
Boc	*tert*-Butoxycarbonyl
BSA	Bovine serum albumin
Caco-2	Human colorectal adenocarcinoma cell line
Cbz	Carboxylbenzyl
CelTOS	Cell-traversal protein for ookinetes and sporozoites
CI	Confidence Interval
COMU	(1-Cyano-2-ethoxy-2-oxoethylidenaminooxy)dimethylamino-morpholino-carbenium hexafluorophosphate
CQ	Chloroquine
CRESIB	Barcelona Center for International Health Research
CSP	Circumsporozoite protein
d	doublet
DBL	Duffy binding-like
DCM	Dichloromethane
dd	doublet of doublets
DIEA	*N,N*-Diisopropylethylamine
DMF	*N,N*-Dimethylformamide
DMSO	Dimethylsulfoxide
DMSO-d_6	Hexadeuterated dimethylsulfoxide
DPAP1	Dipeptidyl Amino Peptidase 1

EBA-175	Erythrocyte binding antigen 175
EDC	1-Ethyl-3-(3-dimethylaminopropyl)carbodiimide
Eq	Molar equivalents
ESI-IT MS	Electrospray ionization-ion trap mass spectrometry
E64	1-[*N*-[(*L*-3-*trans*-carboxyoxirane-2-carbonyl)-*L*-leucyl]amino]-4-guanidinobutane
E64C	[(*2S,3S*)-3-carboxyoxirane-2-carbonyl]-*L*-Leucine (3-Methylbutyl)amide *L*-trans-epoxysuccinyl-Leu-3-methylbutylamide
Fe(III)PPIX	Ferriprotoporphyrin IX
Fig.	Figure
FP	Falcipain
FV	Food Vacuole
GOLD	Genetic optimization for ligand docking
HeLa	Henrietta Lacks (human cervical carcinoma cell line)
H-f	Hemozoin formation
HFF-1	Human foreskin fibroblast cell line
HPLC	High-performance liquid chromatography
HOBT	1-Hydroxybenzotriazole
IC_{50}	Half maximal inhibitory concentration
IFAT	Immunofluorescence antibody test
ITN	Insecticide-treated-net
hPhe	Homophenylalanine
J	Coupling constant (in Hz)
Leu	Leucine
LSA-1	Liver stage antigen-1
m	multiplet
MCF-7	Michigan Cancer Foundation-7 (human breast adenocarcinoma cell line)
MKN-28	Human gastric epithelial carcinoma cell line

mp	Melting point
MSP	Merozoite surface protein
Mu	Morpholine
ND	Not determined
NMR	Nuclear magnetic resonance
NPP	New permeability pathways
P.	*Plasmodium*
PCD	Passive Case Detection
PDB	Protein data bank
Pf	*Plasmodium falciparum*
*Pf*CRT	*Plasmodium falciparum* chloroquine resistant transporter.
PQ	Primaquine
PSAC	*Plasmodium* Surface Anion Channel
p-TsOH	*p*-Toluenesulfonic acid
Py	Pyridine
PyAOP	(7-Azabenzotriazol-1-yloxy)tripyrrolidinophosphonium hexafluorophosphate
PyBOP	Benzotriazolyloxy-tris[pyrrolidino]-phosphonium hexafluorophosphate
PyBrop	Bromo-tris-pyrrolidino phosphoniumhexafluorophosphate
PyClock	6-Chloro-benzotriazole-1-yloxy-tris-pyrrolidinophosphonium hexafluorophosphate
PyOxim	[Ethyl cyano(hydroxyimino)acetato-O^2]tri-1-pyrrolidinylphosphonium hexafluorophosphate
RBC	Red Blood Cell
RESP	Restrained electrostatic potential
RMSD	Root mean standard deviation
rt	Room temperature
s	singlet
SAR	Structure-activity relationships
SN*Ar*	Nuclephilic aromatic substitution

SSP2	Second sporozoite surface protein
Sulfo-NHS	*N*-hydroxysulfosuccinimide
t	triplet
TBAF	Tetra-n-butylammonium fluoride
TBDMSCl	*tert*-Butyldimethylsilyl chloride
TBTU	*O*-(Benzotriazol-1-yl)-*N,N,N',N'*-tetramethyluronium tetrafluoroborate
TEA	Triethylamine
TFA	Trifluoroacetic acid
THF	Tetrahydrofuran
TLC	Thin Layer Chromatography
Uniprot	Universal Protein Resource
WHO	World Health Organization

Foreword

Malaria is an infectious disease responsible for about a half million deaths every year, mostly affecting developing countries in tropical areas.[1, 2] There are five species of the genus *Plasmodium* which cause malaria in humans, *P. malarie*, *P. ovale*, *P. knowlesi*, *P. vivax*, and *P. falciparum* (*Pf*).[3] The latter is the most deadly species, mainly among children under five years of age, and is predominant in Africa.

Malaria is transmitted by female *Anopheles* mosquitoes. Once an infected mosquito bites the human skin, it injects sporozoites which penetrate lymph nodes and capillaries (Fig. 1). The sporozoites that enter the lymph nodes are believed to contribute to the immune response. On the other hand, the sporozoites which go into the capillaries travel to the liver, where they invade hepatocytes to form a schizont, inside which asexual reproduction takes place to produce thousands of merozoites. Subsequently, these merozoites are released into the blood stream to invade red blood cells (RBC) and there reproduce asexually into more merozoites. When the infected RBC collapse, released merozoites are ready to infect other blood cells, thus perpetuating the disease in the human host. Occasionally, some intraerythrocytic parasites differentiate into male and female gametocytes. The life cycle continues when a mosquito bites the infected human and ingests such gametocytes. The sexual reproduction begins within the mosquito gut to end with formation of sporozoites. These sporozoites migrate into the salivary glands of the mosquito that becomes able to infect other human hosts.[4]
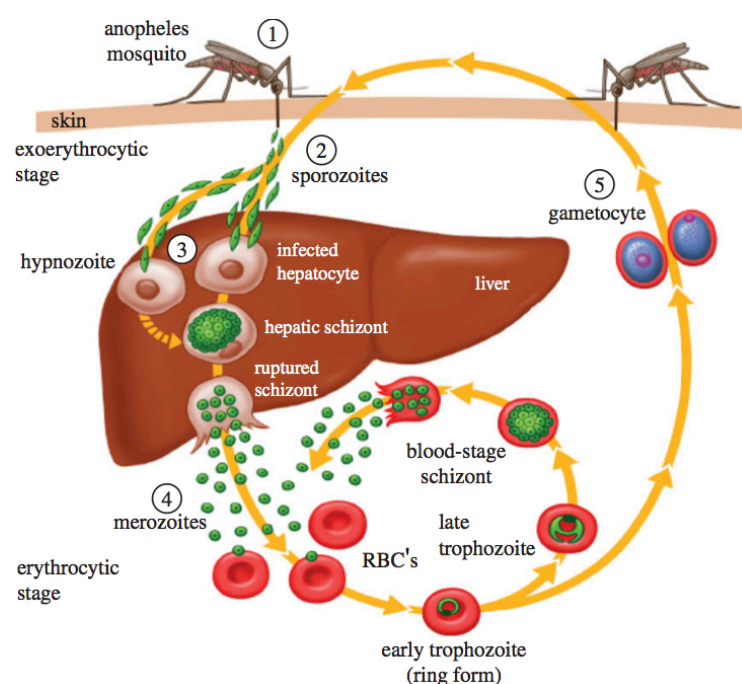
Figure 1. Life cycle of malaria parasites in humans.(Retrieved from Hill *Philos Trans R Soc Lond B Biol Sci* **2011**)

The Malaria Global Plan from 2011 set the challenge of having, by the end of 2015, i) reduced by 75% malaria cases incidence compared to levels in 2000 ii) lowered malaria deaths proximate to zero, and iii) eliminated the disease in ten new countries taking into account the countries where malaria have been eradicated since 2008.[1] Although there have been significant advances in malaria containment to meet this global target, such progress seems to have slowed down recently making it insufficient to meet worldwide needs in this area. Besides, in spite of the fact that the percent of households protected with insecticide-treated-net (ITN) and indoor residual spread (IRS) have increased,[1] parasite resistance to ITN continues to emerge. Additionally, concerns have been arisen regarding the use of bed nets, since by protecting infants from exposure to the malaria parasite, these vector control strategies might be impairing the respective acquirement of natural immunity and consequently, the burden of the disease might be shifting to older age children resulting in little or none long term benefit for vector control.[6] In addition, though the number of diagnostic tests and treatments is increasing, millions of people continue to lack rapid diagnostics and efficient therapies against malaria.[1] Furthermore, the malaria parasite has started to show resistance to artemisinins, the key components of artemisinin-combination therapies (ACT), which are the current first-line treatments against chloroquine (CQ)-resistant malaria. For instance, parasite resistance against artemisinins has already been detected in four countries of Southeast Asia.[1]

Besides political, social, and economic factors which contribute to the malaria burden on the world,[7] malaria eradication is yet an unmet goal due to three main reasons: i) lack of a large scale ecofriendly way to control the vector, and consequently prevent transmission of the disease, ii) widespread parasite resistance to classical antimalarial drugs and emerging resistance to current first-line ones, and iii) lack of an effective and commercially available antimalarial vaccine to prevent infection.[7] Therefore, in order to reduce the malaria incidence and death rates, all these boundaries need to be eliminated.

In this dissertation, the work focused on two of the main and complementary approaches towards malaria eradication, namely, malaria chemotherapy and prevention. The first and major work of the doctoral research, conducted in the area of malaria chemotherapy, centered on the development of economically affordable dual action antimalarials, drugs capable of acting against two different processes in the malaria life cycle to improve efficacy and hinder emergence of parasite resistance. In parallel, work carried in the area of malaria prevention contributed to the understanding of whether the low exposure to *Pf* blood stage antigens could influence the immune response of vaccinated children against malaria in the long term, by obtaining and partially analyzing the antibody (Ab)

response induced by the most clinically advanced pre-erythrocytic antimalarial vaccine, RTS,S.[8]

References

1. World health Organization (WHO). World Malaria Report **2012**. ISBN: 978 92 4 156453 3

2. Rosenthal, P. Antimalarial Chemotherapy: Mechanisms of Action, Resistance and New Directions in Drug Discovery. Published by Humana Press, 2001. ISBN 0896 03670 7

3. Kantele, A.; Jokiranta, S. [Plasmodium knowlesi--the fifth species causing human malaria]. *Duodecim* **2010,** 126, 427-34.

4. Batista, R.; De Jesus Silva Júnior, A.; De Oliveira, A. Plant-Derived Antimalarial Agents: New Leads and Efficient Phytomedicines. Part II. Non-Alkaloidal Natural Products. *Molecules* **2009,** 14, 3037-3072.

5. Hill, A. V. Vaccines against malaria. *Philos Trans R Soc Lond B Biol Sci* **2011,** 366, 2806-14.

6. Chukwuocha, U. M.; Dozie, I. N. Malaria transmission and morbidity patterns in holoendemic areas of Imo River Basin of Nigeria. *BMC Res Notes* **2011,** 4, 514-521.

7. Michalakis, Y.; Renaud, F. Malaria: Evolution in vector control. *Nature* **2009,** 462, 298-300.

8. Regules, J. A.; Cummings, J. F.; Ockenhouse, C. F. The RTS,S vaccine candidate for malaria. *Expert Rev Vaccines* **2011,** 10, 589-99.

List of publications

Chapter 1

Journal article (Appendix A)

1. Pérez, B.; Teixeira, C.; Gomes, J.; Gomes, P. Development of Plasmodium falciparum protease inhibitors in the past decade (2002-2012). *Curr Med Chem* **2013**, 20, 3049-68. Impact factor: 4.07

Chapter 2

Journal article (Appendix B)

1. Pérez, B.; Teixeira, C.; Figueiras, M.; Gut, J.; Rosenthal, P.; Gomes, J.; Gomes, P. Novel cinnamic acid/4-aminoquinoline conjugates bearing non-proteinogenic amino acids: towards the development of potential dual action antimalarials. *Eur J Med Chem* **2012**, *54*, 887-99. (doi: 10.1016/j.ejmech.2012.05.022). Impact factor: 3.356.

Chapter 3

Journal article (Appendix C)

1. Pérez, B.; Domingos, A.; Gomes, J. R. B.; Gomes, P.; Teixeira, C. Toward the discovery of inhibitors of babesipain-1, a Babesia bigemina cysteine protease: in vitro evaluation, homology modeling and molecular docking studies. *J Comput Aid Mol Des*. Accepted in September **2013**, 27, 823-835.

Chapter 4

Journal articles (Appendix D)

1. Pérez, B.; Teixeira, C.; Gut, J.; Rosenthal, P.; Gomes, J.; Gomes, P. Cinnamic Acid/Chloroquinoline Conjugates as Potent Agents against Chloroquine-Resistant *Plasmodium falciparum*. *ChemMedChem* **2012**, *7*, 1537–1540. (doi:10.1002/cmdc.201200257). Impact factor: 3.306.
   Made to Back Cover (Pag 1692).
   http://onlinelibrary.wiley.com/doi/10.1002/cmdc.201290046/abstract

2. Pérez, B.; Teixeira, C.; Albuquerque, I.; Gut, J.; Rosenthal, P.; Gomes, J.; Prudêncio, M.; Gomes, P. *N*-cinnamoylated chloroquine analogues as dual-stage antimalarial leads. *J Med Chem* **2013**, *56*, 556-67. (doi: 10.1021/jm301654b). Impact factor: 5.248.

3. Pérez, B.; Teixeira, C.; Albuquerque, I.; Gut, J.; Rosenthal, P.; Prudêncio, M.; Gomes, P. PRIMACINS, *N*-cinnamoyl-primaquine conjugates with improved liver-stage antimalarial activity. *MedChemComm* **2012**, *3*, 1170-1172. (doi:10.1039/C2MD20113E). Impact factor: 2.8.

   Highlighted in Chemistry World, August 7th, 2012.

   http://www.rsc.org/chemistryworld/2012/08/improved-drugs-treat-malarial-liver-infection

4. Pérez, B.; Teixeira, C.; Gomes, A.; Albuquerque, I.; Gut, J.; Rosenthal, P.; Prudêncio, M.; Gomes, P. In vitro efficiency of 9-(N-cinnamoylbutyl)aminoacridines against blood- and liver-stage malaria parasites. *Bioorg Med Chem Lett* **2013**, *23*, 610-3. (doi: 10.1016/j.bmcl.2012.12.032). Impact factor: 2.554.

   Highlighted in Malaria Nexus, March 15th, 2012.

   http://www.malarianexus.com/articles/in-vitro-efficiency-of-9-n-cinnamoylbutyl-aminoacridines-against/

5. Vale-Costa, S.; Costa Gouveia, J.; Pérez, B.; Silva, T.; Teixeira, C.; Gomes, P.; Gomes, M. S. *N*-cinnamoylated aminoquinolines as promising anti-leishmanial agentes. *Antimicrob Agents Ch* **2013**, *57*, 5112-5.

Conferences

1. Pérez, B.; Teixeira, C.; Gomes, A.; Albuquerque, I.; Gut, J.; Rosenthal, P. J.; Gomes, J. R. B.; Prudêncio, M.; Gomes, P. *N*-cinnamoylated chloroquine analogues as potent dual-stage antimalarial leads. Frontiers in Medicinal Chemistry 2013 (FMC2013). June 23-26th, 2013.

   Travel Grant awarded to attend to FMC2013.

2. Pérez, B.; Teixeira, C.; Albuquerque, I.; Gut, J.; Rosenthal, P.; Gomes, J.; Prudêncio, M.; Gomes, P. *N*-alkylcinnamoylation of 4-amino-7-chloroquinoline: unprecedented discovery of chloroquine surrogates as leads for dual-stage antimalarials. 3º Encontro Nacional de Química Terapêutica/3enqt, Aveiro, Portugal, November 28-30th, 2012 (Poster).

3. Pérez, B.; Teixeira, C.; Gomes, A.; Albuquerque, I.; Gut, J.; Rosenthal, P.; Gomes, J.; Prudêncio, M.; Gomes, P In vitro efficiency of 9-(N-cinnamoylaminobutyl)aminoacridines against blood- and liver-stage malaria parasites. 3º Encontro Nacional de Química Terapêutica/3enqt, Aveiro, Portugal, November 28-30th, 2012 (Poster).

4. Vale-Costa, S.; Gouveia, J. C.; Pérez, B.; Teixeira, C.; Gomes, P.; Gomes, M. S. Cinnamic acid conjugates of primaquine and chloroquine active against

Leishmania infantum. (Poster) II International Conference on Antimicrobial Research, Lisbon, Portugal, November 21- 23th, 2012.

Chapter 5

<u>Conferences</u>

1. Campo, J.; Skinner, J.; Pérez, B.; Nakajima-Sasaki, R.; Molina, D.; Liang, L.; Jahit Sacarlal, J.; Alonso, P.; Crompton, P.; Felgner, P.; Aponte, J.; Dobaño, C. Magnitude and breadth of *P. falciparum* antibody responses after vaccination with RTS,S/AS02 in Mozambican children. Malaria Vaccine for the world, CHUV, Lausanne, Switzerland, 22-23 April, 2013 (Oral communication).

Chapter 6

<u>Journal Article</u> (Appendix E)

1. Pérez, B.; Fernandes, I.; Mateus, N.; Teixeira, C.; Gomes, P. Recycling antimalarial leads for cancer: antitumoral properties of *N*-cinnamoyl chloroquine analogues. *Bioorg Med Chem Lett.* Accepted October **2013**.

Chapter 1

Dual-action antimalarials

The covalent bitherapy approach

1.0. Introduction

Nowadays, there are drugs targeting each stage of the malaria asexual reproduction cycle within the human host. Chloroquine (CQ, **I**) and artemisinin (**II**) both target the erythrocytic stage[1-3] while primaquine (**III**) targets the liver stage parasite.[4, 5] However, most malaria control strategies are in jeopardy due to the emergence of parasite resistance. *Pf* parasites have displayed widespread resistance to one of the safer and most affordable drugs, CQ.[6, 7] Furthermore, there is growing evidence that *Pf* is developing resistance to the key compounds of the first-line antimalarial medicines for CQ-resistant malaria, the artemisinin-combination therapies (ACT), [8] despite the fact that ACT have been designed to improve efficacy and hinder emergence of resistance. Therefore, there is an increasing need to develop new effective and affordable antimalarials capable of delaying parasite resistance.
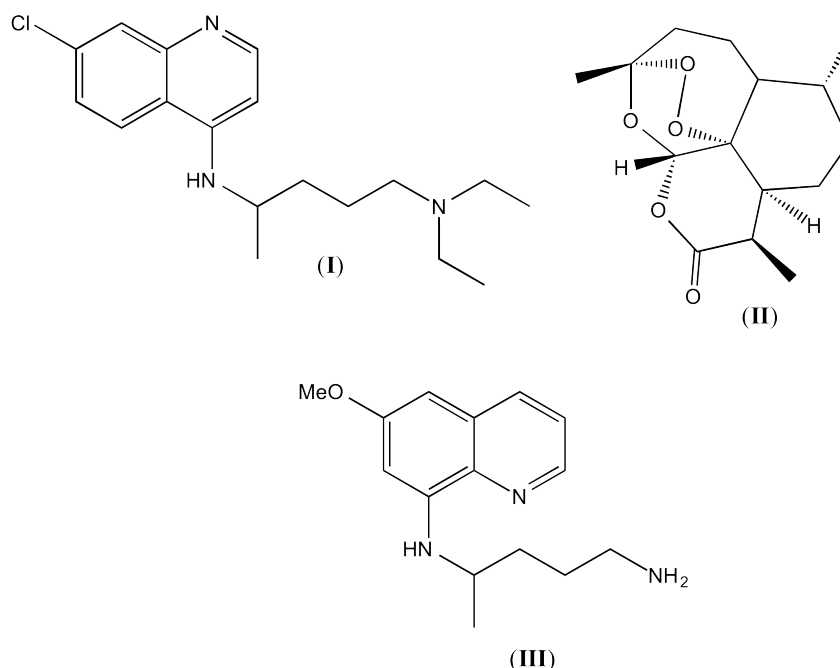
The erythrocytic stage is one of the most relevant stages of the malaria life cycle since the symptoms of malaria appear in this stage. The symptoms include fever, chill, prostration, and anemia and in more severe cases, delirium, metabolic acidosis, cerebral malaria, and multi-organ system failure. Therefore, most antimalarial aim to target this stage of the malarial life cycle. In this stage, the host's hemoglobin is endocytosed to the parasitophorous vacuole (PV) formed inside the infected RBC, and transported to the parasite's food vacuole (FV) where it is degraded into amino acids required for the parasite growth and maturation.[9] In addition, hemoglobin degradation

allows the modulation of the osmotic stability within the host cell.[10] This degradation process is believed to occur in a semi-ordered pathway (Fig. 2), where aspartyl proteases make the initial cleavage of the hemoglobin. Namely, plasmepsins I (PlmI) and II (PlmII) catalyze this first step by breaking down hemoglobin between Phe33 and Leu34 of the α-chain to produce globin and free heme (Fig. 2).[11] On one hand, globin is degraded into small peptide chains by cysteine proteases known as falcipains.[12] Once falcipains have degraded globin into small peptides, these are following broken into oligopeptides of 5 to 10 amino acids by falcilysin.[13] Subsequently, dipeptidyl aminopeptidase 1 (DPAP1) cleaves these oligopeptides into dipeptides.[14] Finally, these dipeptides are transported outside the FV into the PV's cytoplasm where they are degraded into amino acids by exopeptidases.[15] A comprehensive review regarding recent advance towards the development of antimalarial inhibitors of the proteases, which participate in the hemoglobin degradation, has been recently published (See appendix A).
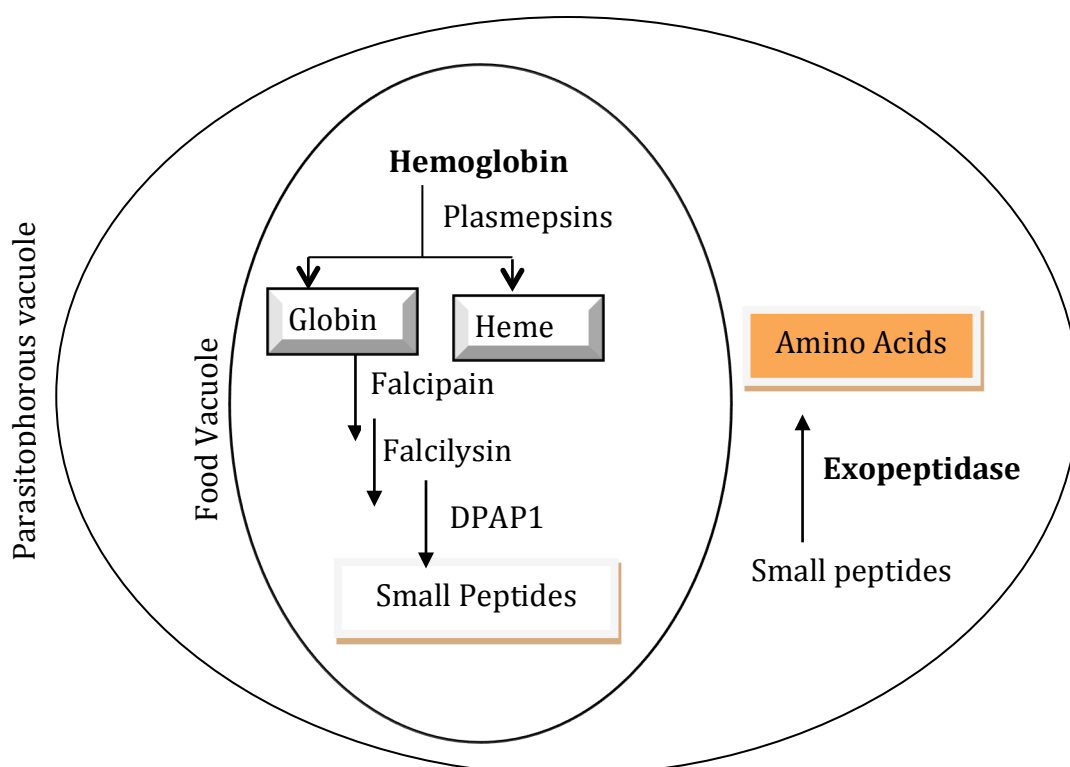
Figure 2. Proteolytic semi-ordered pathway of hemoglobin degradation into amino acids.

On the other hand, heme is readily oxidized to ferriprotoporphyrin IX [Fe(III)PPIX][16] which is toxic to the parasite. [Fe(III)PPIX] is known to cause lipid peroxidation and changes in membrane's permeability.[17] The oxidation of membrane components caused by free heme promotes cell lysis and subsequent death of the parasite,[16] which can't degrade [Fe(III)PPIX] as mammals do (using the enzyme oxygenase) because it lacks a mechanism to sequester the free Fe(III) generated.[17] Therefore, the main detoxification process of [Fe(III)PPIX] involves formation of hemozoin (β-hematin), also known as the malaria pigment. Hemozoin is a dark insoluble biocrystal that contains solely monomers of [Fe(III)PPIX] and is released into the host RBC every time a parasite completes a cycle. Inhibition of hemozoin formation is one of the antimalarial strategies.[18]

1.1. Targeting inhibition of globin degradation by falcipains

Other potential target to impair the malaria parasite development constitutes inhibition of falcipains, which are one of the most studied families of *Pf* proteases.[19] According to the analysis of the *Pf* genome, there are four cysteine proteases, falcipain 1 (FP1), falcipain 2 (FP2), falcipain 2' (FP2'), and falcipain 3 (FP3).[20] FP1 has a low sequence identity compared to the other falcipains and its role in the malaria life cycle is yet to be elucidated. Still reported studies suggest that this protease might participate in the generation of oocysts during parasite development in the mosquito midgut.[21] FP2, FP2', and FP3 show high sequence identity. For instance, FP2 has been demonstrated to be 93% similar to FP2' which is thought to arise by gene duplication.[22] FP2 and FP3 present a sequence identity of 68% and contribute more or less equally in the digestion of globin. In addition, FP2 and FP3 require acidic pH and reducing environment for optimal proteolytic activity. Although FP2 concentration in trophozoites is 1.8 times higher than that of FP3, the latter cleaves globin two times faster than FP2. Today there are several reports in the literature concerning the development of falcipain inhibitors.[20] Inhibitors of falcipains can be generally classified in peptide-based inhibitors and non-peptidic inhibitors. Some of the most active compounds of each family are further below presented. The main catalytic residues of falcipains constituted Cys and His, whose side chains form an ion pair (thiolate/imidazolium) correctly orientated due to influence of a neighboring Asn residue. Molecules bearing electrophilic warheads are generally used to inhibit these enzymes because they form irreversible or reversible covalent bond with the active site cysteine. Examples of such warhead are α-ketoamide,[23] fluoromethyl ketone,[24] epoxysuccinyl[25] or azirine derivatives,[25] and the most used, Michael acceptors. The crystal structures of FP2 (PDB code = 3BPF) and FP3 (PDB code = 3BPM) reported

in complex with known inhibitors of cysteine proteases, such as E64 (**IV**) and leupeptin (**V**), have facilitated the design of new falcipains inhibitors.[12] Accordingly, the substituents in the position P1, P2, and P3 of the ligands, E64 and leupeptin, respectively interact with residues in the S1, S2, and S3 sites of the active cavity of falcipains (Fig. 3). The S2 subsite seems to govern specificity towards FP2 and/or FP3, and to prefer substrates with a leucine residue in the corresponding P2 site. In addition, the catalytic residues of the FP2 and FP3, cysteines, form a covalent irreversible bond with the epoxide moiety of E64 and a covalent reversible bond with the carbonyl motif of leupeptin, respectively.
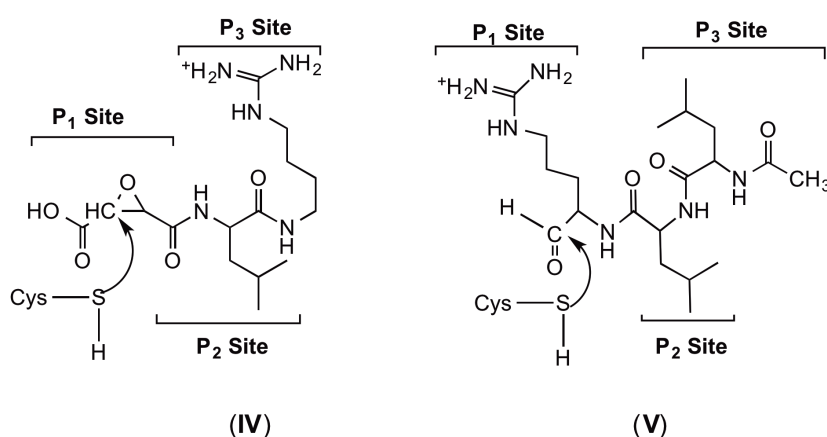
Figure 3. E-64 and leupeptin as inhibitors of falcipains.

One of the most successful examples of the use of Michael acceptor is that of peptidyl-vinyl sulfones which have to shown to inhibit FP2 in the nanomolar range.[26] Inhibition of falcipains by such vinyl sulfones has been shown to correlate with the impairment of *Pf* development.[19] These compounds include a dipeptide segment for better recognition by the parasite's protease, whereas the vinyl sulfone moiety acts as a Michael acceptor to irreversibly alkylate the catalytic Cys residue of the protease (Fig. 4).[27]
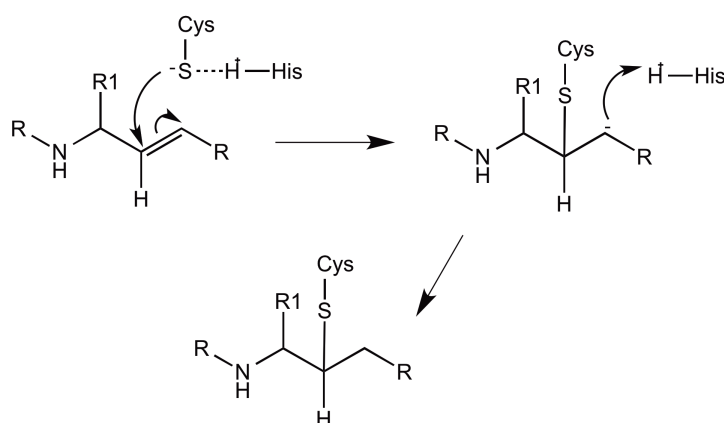
Figure 4. Example of irreversible alkylation of the cysteine residue of falcipains.

Accordingly to Rosenthal's studies, the Leucine-*homo*Phenylalanine (Leu-*h*Phe) dipeptide, has been demonstrated to confer the highest FP inhibitory activity of the respective vinyl sulfones. Further studies reported the structural activity relationship (SAR) of these and related cysteine inhibitors (Fig. 5).[26] In these series, the potency of the compounds against FP2 and FP3, respectively, is not an ideal predictor of the antiplasmodial activity since SAR against falcipain does not completely correlated with the SAR found against the parasite development. For instance, vinyl sulfonamide and vinyl sulfonyl derivatives demonstrated to be more potent than vinyl sulfonate ester against the parasite, contrary to what was found against FP2. In addition, SAR regarding antiplasmodial activity showed that there is a clear preference for -OMe over -H over -F substitution in aromatic ring of the vinyl sulfonate esters, opposite to results found against falcipains.
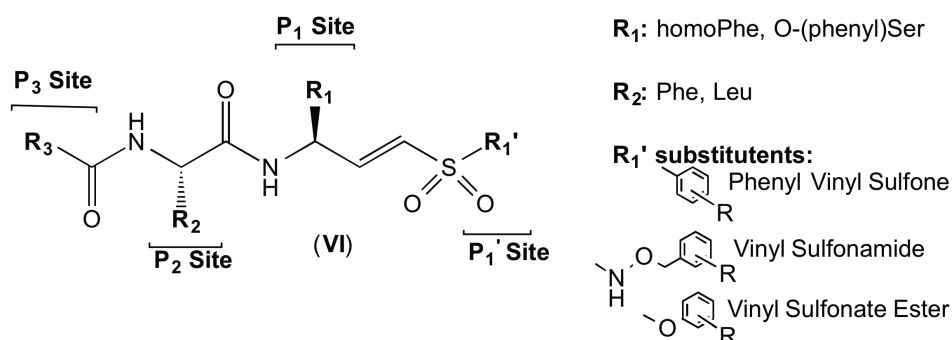
Figure 5. Structure of vinyl sulfone inhibitors of FP2/3 developed by Rosenthal and co-workers.[26]

In addition, other peptide-based inhibitors have been reported to reversibly bind to falcipains and inhibit FP2 and FP3 in the nanomolar level, for instance, compounds reported by O'Neill and co-workers.[28] These compounds possessed the Leu-*h*Phe

dipeptide segment, as the best vinyl sulfone inhibitors reported by Rosenthal's group, but did not include a Michael acceptor moiety; instead, an aldehyde moiety was used in the place of the vinyl sulfone warhead. Compounds (**VII**) and (**VIII**) displayed IC$_{50}$ of 1.4 nM and 16.3 nM against FP2 and 198.9 nM and 214.6 nM against FP3, correspondingly. Also, these compounds (**VII**) and (**VIII**) did inhibit the CQ sensitive *Pf* strain 3D7 with IC$_{50}$ of 27.1 nM and 9.3 nM, respectively, and were found to fit well inside the enzyme's active pocket according to docking studies.

R=Cbz (**VII**); Mu (**VIII**)
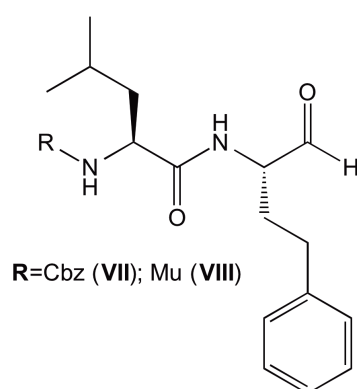
Apart from peptidyl irreversible and reversible inhibitors of FP, non-peptidic compounds, known to not be prone to proteolytic degradation, have also shown to inhibit FP in the nanomolar range, for instance, compounds reported by Fiandor's team.[29] The most potent inhibitors of the series were the 2-cyanopyrimidine derivatives including the 2-cyano-5-chloropyrimidines and 2-cyano-5-bromopyrimidines. Although these compounds were nanomolar inhibitors of FP2 and FP3, they presented antiparasitic activity in the micromolar range. Furthermore, Fiandor and co-workers found that introduction of a protonable amine read to a significant increase in the antiplasmodial activity. For instance, one of the most active compound (**IX**), which contains a protonable amine, displayed an IC$_{50}$ below 0.5 nM against FP2 and FP3 and an IC$_{50}$ of 1 nM against the CQ-resistant parasite.

(**IX**)
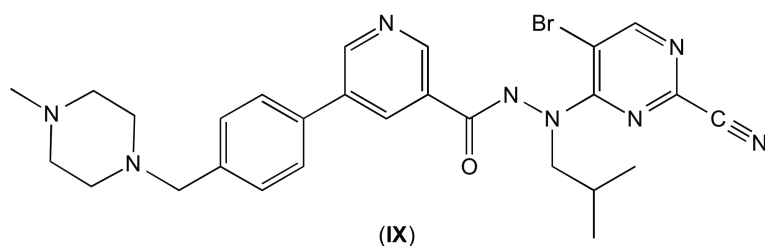
1.2. Targeting inhibition of hemozoin formation

As mentioned above, hemozoin formation is a unique process adopted by *Plasmodium* parasites to detoxify free heme. It is a validated target for most of the well-known existing antimalarial drugs and considered to be suitable target to developed new antimalarials.[30] There are several families of compounds which impair parasite growth through inhibition of hemozoin formation (Fig. 6). The major families are quinolines (**X**), azoles (**XI**), isonitriles (**XII**), methylene blue (**XIII**), and xanthones (**XIV**).[18] For instance, xanthone and derivatives inhibit hemozoin formation through the generation of a soluble complex with heme. Xanthones presenting a single hydroxyl group displayed $IC_{50} > 50\mu M$ against *Pf* clone D6. However, xanthone with multiple hydroxyl substituents, especially on position 4- and 5-, demonstrated to be more active (IC_{50} = 0.1-40 μM) against *Pf* D6.[31] In fact, the antimalarial activity demonstrated to be positively correlated with the number of hydroxyl groups on the compounds. In terms of inhibition of hemozoin formation, xanthones with hydroxyl groups in positions 4- and 5- showed the highest activity of the series. Further reports in the literature showed that xanthones with an *N,N*-diethylaminoalkyl side chain of 5 or 6 carbons presented significantly higher antimalarial activity against *Pf* strain D6 (IC_{50} = 70-100 nM) exhibiting strong heme affinity.
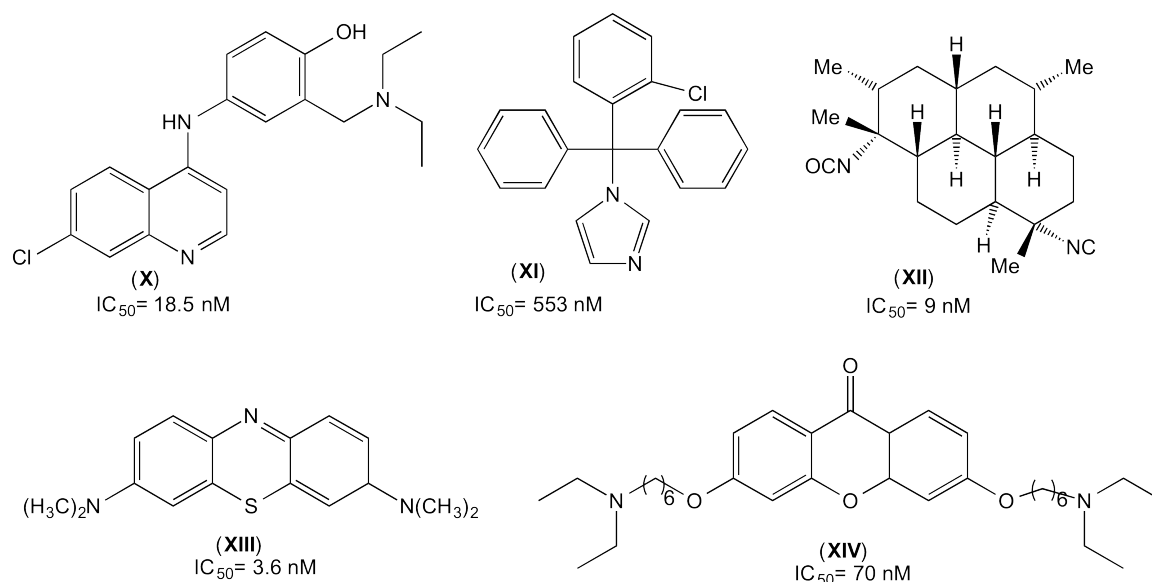
Figure 6. Known inhibitors of hemozoin formation: amodiaquine (**X**), clotrimazole (**XI**), diterpene isonitriles derivative (**XII**), methylene blue (**XIII**), and xanthone derivative (**XIV**),against CQ-sensitive *Pf*.

Other major family of compounds whose SAR against hemozoin formation has been well established constitute quinolines and derivatives such as amodiaquine (**X**) and the

widely used CQ. CQ prevents hemozoin growth by capping the growth of the biocrystal, thus leading to accumulation of free heme to levels that cause parasite death (Fig. 7).[32, 33] The chlorine atom in position seven of the quinoline ring in CQ has been found essential for the drug's activity against hemozoin formation (Fig. 8).[34, 35] In terms of optimal antiparasitic activity of antimalarial 4-aminoquinolines, like CQ, i) a halogen in position seven (-Cl, -Br, or -I but not -F), ii) a protonable amine at position 1 of the quinoline ring, and iii) a dialkylaminoalkylamino side chain are all key structural features.[36] In addition, a dialkylaminoalkylamino side chain of 2 to 12 carbons leads to low nanomolar activities against the CQ-sensitive *Pf* strain. Moreover, it has been show that the protonable amine at position 1 of the quinoline ring and the terminal amine in the dialkylaminoalkylamino side chain are important for the accumulation of the compounds in the food vacuole and consequent inhibition of its target.[37]
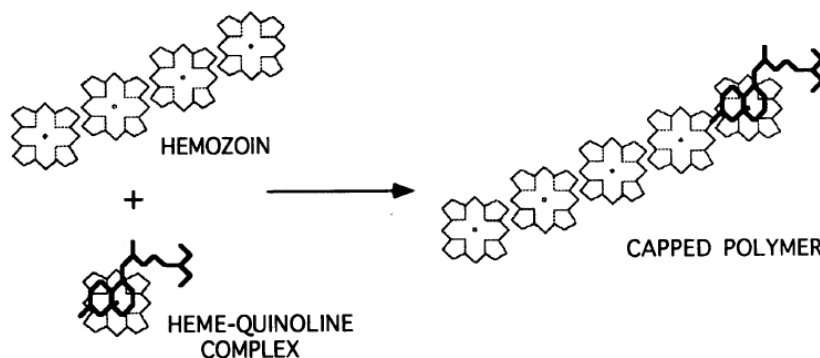
Figure 7. CQ-heme complex incorporate in the forming biocrystal and inhibits hemozoin formation.[32]
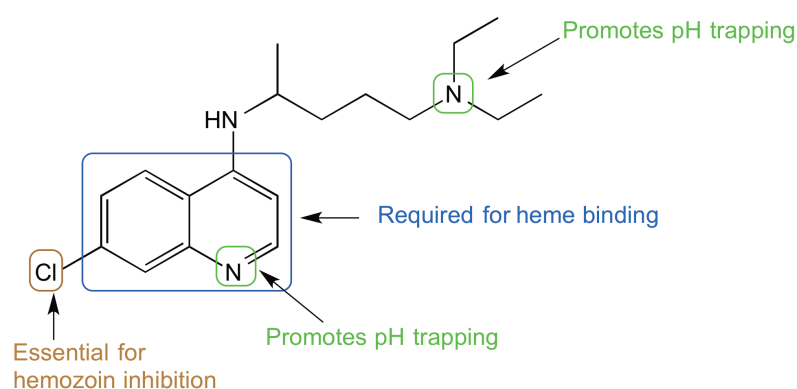
Figure 8. Main characteristics of CQ for the optimal inhibition of hemozoin formation.[38]

Additionally, CQ can accumulate in the FV and subsequently inhibit its target because it is a weak base that can diffuse through the parasite's membrane. Once the drug is inside the FV, it is protonated and consequently, trapped in the acidic FV (pH trapping), which promotes the inhibition of hemozoin. However, the excessive use of CQ due to its high efficacy, low cost, and limited host toxicity led to a gradual decline of the parasite sensitivity to this drug,[39] despite it aims at a non-proteic (i.e., non-genetically coded) target. It has been found that CQ concentrates substantially less in the FV of CQ-resistant *Pf* strains. It is widely believed that this lower accumulation is due to a mutant transmembrane protein, *Pf*CRT, which promotes CQ efflux from the parasite's FV, where the drug should exert its action.[40]

In view of the wide spread parasite resistance to CQ, especially in Africa, nowadays the first line of antimalarial treatment for CQ-resistance malaria is based on ACT, where the potent artemisinins are combined with other antimalarial to hinder the parasite resistance usually associated to monotherapy. However, there has been growing evidence of decreasing sensitivity of plasmodial to ACT. Malaria parasite has started to show resistance to other antimalarials such as artemisinins, the basis compounds of ACT.[41] New approaches to delay parasite emergence resistance consist on the development of dual-action drugs, compounds capable of acting against two processes in the *Pf* malaria life cycle. Hybrid compounds have displayed potent antimalarial activity and no toxicity.[42] Based on their high efficacy and low toxicity, dual-action drugs may constitute the next generation of antimalarials.[42]

1.3. The covalent bitherapy approach against *Pf* malaria

The covalent bitherapy approach against malaria refers to the development of hybrid drugs that covalently link two antimalarial moieties acting against different processes which are essential for parasite survival.[43] One of the advantages of hybrid drugs, as opposed to multicomponent ones, is that they might diminish the risk of drug-drug adverse interactions. An example of hybrid antimalarials is that of trioxaquines, reported by Meunier and co-workers, which combine a trioxolane moiety (mimic of the artemisinin's active core) with the CQ's 4-amino-7-chloroquinoline core.[44] The most promising trioxaquine (**XV**) of the series was synthesized from two precursors: i) 4-(*N*-aminoethyl)amino-7-chloroquinoline obtained from nucleophilic substitution of ethane-1,2-diamine on 4,7-dichloroquinoline, and ii) a trioxane-ketone synthesized from α-terpinene, through photo-oxygenation and subsequent condensation with cyclohexane-1,4-dione (Scheme 1).[45] Trioxaquine (**XV)** was active in the nanomolar range against the asexual intraerythrocytic stage (IC_{50} = 28 nM) and young (IC_{50} = 69 nM) or old

gametocytes (IC_{50} = 67 nM) with activities comparable to those presented by the respective reference drugs of each tested stage, atovaquone on asexual intraerythrocytic forms (IC_{50} = 4.6 nM), and artesunate that targets both young (IC_{50} = 72 nM) and old gametocytes (IC_{50} = 108 nM).
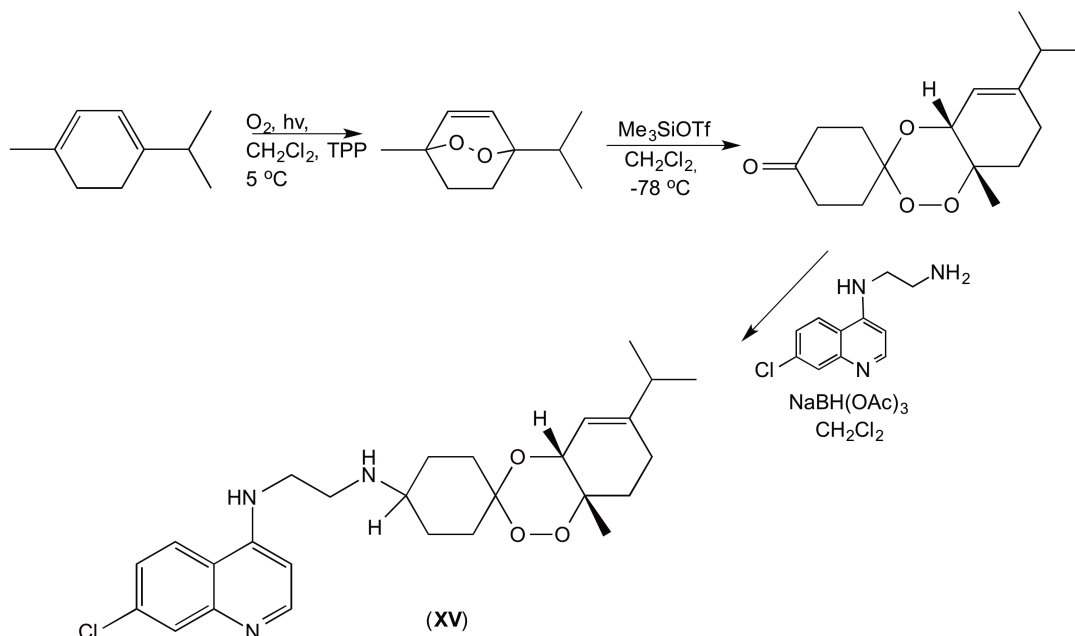
Scheme 1. Synthetic route towards trioxaquine (**XV**), a promising antimalarial built on the covalent bitherapy concept.[44, 45]

In the same year, Bell and co-workers reported a hybrid molecule (**XVI**) where artemisinin was combined with the emblematic antimalarial drug quinine.[46] Accordingly, artemisinin was reduced to dihydroartemisinin and the vinyl functionality of quinine was modified into a carboxylic moiety, so that the two cores were linked to each other through an ester bond (Scheme 2). Other functionalities of the respective building blocks could not be altered without sacrificing activity. For instance, the potent blood-schizontocidal activity of quinine depends on both the quinoline ring and the hydroxyl group. The artemisinin-quinine hybrid (**XVI**) was more active against *Pf* 3D7 (IC_{50} = 10.4 nM) than artemisinin (IC_{50} = 45.3 nM), quinine (IC_{50} = 73.5 nM), or an equimolar mixture of both drugs (IC_{50} = 27.9 nM).
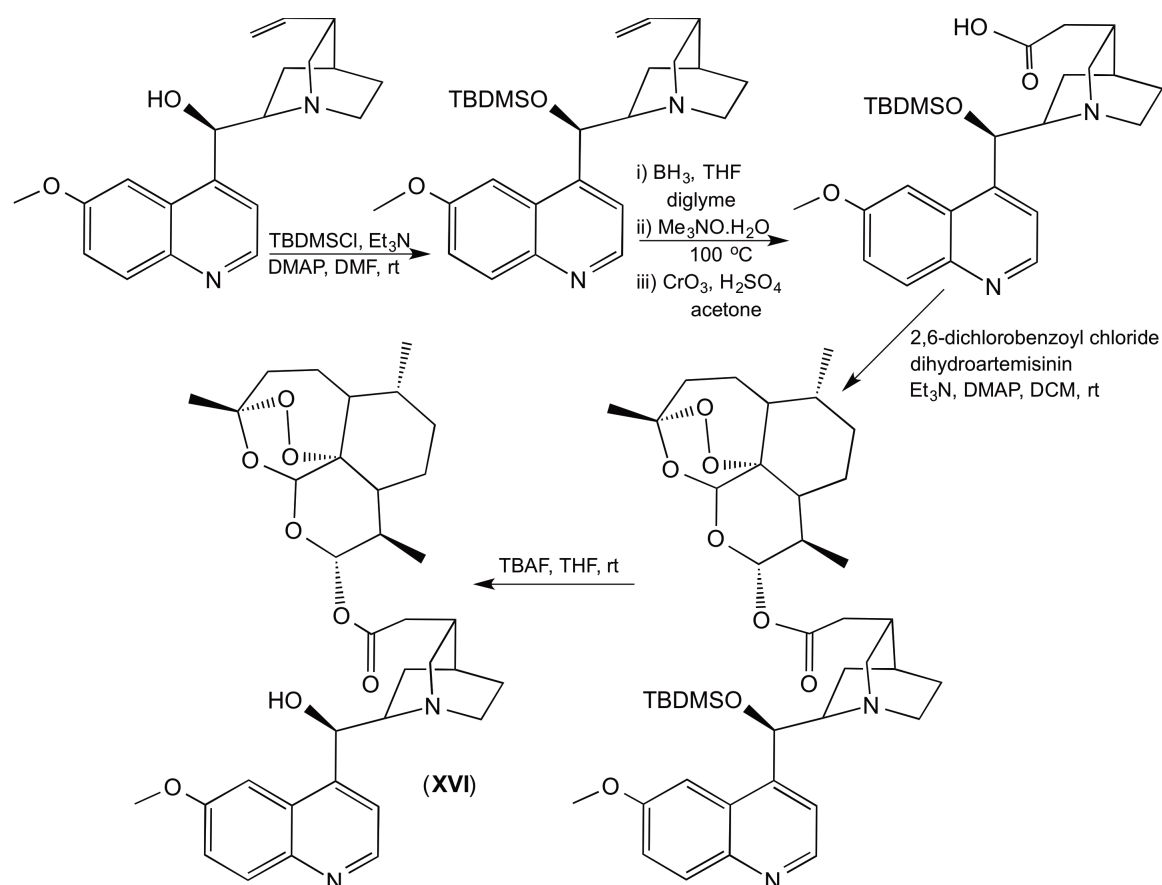
Scheme 2. Synthesis route to an antimalarial artemisinin-quinine hybrid (**XVI**) developed by Bell and co-workers.[46]

Other examples of hybrid molecules, which include the artemisinin core, are those reported by Capela's and co-workers.[47, 48] In the hope to develop a multi-stage drug which did not only target the *Pf* in the RBC but also the replicative and dormant form in the liver stage of the malaria cycle, they decided to join together the ART core and the PQ.[46] The two synthesized compounds (**XVIIa**) and (**XVIIb**) displayed *in vitro* activities against the liver and blood stage comparable to the reference drugs, PQ and ART, respectively. Compound (**XVIIb**) was more active against blood stage (IC_{50} = 9.1 nM) than compound (**XVIIa**) (IC_{50} = 12.5 nM). In the liver stage, compound (**XVIIa**) showed to be the most active *in vivo*, while when testing against blood stage parasite, compound (**XVIIb**) displayed the highest activity *in vivo*; both results were in agreement with the *in vitro* data.

(XVIIa)   (XVIIb)
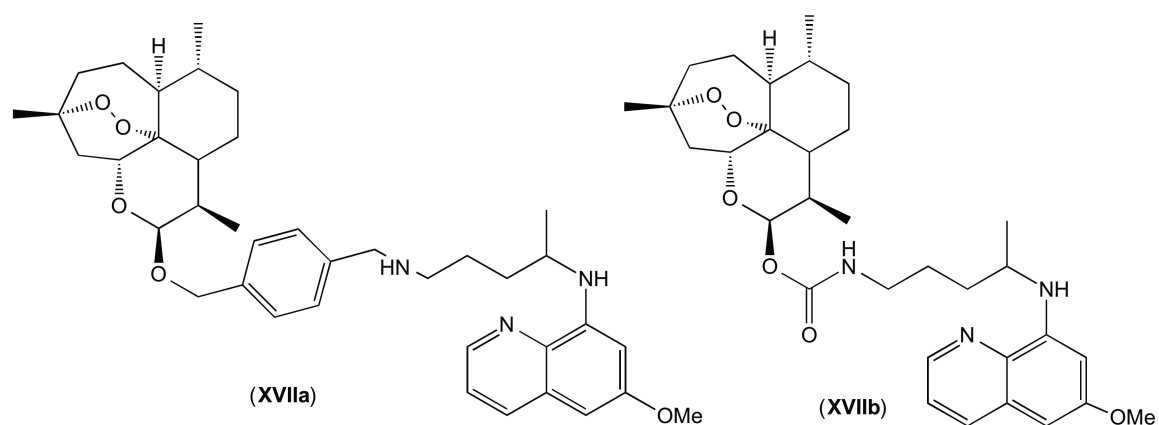
In addition, Capela and co-workers designed and synthesized hybrid compounds (XVIII) which join together the vinyl sulfones, previously demonstrated by Rosenthal to be potent inhibitor of falcipains,[26] to the artemisinin core using a 4-hydroxymethylbenzoic acid as a linker. These derivatives displayed activities comparable to those of the artemisinin. The synthesis pathway consisted in multiple reaction steps. First, it involved the formation of an aldehyde moiety from the respective Boc protected amino acid using Weinreb chemistry followed by the Horner–Wadsworth–Emmons reaction. Later, the Boc protecting group was removed and the obtained amine was coupled to a second Boc protected amino acid to result the dipeptidyl vinyl sulfone. Finally, the corresponding amine was deprotected and coupled to the previously obtained artemisinin/4-hydroxymethylbenzoic acid derivative (Scheme 3). The compounds were evaluated as inhibitors of the activity of CQ sensitive malaria parasite and falcipains action. Although hybrid compounds displayed activity in the nanomolar range against the parasite, they showed to be active only in the micromolar range against FP2 (IC_{50} = 0.35-16.5 μM), suggesting that the main mechanism of action of these derivatives was due to the endoperoxide form of the artemisinin core. The most active compound (XVIIIa) of the synthesized series against FP2 possessed the dipeptide Leu-hPhe which is in agreement with results previously found by Rosenthal's team.[26]

a)

Vinyl sulfone precursor

b)

(XVIII)

(XVIIIa) $R^1 = CH_2CH(Me)_2$; $R^2 = Me$;
$R^3 = (CH_2)_2Ph$
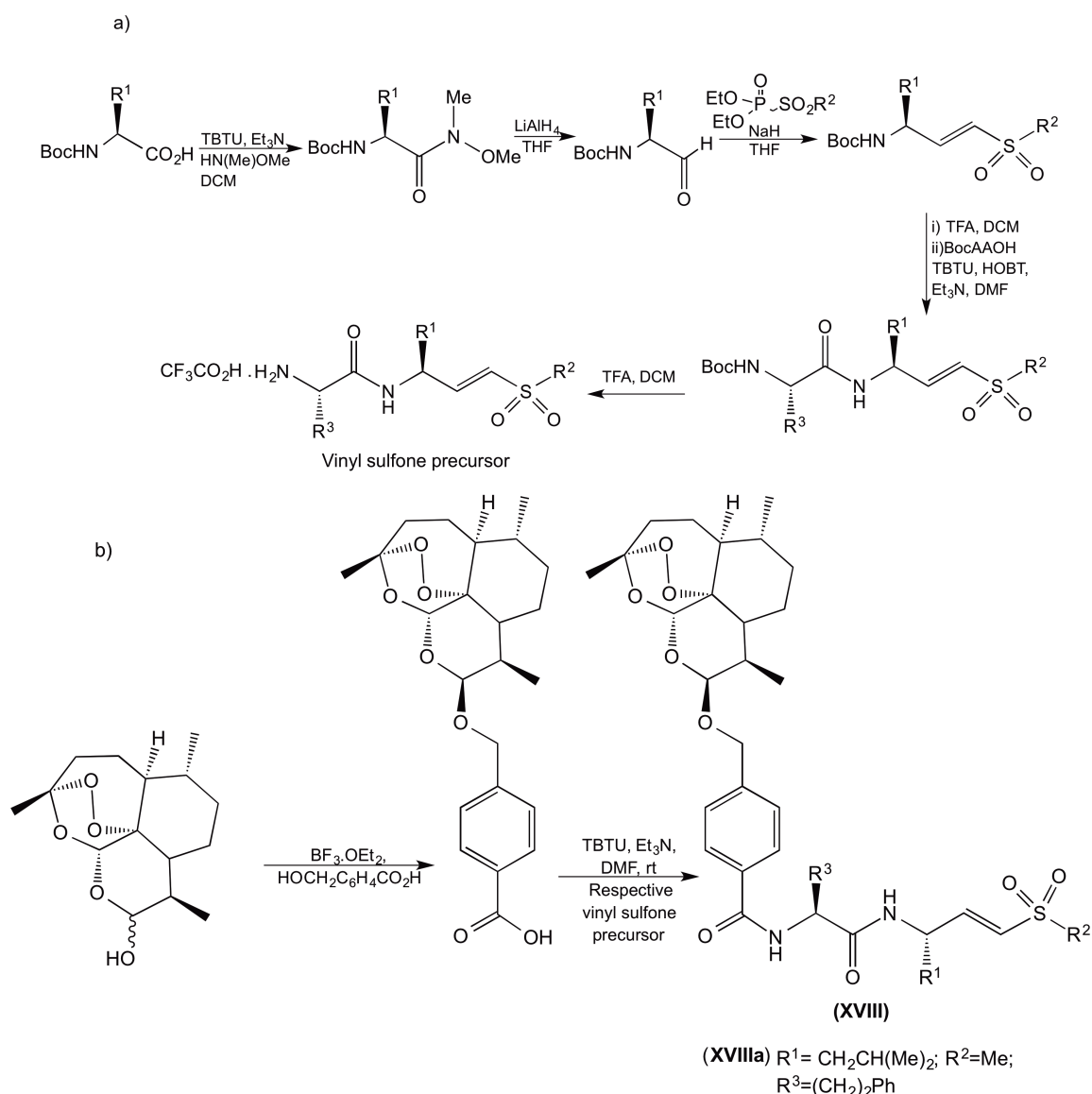
Scheme 3. a) Synthesis of the vinyl sulfone precursor. b) General synthesis of the hybrid molecules designed by Moreira and co-workers. Hybrid molecule (**XVIIIa**) is the most active compound against FP2 that is also active against the parasite.[47]

O'Neill and co-workers applied a similar concept,[28] by synthesizing a series of compounds where an endoperoxide was linked to a morpholine urea (Mu-Urea) or to a benzyloxycarbonyl protecting group (Cbz) through the dipeptide linker Leu-*h*Phe. The resulting hybrids would expectedly disrupt parasite development through two processes: falcipain inhibition and generation of cytotoxic C-radical species. Both the falcipain inhibiting moiety and the C-radical species would be released upon hybrid compound degradation catalyzed by Fe(II) (Scheme 4). The most active compounds against CQ-sensitive *Pf* strain, (**XIXa**) and (**XIXb**) with IC_{50} = 55.5 nM and 35.3 nM, correspondingly, were also active against FP2 (IC_{50} = 425.3 and 510.2 nM for (**XIXa**) and (**XIXb**), respectively) and FP3 (IC_{50} = 947 and 332.3 nM, respectively).
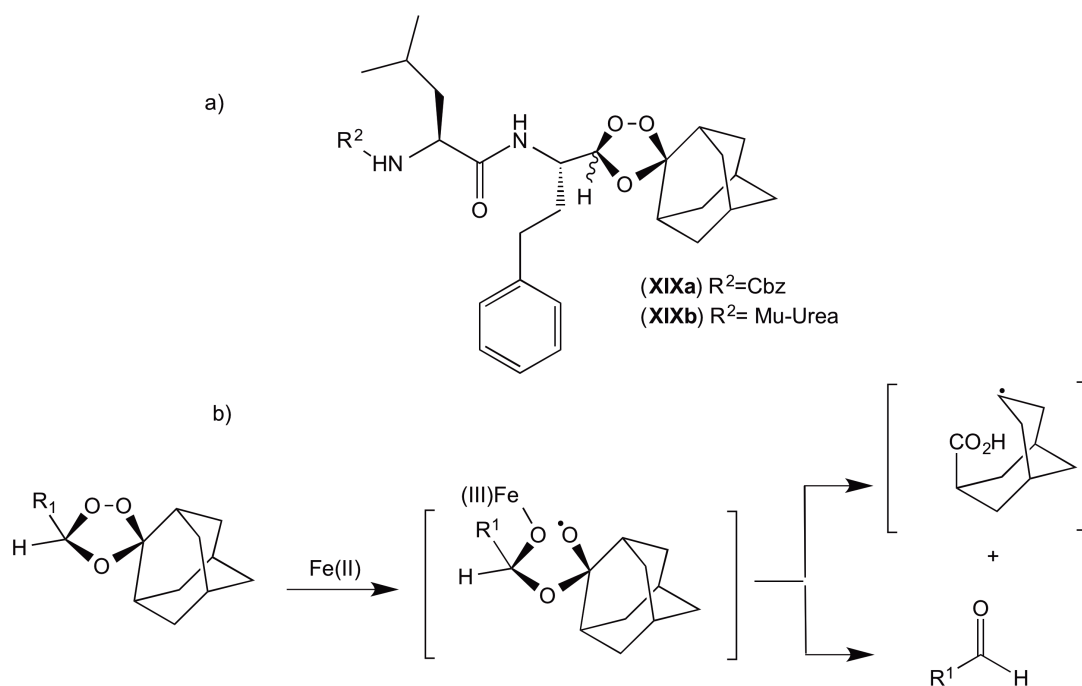
Scheme 4. a) Most active endoperoxide hybrids ((**XIXa**) and (**XIXb**)) reported by O'Neill and co-workers, and b) expected mechanism of hybrid degradation by Fe(II).[28]

Compounds targeting inhibition of both falcipains and hemozoin formation have also been reported. For instance, Chibale and co-workers found 4-amino-7-chloroquinoline derivatives (**XX**) containing the isatin scaffold to present activity against three *Pf* strains, CQ-sensitive D10 (IC_{50} = 0.079−1.33 μM), and CQ-resistant K1 (IC_{50} = 0.054−1.51 μM) and W2 (IC_{50} = 0.051−1.23 μM) (Fig. 9).[49] Also, the compounds displayed activity against falcipains in the micromolar range (IC_{50} > 6.07 μM) though there was no evidence of swollen FV in intraerythrocytic parasites, which is a morphological trait of FP inhibition. The isatin and the 4-amino-7-chloroquinoline cores were linked through a morpholine or alkyl chain, and the isatin core to a ketone or to a thiosemicarbazone warhead meant to alkylate the FP catalytic cysteine. Removal of the quinoline moiety resulted in significant loss of activity against all *Pf* strains tested. The most active compounds were those with an ethylene spacer between the quinoline and the isatin cores (**XX**) with a preference for a methyl group on the isatin ring's C-5 (R^1).
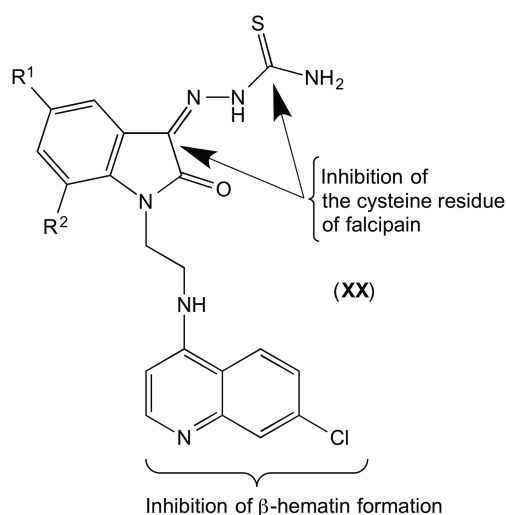
Figure 9. Most active 4-amino-7-chloroquine – isatin conjugates reported by Chibale and co-workers in 2005.[49]

Later on, Chibale's research team reported a series of inhibitors which also included the 4-amino-7-chloroquinoline core.[50] The derivatives were synthesized through multiple reaction steps starting from 4,7-dichloroquinoline (Scheme 5). The compounds were designed to inhibit FP2 while including the quinoline moiety to promote accumulation of the drug in the parasite's FV. Generally, derivatives lacking the 4-amino-7-chloroquinoline core showed lower antimalarial activity. In addition, the most active compound (**XXI**) displayed activity against FP2 (IC_{50} = 3.16 μM) that did not correlate with the corresponding activity against *Pf* CQ-resistant strain W2 (IC_{50} = 77 nM), suggesting that other mechanism(s) could be responsible for the antiplasmodial activity of this compound.
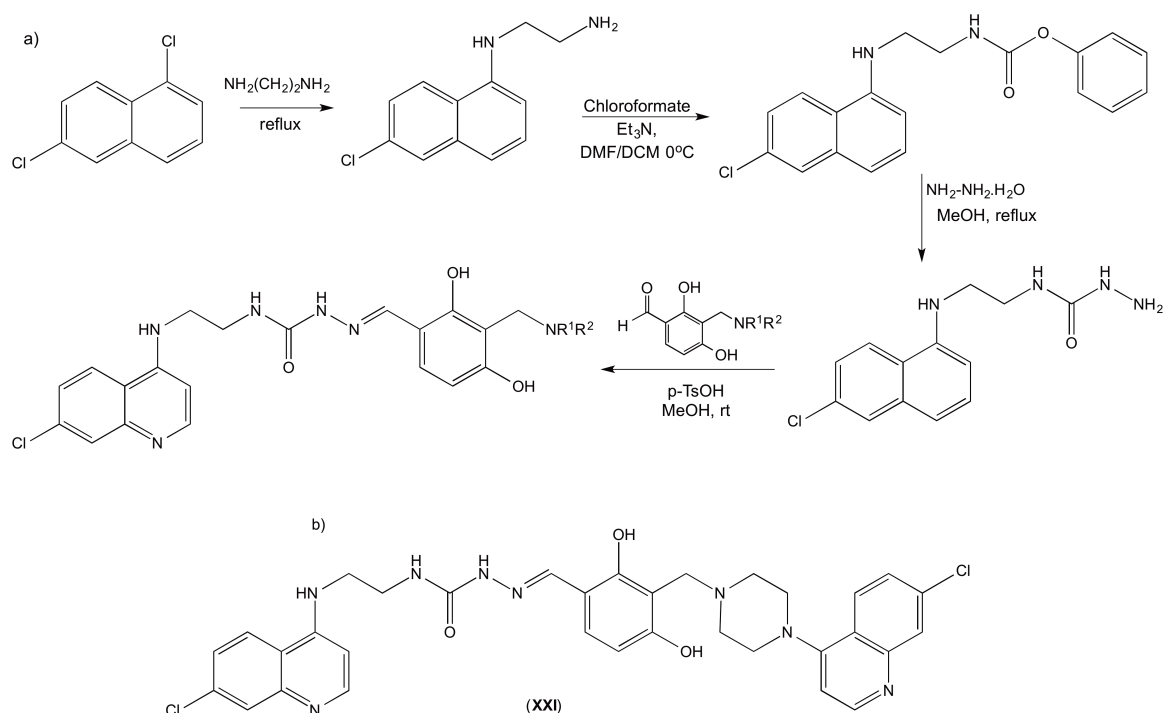
Scheme 5. a) Synthetic pathway developed by Chibale and co-workers in 2007.[50] b) Most active compound of the synthesized series.

Following, the same group reported a series of γ- and δ-lactams linked to 4-amino-7-chloroquinoline through an alkyl chain (**XXII**).[51] The synthetic pathway involved, first, the nucleophilic substitution on 4,7-dichloroquinoline with the relevant alkanediamine. Posteriorly, the resulted 4-(*N*-aminoalkyl)amino-7-chloroquinoline was reacted with levulinic acid or 4-acetylbutyric acid and the relevant isocyanide, through a one-pot Ugi reaction (Scheme 6). The most active compound (**XXIIa**) displayed activity in the nanomolar range against *Pf* CQ-resistant W2 strain (IC$_{50}$ = 96 nM) that did not correlate with its ability to inhibit FP2 action (IC$_{50}$ = 17.6 μM). The lack of correlation between antiplasmodial and FP-inhibitory activity and the fact that the compounds presented lower IC$_{50}$ compared to CQ (IC$_{50}$ = 240 nM) may suggest that these molecules might be eluding efflux from the FV.
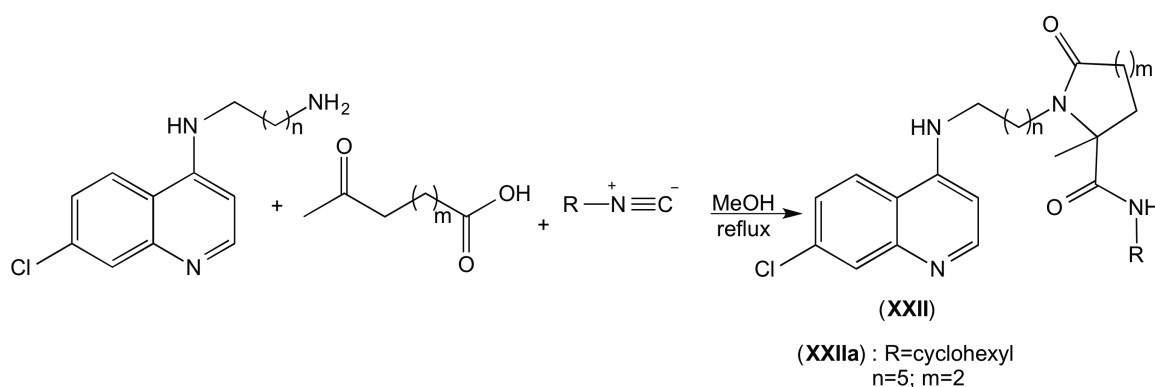
Scheme 6. One-pot Ugi reaction in methanol at room temperature (rt) carried out by Chibale and co-workers.[51]

Furthermore, Chibale's team synthesized a new series of compounds (**XXIII**) that joined chloroquinoline to chalcone through a triazole linker aiming at inhibition of both hemozoin formation and FP2 action.[52, 53] The synthesis pathway globally involved the previous obtainment of suitable precursors, namely, chalcones and 4-azido-7-chloroquinoline, followed by an azide-alkyne coupling (Huisgen's cycloaddition) to yield 1,2,3-triazoles (Scheme 7). The most active compound of series (**XXIIIa**) presented activity (IC$_{50}$ = 40 nM) comparable to CQ (IC$_{50}$ = 17 nM) against the *Pf* W2 strain. Although the compounds showed to inhibit hemozoin formation as CQ did, they only displayed activity in the micromolar range against FP2, suggesting that the main mechanism of these series was inhibition of hemozoin formation.
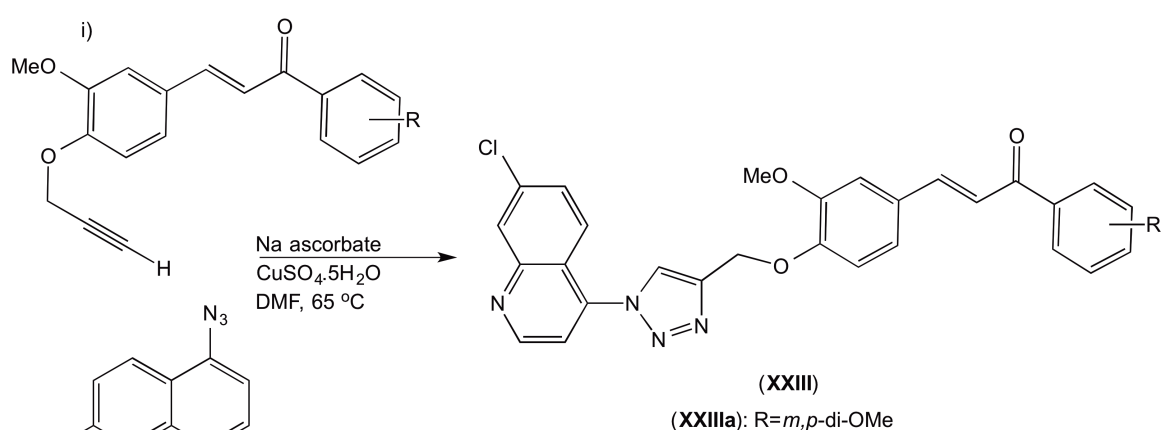
Scheme 7. Synthethic pathway developed by Chibale's team in 2010.[53]

More recently, Gomes and co-workers developed potential dual-action antimalarials (**XXIV**), expectedly able to also inhibit hemozoin formation and falcipain activity. These compounds included the 4-amino-7-chloroquinoline core, meant to impair hemozoin formation, linked to an α,β-unsaturated carbonyl moiety expected to act as a Michael

acceptor, and thus alkylate the catalytic Cys in falcipains.[54] The authors believed those two moieties should be linked through the Leu-*h*Phe dipeptide, previously described by Rosenthal to enhance inhibitor recognition by falcipains. However, in order to prevent premature proteolytic degradation of the dipeptide spacer, the authors used the corresponding retro-inverso dipeptide, using the respective D-amino acids (Fig. 10).[55, 56]
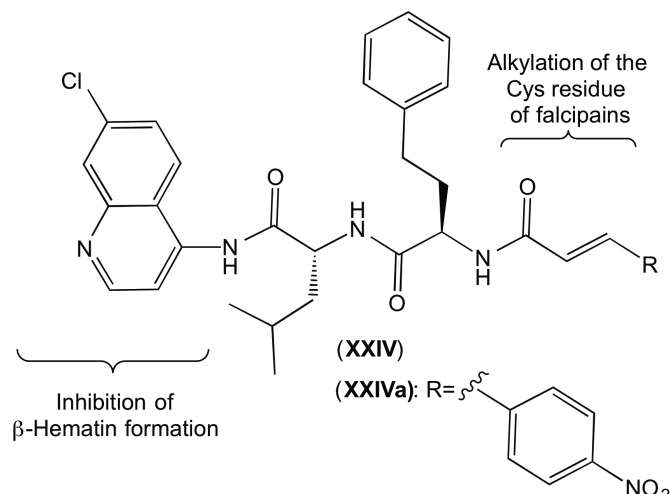
Figure 10. General structure of hybrid compounds (**XXIV**) designed by Gomes's team.[54] Most promising compound (**XXIVa**) synthesized.

Gomes's team chose cinnamic acid derivatives motivated by cinnamic acid potential ability to act as inhibitor of enzyme catalytic Cys residues,[57] due to the α,β-unsaturated carbonyl moiety, and by previous reports on the antimalarial properties of cinnamoyl derivatives.[58-60] One such report, by Schlitzer and co-workers, suggested that the use of 4-alkoxy-substituted cinnamic acids improved the antiplasmodial activity of identified antimalarial leads (Fig. 11).[58] Specifically, replacement of the 3-phenylpropionyl moiety of the lead structure (**XXV**) by a 4-propoxycinnamoyl functionality (**XXVI**) resulted in higher activity (IC$_{50}$ (**XXV**)= 2.7 μM *vs* IC$_{50}$ (**XXVI**) = 0.20 μM) against the CQ-resistance *Pf* strain Dd2. In addition, they also demonstrated that substitution of the 3-phenylpropionyl moiety by the 4-phenylcinnamoyl functionality (**XXVII**) led to significantly lower cytotoxicity (IC$_{50}$ (**XXV**) < 36.9 μM *vs* IC$_{50}$ (**XXVII**) >180 μM against HeLa) and 5-fold increase on activity (IC$_{50}$ (**XXV**) = 2.7 μM *vs* IC$_{50}$ (**XXVII**) = 0.65 μM) against *Pf* Dd2.[59]
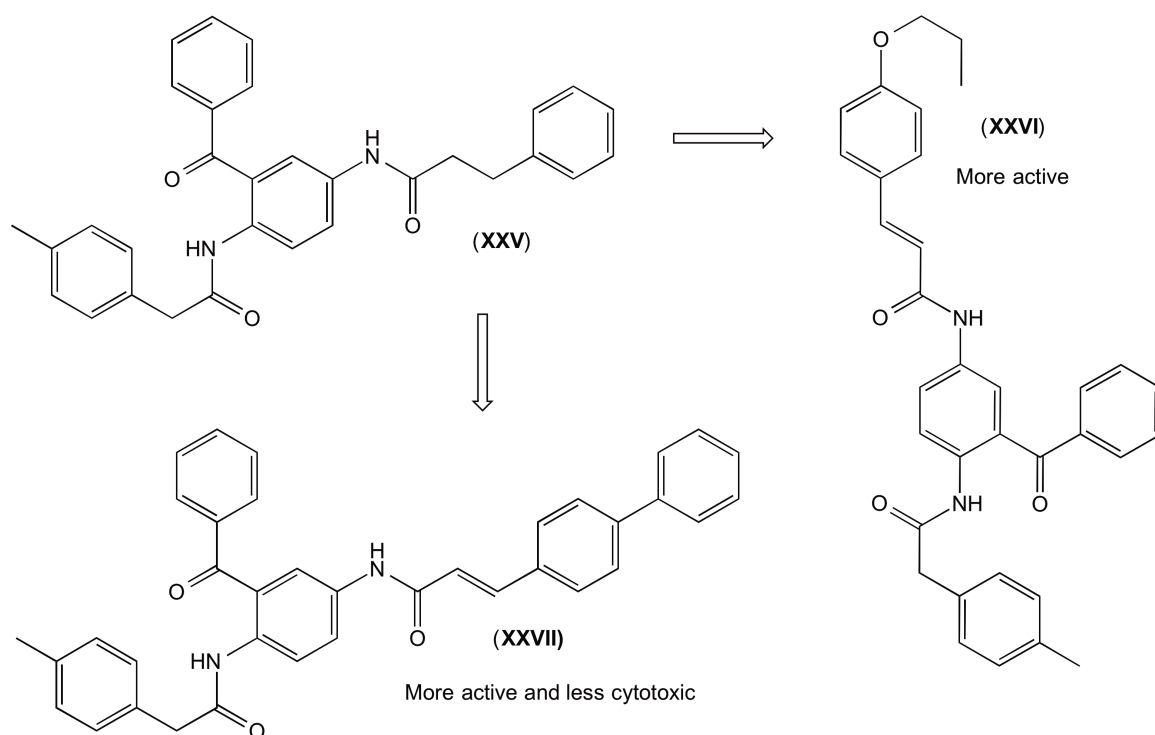
Figure 11. Cinnamic acid derivatives found by Schlitzer research team.[58, 59]

Gomes et al's *in vitro* results demonstrated two of the synthesized derivatives to be active in the micromolar range, with the best compound (**XXIVa**) displaying an IC_{50} of 1.4 μM against *Pf* strain W2. Although the approach showed promising results, further studies were required to improve the antimalarial activity of these cinnamic derivatives.

1.4. References

1.   Eckstein-Ludwig, U.; Webb, R. J.; Van Goethem, I. D.; East, J. M.; Lee, A. G.; Kimura, M.; O'Neill, P. M.; Bray, P. G.; Ward, S. A.; Krishna, S. Artemisinins target the SERCA of Plasmodium falciparum. *Nature* **2003,** 424, 957-61.

2.   Price, R. N.; Nosten, F.; Luxemburger, C.; ter Kuile, F. O.; Paiphun, L.; Chongsuphajaisiddhi, T.; White, N. J. Effects of artemisinin derivatives on malaria transmissibility. *Lancet* **1996,** 347, 1654-8.

3.   Slater, A. F. Chloroquine: mechanism of drug action and resistance in Plasmodium falciparum. *Pharmacol Ther* **1993,** 57, 203-35.

4.   Rodrigues, T.; Prudêncio, M.; Moreira, R.; Mota, M. M.; Lopes, F. Targeting the Liver Stage of Malaria Parasites: A Yet Unmet Goal. *J Med Chem* **2011,** 55, 995-1012.

5.   White, N. J. Primaquine to prevent transmission of falciparum malaria. *Lancet Infect Dis* **2013,** 13, 175-81.

6.   Vathsala, P. G.; Pramanik, A.; Dhanasekaran, S.; Devi, C. U.; Pillai, C. R.; Subbarao, S. K.; Ghosh, S. K.; Tiwari, S. N.; Sathyanarayan, T. S.; Deshpande, P. R.; Mishra, G. C.; Ranjit, M. R.; Dash, A. P.; Rangarajan, P. N.; Padmanaban, G. Widespread occurrence of the Plasmodium falciparum chloroquine resistance transporter (Pfcrt) gene haplotype SVMNT in P. falciparum malaria in India. *Am J Trop Med Hyg* **2004,** 70, 256-9.

7.   Rab, M. A.; Freeman, T. W.; Durrani, N.; de Poerck, D.; Rowland, M. W. Resistance of Plasmodium falciparum malaria to chloroquine is widespread in eastern Afghanistan. *Ann Trop Med Parasitol* **2001,** 95, 41-6.

8.   WHO. Global plan for artemisinin resistance containment (GPARC). **2011**.

9.   Goldberg, D. E.; Slater, A. F.; Cerami, A.; Henderson, G. B. Hemoglobin degradation in the malaria parasite Plasmodium falciparum: an ordered process in a unique organelle. *P Natl Acad Sci USA* **1990,** 87, 2931-5.

10.   Lew, V. L.; Tiffert, T.; Ginsburg, H. Excess hemoglobin digestion and the osmotic stability of Plasmodium falciparum-infected red blood cells. *Blood* **2003,** 101, 4189-94.

11.   Liu, J.; Istvan, E. S.; Goldberg, D. E. Hemoglobin-degrading plasmepsin II is active as a monomer. *J Biol Chem* **2006,** 281, 38682-8.

12.   Kerr, I. D.; Lee, J. H.; Pandey, K. C.; Harrison, A.; Sajid, M.; Rosenthal, P. J.; Brinen, L. S. Structures of falcipain-2 and falcipain-3 bound to small molecule inhibitors: implications for substrate specificity. *J Med Chem* **2009,** 52, 852-7.

13. Ponpuak, M.; Klemba, M.; Park, M.; Gluzman, I. Y.; Lamppa, G. K.; Goldberg, D. E. A role for falcilysin in transit peptide degradation in the Plasmodium falciparum apicoplast. *Mol Microbiol* **2007,** 63, 314-34.

14. Wang, F.; Krai, P.; Deu, E.; Bibb, B.; Lauritzen, C.; Pedersen, J.; Bogyo, M.; Klemba, M. Biochemical characterization of Plasmodium falciparum dipeptidyl aminopeptidase 1. *Mol Biochem Parasitol* **2011,** 175, 10-20.

15. Gavigan, C. S.; Dalton, J. P.; Bell, A. The role of aminopeptidases in haemoglobin degradation in Plasmodium falciparum-infected erythrocytes. *Mol Biochem Parasitol* **2001,** 117, 37-48.

16. Monti, D.; Vodopivec, B.; Basilico, N.; Olliaro, P.; Taramelli, D. A Novel Endogenous Antimalarial: Fe(II)-Protoporphyrin IXα (Heme) Inhibits Hematin Polymerization to β-Hematin (Malaria Pigment) and Kills Malaria Parasites†. *Biochemistry* **1999,** 38, 8858-8863.

17. Egan, T. J. Recent advances in understanding the mechanism of hemozoin (malaria pigment) formation. *J Inorg Biochem* **2008,** 102, 1288-99.

18. Kumar, S.; Guha, M.; Choubey, V.; Maity, P.; Bandyopadhyay, U. Antimalarial drugs inhibiting hemozoin (beta-hematin) formation: a mechanistic update. *Life Sci* **2007,** 80, 813-28.

19. Rosenthal, P. J.; Olson, J. E.; Lee, G. K.; Palmer, J. T.; Klaus, J. L.; Rasnick, D. Antimalarial effects of vinyl sulfone cysteine proteinase inhibitors. *Antimicrob Agents Ch* **1996,** 40, 1600-3.

20. Teixeira, C.; Gomes, J. R.; Gomes, P. Falcipains, Plasmodium falciparum cysteine proteases as key drug targets against malaria. *Curr Med Chem* **2011,** 18, 1555-72.

21. Eksi, S.; Czesny, B.; Greenbaum, D. C.; Bogyo, M.; Williamson, K. C. Targeted disruption of Plasmodium falciparum cysteine protease, falcipain 1, reduces oocyst production, not erythrocytic stage growth. *Mol Microbiol* **2004,** 53, 243-50.

22. Nielsen, K. M.; Kasper, J.; Choi, M.; Bedford, T.; Kristiansen, K.; Wirth, D. F.; Volkman, S. K.; Lozovsky, E. R.; Hartl, D. L. Gene conversion as a source of nucleotide diversity in Plasmodium falciparum. *Mol Biol Evol* **2003,** 20, 726-34.

23. Lee, B. J.; Singh, A.; Chiang, P.; Kemp, S. J.; Goldman, E. A.; Weinhouse, M. I.; Vlasuk, G. P.; Rosenthal, P. J. Antimalarial activities of novel synthetic cysteine protease inhibitors. *Antimicrob Agents Ch* **2003,** 47, 3810-4.

24. Powers, J. C.; Asgian, J. L.; Ekici, O. D.; James, K. E. Irreversible inhibitors of serine, cysteine, and threonine proteases. *Chem Rev* **2002,** 102, 4639-750.

25. Schulz, F.; Gelhaus, C.; Degel, B.; Vicik, R.; Heppner, S.; Breuning, A.; Leippe, M.; Gut, J.; Rosenthal, P. J.; Schirmeister, T. Screening of protease inhibitors as

antiplasmodial agents. Part I: Aziridines and epoxides. *ChemMedChem* **2007,** 2, 1214-24.

26. Shenai, B. R.; Lee, B. J.; Alvarez-Hernandez, A.; Chong, P. Y.; Emal, C. D.; Neitz, R. J.; Roush, W. R.; Rosenthal, P. J. Structure-Activity Relationships for Inhibition of Cysteine Protease Activity and Development of Plasmodium falciparum by Peptidyl Vinyl Sulfones. *Antimicrob Agents Ch* **2003,** 47, 154-160.

27. Santos, M. M.; Moreira, R. Michael acceptors as cysteine protease inhibitors. *Mini Rev Med Chem* **2007,** 7, 1040-50.

28. Gibbons, P.; Verissimo, E.; Araujo, N. C.; Barton, V.; Nixon, G. L.; Amewu, R. K.; Chadwick, J.; Stocks, P. A.; Biagini, G. A.; Srivastava, A.; Rosenthal, P. J.; Gut, J.; Guedes, R. C.; Moreira, R.; Sharma, R.; Berry, N.; Cristiano, M. L.; Shone, A. E.; Ward, S. A.; O'Neill, P. M. Endoperoxide carbonyl falcipain 2/3 inhibitor hybrids: toward combination chemotherapy of malaria through a single chemical entity. *J Med Chem* **2010,** 53, 8202-6.

29. Coteron, J. M.; Catterick, D.; Castro, J.; Chaparro, M. J.; Diaz, B.; Fernandez, E.; Ferrer, S.; Gamo, F. J.; Gordo, M.; Gut, J.; de las Heras, L.; Legac, J.; Marco, M.; Miguel, J.; Munoz, V.; Porras, E.; de la Rosa, J. C.; Ruiz, J. R.; Sandoval, E.; Ventosa, P.; Rosenthal, P. J.; Fiandor, J. M. Falcipain inhibitors: optimization studies of the 2-pyrimidinecarbonitrile lead series. *J Med Chem* **2010,** 53, 6129-52.

30. Weissbuch, I.; Leiserowitz, L. Interplay between malaria, crystalline hemozoin formation, and antimalarial drug action and design. *Chem Rev* **2008,** 108, 4899-914.

31. Ignatushchenko, M. V.; Winter, R. W.; Bachinger, H. P.; Hinrichs, D. J.; Riscoe, M. K. Xanthones as antimalarial agents; studies of a possible mode of action. *FEBS Lett* **1997,** 409, 67-73.

32. Sullivan, D. J.; Gluzman, I. Y.; Russell, D. G.; Goldberg, D. E. On the molecular mechanism of chloroquine's antimalarial action. *P Natl Acad Sci USA* **1996,** 93, 11865-11870.

33. Sullivan, D. J., Jr.; Matile, H.; Ridley, R. G.; Goldberg, D. E. A common mechanism for blockade of heme polymerization by antimalarial quinolines. *J Biol Chem* **1998,** 273, 31103-7.

34. Vippagunta, S. R.; Dorn, A.; Matile, H.; Bhattacharjee, A. K.; Karle, J. M.; Ellis, W. Y.; Ridley, R. G.; Vennerstrom, J. L. Structural specificity of chloroquine-hematin binding related to inhibition of hematin polymerization and parasite growth. *J Med Chem* **1999,** 42, 4630-9.

35. Portela, C.; Afonso, C. M.; Pinto, M. M.; Ramos, M. J. Definition of an electronic profile of compounds with inhibitory activity against hematin aggregation in malaria parasite. *Bioorg Med Chem* **2004,** 12, 3313-21.

36. Hocart, S. J.; Liu, H.; Deng, H.; De, D.; Krogstad, F. M.; Krogstad, D. J. 4-aminoquinolines active against chloroquine-resistant Plasmodium falciparum: basis of antiparasite activity and quantitative structure-activity relationship analyses. *Antimicrob Agents Ch* **2011,** 55, 2233-44.

37. O'Neill, P.; Barton, V.; Ward, S.; Chadwick, J. 4-Aminoquinolines: Chloroquine, Amodiaquine and Next-Generation Analogues. In *Treatment and Prevention of Malaria*, Staines, H. M.; Krishna, S., Eds. Springer Basel: 2012; pp 19-44.

38. Egan, T. J.; Kuter, D. Dual-functioning antimalarials that inhibit the chloroquine-resistance transporter. *Future Microbiol* **2013,** 8, 475-89.

39. Foley, M.; Tilley, L. Quinoline Antimalarials: Mechanisms of Action and Resistance and Prospects for New Agents. *Pharmacol Therapeut* **1998,** 79, 55-87.

40. Ecker, A.; Lehane, A. M.; Clain, J.; Fidock, D. A. PfCRT and its role in antimalarial drug resistance. *Trends Parasitol* **2012,** 28, 504-514.

41. WHO. World Malaria Report. **2012**.

42. Muregi, F. W.; Ishih, A. Next-Generation Antimalarial Drugs: Hybrid Molecules as a New Strategy in Drug Design. *Drug Dev Res* **2010,** 71, 20-32.

43. Meunier, B. Hybrid Molecules with a Dual Mode of Action: Dream or Reality?†. *Accounts Chem Res* **2007,** 41, 69-77.

44. Benoit-Vical, F.; Lelièvre, J.; Berry, A.; Deymier, C.; Dechy-Cabaret, O.; Cazelles, J.; Loup, C.; Robert, A.; Magnaval, J.-F.; Meunier, B. Trioxaquines Are New Antimalarial Agents Active on All Erythrocytic Forms, Including Gametocytes. *Antimicrob Agents Ch* **2007,** 51, 1463-1472.

45. Dechy-Cabaret, O.; Benoit-Vical, F.; Loup, C.; Robert, A.; Gornitzka, H.; Bonhoure, A.; Vial, H.; Magnaval, J. F.; Seguela, J. P.; Meunier, B. Synthesis and antimalarial activity of trioxaquine derivatives. *Chemistry* **2004,** 10, 1625-36.

46. Walsh, J. J.; Coughlan, D.; Heneghan, N.; Gaynor, C.; Bell, A. A novel artemisinin-quinine hybrid with potent antimalarial activity. *Bioorg Med Chem Lett* **2007,** 17, 3599-602.

47. Capela, R.; Oliveira, R.; Goncalves, L. M.; Domingos, A.; Gut, J.; Rosenthal, P. J.; Lopes, F.; Moreira, R. Artemisinin-dipeptidyl vinyl sulfone hybrid molecules: design, synthesis and preliminary SAR for antiplasmodial activity and falcipain-2 inhibition. *Bioorg Med Chem Lett* **2009,** 19, 3229-32.

48. Capela, R.; Cabal, G. G.; Rosenthal, P. J.; Gut, J.; Mota, M. M.; Moreira, R.; Lopes, F.; Prudêncio, M. Design and evaluation of primaquine-artemisinin hybrids as a multistage antimalarial strategy. *Antimicrob Agents Ch* **2011,** 55, 4698-706.

49. Chiyanzu, I.; Clarkson, C.; Smith, P. J.; Lehman, J.; Gut, J.; Rosenthal, P. J.; Chibale, K. Design, synthesis and anti-plasmodial evaluation in vitro of new 4-aminoquinoline isatin derivatives. *Bioorg Med Chem* **2005,** 13, 3249-61.

50. Chipeleme, A.; Gut, J.; Rosenthal, P. J.; Chibale, K. Synthesis and biological evaluation of phenolic Mannich bases of benzaldehyde and (thio)semicarbazone derivatives against the cysteine protease falcipain-2 and a chloroquine resistant strain of Plasmodium falciparum. *Bioorg Med Chem* **2007,** 15, 273-82.

51. Musonda, C. C.; Gut, J.; Rosenthal, P. J.; Yardley, V.; Carvalho de Souza, R. C.; Chibale, K. Application of multicomponent reactions to antimalarial drug discovery. Part 2: New antiplasmodial and antitrypanosomal 4-aminoquinoline gamma- and delta-lactams via a 'catch and release' protocol. *Bioorg Med Chem* **2006,** 14, 5605-15.

52. Guantai, E. M.; Ncokazi, K.; Egan, T. J.; Gut, J.; Rosenthal, P. J.; Smith, P. J.; Chibale, K. Design, synthesis and in vitro antimalarial evaluation of triazole-linked chalcone and dienone hybrid compounds. *Bioorg Med Chem* **2010,** 18, 8243-56.

53. Guantai, E. M.; Ncokazi, K.; Egan, T. J.; Gut, J.; Rosenthal, P. J.; Bhampidipati, R.; Kopinathan, A.; Smith, P. J.; Chibale, K. Enone– and Chalcone–Chloroquinoline Hybrid Analogues: In Silico Guided Design, Synthesis, Antiplasmodial Activity, in Vitro Metabolism, and Mechanistic Studies. *J Med Chem* **2011,** 54, 3637-3649.

54. Figueiras, M. Potenciais Fármacos de Acção Dual Contra Fase Sanguínea da Malária. *Master Thesis, Faculdade de Ciências da Universidade do Porto* **2010**.

55. Hong, S. Y.; Oh, J. E.; Lee, K.-H. Effect of d-amino acid substitution on the stability, the secondary structure, and the activity of membrane-active peptide. *Biochem Pharmacol* **1999,** 58, 1775-1780.

56. Müller-Schiffmann, A.; Petsch, B.; Leliveld, S. R.; Muyrers, J.; Salwierz, A.; Mangels, C.; Schwarzinger, S.; Riesner, D.; Stitz, L.; Korth, C. Complementarity determining regions of an anti-prion protein scFv fragment orchestrate conformation specificity and antiprion activity. *Mol Immunol* **2009,** 46, 532-540.

57. Kouassi, Y. A. O.; Shelef, L. A. INHIBITION OF LISTERIA MONOCYTOGENES BY CINNAMIC ACID: POSSIBLE INTERACTION OF THE ACID WITH CYSTEINYL RESIDUES. *J Food Safety* **1998,** 18, 231-242.

58. Wiesner, J.; Mitsch, A.; Wissner, P.; Jomaa, H.; Schlitzer, M. Structure-activity relationships of novel anti-malarial agents. Part 2: cinnamic acid derivatives. *Bioorg Med Chem Lett* **2001,** 11, 423-4.

59. Wiesner, J.; Wissner, P.; Dahse, H. M.; Jomaa, H.; Schlitzer, M. Discovery of a novel lead structure for anti-malarials. *Bioorg Med Chem* **2001,** 9, 785-92.

60. Herrin, T. R.; Pauvlik, J. M.; Schuber, E. V.; Geiszler, A. O. Antimalarials. Synthesis and antimalarial activity of 1-(4-methoxycinnamoyl)-4-(5-phenyl-4-oxo-2-oxazolin-2-yl)piperazine and derivatives. *J Med Chem* **1975,** 18, 1216-23.

Chapter 2

_HEDICIN_s as dual-action antimalarials

2.0. Preamble

Research work within the area of malaria chemotherapy of the present dissertation followed preliminary efforts in the research group towards development of dual-action antimalarials (c.f. Fig. 10 in chapter 1) and was supervised by Prof. Paula A. C. Gomes, from CIQUP - *Departamento de Química e Bioquímica da Faculdade de Ciências da Universidade do Porto*, in Portugal (DQB-FCUP), and co-supervised by Dr. Cátia A. S. Teixeira, from *CICECO - Departamento de Química da Universidade de Aveiro*, also in Portugal.

The doctoral research work started by the synthesis and evaluation of compounds expectedly capable of targeting two essential processes for the malaria parasite survival, namely, heme detoxification and globin digestion. Such compounds, called *HEDICIN*s (Fig. 12), contained a *HE*teroaromatic core from a well-known antimalarial (known to inhibit hemozoin formation), a *DI*peptide spacer (known to promote binding to falcipains), and a *CIN*namoyl group (meant to act as a Michael acceptor by alkylating the catalytic cysteine residue of falcipains). D-amino acids instead of L-amino acids were used in the dipeptide spacer, in order to prevent premature proteolytic degradation.[1, 2] A second family lacking the dipeptide spacer, called *HECIN*s (*HE*teroaromatic-*CIN*namoyl conjugates), was also synthesized and included in the study, to assess the effect of such spacer in the compounds' bioactivity.
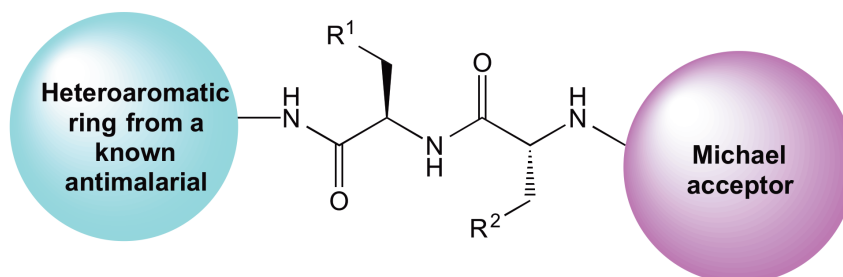
Figure 12. General structure of *HEDICIN*s, the first generation of compounds studied in this dissertation.

The doctoral candidate was in charge of the chemical synthesis of the compounds and their evaluation as inhibitors of hemozoin or β-hematin (β-H) formation, whereas *in vitro* assessment of their inhibitory activity against both falcipains and development of blood-stage *Pf* parasites was carried out by Prof Philip J. Rosenthal's team at the School of Medicine of the University of California – San Francisco, in the United States of America. The experimental research work was developed alongside an *in silico* study against falcipains carried out by the thesis co-supervisor, Dr. Cátia Teixeira.

2.1. *HE[DI]CIN*s

HEDICINs were designed according to general structure **1** using 4-amino-7-quinoline as the core responsible for inhibition of hemozoin formation, linked to a cinnamoyl moiety as the electrophilic warhead eventually able to irreversibly inhibit falcipains, through the dipeptide chain. As compared to cinnamoylated derivatives previously synthesized in the research group which used D-Leu-D-*h*Phe as a spacer, *HEDICIN*s included the D-*h*Phe–D-Leu as the dipeptide chain instead, since i*n silico* studies in the group have suggested that the latter dipeptide chain would allow a better fit into falcipains active site and place the α,β-unsaturated system closer to the enzyme's catalytic cysteine (Fig. 13). Moreover, *HECIN*s **2**, analogs lacking the dipeptide spacer, were also synthesized to assess the relevance of this spacer on compounds' ability to inhibit both falcipains and development of intraerythrocytic *Plasmodia in vitro*.
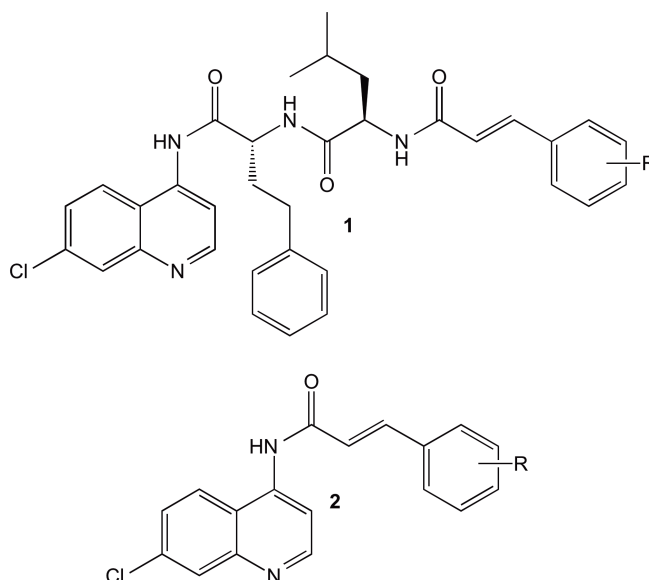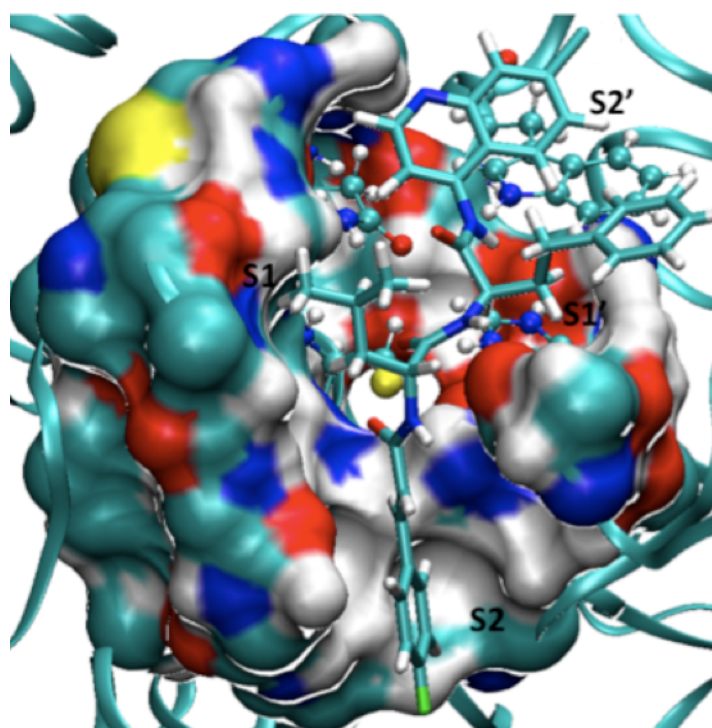
Figure 13. Structure of *HEDICIN* in complex with FP2 .

2.1.1. Synthesis of *HEDICIN*s and *HECIN*s

a) *HEDICIN*s

The synthetic procedure followed to obtain *HEDICIN*s **1** comprised a nucleophilic aromatic substitution (S$_N$*Ar*) on 4,7-dichloroquinoline using ammonia in the presence of phenol, and subsequent stepwise condensation of the *N*$^\alpha$-*tert*-butoxycarbonyl-protected amino acids (Boc-AA-OH) and removal of the *N*$^\alpha$-Boc protecting group and finally, condensation of the cinnamic acid (Scheme 8). The first S$_N$*Ar* reaction step was a straightforward procedure already reported in the literature,[3] thus 4-amino-7-chloroquinoline **2** was easily obtained in good yields (89%). The following coupling reactions involved a prior activation of the relevant carboxylic acid with *O*-(benzotriazol-1-yl)-*N,N,N',N'*-tetramethyluronium tetrafluoroborate (TBTU) or benzotriazolyloxy-tris[pyrrolidino]-phosphonium hexafluorophosphate (PyBOP) in either dichloromethane (DCM) or *N,N*-dimethylformamide (DMF), and in the presence of *N*-ethyl-*N,N*-diisopropylamine (DIEA). These steps resulted in moderate to good yields (40-78%), except for the coupling of i) **3** to Boc-D-*h*Phe-OH (% yield = 35 %), ii) **7** to *p*-nitrocinnamic acid (% yield = 17), and iii) **7** to *p*-(*N-tert*-butoxycarbonyl)aminocinnamic acid (% yield = 13). In regard to Boc removal steps, these were carried out by treatment of Boc-protected compounds (**4** and **6**) with neat trifluoroacetic acid (TFA) at room temperature (2 h), and the desired products were obtained in quantitative yield.
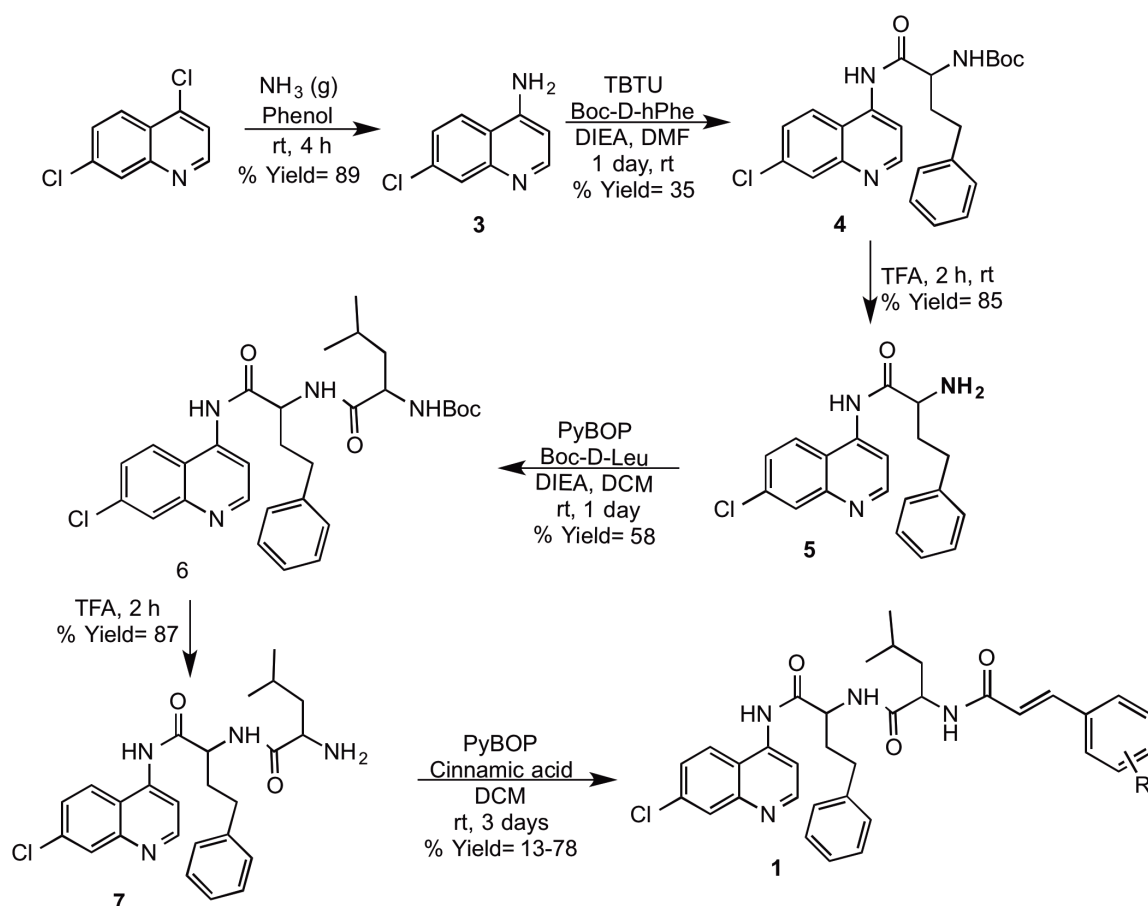
Scheme 8. Synthesis pathway to obtain *HEDICIN*s **1**.

The yield-limiting step in the synthesis pathway to *HEDICIN*s was the coupling of **3** to Boc-D-*h*Phe-OH, probably because of the low nucleophilicity of the amino group in **3**. In fact, the nitrogen atom at position 1 of 4-amino-7-chloroquinoline **3** withdraws electron density from the amino substituent at position 4, making the latter less prone to attack an electrophile. Hence, looking for the appropriate reaction conditions to improve yield, highly efficient *in situ* amide coupling reagent were used as: PyBOP, ethyl cyano(hydroxyimino)acetato-O^2]tri-1-pyrrolidinylphosphonium hexafluorophosphate (PyOXIM), (1-cyano-2-ethoxy-2-oxoethylidenaminooxy)dimethylamino-morpholino-carbenium hexafluorophosphate (COMU), 6-chloro-benzotriazole-1-yloxy-tris-pyrrolidinophosphonium hexafluorophosphate (PyClock), bromo-tris-pyrrolidino phosphonium hexafluorophosphate (PyBrop), and (7-azabenzotriazol-1-yloxy)tripyrrolidinophosphonium hexafluorophosphate (PyAOP) (Fig. 14), still the highest yield obtained was 35% (Table 1). The coupling reagent that resulted the best yield in this step was TBTU.[4] This was an unexpected observation, since PyAOP has been described to significantly improve coupling yields when using poor nucleophiles and hindered amino acids.[4, 5] In addition, increasing the temperature of the reaction up to 50

°C and the amount of DIEA base up to 3.3 molar equivalents (eq), even risking the possibility of racemization of the desired product,[6] did not increase the yield achieved in the reaction step.
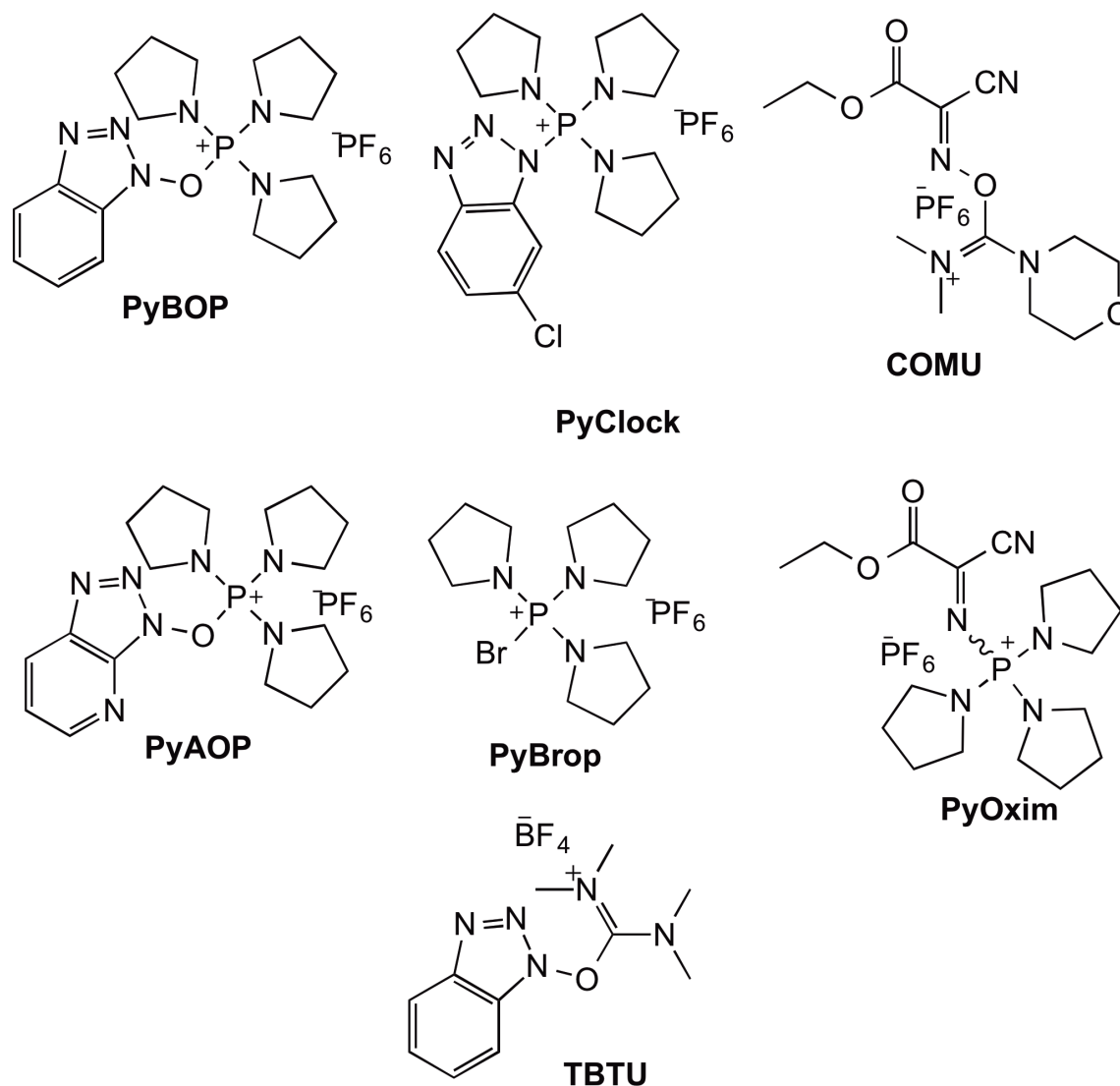
Figure 14. Coupling reagents used to promote *in situ* coupling of **3** with Boc-*h*Phe-OH.

Table 1. Reaction conditions for the coupling of Boc-D-*h*Phe-OH to obtain **4**.

Coupling Reagent	DIEA	Day(s)	Temperature (°C)	Solvent	% Yield
PyBOP	2.2	2	rt	DMF:DMSO (1:1)	8
	2.2	2	50		6
	3.3	2	50		9
	2.2	2	rt	DCM + Drops of DMF	21
	2.2	1	rt		22
	2.2	1	rt	DMF	7
COMU	2.2	2	rt	DMF	14
PyOXIM	2.2	2	rt	DMF	14
PyBrop	2.2	2	rt	DMF	29
		3	rt	DMF	31
PyClock	2.2	2	rt	DMF	8
PyAOP	2.2	2	rt	DMF	20
TBTU	2	1	rt	DMF	35

Table 1 also shows that when increasing temperature or reaction time, no significant difference was observed among the yields obtained. However, a decrease of the amount of DMF used as a solvent when using PyBOP as a coupling reagent led to approximately two-fold yield increment. This could suggest that the DMF used to synthesize the desired compounds possessed water, which could be solvating the nucleophile, and impeding its subsequent reaction with the corresponding activated cinnamic acid.

Moreover, in order to evaluate the influence of the configuration of the amino acid in the bioactivity of *HEDICIN*s, an additional *HEDICIN* (**1a'**) was synthesized using L-amino acids instead of D-amino acids following the synthetic procedure presented in scheme 8. Furthermore, to evaluate the effect of chloroquinoline ring on the antiplasmodial activity of the compounds, cinnamoylated derivative **8** was also synthesized. Compound **8** was obtained following similar procedure to that used for *HEDICIN*s but using as a starting material morpholine instead of 4-amino-7-chloroquinoline (Scheme 9). As expected the coupling of *h*-Phe was carried in good yields which confirmed that in the synthetic pathway of *HEDICIN*s **1**, the coupling of Boc-D-*h*Phe-OH to obtain compound **4** is limited by the poor nucleophilicity of 4-amino-7-choloroquinoline **3**. Morpholine was selected

based on the structure of the vinyl sulfone reported by Rosenthal's team and its flexibility. The latter could promote a better fit of the ligand into falcipain catalytic site although the inhibition of hemozoin formation would be disregarded.
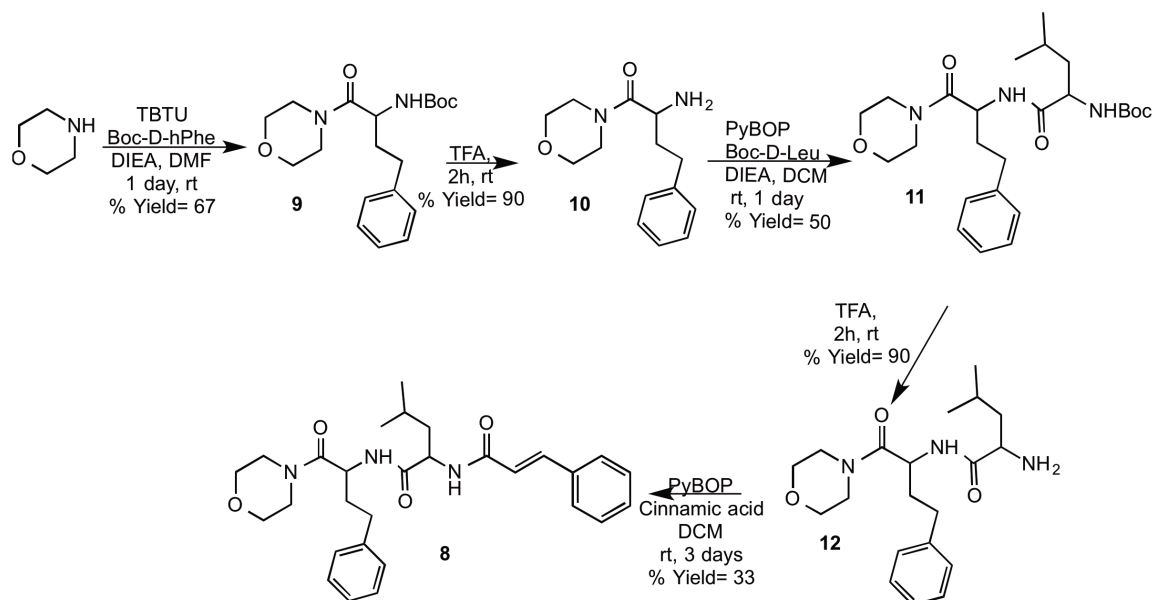
Scheme 9. Synthetic pathway to obtain morpholine derivative **8**.

b) *HECIN*s
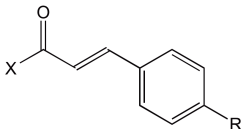
In parallel to the synthesis of *HEDICIN*s, *HECIN*s **2a-k** were obtained by coupling different cinnamic acids, or the respective acyl chlorides, to compound **3** (Scheme 10), previously obtained by ammonolysis of 4,7-dichloroquinoline. Initially, PyBOP was used as the coupling reagent to couple the respective cinnamic acids. However, the latter reaction conditions led to low yields, which encouraged us to try different reaction conditions to improve the yields obtained. In this context, the respective acyl chloride, when available, and K_2CO_3 and 18-crown-6 (catalytic amounts) were used to obtain the desired *HECIN*s. Accordingly, this reaction conditions provided better results. For instance, in the case of the *p*-metoxy cinnamoyl derivative **2d**, when using PyBOP as coupling reagents and DMF as solvent, the desired product **2d** was obtained with 1% yield. However, when using *trans*-4-methoxycinnamoyl chloride, the desired product was achieved with an 18% yield (Table 2); a significant increase that facilitates the characterization of the desired compound **2d**. Additional experimental procedures carried out to improve the yields obtained for *HECIN*s demonstrated that, when using PyBOP as a coupling reagent with DCM and some drops of DMF instead of exclusively DMF as a solvent, the yields increased but not higher than 20% which is in agreement

with results obtained for *HEDICIN*s when coupling compound **3** to Boc-D-*h*Phe-OH and using the same reaction conditions.
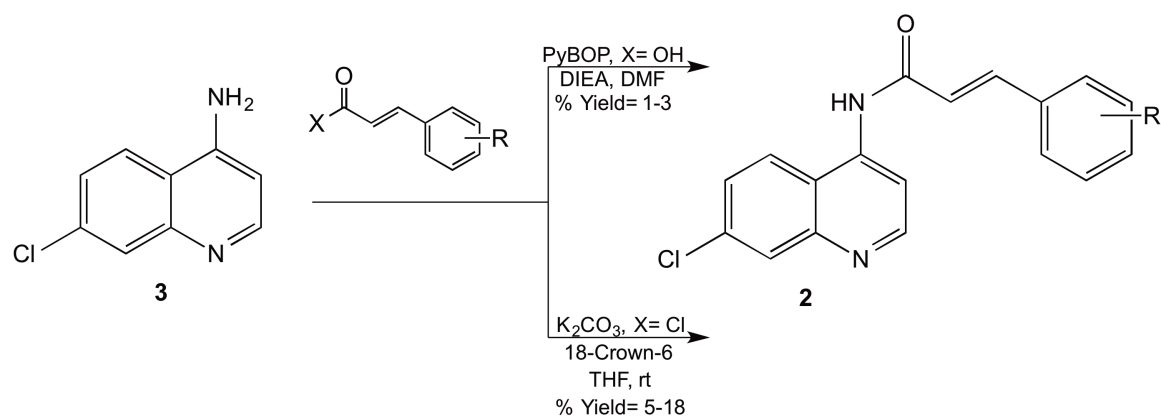
Scheme 10. Synthesis pathways to obtain *HECIN*s.

Table 2. Amide bond formation for *HECIN*s.

X= -Cl, -OH	Reaction conditions	
	PyBOP, DIEA, DMF, rt Respective cinnamic acid	**K₂CO₃, 18-Crown-6, THF, rt**
	% Yield	**% Yield**
R= H	3	18
R= -OMe	1	18
R= -NO₂	Not Obtained	5

2.1.2. Characterization of *HEDICIN*s and *HECIN*s

All *HEDICIN*s **1a'**, **1a-l**, and **8** and *HECIN*s **2a-k** were characterized by electrospray ionization-ion trap mass spectrometry (ESI-IT MS) as well as by proton (1H-) and carbon (13C-) nuclear magnetic resonance (NMR) and high-performance liquid chromatography (HPLC). Results were in agreement with the desired structures and are provided in the experimental section at the end of this chapter. The HPLC results displayed a peak for the relevant sample with a percent of purity that allow further *in vitro* evaluation. In addition, the characteristic signals of the corresponding samples in the ESI-IT MS and NMR were observed. As an example for *HEDICIN*s, the relevant NMR and MS spectra of the *p*-methoxycinnamic acid derivative **1d** is provided in figures 15−17.
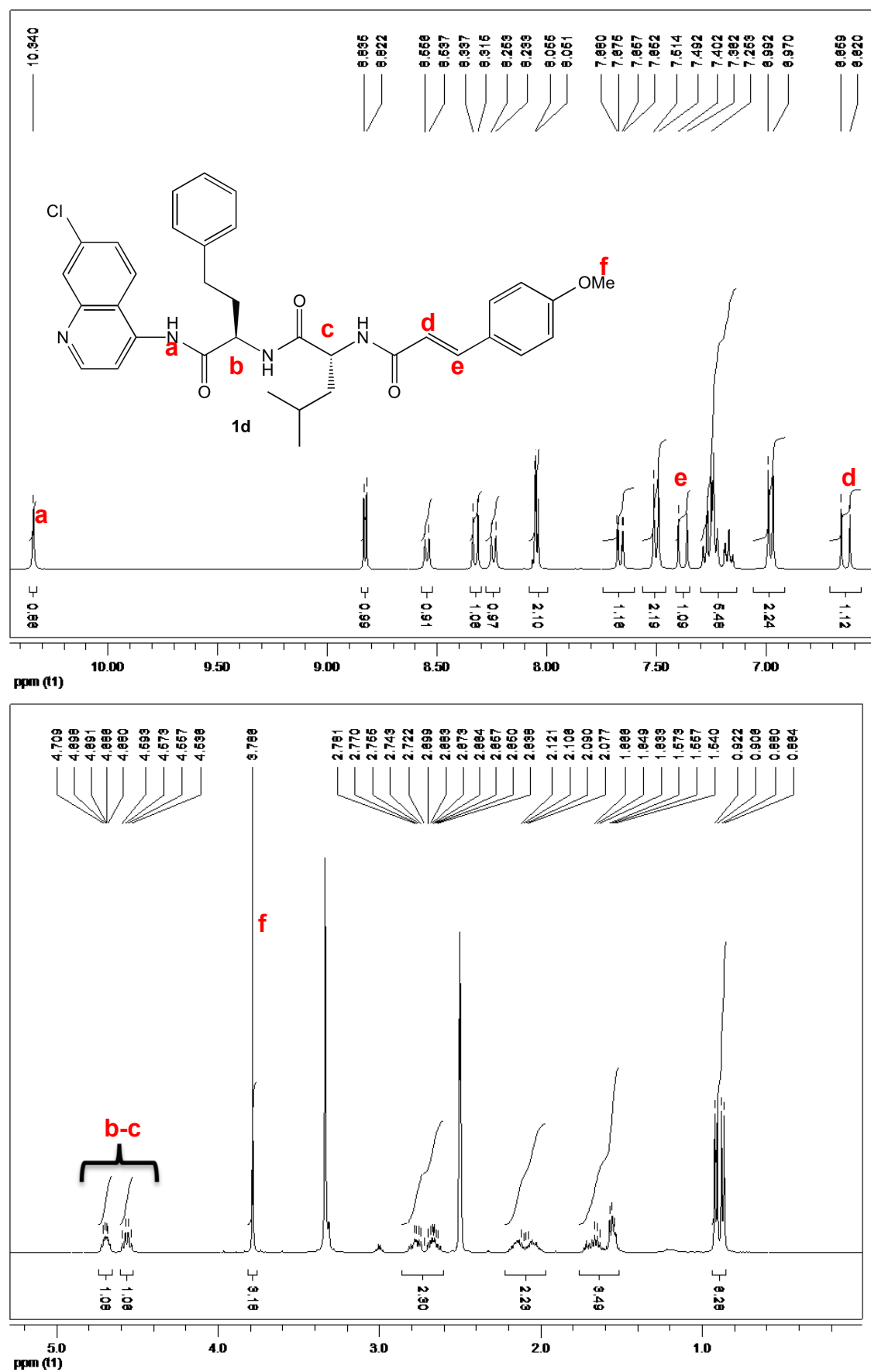
Figure 15. 1H-NMR (400 MHz, DMSO-d$_6$) of *HEDICIN* **1d** above 6 ppm (Upper corner) and below 5 ppm (bottom corner).
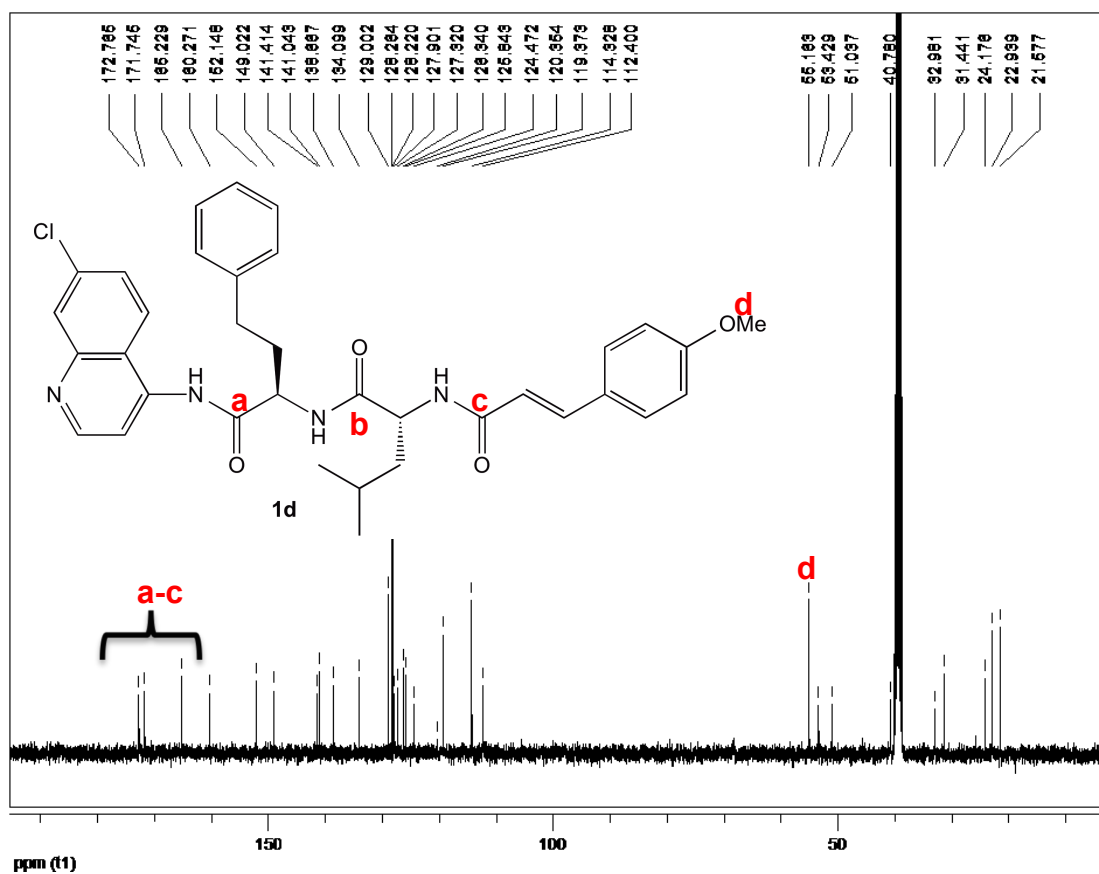
Figure 16. 13C-NMR (100 MHz, DMSO-d$_6$) spectrum of the *HEDICI*N **1d**.
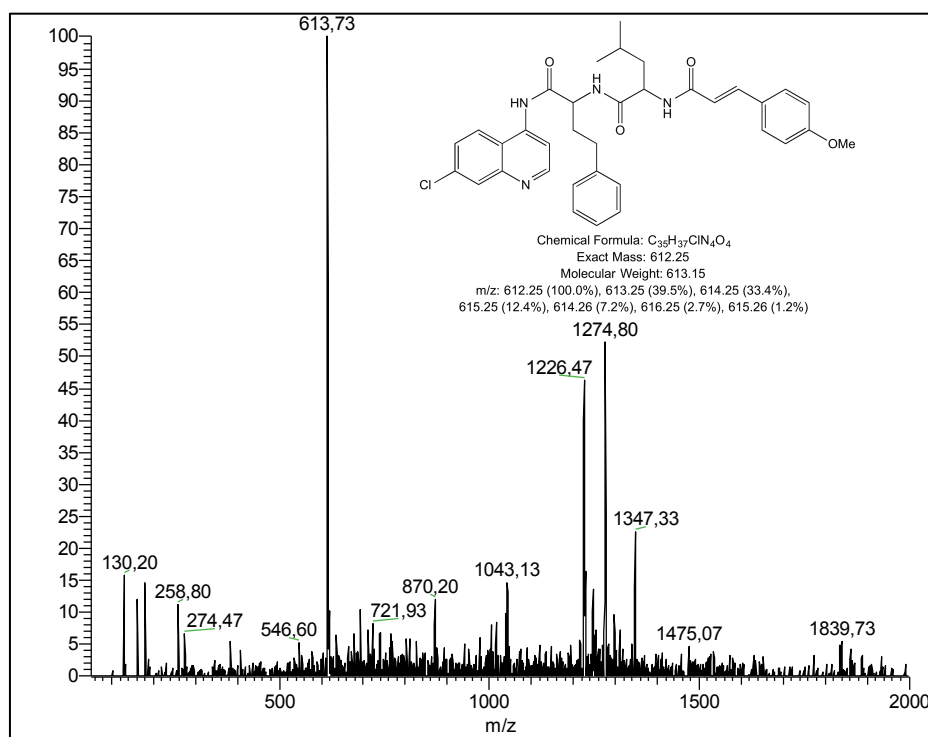
Figure 17. ES-IT MS of *HEDICIN***s 1d.**

Fig. 15 shows the protons downfield and upfield in the 1H-NMR spectrum of **1d**. The downfield region displays the vinyl protons of the α,β-unsaturated carbonyl moiety, the proton of the Cα at 6.63 ppm and the proton of the Cβ at 7.38 ppm with coupling constant J = 16 Hz which is characteristic of *trans*-vicinal vinyl protons. Also, the 1H-NMR spectrum displays the signal of the amide bond attached to the quinoline ring at 10.34 ppm. In the upfield region (Fig. 15), the 1H-NMR spectrum shows the multiplets of the protons of the Cα to the amide functionalities, respectively, at 4.70 ppm and 4.56 ppm. The singlet at 3.79 ppm represents the three deshielded protons of the methoxy substituent in the molecule. In addition, the six shielded protons of the methyl group of the leucine isobutyl side chain are also observed. In fig. 16, the 13C-NMR spectrum displayed the signals in agreement with the structure of compound **1d**, for instance, the deshielded signals of the carbonyl groups above 166 ppm and the signal of the methoxy group at 55.2 ppm. Please refer to the experimental section of this chapter for a more detailed analysis of the spectra of *HE[DI]CIN*s. Moreover, the mass spectrum (Fig. 17) shows an intense peak at 613.73 ppm which corresponds to the *quasi*-molecular ion of **1d**.

Spectroscopy data of *HECIN*s also correspond with the desired compounds. For example, for *HECIN* **2d**, in the upfield region, apart from the respective signal of DMSO and water, the signal of protons of the methoxy substituent in the cinnamoyl moiety at 3.82 ppm (Fig. 18) is displayed. The 1H-NMR spectrum also displays a singlet at 10.34 ppm that corresponds to the proton of the amide bond and a doublet with a small coupling constant of 2 Hz at 8.05 ppm that belongs to the proton of the carbon at position 8 of the quinoline ring. In addition, a doublet with a coupling constant of 15.6 Hz at 7.12 ppm was observed, which agrees with the proton of the Cα of α,β-unsaturated carbonyl. In fig. 18, the 13C-NMR spectrum displays the number of signal in agreement with the desired compounds **2d**, for instance, the upfield region shows one signal which represents the methoxy group at 55.3 ppm and 16 signals in the downfield region, from 111 ppm to 165.1 ppm. The most deshielded signal of the spectrum (δ_C = 165.1 ppm) belongs to the carbonyl. In addition, the mass spectrum (Fig. 19) displays the peak corresponding to the *quasi*-molecular ion of **2d** at 339.33 and also the corresponding dimer at 676.93.
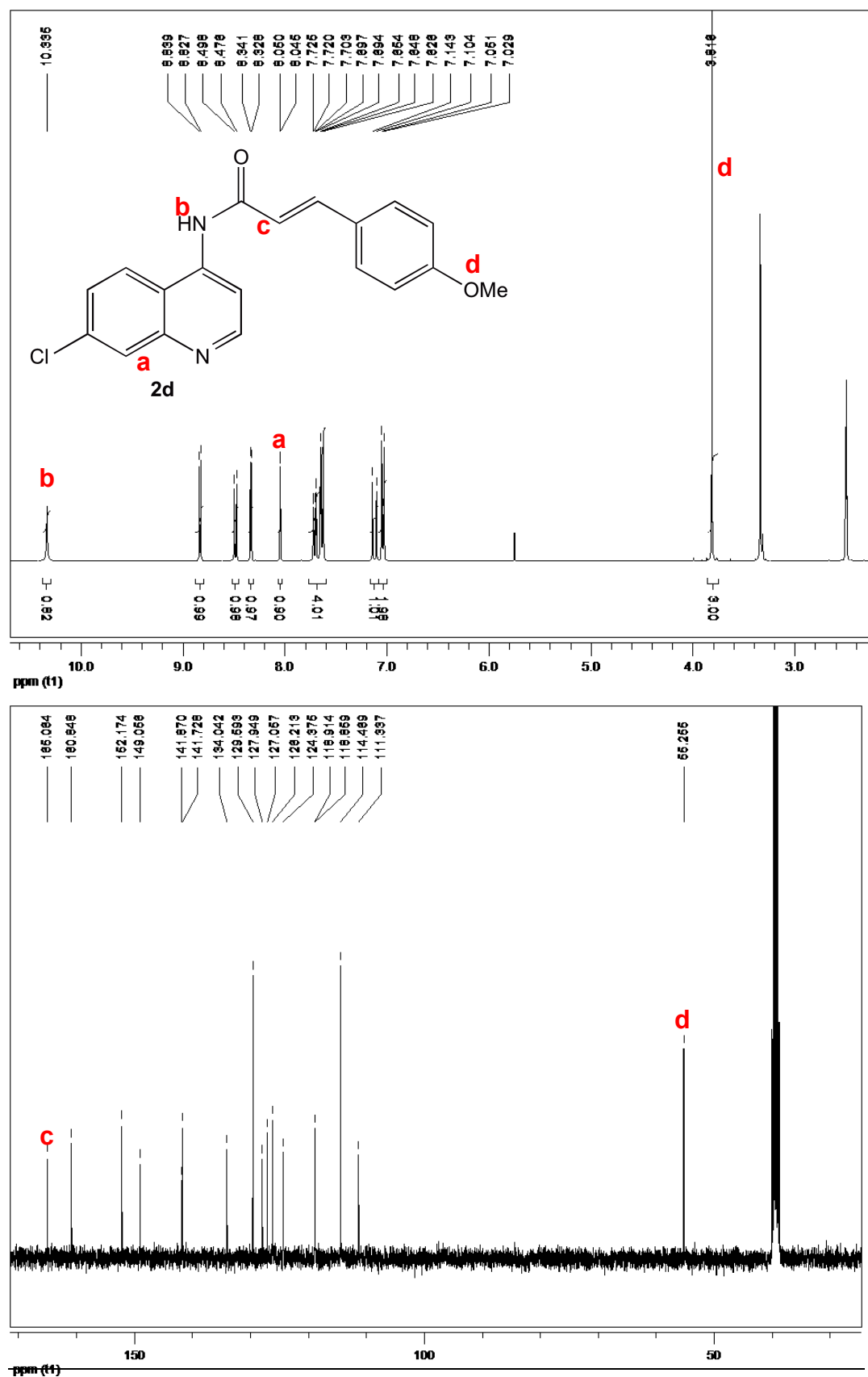
Figure 18. 1H-NMR (400 MHz, DMSO-d$_6$) spectrum of *HECIN* **2d** (Top corner) and 13C-NMR (100 MHz, DMSO-d$_6$) spectrum of *HECIN* **2d** (Bottom corner).
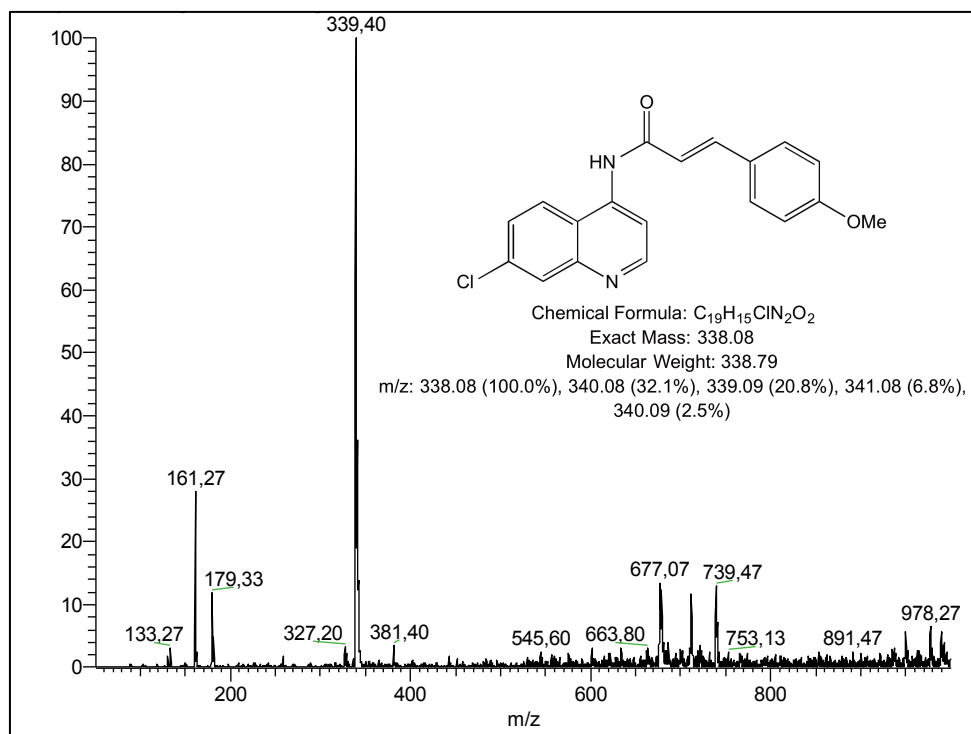
Figure 19. ES-IT MS of *HECIN* **2d**.

2.1.3. Assessment of cinnamoylated derivatives

Once all cinnamoylated derivatives were synthesized and characterized, they were tested *in vitro* against, β-H formation, falcipain action, and blood stage parasite. The ability of the cinnamoylated/quinoline derivatives to inhibit β-H formation was assessed following reported procedure.[7, 8] Assays to evaluate compounds' ability to inhibit falcipains action and antiplasmodial activity were carried by Rosenthal's team following methodology already described in the literature.[9-11] In addition, *in silico* studies were carried out by Dr. Cátia Teixeira. Results are presented in table 3.

Table 3. *In vitro* data of *HEDICIN*s (**1** and **8**) and *HECIN*s (**2**). included.
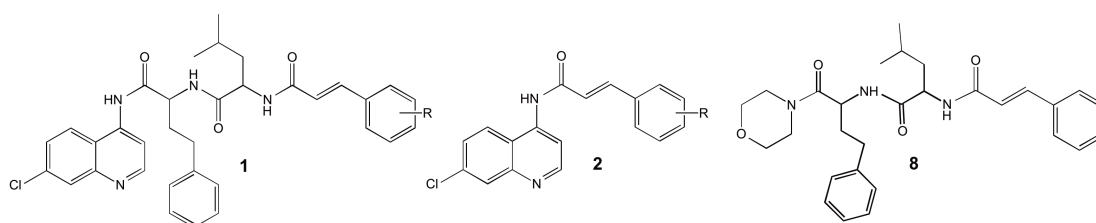
Compound	R	β-H Inhibition[a]	IC$_{50}$ *Pf* W2[b] (μM)	IC$_{50}$ FP2[c] (μM)	IC$_{50}$ FP3 (μM)	logP[d]
1a	H	-	4.89 ± 1.01	19.6 ± 0.4	>50	6.6
1a'[e]	H	ND[f]	~8.00	50.0	ND	6.6
1b	*p*-Me	++	1.96 ± 0.09	>50	ND	7.1
1c	*p*-*i*Pr	-	0.83 ± 0.08	>50	ND	7.9
1d	*p*-OMe	+	10.8 ± 3.77	>50	ND	6.5
1e	*p*-NH$_2$	++	3.28 ± 0.06	20.3 ± 2.4	>50	5.8
1f	*m*-F	-	5.43 ± 0.63	23.1 ± 1.6	>50	6.8
1g	*p*-F	-	4.67 ± 0.36	50.0	ND	6.8
1h	*p*-Cl	-	2.89 ± 0.08	>50	ND	7.2
1i	*p*-Br	-	2.55 ± 0.02	48.3 ± 2.4	>50	7.4
1j	*o*-NO$_2$	+	1.66 ± 0.06	>50	ND	6.6
1k	*m*-NO$_2$	-	2.10 ± 0.09	28.1 ± 3.5	>50	6.6
1l	*p*-NO$_2$	++	1.23 ± 0.12	>50	ND	6.6
2a	H	-	>10	>50	ND	4.3
2b	*p*-Me	-	>10	28.5 ± 0.3	>50	4.8
2c	*p*-*i*Pr	-	>10	>50	ND	5.6
2d	*p*-OMe	-	>10	>50	ND	4.2
2e	*m*-F	-	>10	>50	ND	4.5
2f	*p*-F	-	>10	>50	ND	4.5
2g	*p*-Cl	-	>10	41.3 ± 1.2	>50	4.9
2h	*p*-Br	-	>10	33.1 ± 3.0	>50	5.1
2i	*o*-NO$_2$	-	>10	23.6 ± 5.0	>50	4.3
2j	*m*-NO$_2$	-	>10	14.2 ± 0.4	>50	4.3
2k	*p*-NO$_2$	-	>10	>50	ND	4.3
8	H[g]	-	> 10	ND[g]	ND	
E64		ND	ND	0.0246 ± 0.0012	ND	
ART		ND	0.00876	ND	ND	
CQ		++	0.0138[h]	ND	ND	

[a] ability to β-H formation *in vitro* was calculated as a % of the inhibitory effect displayed by reference drug CQ in the same experiment; test compounds were ranked as follows: <50%, not active (-); between 50 and 75%, moderately active (+); ≥75%, highly active (++); [b] blood-stage antiplasmodial activity was determined against the CQ-resistant *Pf* strain W2, using artemisinin (ART) and CQ as reference drugs; [c] falcipain inhibition capacity was evaluated against FP2 using E64 as reference inhibitor and compound with IC$_{50}$ < 50 μM were further evaluated against FP3; [d] the logP values were estimated with the MarvinSketch software;[12] [e] compound **1a'** is the L-amino acid analogue of **1a**; [f] ND, not determined; [g] Morpholine/cinnamoylated derivative; [h] Retrieved from ref.[13]

a) Inhibition of hemozoin formation

The β-H formation assays were carried out in 96-wells plates. Briefly, the hemin was incubated at 37^oC at pH=4.4 for 48 hours with *HEDICIN*s and *HECIN*s, respectively, at 1mM. Later on, the plates were centrifuged, the supernatant was discarded, and the DMSO was used to wash the plates (Fig. 20). The respective absorbance was measured once the formed crystals of β-H were hydrolyzed and later dissolved in an aqueous solution of NaOH. In this assay, the process of hemozoin formation that takes places in the food vacuole was basically simulated using CQ as a positive control and H_2O and DMSO as negative control of CQ, and the compounds, respectively.

i) Hemin
ii) pH=4.4
iii)Chloroquine/
*HEDICIN*s/
*HECIN*s/
DMSO/H_2O

96-well plates

37^oC
48hours

i) Centrifugate (3000x15 min)
   Discard supernatant
ii) Wash with DMSO
   Centrifugate (3000x15 min)
   3 to 4 times
iii) Hydrolisis
   NaOH (0.2M)
iv) Dilution in NaOH (0.1M)

Read
405nM
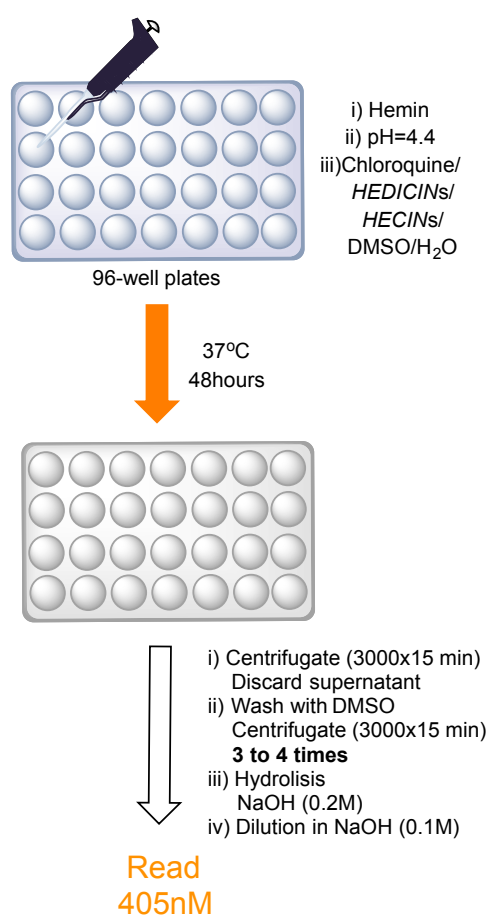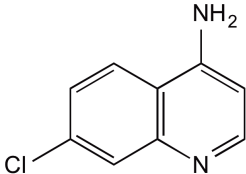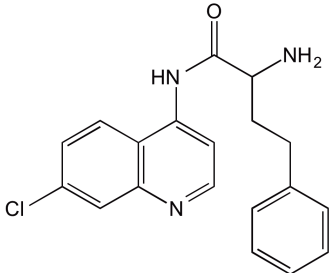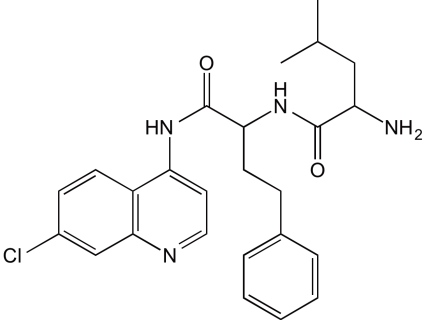
Figure 20. *In vitro* assay of inhibition of β-H formation.

Results in this assay only enable us to find those compounds able to inhibit β-H formation with an activity range similar to the one displayed by CQ in the corresponding assay. Although none of *HECIN*s showed activity against β-H formation, some *HEDICIN*s were active but no clear SAR could be established between inhibition of β-H formation and impairment of the parasite development based on *HEDICIN*s results. Furthermore, since chloroquinoline is known to be the core

responsible for activity of the compounds against hemozoin formation and *HECIN*s did not result active against β-H formation, this suggests that coupling directly the cinnamoyl moiety to 4-amino-7-chloroquinoline does not promote inhibition of such a process. Moreover, the influence of the dipeptide link was assessed by also testing the ability of compounds **3**, **5**, and **7** to inhibit β-H formation (Table 4). Based on the results, coupling the first amino acid or the subsequent D-Leu, led to the loss of the activity presented by compound **3**. However, when coupling *p*-Me, *p*-OMe, *p*-NH$_2$, *o*-NO$_2$, or the *p*-NO$_2$ cinnamic acid resulting compound **1b**, **1d**, **1e**, **1j**, **1l**, respectively, the corresponding derivative displays activity or becomes more active than compound **3**. Results demonstrate that the later cynnamoyl moieties join together with compound **7** promote the activity against β-H formation. However, in order to draw more detailed conclusion regarding the inhibition of β-H formation by *HEDICIN*s, a more precise method should be carried to evaluate the ability of these compounds to inhibit β-H formation such as the one reported by Wright's team.[14] Nevertheless, the latter results suggest the importance of the hydrophobic link for the antiplasmodial activity of *HEDICIN*s.

Table 4. *In vitro* results against β-H for compounds **3**, **5**, and **7**.

Compound	% inhibition of β-H formation at 1mM[a]
3	+
5	-
7	-

[a] Observed legend of table 3 for compound ranking.

b) Inhibition of falcipain action

Besides evaluating compounds ability to inhibit β-H formation, cinnamoylated derivatives were also assessed as inhibitors of falcipains. In the case of *HEDICIN*s, the most active derivatives against falcipains' action were the non-substituted cinnamoyl derivative **1a** and the *m*-NO$_2$ derivative **1k**. However, results showed that *HECIN*s were generally more active than *HEDICIN*s, which contrast to previous results found against β-H. General ability of *HECIN*s to better inhibit falcipain as compared to *HEDICIN*s could be explained by *in silico* results against falcipains carried by Dr. Teixeira. The latter demonstrated that the α,β-unsaturated system of *HECIN*s come closer to the cysteine residue of the active pocket of the proteases compared to the distance between the beta

carbon of the Michael acceptor functionality and catalytic residue of falcipains afforded by *HEDICIN*s (Fig. 21). Furthermore as observed in fig. 21, docking results against FP3 confirmed that the FP3 cavity is too narrow and the cinnamoyl moiety is placed too far away from the cysteine residue hindering a possible inhibition of the enzyme (Fig. 21 B). Only those compounds which displayed activity against FP2 were evaluated against FP3, since FP3's cavity is narrower,[15] therefore, the latter allows lower range of inhibitors compared to FP2. Accordingly, none of the derivatives active against FP2 were active against FP3 (IC$_{50}$ > 50 μM). Moreover, the effect of the use of D-amino acids was evaluated through the synthesis and assessment of compound **1a'** that contained L-amino acids instead. Interesting, the use of L-amino acids led to a clear decrease of inhibition of FP2. The latter suggests that D-amino acid configuration does not impair inhibition of falcipain action, in fact, in *HEDICIN*s case, D-amino acids seem to be preferable.
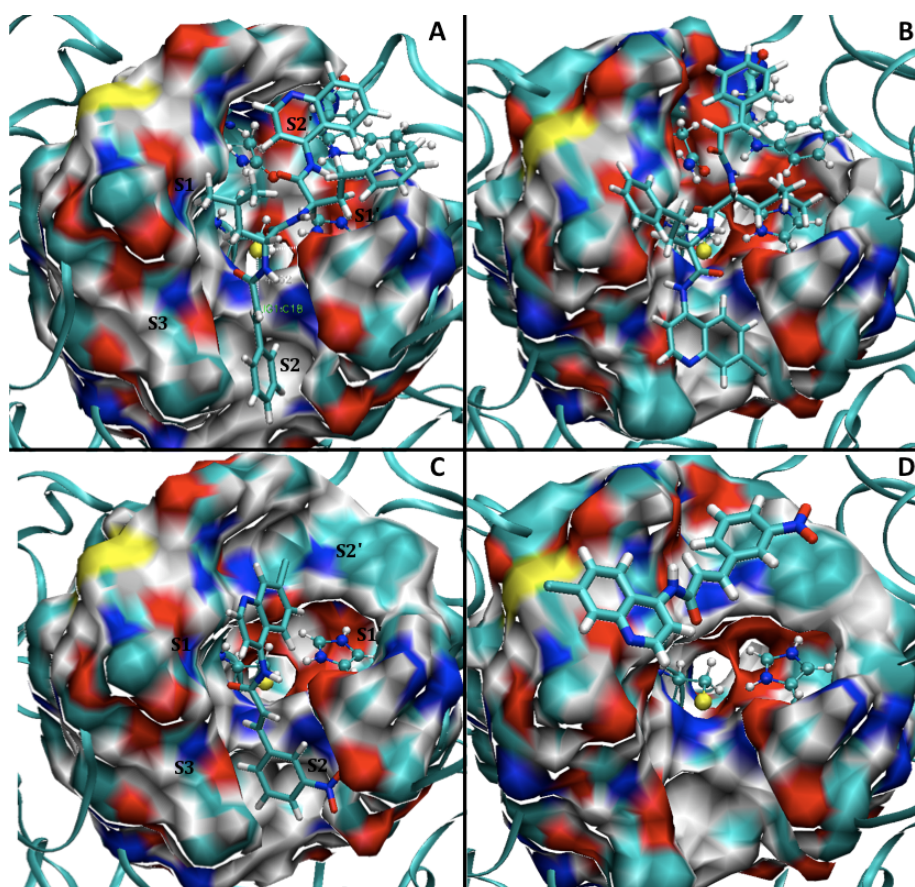
Figure 21. Preferred binding modes of the unsubstituted (A and B) and *m*-NO$_2$ (C and D) cinnamoyl derivative **1a** and **2j** into FP2 and FP3 binding sites, respectively.

c) Antiplasmodial assays

According to antiplasmodial results, all *HEDICIN*s displayed activity in the micromolar range against the parasite (IC$_{50}$ = 0.83-10.8 μM), contrary to *HECIN*s which were not active against the parasite (Table 3). Interesting, the most active compound of the series **1c** was the most lipophilic, demonstrating that this property plays a important role in antiplasmodial activity as found by Miller and Lin.[16] This could also explain the lack of activity of *HECIN*s, since *HEDICIN*s are more lipophilic than *HECIN*s due to dipeptide spacer use to join the cinnamoyl moiety and the chloroquinoline ring. In addition, there was no correlation regarding the activity of the compounds and the electro-donating properties of the substituents in the cinnamoyl moiety. Contrary, results suggest that as the electronegativity of the *para* substituent increases, the activity decreases. For instance, the *p*-Br derivative **1i** (IC$_{50}$ = 2.55 μM) and the *p*-Cl **1h** (IC$_{50}$ = 2.89 μM) were more active than the *p*-F **1g** (IC$_{50}$ = 4.67 μM). Also, *para* substituent seems to be preferable over the *meta* substituents as demonstrated by the *p*-F (IC$_{50}$ = 4.67 μM) *vs* the *m*-F (IC$_{50}$ = 5.43 μM) derivatives and the *p*-NO$_2$ (IC$_{50}$ = 1.23 μM) *vs* the *m*-NO$_2$ derivative (IC$_{50}$ = 2.10μM). Results demonstrated the relevance of the chloroquinoline moiety in the antiplasmodial activity of the compounds since compound **8** was not active against the malaria parasite (IC$_{50}$ > 10 μM). Moreover, as in the case of inhibition of falcipain action, D-amino acids, in the case of *HEDICIN*s, seems to be promoting impairment of parasite growth.

Results demonstrated that compounds ability to inhibit of hemozoin formation or falcipain action does not correlate with compounds ability to impair parasite growth. However, *HEDICIN*s displaying antiplasmodial activity below 2μM which were also active against β-H formation, for instance, the *p*-Me derivative **1b** (IC$_{50}$ = 1.96 μM) and the *p*-NO$_2$ derivative **1k** (IC$_{50}$ = 1.23 μM), suggests that inhibition of hemozoin formation might be one of the mechanism through which these derivatives exert their activity. In addition, the fact that, for instance, the *m*-NO$_2$ derivative **2j**, the most active of *HECIN*s against FP2 (IC$_{50}$ = 14.2μM) was not active against the *Pf* parasite (IC$_{50}$ > 10 μM), might be suggesting that *HECIN*s may not be reaching its corresponding target. The latter could be explained by the low basicity of the *HECIN*s which could be impeding the necessary accumulation of the molecules in the FV to inhibit the respective target. Overall, the relevance of the hydrophobic link and chloroquine moiety to impair parasite growth are demonstrated.

2.2. Experimental Section

2.2.1. Chemistry

2.2.1.1. Chemicals and instrumentation

All solvents and common chemicals were from Sigma Aldrich (Spain), whereas Boc-protected amino acids were from NovaBiochem (VWR International, Portugal) and TBTU was from Bachem (Switzerland). NMR spectra were acquired on a Bruker Avance III 400 spectrometer from solutions in either deuterated chloroform or deuterated dimethylsulfoxide (DMSO-d_6) containing tetramethylsilane as internal reference. MS spectra were obtained on a Thermo Finnigan LCQ Deca XP Max LC/MSn instrument operating with electrospray ionization and ion-trap (ESI-IT) quadrupole detection. HPLC analyses were run for target compounds (**1**-**2** and **8**) using the following conditions: 30-100% of B in A (A =H_2O with 0.05% of trifluoroacetic acid; B =acetonitrile) in 22 min with a flow rate of 1 mL/min on a MerckeHitachi Lachrom Elite instrument equipped with a diode-array detector (DAD) and thermostated (Peltier effect) autosampler, using a Purospher STAR RP-18e column (150 4.0 mm; particle size, 5 μM).

2.2.1.2. Synthesis of compounds 3-7

4-amino-7-chloroquinoline (3).
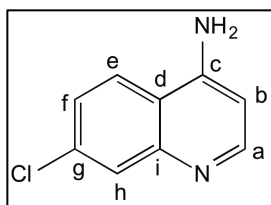
An earlier method by Reitsema and co-workers was followed:[3] 4,7-dichloroquinoline (6 g, 0.03 mol) and phenol (30 g, 0.3 mol) were mixed at room temperature in a round bottom flask. After increasing the temperature to 150°C, ammonia was bubbled into the solution for 2 hours. After cooling the mixture back to room temperature, a solution of glacial acetic acid (7.5 mL) in water (15 mL) was added with stirring, followed by addition of ice-cold ethyl ether (30 mL). The white precipitate formed was collected by suction filtration and dissolved in hot water. The pH of the resulting solution was adjusted to 11 with 1M NaOH (aq) and, after cooling the mixture, a white solid precipitated and was collected, dried and identified as the target 4-amino-7-chloroquinoline, **2** (4.8g, 89%); mp 110-112 ^{o}C; R_F (DCM/MeOH 20:1) 0.59; δ_H (400 MHz, DMSO-d_6) 8.31 (d, J= 5.2 Hz, 1H, Ha), 8.19 (d, J=9.2 Hz, 1H, He), 7.76 (d, J= 2 Hz, 1H, Hh), 7.40 (dd, J= 8.5 Hz, J= 2 Hz, 1H, Hf), 6.93 (s, 2H, -NH_2), 6.55 (d, J= 5.2 Hz, 1H, Hb); δ_C (100 MHz, DMSO-d_6) 151.6, 151,5, 149.4 (Ca, Cc, Ci), 133.4, 127.3, 124.6, 123.7 (Ce-Ch), 117.0 (Cd), 102.6 (Cb); ESI-IT MS: m/z (M+H$^+$) 179.33 ($C_9H_7ClN_{23}$ requires 178.03).

4-[(2R)-2-(tert-butoxycarbonyl)amino-4-phenylbutanoyl]amino-7-chloroquinoline (4)
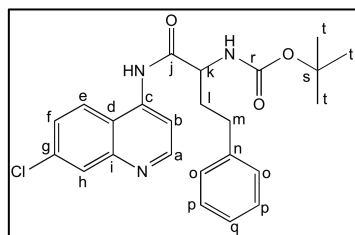
Boc-*D-homo*phenylalanine (0.43 g, 1.5 mmol), TBTU (0.49 g, 1.54 mmol), DIEA (0.36 mL, 2.8 mmol) and dimethylformamide (DMF, 7 mL) were mixed in a round bottom flask at 0 ºC. After 10 minutes, a solution of 4-amino-7-chloroquinoline **3** in DMF (7 mL) was added and the reaction was allowed to proceed for one day at room temperature. Following, water was added to the reaction mixture and the product was extracted with dichloromethane (3 times); the organic layers were pooled and sequentially washed with 1% aq. HCl (3 times) and 5% aq. Na_2CO_3 (3 times). Finally, the organic layer was dried over anhydrous Na_2SO_4, filtered, and evaporated to dryness under reduced pressure. The crude product was purified by column liquid chromatography on silica, using dichloromethane:acetone (DCM/Me$_2$CO) 6:1 v/v as eluent. The resulting product was obtained as a white solid and corresponded to the target compound **4** (218 mg, 35%); mp 150-152ºC; R_F (DCM/Me$_2$CO 6:1) 0.57; δ_H (400 MHz, CDCl$_3$) 9.72 (s, 1H, -NH-QN), 8.8 (d, J= 5.2 Hz, 1H, Ha), 8.29 (d, J= 5.2 Hz, 1H, Hb), 8.05 (d, J= Hz, 1H, Hh), 7.95 (d, J= 8.8 Hz, 1H, He), 7.47 (dd, J= 8 Hz, J= 2 Hz, Hf), 7.33-7.29 (m, 2H), 7.24-7.15 (m, 4H) (-NH-hPhe, Ho-Hq), 4.26 (q, J= 7.3 Hz, 1H, Hk), 2.83-2.79 (m, 2H, Hm), 1.50 (s, 9H, Ht), 1.45-1.44 (m, 2H, Hl); δ_C (100 MHz, CDCl$_3$); 170.8 (Cj), 157.2, 152.3, 149.3, 141.0, 140.3, 135.3, 129.1, 128.7, 128.4, 127.2, 126.4, 121.5 (Ca, Cc, Ce-Ci, Cn-r), 118.3 (Cd), 110.4 (Cb), 81.7 (Cs), 54.7 (Ck), 32.0, 31.3, 28.3 (Cm, Ct, Cl); ESI-IT MS: m/z (M+H$^+$) 440.20 (C$_{24}$H$_{26}$ClN$_3$O$_3$ requires 439.17).

4-[(2R)-2-amino-4-phenylbutanoyl]amino-7-chloroquinoline (5)
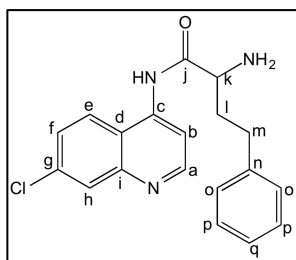
Compound **4** (0.13 g, 0.3 mmol) was reacted with neat trifluoroacetic acid (TFA, 1 mL) for 2 at room temperature, under constant stirring. Then, the pH was adjusted to 12 with 30% Na_2CO_3 (aq) and the solution extracted with DCM. The organic layer was dried with anhydrous Na_2SO_4 and evaporated to dryness under reduced pressure. Compound **5** was thus obtained as a yellow oil (85.3 mg, 85%); R_F (DCM/Me$_2$CO 6:1) 0.26; δ_H (400 MHz, CDCl$_3$) 10.89 (s, 1H, -NH-QN), 8.81 (d, J= 5.2 Hz, 1H, Ha), 8.38 (d, J= 5.2 Hz, 1H, Hb), 8.08 (d, J= 2 Hz, 1H, Hh), 7.77 (d, J=9.2Hz, 1H, He), 7.48 (dd, J= 9Hz, J= 2Hz, 1H, Hf), 7.33-7.18 (m, 7H, Ho-Hq, -NH$_2$), 3.63-3.59 (m, 1H, Hk), 2.90-2.75 (m, 2H, Hm), 2.01-1.85 (m, 2H, Hl); δ_C (100 MHz, CDCl$_3$) 173.3 (Cj), 152.2, 148.9, 140.1, 139.9, 134.8, 128.9, 128.3, 128.0, 126.8, 126.0, 120.5 (Ca, Cc, Ce-

Ci, Cn-Cq), 118.0 (Cd), 109.3 (Cb), 55.1 (Ck), 35,7, 31.8 (Cl-Cm); ESI-IT MS: m/z (M+H$^+$) 340.33 (C$_{19}$H$_{18}$ClN$_3$O requires 339.11).

4-{(2R)-2-[(2R)-2-(tert-butoxycarbonyl)amino-4-methylpentanoyl]amino-4-phenylbutanoyl}amino-7-chloroquinoline (6)
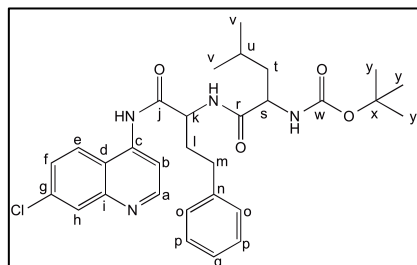
Boc-*D*-leucine (0.13 g, 0.38 mmol), PyBOP (0.22 g, 0.42 mmol), DIEA (0.162 mL, 1.25 mmol) and DCM (2 mL) were mixed in a round bottom flask at 0 ºC and put under stirring for 20 minutes. Then, a solution of **5** in DCM (2 mL) was added and the reaction allowed to proceed for one day at room temperature. Following, the reaction mixture was diluted with 14 mL of DCM and sequentially washed with 1% aq. HCl (3×18 mL) and 5% aq. Na$_2$CO$_3$ (3×18 mL). Finally, the organic layer was dried with anhydrous Na$_2$SO$_4$, filtered, and evaporated to dryness. The crude product was purified by column liquid chromatography on silica, using DCM/Me$_2$CO 6:1 v/v as eluent. The target compound, **6**, was isolated as a yellowish oil (122 mg, 58%); R$_F$ (DCM/Me$_2$CO 6:1) 0.53; δ$_H$ (400 MHz, CDCl$_3$); 9.75 (s, 1H, -NH-QN), 8.79 (d, J= 5.2 Hz, 1H, Ha), 8.22 (d, J= 4.8 Hz, 1H, Hb), 8.07 (d, J= 2 Hz, 1H, Hh), 7.95 (d, J= 9.2 Hz, 1H, He), 7.49 (dd, J= 8.8 Hz, J= 2 Hz, 1H, Hf), 7.30-7.26 (m, 2H, -NH-Leu, -NH-hPhe), 7.24-7.17 (m, 5H, Ho-Hq), 4.60 (q, J= 7.2 Hz, 1H, Hk), 4.16 (b, 1H, Hs), 2.83-2.74 (m, 2H, Hm), 2.22-2.11 (m, 2H, Hl), 1.81-1.71 (m, 2H, Ht), 1.65-1.55 (m, 1H, Hu), 1.4 (s, 9H, Hy), 0.9 (d, J= 6.8 Hz, 6H, Hv); δ$_C$ (100 MHz, CDCl$_3$) 174.5 (Cj), 170.1 (Cr), 155.9 (Cw), 152,1, 149.3, 141.2, 140.4, 135.3, 129.0, 128.7, 128.4, 127.3, 126.4, 121.9 (Ca, Cc, Ce-Ci, Cn-Cq), 118.5 (Cd), 110.9 (Cb), 69.7 (Cx), 53.9, 53.1 (Ck, Cs), 40.3, 30.8, 28.2, 24.7, 22.7, 18.8 (Cl-Cm, Ct-Cv, Cy); ESI-IT MS: m/z (M+H$^+$) 553.27 (C$_{30}$H$_{37}$ClN$_4$O$_4$ requires 552.25).

4-{(2R)-2-[(2R)-2-amino-4-methylpentanoyl]amino-4-phenylbutanoyl}amino-7-chloroquinoline (7)
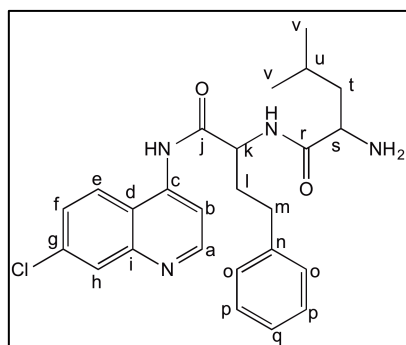
Compound **6** (0.122 g, 0.22 mmol) was reacted with neat trifluoroacetic acid (TFA, 1 mL) for 2 at room temperature, under constant stirring. Then, the pH was adjusted to 12 with 30% aq. Na$_2$CO$_3$ and the desired compound was extracted with DCM. The organic layer was dried with anhydrous Na$_2$SO$_4$ and evaporated to dryness under reduced pressure. Compound **6** was thus obtained as a yellowish oil (72 mg, 87%); R$_F$ (DCM/Me$_2$CO 6:1) 0.16; δ$_H$ (400 MHz, CDCl$_3$) 10.15 (s, 1H, -NH-QN), 8.77 (d, J=5.2Hz, 1H, Ha), 8.28 (b,

1H, Hb), 8.11-8.01 (m, 3H, -NH-hPhe, He, Hh), 7.51 (d, J=8.8Hz, 1H, Hf), 7.31-7.13 (m, 7H, -NH$_2$, Ho-Hq), 4.57 (b, 1H, Hk), 3.52-3.36 (m, 1H, Hs), 2.81-2.78 (m, 2H, Hm), 2.04-1.84 (m, 2H, Hl), 1.44-1.29 (m, 3H, Hu-Ht), 1.03-0.87 (m, 6H, Hv); δ_C (100 MHz, CDCl$_3$) 178.8 (Cj), 171.3 (Cr), 153.1, 150,2, 142.2, 141.4, 136.2, 129.9, 129.6, 129.3, 128.3, 127.3, 122.9 (Ca, Cc, Ce-Ci, Cn-Cq), 119.3 (Cd), 111.3 (Cb), 54.6, 54.1 (Ck, Cs), 44.5, 33.0, 25.8, 24.3, 22.2 (Cm-Cl, Ct-Cv); ESI-IT MS: m/z (M+H$^+$) 453.27 (C$_{25}$H$_{29}$ClN$_4$O$_2$ requires 452.20).

2.2.1.3. Synthesis of compounds 1a-l and 1a' (*HEDICIN*s)

The relevant cinnamic acid (1.1 eq), PyBOP (1.1 eq), DIEA (2 eq.) and DCM (2 mL) were mixed in a round bottom flask and put under stirring for 20 min. Then, a solution of 7 in DCM (2 mL) was added and the reaction allowed to proceed for three days. Precipitation was observed and the precipitate was collected by suction filtration, washed with ice-cold DCM, dried and identified as the pure target compound, except in the case of **1l** (*p*-nitrocinnamic acid derivative), which was further submitted to liquid chromatography on silica, using DCM/Me$_2$CO 6:1 (v/v) as eluent. In the particular case of compound **1e**, derived from *p*-aminocinnamic acid, the *N*-Boc-protected precursor of this cinnamic acid derivative was coupled to **7** as described, and the resulting Boc-protected compound (**1e'**) was treated with neat TFA as described for the synthesis of **5** and **7**, to give the final unprotected compound, **1e**. Analytical and spectroscopic data for *HEDICIN*s are given below.

4-{(2R)-2-[(2R)-2-(cinnamoyl)amino-4-methylpentanoyl]amino-4-phenylbutanoyl}amino-7-chloroquinoline (1a)
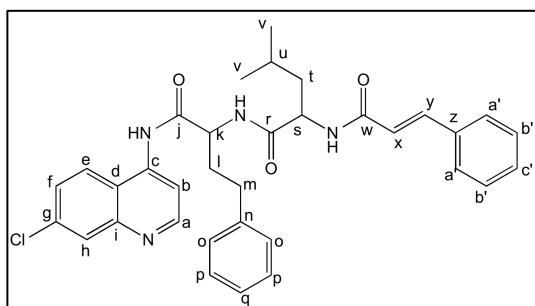
White solid (29.5 mg, 66%); mp 241-245 ^{o}C; R$_F$ (DCM/Me2CO 6:1) 0.36; δ_H (400 MHz, DMSO-d$_6$) 10.36 (s, 1H, -NH-QN), 8.84 (d, J=5.2 Hz, 1H, Ha), 8.59 (d, J=7.6 Hz, 1H, He), 8.37-8.32 (m, 2H, -NH-Leu, -NH-hPhe), 8.05-8.04 (m, 2H, Hb, Hh), 7.67 (dd, J= 9.28 Hz, J= 2 Hz, 1H, Hf), 7.56 (d, J=7.2 Hz, 2H), 7.46-7.34 (m, 4H) (Ha'-Hc', Hy), 7.29-7.15 (m, 5H, Ho-Hq); 6.79 (d, J= 15.6 Hz, 1H, Hx); 4.72-4.67 (m, 1H), 4.58 (q, J= 7.6 Hz, 1H) (Hk, Hs), 2.85-2.60 (m, 2H, Hm), 2.19-2.01 (m, 2H, Hl), 1.72-1.61 (m, 1H, Hu), 1.61-1.51 (m, 2H, Ht), 0.90 (dd, J= 16 Hz, J= 6.4 Hz, 6H, Hv); δ_C (100 MHz, DMSO-d$_6$); 172.7, 171.8, 164.9 (Cj, Cr, Cw), 152.2, 149.1, 141.5, 141.1, 139.0, 134.8, 134.2, 129.5, 128.9, 128.3, 128.3, 128.0, 127.5, 126.4, 125.9, 124.5, 121.9, 119.4, 112.4 (Ca-Ci, Cn-Cq, Cx-Cc'), 53.5, 51.1 (Ck, Cs),

40.9, 33.0, 31.5, 24.2, 23.0, 21.6 (Cl-Cm, Ct-Cv); ESI-IT MS: m/z (M+H$^+$) 583.47 ($C_{34}H_{35}ClN_4O_3$ requires 582.24); HPLC-DAD: rt = 12.4 min (% Area = 96%).

4-{(2R)-2-[(2R)-2-((*p*-methyl)cinnamoyl)amino-4-methylpentanoyl]amino-4-phenylbutanoyl}amino-7-chloroquinoline (1b)
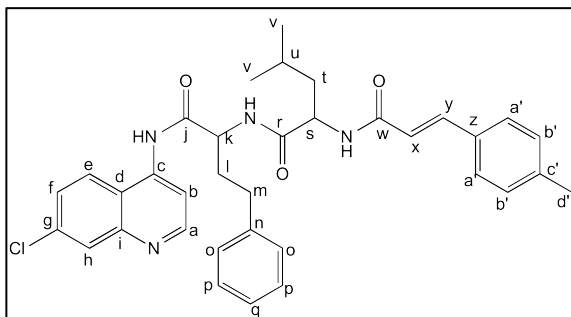
White solid (30.1 mg, 76%); mp 230-235 °C; R_F (DCM/Me$_2$CO 6:1) 0.24; δ_H (400 MHz, DMSO-d$_6$) 10.35 (s, 1H, -NH-QN), 8.83 (d, J= 5.2 Hz, 1H, Ha), 8.55 (d, J= 7.6 Hz, 1H, He), 8.36-8.26 (m, 2H, -NH-Leu, -NH-hPhe), 8.06-8.04 (m, 2H, Hb, Hh), 7.66 (dd, J= 9 Hz, *J*= 2 Hz, 1H, Hf), 7.46-7.35 (m, 3H, Ha',Hy), 7.31-7.10 (m, 7H, Ho-q, Hb'), 6.75 (d, J= 16 Hz, 1H, Hx), 4.72-4.67 (m, 1H), 4.57 (q, J= 7.7, 1H) (Hk, Hs), 2.81-2.62 (m, 2H, Hm), 2.32 (s, 3H, Hd'), 2.20-2.00 (m, 2H, Hl), 1.74-1.50 (m, 3H, Ht-u), 0.90 (dd, J= 16 Hz, J= 6.4 Hz, 6H, Hv); δ_C (100 MHz, DMSO-d$_6$) 172.7, 171.7, 165.0 (Cj, Cr, Cw), 152.2, 149.0, 141.4, 141.0, 139.2, 134.9, 134.1, 132.0, 129.5, 128.3, 128.2, 127.9, 127.4, 126.3, 125.8, 124.5, 120.8, 119.3, 112.4 (Ca-Ci, Cn-Cq, Cx-Cc'), 53.4, 51.6 (Ck, Cs), 40.8, 32.9, 31.4, 24.8, 22.9, 21.6, 20.9 (Cl-Cm, Ct-Cv, Cd'); ESI-IT MS: m/z (M+H$^+$) 597.60 ($C_{35}H_{37}ClN_4O_3$ requires 596.26); HPLC-DAD: rt = 18.3 min (% Area = 98%).

4-{(2R)-2-[(2R)-2-((*p*-isopropyl)cinnamoyl)amino-4-methylpentanoyl]amino-4-phenylbutanoyl}amino-7-chloroquinoline (1c)
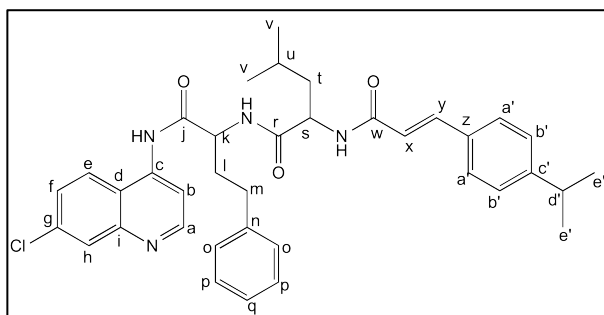
White solid (23 mg, 47%); mp 238-240 °C; R_F (DCM/Me$_2$CO 6:1) 0.44; δ_H (400 MHz, DMSO-d$_6$) 10.34 (s, 1H, -NH-QN), 8.83 (d. J= 5.2 Hz, 1H, Ha), 8.56 (d, J= 6.8 Hz, 1H, He), 8.36-8.26 (m, 2H, -NH-Leu, -NH-hPhe), 8.06-8.04 (m, 2H, Hb, Hh), 7.67 (d, J= 8.8 Hz, 1H, Hf), 7.50-7.38 (m, 4H, Ha'-b'), 7.30-7.23 (m, 6H, Ho-q, Hy), 6.73 (d, J= 16 Hz, 1H, Hx), 4.72-4.67 (m, 2H, Hk, Hs), 2.97-2.62 (m, 3H, Hm, Hd'), 2.20-2.00 (m, 2H, Hl), 1.77-1.51 (m, 3H, Ht-u), 1.20 (d, J= 6.8 Hz, 6H, He'), 0.90 (dd, J= 16.6 Hz, J= 6.4 Hz, 6H); δ_C (100 MHz, DMSO-d$_6$) 172.7, 171.7, 165.0 (Cj, Cr, Cw), 152.1, 150.0, 149.0, 141.4, 141.0, 138.9, 134.1, 132.4, 128.3, 128.2, 127.9, 127.5, 126.8, 126.3, 125.8, 124.5, 120.9, 119.36, 112.4 (Ca-Ci, Cn-Cq, Cx-Cc'), 53.4, 51.0 (Ck, Cs), 40.8, 33.2, 33.0, 31.4, 24.8, 23.6,

22.9, 21.6 (Cl-Cm, Ct-Cv, Cd'-Ce'); ESI-IT MS: m/z (M+H$^+$) 625.36 (C$_{37}$H$_{41}$ClN$_4$O$_3$ requires 624.29); HPLC-DAD: rt = 14.5 min (% Area = 93%).

4-{(2R)-2-[(2R)-2-((*p*-methoxy)cinnamoyl)amino-4-methylpentanoyl]amino-4-phenylbutanoyl}amino-7-chloroquinoline (1d)
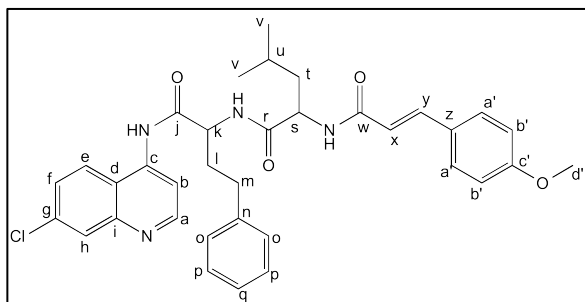
White solid (38 mg, 47%); mp 223-241 ^{o}C; R$_F$ (DCM/Me$_2$CO 6:1) 0.35; δ$_H$ (400 MHz, DMSO-d6) 10.34 (s, 1H, -NH-QN), 8.83 (d, J= 5.2 Hz, 1H, Ha), 8.54 (d, J= 7.6 Hz, 1H, He), 8.32 (d, J= 8.8 Hz, 1H), 8.24 (d, J= 8 Hz, 1H) (-NH-Leu, -NH-hPhe), 8.06-8.04 (m, 2H, Hb, Hh), 7.66 (d, J= 9.2 Hz, J=2 Hz, 1H, Hf), 7.50 (d, J= 8.8 Hz, 2H, Ha'), 7.38 (d, J= 16 Hz, 1H, Hy), 7.29-7.15 (m, 5H, Ho-q), 6.98 (d, J= 8.8 Hz, 2H, Hb'), 6.63 (d, J= 15.6 Hz, 1H, Hx), 4.72-4.68 (m, 1H), 4.61-4.52 (m, 1H) (Hk, Hs), 3.79 (s, 3H, OCH$_3$), 2.85-2.62 (m, 2H, Hm), 2.20-2.00 (m, 2H, Hl), 1.77-1.51 (m, 3H, Ht-u), 0.90 (dd, J= 16.8 Hz, J= 6.4 Hz, 6H, Hv); δ$_C$ (100 MHz, DMSO-d$_6$) 172.8, 171.7, 165.2 (Cj, Cr, Cw), 160.3, 152.1, 149.0, 141.4, 141.0, 138.7, 134.1, 129.0, 128.3, 128.2, 127.9, 127.3, 126.3, 125.8, 124.5, 120.4, 119.4, 114.3, 112.4 (Ca-Ci, Cn-Cq, Cx-Cc'), 55.2, 53.4, 51.0 (Ck, Cs, Cd'), 40.8, 33.0, 31.4, 24.2, 22.9, 21.6 (Cl-Cm, Ct-Cv); ESI-IT MS: m/z (M+H$^+$) 613.73 (C$_{35}$H$_{37}$ClN$_4$O$_4$ requires 612.25); HPLC-DAD: rt = 12.3 min (% Area = 91%).

4-{(2R)-2-[(2R)-2-((*p*-(tert-butoxycarbonyl)amino)cinnamoyl)amino-4-methylpentanoyl]amino-4-phenylbutanoyl}amino-7-chloroquinoline (1e')
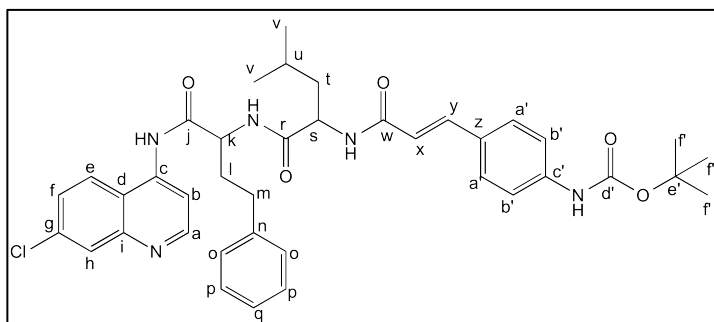
Yellow solid (10 mg, 13%); mp (dec.) 238 ^{o}C; R$_F$ (DCM/Me$_2$CO 6:1) 0.35; δ$_H$ (400 MHz, DMSO-d$_6$) 10.33 (s, 1H, -NH-QN), 9.55 (s, 1H, -NHBoc), 8.83 (d, J= 4.8 Hz, 1H, Ha), 8.53 (d, J= 7.2 Hz, 1H, He), 8.32 (d, J= 9.2 Hz, 1H), 8.26 (d, J= 8 Hz, 1H) (-NH-Leu, -NH-hPhe), 8.06-8.04 (m, 2H, Hb, Hh), 7.66 (dd, J= 9.2 Hz, J= 2 Hz, 1H, Hf), 7.50-7.38 (m, 4H, Ha'-Hb'), 7.34 (d, J= 16 Hz, 1H, Hy), 7.23 (m, 5H, Ho-q), 6.65 (d, J= 15.6 Hz, 1H, Hx), 4.72-4.68 (m, 1H), 4.61-4.52 (m, 1H) (Hk, Hs), 2.85-2.62 (m, 2H, Hm), 2.20-2.00 (m, 2H, Hl), 1.77-1.51 (m, 3H, Ht-u), 1.48 (s, 9H, Hf'), 0.90 (dd, J= 17.2 Hz, J= 6.4 Hz, 6H, Hv'); δ$_C$ (100 MHz, DMSO- d$_6$) 172.8, 171.8, 165.2 (Cj, Cr, Cw), 152.5, 152.2,

149.0, 141.4, 141.0, 140.8, 138.7, 134.1, 128.5, 128.3, 128.2, 128.1, 127.1, 126.4, 125.9, 124.5, 119.7, 119.4, 118.0, 112.0 (Ca-Ci, Cn-Cq, Cx-Cd'), 79.3 (Ce'), 53.4, 51.1 (Ck, Cs), 40.7, 33.0, 31.4, 28.0, 24.2, 22.9, 21.6 (Cl-Cm, Ct-Cv, Cf'); ESI- IT MS: m/z (M+H$^+$) 698.47 (C$_{39}$H$_{44}$ClN$_5$O$_5$ requires 697.30); HPLC- DAD: rt = 16.5 min (% Area = 97%).

4-{(2R)-2-[(2R)-2-((*p*-amino)cinnamoyl)amino-4-methylpentanoyl]amino-4-phenylbutanoyl}amino-7-chloroquinoline (1e)
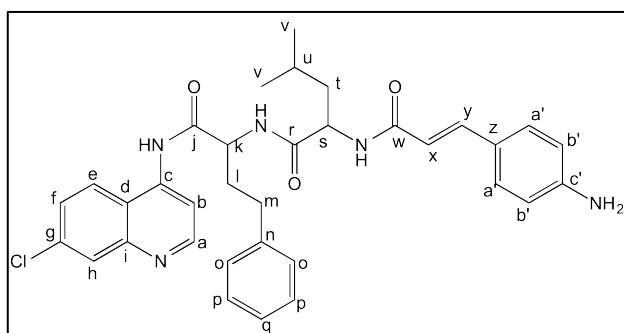
Yellow solid (12 mg, 78%); mp 240-242 °C; R$_F$ (DCM/Me$_2$CO 6:1) 0.11; δ$_H$ (400 MHz, DMSO-d$_6$) 10.32 (s, 1H, -NH-QN), 8.83 (d, J= 5.2 Hz, 1H, Ha), 8.49 (d, J= 7.6 Hz, 1H, He), 8.32 (d, J= 9.2 Hz, 1H), 8.08 (d, J= 8 Hz, 1H) (-NH-Leu, -NH-hPhe), 8.06-8.04 (m, 2H, Hb, Hh), 7.66 (dd, J= 9 Hz, J=2 Hz, 1H, Hf), 7.29-7.16 (m, 8H, Ho-q, Hy, Ha'), 6.56 (d, J= 8.4 Hz, 2H, Hb'), 6.43 (d, J= 16 Hz, 1H, Hx), 5.57 (s, 2H, -NH$_2$), 4.71-4.65 (m, 1H), 4.55-4.49 (m, 1H) (Hk, Hs), 2.80-2.59 (m, 2H, Hm), 2.20-2.00 (m, 2H, Hl), 1.75-1.50 (m, 3H, Ht-u), 0.90 (dd, J= 18.4 Hz, J= 6.4 Hz, 6H, Hv); δ$_C$ (100 MHz, DMSO-d$_6$) 172.9, 171.8, 165.9 (Cj, Cr, Cw), 152.1, 150.5, 149.0, 141.4, 141.1, 139.9, 134.1, 129.0, 128.3, 128.2, 127.9, 126.4, 125.8, 124.5, 122.0, 119.4, 115.4, 113.6, 112.4 (Ca-Ci, Cn-Cq, Cx-Ca', Cc'-Cd'), 53.4, 51.2 (Ck, Cs), 40.7, 33.0, 31.4, 24.2, 22.9, 21.6 (Cl-Cm, Ct-Cv); ESI-IT MS: m/z (M+H$^+$) 598.30 (C$_{34}$H$_{36}$ClN$_5$O$_3$ requires 597.25); HPLC-DAD: rt =16.5 min (% Area = 97%).

4-{(2R)-2-[(2R)-2-((*m*-fluoro)cinnamoyl)amino-4-methylpentanoyl]amino-4-phenylbutanoyl}amino-7-chloroquinoline (1f)
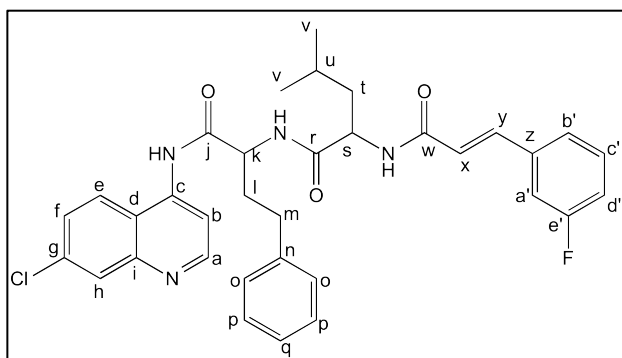
White solid (28 mg, 56%); mp 249-254 °C; R$_F$ (DCM/Me$_2$CO 6:1) 0.35; δ$_H$ (400 MHz, DMSO-d$_6$) 10.36 (s, 1H, -NH-QN), 8.83 (d, J= 4.8 Hz, 1H, Ha), 8.58 (d, J= 7.2 Hz, 1H, He), 8.37-8.30 (m, 2H, -NH-Leu, -NH-hPhe), 8.06-8.05 (m, 2H, Hb, Hh), 7.67 (d, J= 9.2 Hz, J= 2 Hz 1H, Hf), 7.50-7.38 (m, 4H, Ha'-d'), 7.31-7.15 (m, 6H, Ho-q, Hy), 6.83 (d, J= 16 Hz, 1H, Hx), 4.73-4.68 (m, 1H), 4.63-4.56 (m, 1H) (Hs, Hk), 2.82-2.63 (m, 2H, Hm), 2.20-2.00 (m, 2H, Hl), 1.75-1.52 (m, 3H, Ht-u),

0.90 (dd, J= 15.4 Hz, J= 6.8 Hz, 6H, Hv); δ_C (100 MHz, DMSO-d_6) 172.6, 171.7, 164.5, (Cj, Cr, Cw), 163.6, 161.1, 152.2, 149.0, 141.4, 141.0, 137.6, 137.4, 134.1, 130.9, 128.3, 128.2, 127.9, 126.3, 125.8, 124.5, 123.5, 119.4, 116.1, 113.8, 112.4 (Ca-Ci, Cn-Cq, Cx-Ce'), 53.5, 51.1 (Ck, Cs), 40.8, 33.0, 31.5, 24.2, 22.9, 21.6 (Cl-Cm, Ct-Cv); ESI-IT MS: m/z (M+H$^+$) 601.40 ($C_{34}H_{34}ClFN_4O_3$ requires 600.23); HPLC-DAD: rt = 11.2 min (% Area = 100%).

4-{(2R)-2-[(2R)-2-((*p*-fluoro)cinnamoyl)amino-4-methylpentanoyl]amino-4-phenylbutanoyl}amino-7-chloroquinoline (1g)
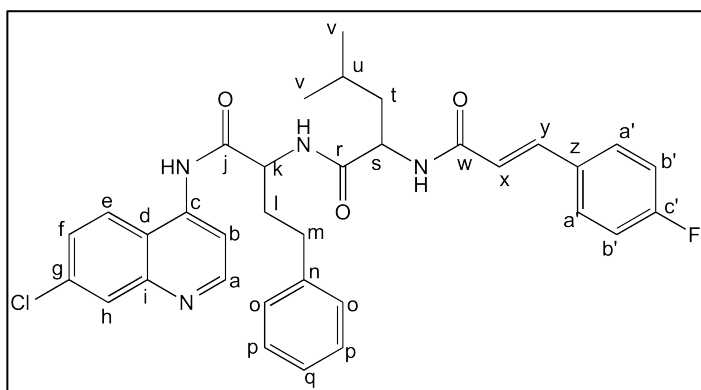
White solid (39 mg, 78%); mp 246-249 °C; R_F (DCM/Me$_2$CO 6:1) 0.35; δ_H (400 MHz, DMSO-d_6) 10.35 (s, 1H, -NH-QN), 8.83 (d, J= 5.2 Hz, 1H, Ha), 8.56 (d, J= 7.2 Hz, 1H, He), 8.32 (d, J= 9.2 Hz, 2H, -NH-Leu, -NH-hPhe), 8.06-8.04 (m, 2H, Hb, Hh), 7.67-7.60 (m, 3H, Ha', Hf), 7.44 (d, J= 15.6 Hz, 1H, Hy), 7.29-7.14 (m, 7H, Ho-q, Hb'), 6.73 (d, J= 15.6 Hz, 1H, Hx), 4.73-4.68 (m, 1H), 4.61-4.55 (m, 1H) (Hk, Hs), 2.82-2.62 (m, 2H, Hm), 2.20-2.00 (m, 2H, Hl), 1.75-1.52 (m, 3H, Ht-u), 0.90 (dd, J= 16 Hz, J= 6.4 Hz, 6H, Hv); δ_C (100 MHz, DMSO-d_6) 172.7, 171.7, 164.8 (Cj, Cr, Cw), 152.2, 149.0, 141.4, 141.0, 137.8, 134.1, 131.4, 129.6, 128.3, 128.2, 127.9, 126.3, 125.8, 124.5, 121.8, 119.4, 116.0, 115.7, 112.4 (Ca-Ci, Cn-Cq, Cx-Cc'), 53.5, 51.0 (Ck, Cs), 40.8, 33.0, 31.5, 24.2, 22.9, 21.6 (Cl-Cm, Ct-Cv); ESI-IT MS: m/z (M+H$^+$) 601.47 ($C_{34}H_{34}ClFN_4O_3$ requires 600.23); HPLC-DAD: rt= 12.5 min (% Area = 85%).

4-{(2R)-2-[(2R)-2-((*p*-chloro)cinnamoyl)amino-4-methylpentanoyl]amino-4-phenylbutanoyl}amino-7-chloroquinoline (1h)
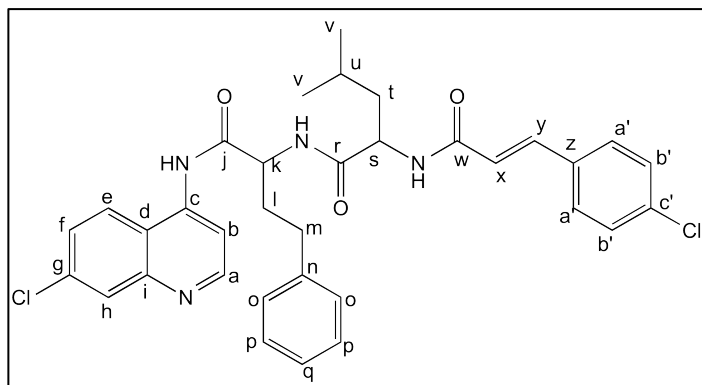
White solid (25 mg, 59%); mp 249-260 °C; R_F (DCM/Me$_2$CO 6:1) 0.35; δ_H (400 MHz, DMSO-d_6) 10.35 (s, 1H, -NH-QN), 8.83 (d, J= 4.8 Hz, 1H, Ha), 8.57 (d, J= 7.6 Hz, 1H, He), 8.34-8.30 (m, 2H, -NH-Leu, -NH-hPhe), 8.06-8.04 (m, 2H, Hb, Hh), 7.66 (dd, J= 9 Hz, J=2, 1H, Hf), 7.58 (d, J= 8.8 Hz, 2H), 7.48 (d, J= 8.4 Hz,

2H) (Ha'-b'), 7.42 (d, J= 16 Hz, 1H, Hy), 7.22 (m, 5H, Ho-q), 6.79 (d, J= 15.6 Hz, 1H, Hx), 4.73-4.68 (m, 1H), 4.61-4.55 (m, 1H) (Hk, Hs), 2.82-2.62 (m, 2H, Hm), 2.20-2.00 (m, 2H, Hl), 1.75-1.52 (m, 3H, Ht-u), 0.90 (dd, J= 16 Hz, J= 6.4 Hz, 6H, Hv); δ_C (100 MHz, DMSO-d_6) 172.6, 171.7, 164.7 (Cj, Cr, Cw), 152.2, 149.0, 141.4, 141.0, 137.6, 134.1, 133.8, 133.7, 129.1, 128.9, 128.3, 128.2, 127.9, 126.3, 125.8, 124.5, 122.7, 119.4, 112.4 (Ca-Ci, Cn-Cq, Cx-Cc'), 53.5, 51.1 (Ck, Cs), 40.8, 33.0, 31.5, 24.2, 22.9, 21.6 (Cl-Cm, Ct-Cv); ESI-IT MS: m/z (M+H$^+$) 617.23 (C$_{34}$H$_{34}$Cl$_2$N$_4$O$_3$ requires 616.20); HPLC-DAD: rt = 18.5 min (% Area = 100%)

4-{(2R)-2-[(2R)-2-((p-bromo)cinnamoyl)amino-4-methylpentanoyl]amino-4-phenylbutanoyl}amino-7-chloroquinoline (1i)
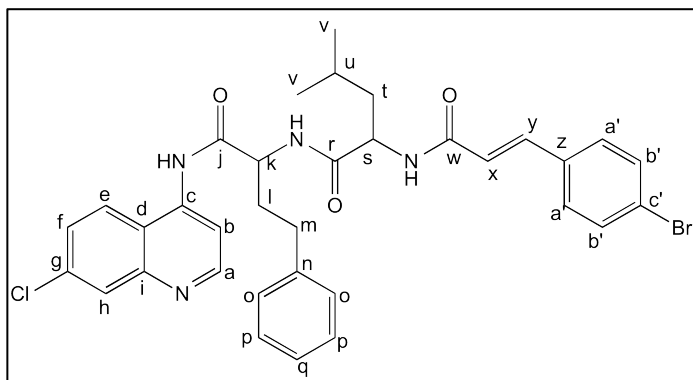
White solid (31 mg, 70%); mp 240-246 ^{o}C; R$_F$ (DCM/Me$_2$CO 6:1) 0.35; δ_H (400 MHz, DMSO-d_6) 10.35 (s, 1H, -NH-QN), 8.83 (d, J= 4.8 Hz, 1H, Ha), 8.57 (d, J= 7.2 Hz, 1H, He), 8.39-8.31 (m, 2H, -NH-Leu, -NH-hPhe), 8.06-8.04 (m, 2H, Hb, Hh), 7.71-7.61 (m, 3H), 7.51 (d, J= 8.4 Hz, 2H) (Ha'-b', Hf), 7.40 (d, J= 15.6 Hz, 1H, Hy), 7.31-7.14 (m, 5H, Ho-q), 6.80 (d, J= 16 Hz, 1H, Hx), 4.73-4.68 (m, 1H), 4.61-4.55 (m, 1H) (Hk, Hs), 2.82-2.62 (m, 2H, Hm), 2.20-2.00 (m, 2H, Hl), 1.74-1.49 (m, 3H, Ht-v), 0.90 (dd, J= 16 Hz, J= 6.4 Hz, 6H, Hv); δ_C (100 MHz, DMSO-d_6) 172.6, 171.7, 164.6 (Cj, Cr, Cw), 152.2, 149.0, 141.4, 141.0, 137.7, 134.1, 131.8, 129.4, 128.3, 128.2, 127.9, 126.3, 125.8, 124.5, 122.8, 122.6, 119.4, 112.4 (Ca-Ci, Cn-Cq, Cx-Cc'), 53.4, 51.1 (Ck, Cs), 40.8, 33.0, 31.4, 24.2, 22.9, 21.6 (Ct-Cv); ESI-IT MS: m/z (M+H$^+$) 663.40 (C$_{34}$H$_{34}$BrClN$_4$O$_3$ requires 660.15); HPLC-DAD: rt = 18.6 min (% Area = 98%).

4-{(2R)-2-[(2R)-2-((*o*-nitro)cinnamoyl)amino-4-methylpentanoyl]amino-4-phenylbutanoyl}amino-7-chloroquinoline (1j)
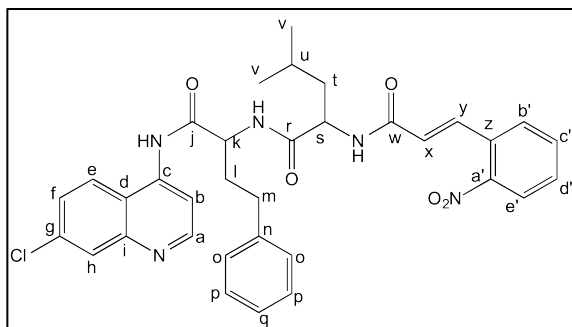
White solid (25 mg, 40%); mp 260-265 °C; R_F (DCM/Me$_2$CO 6:1) 0.35; δ_H (400 MHz, DMSO-d$_6$) 10.38 (s, 1H, -NH-QN), 8.83 (d, J= 5.2 Hz, 1H, Ha), 8.62 (d, J= 6 Hz, 1H, He), 8.49 (d, J= 9.2 Hz,1H), 8.32 (d, J= 7.2 Hz, 1H) (-NH-Leu, -NH-hPhe), 8.07-8.04 (m, 3H, Hb, Hh, He'), 7.83-7.62 (m, 5H, Hf, Hy, Hb'-d'), 7.30-7.15 (m, 5H, Ho-q), 6.79 (d, J= 15.6 Hz, 1H, Hx), 4.73-4.68 (m, 1H), 4.63-4.58 (m, 1H) (Hk, Hs), 2.87-2.63 (m, 2H, Hm), 2.20-2.00 (m, 2H, Hl), 1.73-1.51 (m, 3H, Ht-u), 0.90 (dd, J= 14.4 Hz, J= 6.4 Hz, 6H, Hv); δ_C (100 MHz, DMSO-d$_6$) 172.5, 171.8, 163.9 (Cj, Cr, Cw), 152.2, 149.0, 148.3, 141.4, 141.0, 134.1, 133.8, 133.7, 130.2, 129.8, 128.5, 128.3, 128.2, 127.9, 126.6, 126.3, 125.8, 124.6, 124.5, 119.4, 112.4 (Ca-Ci, Cn-Cq, Cx-Ce'), 53.5, 51.0 (Ck, Cs), 40.9, 33.0, 31.5, 24.2, 22.9, 21.6 (Cl-Cm, Ct-Cv); ESI-IT MS: m/z (M+H$^+$) 628.47 (C$_{34}$H$_{34}$ClN$_5$O$_5$ requires 627.22); HPLC-DAD: rt = 17.8 min (% Area = 98%).

4-{(2R)-2-[(2R)-2-((*m*-nitro)cinnamoyl)amino-4-methylpentanoyl]amino-4-phenylbutanoyl}amino-7-chloroquinoline (1k)
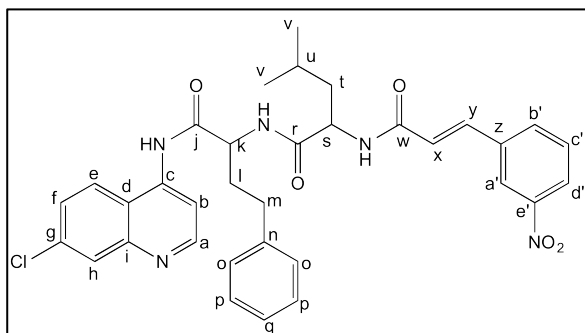
White solid (26 mg, 50%); mp 202-221 °C; R_F (DCM/Me$_2$CO 6:1) 0.35; δ_H (400 MHz, DMSO-d$_6$) 10.36 (s, 1H, -NH-QN), 8.83 (d, J= 4.8 Hz, 1H, Ha), 8.60 (d, J= 7.2 Hz, 1H, He), 8.41-8.40 (m, 2H), 8.33 (d, J= 8.8 Hz, 1H) (-NH-Leu, -NH-hPhe, Hd'), 8.21 (dd, J= 8.2 Hz, J=1.2 Hz, 1H, Hb'), 8.07-7.98 (m, 3H, Hb, Hh, Ha'), 7.74-7.67 (m, 2H, Hf, Hc'), 7.56 (d, J= 15.6 Hz, 1H, Hy), 7.29-7.14(m, 5H, Ho-q), 6.99 (d, J= 16 Hz, 1H, Hx), 4.73-4.68 (m, 1H), 4.63-4.58 (m, 1H) (Hk, Hs), 2.87-2.63 (m, 2H, Hm), 2.20-2.00 (m, 2H, Hl), 1.74-1.49 (m, 3H, Ht-u), 0.90 (dd, J= 14.4 Hz, J= 6.4 Hz, 6H, Hv); δ_C (100 MHz, DMSO-d$_6$) 172.5, 171.7, 164.3 (Cj, Cr, Cw), 152.2, 149.0, 148.2, 141.4, 141.0, 136.7, 136.6, 134.1, 133.6, 130.4, 128.3, 128.2, 127.9, 126.3, 125.9, 124.8, 124.5, 123.7, 121.4, 119.4, 112.4 (Ca-Ci, Cn-Cq, Cx-Ce'), 53.5, 51.1 (Ck, Cs), 40.8, 33.0, 31.5, 24.2, 23.0, 21.6 (Cl-Cm, Ct-Cv); ESI-IT MS: m/z (M+H$^+$) 628.53 (C$_{34}$H$_{34}$ClN$_5$O$_5$ requires 627.22); HPLC-DAD: rt = 11.1 min (% Area = 100%).

4-{(2R)-2-[(2R)-2-((*p*-nitro)cinnamoyl)amino-4-methylpentanoyl]amino-4-phenylbutanoyl}amino-7-chloroquinoline (1l)
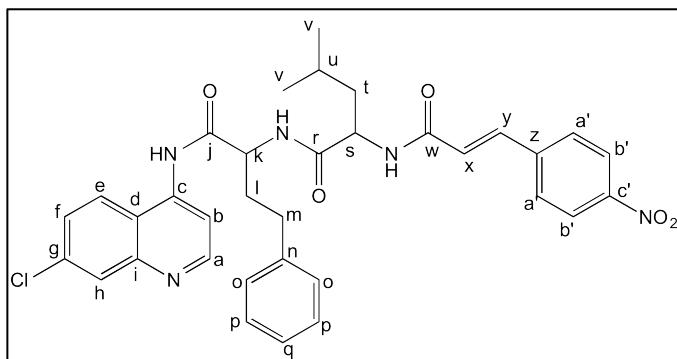
Yellowish solid (11 mg, 17%); mp 252-257 °C; R$_F$ (DCM/Me$_2$CO 6:1) 0.35; δ$_H$ (400 MHz, DMSO-d$_6$) 10.34 (s, 1H, -NH-QN), 8.82 (d, J= 5.2 Hz, 1H, Ha), 8.60 (d, J= 7.2 Hz, 1H, He), 8.49 (d, J= 8 Hz, 1H), 8.33 (d, J= 9.2 Hz, 1H) (-NH-Leu, -NH-hPhe), 8.27 (d, J= 8.4 Hz, 2H, Hb'), 8.04 (m, 2H, Hb, Hh), 7.81 (d, J= 9.2 Hz, 2H, Ha'), 7.66 (dd, J= 9.2 Hz, J= 2 Hz, 1H, Hf), 7.53 (d, J= 15.6 Hz, 1H, Hy), 7.29-7.15 (m, 5H, Ho-q), 6.96 (d, J= 16 Hz, 1H, Hx), 4.74-4.68 (m, 1H), 4.64-4.57 (m, 1H) (Hk, Hs), 2.87-2.62 (m, 2H, Hm), 2.20-2.10 (m, 2H, Hl), 1.74-1.52 (m, 3H, Ht-u), 0.90 (dd, J= 15.6 Hz, J= 6.4 Hz, 6H, Hv); δ$_C$ (100 MHz, DMSO-d$_6$) 172.6, 171.8, 164.3 (Cj, Cr, Ct), 152.3, 149.1, 147.6, 141.5, 141.4, 141.1, 136.8, 134.3, 128.6, 128.4, 128.3, 128.0, 126.5, 126.0, 124.6, 124.2, 122.8, 119.5, 112.6 (Ca-Ci, Cn-Cq, Cx-Cc'), 53.4, 51.2 (Ck, Cs), 40.7, 33.0, 31.4, 24.2, 22.9, 21.6 (Cl-Cm, Ct-Cv); ESI-IT MS: m/z (M+H$^+$) 628.73 (C$_{34}$H$_{34}$ClN$_5$O requires 627.22); HPLC-DAD: rt = 18.0 min (% Area = 92%).

## 4-{(2S)-2-[(2S)-2-(cinnamoyl)amino-4-methylpentanoyl]amino-4-phenylbutanoyl}amino-7-chloroquinoline (1a')
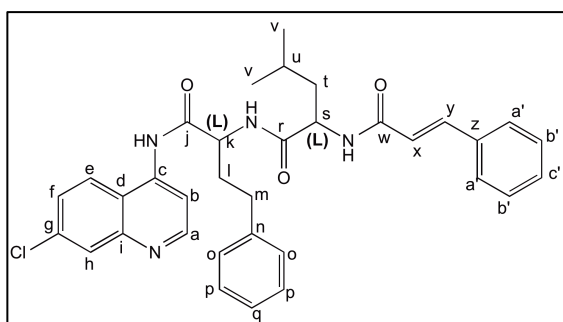
The L-amino acid analogues of precursors **5-7** (**5'-7'**) were prepared by methods similar to those above described for their D-amino acid counterparts. Compound **7'** was subsequently used to synthesize **1a'** as previously described for **1a**, and the target product **1a'** was isolated as white solid (10 mg, 26%); mp 240-242 °C; R$_F$ (DCM/Me$_2$CO 6:1) 0.36; δ$_H$ (400 MHz, DMSO-d$_6$) 10.35 (s, 1H, -NH-QN), 8.83 (d, J= 5.2 Hz, 1H, Ha), 8.57 (d, J= 7.6 Hz, 1H, He), 8.35-8.31 (m, 2H, -NH-Leu, -NH-hPhe), 8.06-8.04 (m, 2H, Hb, Hh), 7.67 (dd, J= 9.2 Hz, J= 2 Hz, 1H, Hf), 7.49 (d, J= 7.2Hz, 2H), 7.48-7.33 (m, 4H) (Ha'-c', Hy), 7.32-7.16 (m, 5H, Ho-q), 6.79 (d, J= 16 Hz, 1H, Hx), 4.76-4.51 (m, 2H, Hk, Hs), 2.84-2.63 (m, 2H, Hm), 2.20-2.00 (m, 2H, Hl), 1.73-1.51 (m, 3H, Ht-u), 0.90 (d, J= 16 Hz, J= 6.4 Hz, 6H, Hv); δ$_C$ (100 MHz, DMSO-d$_6$) 172.7, 171.7, 164.9 (Cw, Cr, Ct), 152.2, 149.0, 141.4, 141.0, 138.9, 134.8, 134.1, 129.4, 128.9, 128.3, 128.2, 127.9, 127.4, 126.3, 125.8, 124.5, 121.9, 119.4, 112.4 (Ca-I,

Cn-q, Cx-c'), 53.4, 51.1 (Ck, Cs), 40.8, 33.0, 31.4, 24.2, 22.9, 21.6 (Cl-Cm, Ct-Cv); ESI-IT MS: m/z (M+H$^+$) 583.60 (C$_{34}$H$_{35}$ClN$_4$O$_3$ requires 582.24); HPLC-DAD: rt = 17.1 min (% Area = 100%).

(2R)-4-methyl-N-[(1R)-(morpholine-4-carbonyl)-3-phenyl-propyl]-2-[(cinnamoyl) amino]pentanamide (8):
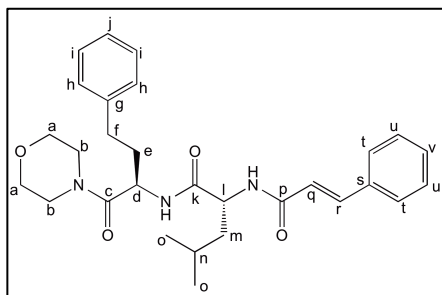
Compound **8** was obtained following a synthetic procedure similar to the one described for *HEDICIN*s but starting from morpholine instead of 4-amino-7-chloroquinoline **3** (Scheme 9). In a round bottom at 0°c, 1eq of the D*h*Phe-OH (0.2g, 0.72 mmol) was activated using 1 eq of TBTU (0.23 g, 0.72 mmol) and 2 eq of DIEA in DMF. After 10 min, 1.1 eq of morpholine (0.07 g, 0.78 mmol) was added and the reaction ran for a day. To extract the desired product **9**, 15 mL of DCM were added and the organic layer was washed three times with HCl 1% and NaCO$_3$ 5%. The organic layer was dried over Na$_2$SO$_4$ anhydrous, filtered, and evaporated down. Liquid chromatography was required to obtain the Mu-*h*Phe **9** with a 67 % yield. TFA was used to remove the corresponding Boc-protecting group and obtained the Mu-D*h*Phe-NH$_2$ **10**. Posteriorly, the latter resulted compound was coupled to Boc-D-Leu using 1.1 eq of PyBOP as coupling reagent and DIEA in DCM. The subsequent Boc protecting group was also removed with TFA. The resulted amine (Mu-*h*Phe-Leu-NH$_2$ **12**) was coupled to cinnamic acid using again PyBOP as coupling reagent, DIEA, and DCM. Liquid chromatography using as eluent DCM/Me$_2$CO 6:1 v/v was also required to purify compounds **12** and **8**. Compound **8** resulted a white solid (39mg, 33%); mp 95-100°C; R$_F$ (DCM/Me$_2$CO 6:1) 0.2; δ$_H$ (400 MHz, CDCl$_3$) 7.58 (d, J= 16 Hz, 1H, Hr), 7.47 (m, 1H, -NHC=O), 7.40-7.38 (m, 2H, Ht), 7.31-7.09 (m, 8H, Hh-Hj, Hu-Hv), 6.85-6.76 (m, 1H, -NHC=O), 6.46 (d, J= 15.6 Hz, 1H, Hq), 4.97-4.89 (m, 1H), 4.80-4.74 (m, 1H) (Hd, Hl), 3.65-3.21 (m, 8H, Ha-Hb), 2.62-2.58 (m, 2H, Hf), 2.01-1.84 (m, 2H, He), 1.73-1.52 (m, 3H, Hm-Hn), 0.91-0.88 (m, 6H, Ho); δ$_C$ (100 MHz, CDCl$_3$) 172.9, 170.0, 165.7 (Cc, Ck, Cp), 141.5, 140.8, 134.7, 129.6, 128.7, 128.4, 128.4, 127.8, 126.1, 120.3, (Cg-Cj, Cq-Cv) 66.6 (Ca), 51.9, 48.1, 45.8 (Cb, Cd, Cl), 41.9, 34.9, 31.3, 24.8, 23.0, 22.1 (Ce-Cf, Cm-Co); ESI-IT MS: m/z (M+H$^+$) 492.27 (C$_{29}$H$_{37}$N$_3$O$_4$ requires 491.28); HPLC-DAD rt = 17.5 (% Area 100).

2.2.1.4. Synthesis of compounds 2a-k (*HECIN*s)

2.2.1.4.1. Coupling reaction using the relevant cinnamic acid

The respective cinnamic acid (1.1 eq), PyBOP (1.1 eq), DIEA (2 eq.) and DCM (2 mL) were mixed in a round bottom flask and put under stirring for 20 min. Then, a solution of **3** (0.250 g, 1.40 mmol) in DMF (2 mL) was added and the reaction allowed to proceed for one day at room temperature. Following, the reaction mixture was diluted with 14 mL of DCM and sequentially washed with 1% aq. HCl (3×18 mL) and 5% aq. Na_2CO_3 (3×18 mL). Finally, the organic layer was dried with anhydrous Na_2SO_4, filtered, and evaporated to dryness. In all cases, the crude product had to be purified by liquid chromatography on silica, using DCM/Me_2CO 6:1 v/v as eluent. Target compounds were isolated as solids, with analytical, and spectral data given below.

2.2.1.4.2. Coupling reaction using the relevant acyl chloride

In a round bottom flask at room temperature, it was added 1 eq of compound **3**, 1.1 eq of the respective acyl chloride, 2.5 eq of K_2CO_3, and catalytic amount of 18-crown-6 in tetrahydrofuran (THF). The reaction ran overnight. Later it was added HCl 1% and the desired product was extracted with ethyl acetate. The organic layer was washed with Na_2CO_3 15 %, dried over Na_2SO_4 anhydrous, filtered, and evaporated down. Liquid chromatography was required to obtain the corresponding cinnamoylated derivative. The eluent used was DCM/Me_2CO 3:1.

4-(cinnamoyl)amino-7-chloroquinoline (2a)
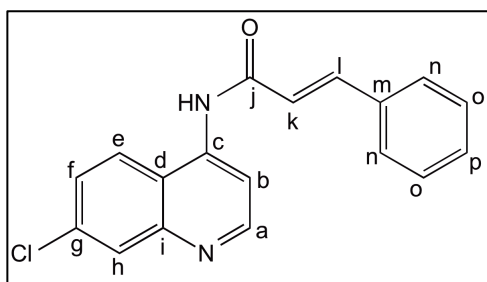
White solid (62 mg, 18%); mp 170-176 °C; R_F (DCM/Me_2CO 3:1) 0.56; δ_H (400 MHz, DMSO-d_6) 10.42 (s, 1H, -NH-QN), 8.85 (d, J= 5.2 Hz, 1H, Ha), 8.48 (d, J= 9.2 Hz, 1H, He), 8.33 (d, J=5.2 Hz, 1H, Hb), 8.05 (d, J= 2.4 Hz, 1H, Hh), 7.74-7.68 (m, 4H), 7.51-7.42 (m, 3H, Hf, Hl, Hn-Hp), 7.27 (d, J=15.6 Hz, 1H, Hk); δ_C (100 MHz, DMSO-d_6) 164.8 (Cj), 152.2, 149.1, 141.9, 141.7, 134.5, 134.1, 130.1, 129.0, 128.0, 127.9, 126.3, 124.4, 121.5, 119.0, 111.5 (Ca-i, Ck-p); ESI-IT MS: m/z (M+H$^+$) 309.33 ($C_{18}H_{13}ClN_2O$ requires 308.07); HPLC-DAD: rt = 8.10 min (% Area = 85%).

4-[(*p*-methyl)cinnamoyl]amino-7-chloroquinoline *(2b)*
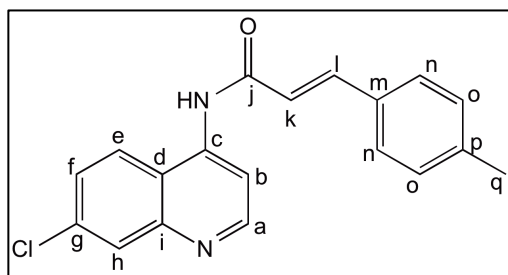
Beige solid (11 mg, 2%); mp 209-218 $^{\circ}$C; R_F (DCM/Me$_2$CO 3:1) 0.56; δ_H (400 MHz, DMSO-d$_6$) 10.38 (s, 1H, -NH-QN), 8.85 (d, J= 5.2 Hz, 1H, Ha), 8.49 (d, J= 9.2 Hz, 1H, He), 8.33 (d, J= 5.2 Hz, 1H, Hb), 8.05 (d, J= 2 Hz, 1H, Hh), 7.74-7.67 (m, 2H, Hf, Hl), 7.58 (d, J= 8.4 Hz, 2H, Hn), 7.29 (d, J= 8 Hz, 2H, Ho), 7.21 (d, J= 15.6 Hz, 1H, Hk), 2.35 (s, 3H, Hq); δ_C (100 MHz, DMSO-d$_6$) 164.9 (Cj), 152.2, 149.1, 141.9, 141.8, 140.0, 134.1, 131.8, 129.6, 128.0, 127.9, 126.3, 124.4, 120.4, 119.0, 111.5 (Ca-Ci, Ck-Cp), 20.9 (Cq); ESI-IT MS: m/z (M+H$^+$) 323.40 (C$_{19}$H$_{15}$ClN$_2$O requires 322.09); HPLC-DAD: rt = 9.30 min (% Area = 85%).

4-[(*p*-isopropyl)cinnamoyl]amino-7-chloroquinoline (2c)
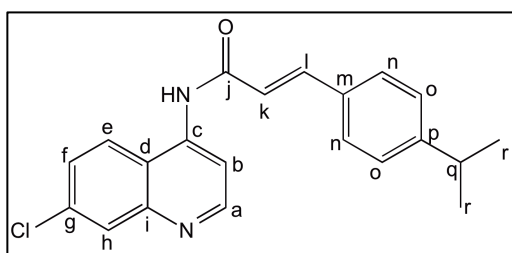
Beige solid (17 mg, 3%); mp 187-204 $^{\circ}$C; R_F (DCM/Me$_2$CO 3:1) 0.56; δ_H (400 MHz, DMSO-d$_6$) 10.40 (s, 1H, -NH-QN), 8.84 (d, J= 5.2 Hz, 1H, Ha), 8.49 (d, J= 9.2 Hz, 1H, He), 8.33 (d, J= 5.2 Hz, 1H, Hb), 8.05 (d, J= 2.4 Hz, 1H, Hh), 7.74-7.67 (m, 2H, Hf, Hl), 7.61 (d, J= 8.4 Hz, 2H, Hn), 7.35 (d, J= 8 Hz, 2H, Ho), 7.23 (d, J= 15.6 Hz, 1H, Hk), 2.96-2.90 (m, 1H, Hq), 1.22 (d, J= 6.8 Hz, 6H, Hr); δ_C (100 MHz, DMSO-d$_6$) 164.9 (Cj), 152.2, 150.8, 149.1, 141.9, 141.8, 134.1, 132.1, 128.0, 127.0, 126.7, 126.3, 124.4, 120.8, 118.9, 111.5 (Ca-i, Ck-p), 33.3, 23.5 (Cq-Cr); ESI-IT MS: m/z (M+H$^+$) 351.27 (C$_{21}$H$_{19}$ClN$_2$O requires 350.12); HPLC-DAD: rt = 11.4 min (% Area = 85%).

4-[(*p*-methoxy)cinnamoyl]amino-7-chloroquinoline (2d)
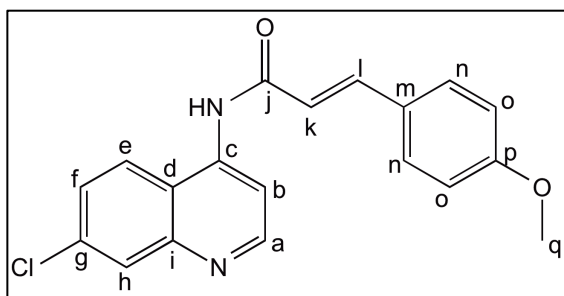
Beige solid (83 mg, 18%); mp 240-242 $^{\circ}$C; R_F (DCM/Me$_2$CO 3:1) 0.56; δ_H (400 MHz, DMSO-d$_6$) 10.34 (s, 1H, -NH-QN), 8.83 (d, J= 4.8 Hz, 1H, Ha), 8.49 (d, J= 8.8 Hz, 1H, He), 8.33 (d, J= 5.2 Hz, 1H, Hb), 8.05 (d, J= 2 Hz, 1H, Hh), 7.73-7.63 (m, 4H, Hf, Hl, Hn), 7.12 (d, J= 15.6 Hz, 1H, Hk), 7.04 (d, J= 8.8 Hz, 2H, Ho), 3.82 (s, 3H, Hq); δ_C (100 MHz, DMSO-d$_6$) 165.1 (Cj), 160.8, 152.2, 149.1, 141.9, 141.7, 134.0, 129.6, 127.9, 127.1, 126.2, 124.4, 118.9, 118.9, 114.5, 111.3

(Ca-Ci, Ck-Cp), 55.3 (Cq); ESI-IT MS: m/z (M+H$^+$) 339.33 (C$_{19}$H$_{15}$ClN$_2$O$_2$ requires 338.08); HPLC- DAD: rt= 6.80 min (% Area= 97%).

4-[(*m*-fluoro)cinnamoyl]amino-7-chloroquinoline (2e)
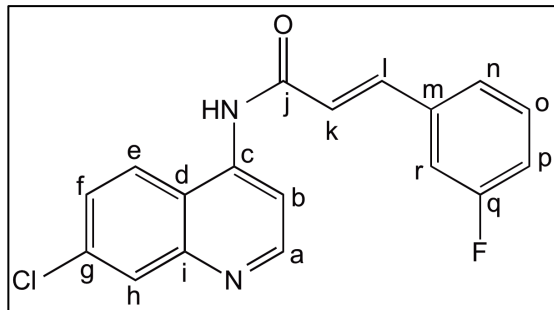
Yellow solid (4 mg, 1%); mp 181-190 ^{o}C; R$_F$ (DCM/Me$_2$CO 3:1) 0.56; δ$_H$ (400 MHz, DMSO-d$_6$) 10.45 (s, 1H, -NH-QN), 8.85 (d, J= 5.2 Hz, 1H, Ha), 8.47 (d, J= 8.8 Hz, 1H, He), 8.32 (d, J= 5.2 Hz, 1H, Hb), 8.06 (d, J= 2 Hz, 1H, Hh), 7.74-7.69 (m, 2H, Hf, Hl), 7.54-7.50 (m, 3H, Hn, Hp, Hr), 7.26-7.31 (m, 2H, Hk, Ho); δ$_C$ (100 MHz, DMSO-d$_6$) 164.5 (Cj), 163.6, 152.2, 149.1, 141.7, 140.5, 137.1, 134.1, 131.0, 128.0, 126.4, 124.3, 124.0, 123.1, 119.0, 116.6, 114.4, 111.6 (Ca-Ci, Ck-Cq); ESI-IT MS: m/z (M+H$^+$) 327.33 (C$_{18}$H$_{12}$ClFN$_2$O requires 326.06); HPLC-DAD: rt= 8.70 min (% Area = 98%).

4-[(*p*-fluoro)cinnamoyl]amino-7-chloroquinoline (2f)
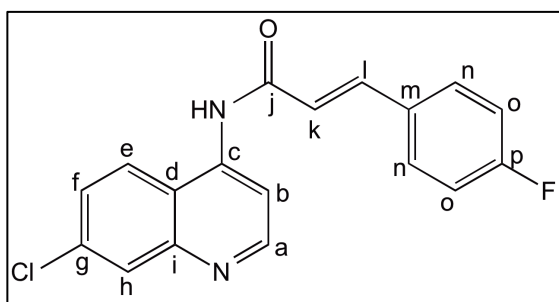
White solid (19 mg, 4%); mp 210-212 ^{o}C; RF (DCM/Me$_2$CO 3:1) 0.56; δ$_H$ (400 MHz, DMSO-d$_6$) 10.42 (s, 1H, -NH-QN), 8.85 (d, J= 4.8 Hz, 1H, Ha), 8.48 (d, J= 9.2 Hz, 1H, He), 8.32 (d, J= 4.8 Hz, 1H, Hb), 8.06 (d, J= 2 Hz, 1H, Hh), 7.78-7.70 (m, 4H, Hf, Hl, Hn), 7.33 (t, J= 9 Hz, 2H, Ho), 7.21 (d, J= 15.6 Hz, 1H, Hk); δ$_C$ (100 MHz, DMSO-d$_6$) 164.7 (Cj), 152.2, 149.1, 141.7, 140.7, 134.1, 131.2, 130.1, 128.0, 126.3, 124.4, 121.4, 119.0, 116.1, 115.9, 111.5 (Ca-Ci, Ck-Cp); ESI-IT MS: m/z (M+H$^+$) 327.11 (C$_{18}$H$_{12}$ClFN$_2$O requires 326.06); HPLC-DAD: rt = 8.50 min (% Area = 89%).

4-[(*p*-chloro)cinnamoyl]amino-7-chloroquinoline (2g)
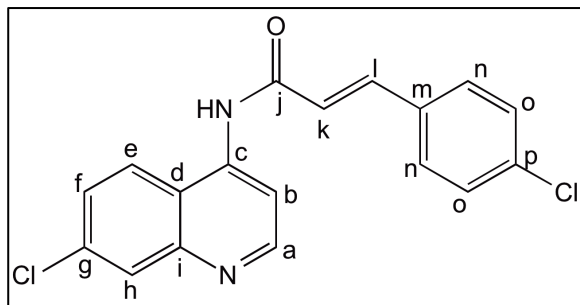
White solid (44 mg, 21%); mp 240-250 ^{o}C; R_F (DCM/Me$_2$CO 3:1) 0.56; δ_H (400 MHz, DMSO-d$_6$) 10.44 (s, 1H, -NH-QN), 8.85 (d, J= 5.2 Hz, 1H, Ha), 8.47 (d, J= 9.2 Hz, 1H, He), 8.32 (d, J= 4.8 Hz, 1H, Hb), 8.06 (d, J= 2 Hz, 1H, Hh), 7.72 (m, 4H, Hf, Hl, Hn), 7.55 (d, J= 8.4 Hz, 2H, Ho), 7.26 (d, J= 16 Hz, 1H, Hk); δ_C (100 MHz, DMSO-d$_6$) 164.6 (Cj), 152.2, 149.1, 141.7, 140.5, 134.5, 134.1, 133.5, 129.5, 129.1, 128.0, 126.3, 124.3, 122.3, 119.0, 111.6 (Ca-Ci, Ck-Cp); ESI-IT MS: m/z (M+H$^+$) 343.33 (C$_{18}$H$_{12}$Cl$_2$N$_2$O requires 342.03); HPLC-DAD: rt = 8.30 min (% Area = 96%).

4-[(*p*-bromo)cinnamoyl]amino-7-chloroquinoline (2h)
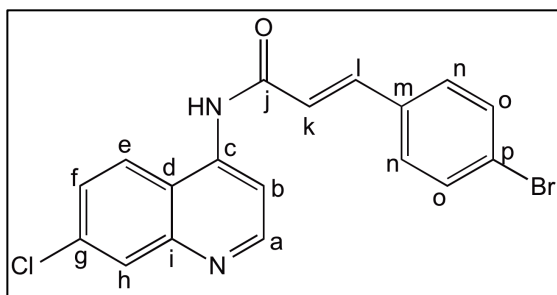
Green solid (38 mg, 7%); mp (dec.) 190 ^{o}C; R_F (DCM/Me$_2$CO 3:1) 0.56; δ_H (400 MHz, DMSO-d$_6$) 10.44 (s, 1H, -NH-QN), 8.85 (d, J= 5.2 Hz, 1H, Ha), 8.47 (d, J= 8.8Hz, 1H, He), 8.32 (d, J=4.8 Hz, 1H, Hb), 8.08 (d, J= 2.4 Hz,1H, Hh), 7.74-7.70 (m, 6H, Hf, Hl, Hn-o), 7.27 (d, J= 16 Hz, 1H, Hk); δ_C (100 MHz, DMSO-d$_6$) 164.6 (Cj), 152.2, 149.1, 141.7, 140.5, 134.1, 133.8, 132.0, 129.8, 128.0, 126.3, 124.3, 123.3, 122.4, 118.9, 111.6 (Ca-Ci, Ck-Cp); ESI-IT MS: m/z (M+H$^+$) 387.27 (C$_{18}$H$_{12}$BrClN$_2$O requires 385.98); HPLC-DAD: rt = 8.60 min (% Area = 97%).

4-[(*o*-nitro)cinnamoyl]amino-7-chloroquinoline (2i)
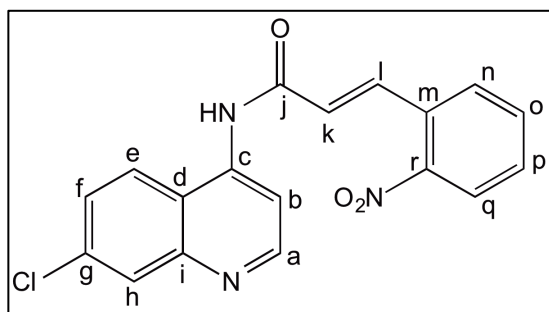
Yellow solid (36 mg, 7%); mp 168-200 ^{o}C; R_F (DCM/Me$_2$CO 3:1) 0.56; δ_H (400MHz,DMSO-d$_6$) 10.56 (s, 1H, -NH-QN), 8.87 (d, J= 5.2 Hz, 1H, Ha), 8.47 (d, J= 8.8 Hz, 1H, He), 8.32 (d, J= 4.8 Hz, 1H, Hb), 8.12 (d, J= 8 Hz, 1H, Hq), 8.07 (d, J= 2 Hz, 1H, Hh), 7.99 (d, J= 15.6 Hz, 1H, Hl), 7.88-7.86 (m, 2H), 7.76-7.69 (m, 2H, Hf, Hn-p), 7.25 (d, J= 15.6 Hz, 1H, Hk); δ_C (100 MHz, DMSO-d$_6$) 163.9 (Cj), 152.2, 149.0, 148.2, 141.4, 137.0, 134.1, 133.9, 130.7, 129.8, 128.8, 128.0, 126.4, 126.1, 124.8, 124.3, 119.0, 111.7 (Ca-Ci, Ck-Cr); ESI-IT MS: m/z

(M+H$^+$) 354.33 (C$_{18}$H$_{12}$ClN$_3$O$_3$ requires 353.06); HPLC-DAD: trt = 7.90 min (% Area= 97%).

4-[(*m*-nitro)cinnamoyl]amino-7-chloroquinoline (2j)
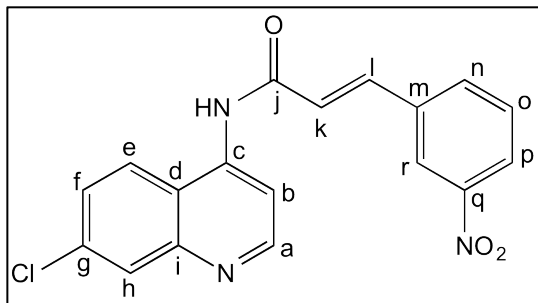
White solid (11 mg, 2%); mp (dec.) 240-247 °C; R$_F$ (DCM/Me$_2$CO 3:1) 0.56; δ$_H$ (400 MHz, DMSO-d$_6$) 10.49 (s, 1H, -NH-QN), 8.86 (d, J= 4.8 Hz, 1H, Ha), 8.53 (m, 1H, Hr), 8.49 (d, J= 9.2 Hz, He), 8.34 (d, J= 5.2Hz, 1H, Hb), 8.27 (dd, J= 8.2 Hz, J= 1.2 Hz, 1H, Hp), 8.11 (d, J= 8 Hz, 1H, Hn), 8.07 (d, J= 2 Hz, 1H, Hh), 7.84 (d, J= 16 Hz, 1H, Hl), 7.80-7.73 (m, 2H, Hf, Ho), 7.46 (d, J= 16 Hz, 1H, Hk); δ$_C$ (100 MHz, DMSO-d$_6$) 164.2 (Cj), 152.2, 149.1, 148.2, 141.5, 139.4, 136.3, 134.5, 134.2, 130.6, 128.0, 126.4, 124.4, 124.3, 121.5, 118.9, 111.5 (Ca-Ci, Ck-Cr); ESI- IT MS: m/z (M+H$^+$) 354.53 (C$_{18}$H$_{12}$ClN$_3$O$_3$ requires 353.06); HPLC-DAD: rt = 7.20 min (% Area = 100%).

4-[(*p*-nitro)cinnamoyl]amino-7-chloroquinoline (2k)
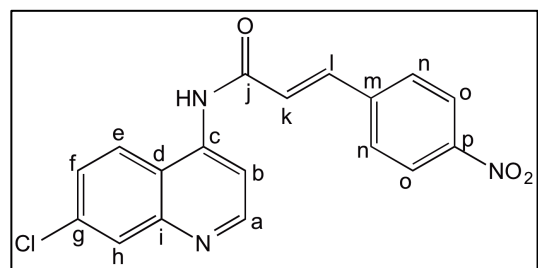
Beige solid (9 mg, 5%); mp desc. 205 °C; R$_F$ (DCM/Me$_2$CO 3:1) 0.56; δ$_H$ (400 MHz, DMSO-d$_6$) 10.58 (s, 1H, -NH-QN), 8.87 (d, J= 5.2 Hz, 1H, Ha), 8.48 (d, J= 9.2 Hz, 1H, He), 8.35-8.32 (m, 3H, Hb, Ho), 8.07 (d, J= 2.4 Hz, 1H, Hh), 7.94 (d, J= 8.8 Hz, 2H, Hn), 7.83 (d, J= 16 Hz, 1H, Hl), 7.74 (dd, J= 9 Hz, J= 2 Hz, 1H, Hf), 7.44 (d, J= 15.6 Hz, 1H, Hk); δ$_C$ (100 MHz, DMSO-d$_6$) 164.1 (Cj), 152.2, 149.1, 147.8, 141.5, 141.0, 139.3, 134.2, 128.9, 128.0, 126.4, 125.8, 124.3, 124.2, 119.0, 111.7 (Ca-Cl, Ck-Cp); ESI-IT MS: m/z (M+H$^+$) 354.27 (C$_{18}$H$_{12}$ClN$_3$O$_3$ requires 353.06); HPLC-DAD: rt = 7.20 min (% Area= 92%).

2.2.2. *In vitro* assessment of inhibition of β-H formation

The inhibition of β-H formation assay was performed as previously described.[7, 8] Briefly, in a 96-microwell plate it was respectively added i) 50 μL of different concentrations (0.1-1 mM) of test compounds dissolved in DMSO, in triplicate, and ii) 50 μL hemin chloride dissolved in DMSO (5.2 mg/mL). Controls contained equal volumes of water or DMSO. β-H formation was initiated by the addition of acetate buffer 0.2 M (100 μL, pH 4.4), following plates were incubated at 37 ^{o}C for 48 h, and subsequently, they were centrifuged at 3000 rpm for 15 min (SIGMA 3-30K). After discarding the supernatant, the pellet was washed four times with DMSO (3×200 μL), and finally dissolved in 0.2 M aq. NaOH (200 μL). The solubilized aggregates were further diluted 1:6 with 0.1 M aq. NaOH and absorbances recorded at 405 nm on a Biotek Powerwave XS with software Gen5 1.07.

2.3. References

1. Hong, S. Y.; Oh, J. E.; Lee, K.-H. Effect of d-amino acid substitution on the stability, the secondary structure, and the activity of membrane-active peptide. *Biochem Pharmacol* **1999,** 58, 1775-1780.

2. Müller-Schiffmann, A.; Petsch, B.; Leliveld, S. R.; Muyrers, J.; Salwierz, A.; Mangels, C.; Schwarzinger, S.; Riesner, D.; Stitz, L.; Korth, C. Complementarity determining regions of an anti-prion protein scFv fragment orchestrate conformation specificity and antiprion activity. *Mol Immunol* **2009,** 46, 532-540.

3. Price, C. C.; Leonard, N. J.; Peel, E. W.; Reitsema, R. H. Some 4-Amino-7-chloroquinoline Derivatives1. *J Am Chem Soc* **1946,** 68, 1807-1808.

4. Albericio, F.; Cases, M.; Alsina, J.; Triolo, S. A.; Carpino, L. A.; Kates, S. A. On the Use of PyAOP, a phosphonium salt derived from HOAt, in Solid-Phase Peptide Synthesis. *Tetrahedron Lett* **1997,** 38, 4853-4856.

5. Han, S.-Y.; Kim, Y.-A. Recent development of peptide coupling reagents in organic synthesis. *Tetrahedron* **2004,** 60, 2447-2467.

6. Lassen, M. J. K. Evolution of amide bond formation. *ARKIVOC* **2010,** 8.

7. Baelmans, R.; Deharo, E.; Munoz, V.; Sauvain, M.; Ginsburg, H. Experimental conditions for testing the inhibitory activity of chloroquine on the formation of beta-hematin. *Exp Parasitol* **2000,** 96, 243-8.

8. Barazarte, A.; Lobo, G.; Gamboa, N.; Rodrigues, J. R.; Capparelli, M. V.; Alvarez-Larena, A.; Lopez, S. E.; Charris, J. E. Synthesis and antimalarial activity of pyrazolo and pyrimido benzothiazine dioxide derivatives. *Eur J Med Chem* **2009,** 44, 1303-10.

9. Shenai, B. R.; Sijwali, P. S.; Singh, A.; Rosenthal, P. J. Characterization of native and recombinant falcipain-2, a principal trophozoite cysteine protease and essential hemoglobinase of Plasmodium falciparum. *J Biol Chem* **2000,** 275, 29000-10.

10. Sijwali, P. S.; Shenai, B. R.; Gut, J.; Singh, A.; Rosenthal, P. J. Expression and characterization of the Plasmodium falciparum haemoglobinase falcipain-3. *Biochem J* **2001,** 360, 481-9.

11. Vale, N.; Prudêncio, M.; Marques, C. A.; Collins, M. S.; Gut, J.; Nogueira, F.; Matos, J.; Rosenthal, P. J.; Cushion, M. T.; do Rosário, V. E.; Mota, M. M.; Moreira, R.; Gomes, P. Imidazoquines as antimalarial and antipneumocystis agents. *J Med Chem* **2009,** 52, 7800-7.

12. ChemAxon. MarvinSketch 5.2.2. http://www.chemaxon.com. **2009**.

13. Lavrado, J.; Gani, K.; Nobre, P. A.; Santos, S. A.; Figueiredo, P.; Lopes, D.; Rosário, V.; Gut, J.; Rosenthal, P. J.; Moreira, R.; Paulo, A. Bis-alkylamine quindolone derivatives as new antimalarial leads. *Bioorg Med Chem Lett* **2010,** 20, 5634-7.

14. Sandlin, R. D.; Carter, M. D.; Lee, P. J.; Auschwitz, J. M.; Leed, S. E.; Johnson, J. D.; Wright, D. W. Use of the NP-40 detergent-mediated assay in discovery of inhibitors of beta-hematin crystallization. *Antimicrob Agents Ch* **2011,** 55, 3363-9.

15. Sabnis, Y. A.; Desai, P. V.; Rosenthal, P. J.; Avery, M. A. Probing the structure of falcipain-3, a cysteine protease from Plasmodium falciparum: comparative protein modeling and docking studies. *Protein Sci* **2003,** 12, 501-9.

16. Lin, A. J.; Miller, R. E. Antimalarial Activity of New Dihydroartemisinin Derivatives. 6. .alpha.-Alkylbenzylic Ethers. *J Med Chem* **1995,** 38, 764-770.

Chapter 3

*HE[DI]CIN*s against a malaria-like disease

3.0. Preamble

*HEDICIN*s and *HECIN*s were also evaluated against another parasitic cysteine protease, babesipain-1 from *Babesia bigemina*, one of the causing agents of babesiosis, a malaria-like disease that mainly affects cattle and represents a huge economic burden in the cattle industry.[1, 2] *In vitro* evaluation of babesipain-1 inhibition by *HEDICIN*s and *HECIN*s was carried out by Dr. Ana Domingos's team at the *Instituto de Higiene e Medicina Tropical – Universidade Nova de Lisboa*. The doctoral candidate performed a parallel study *in silico*, in order to evaluate the interaction of *HEDICIN*s and *HECIN*s with babesipain-1 at the atomic level bbspn-1. As such, and given that there was no three-dimensional (3D) structure available for babesipain-1, a homology model was built and validated, followed by the respective molecular docking of the ligands.

3.1. Babesiosis and Babesia parasites – brief overview

Babesiosis is a worldwide distributed disease caused by protozoans of the genus *Babesia*, which is transmitted by *Rhipicephalus* (*Boophilus)* sp. ticks.[2] The symptoms of babesiosis included fever, anemia, hemoglobinuria, malaise, and anorexia.[2] There are several species which cause babesiosis, but the two species which cause more economical impact are *Babesia bovis* and *Babesia bigemina*.[2] The reproductive life cycle of *Babesia* is similar to that of *Plasmodia* parasites. The sporogony and the gamogony takes places in the invertebrate host while merogony, the asexual dividing stage, occurs within the erythrocyte of the human host (Fig. 22).[3, 4]

Vaccines containing live attenuated parasites are the main strategy to control this disease but failures of protective immunity provided by vaccination have been observed since these vaccines do not offer cross protection against the different variants in the field.[5, 6] Moreover, chemoprophylaxis is used as short-term protection during epidemics when cattle are being relocated, or to treat pregnant cows. Some examples of drugs used to treat babesiosis are diminazene aceturate (**XXVIII**) or imidocarb (**XXIX**), and in clinical cases clindamycin (**XXX**) and quinine (**XXXI**), the latter two are also known to treat against malaria.[4] Nonetheless, there is the need for a more specific, fast acting, and safe chemotherapy to combat the disease.[7]
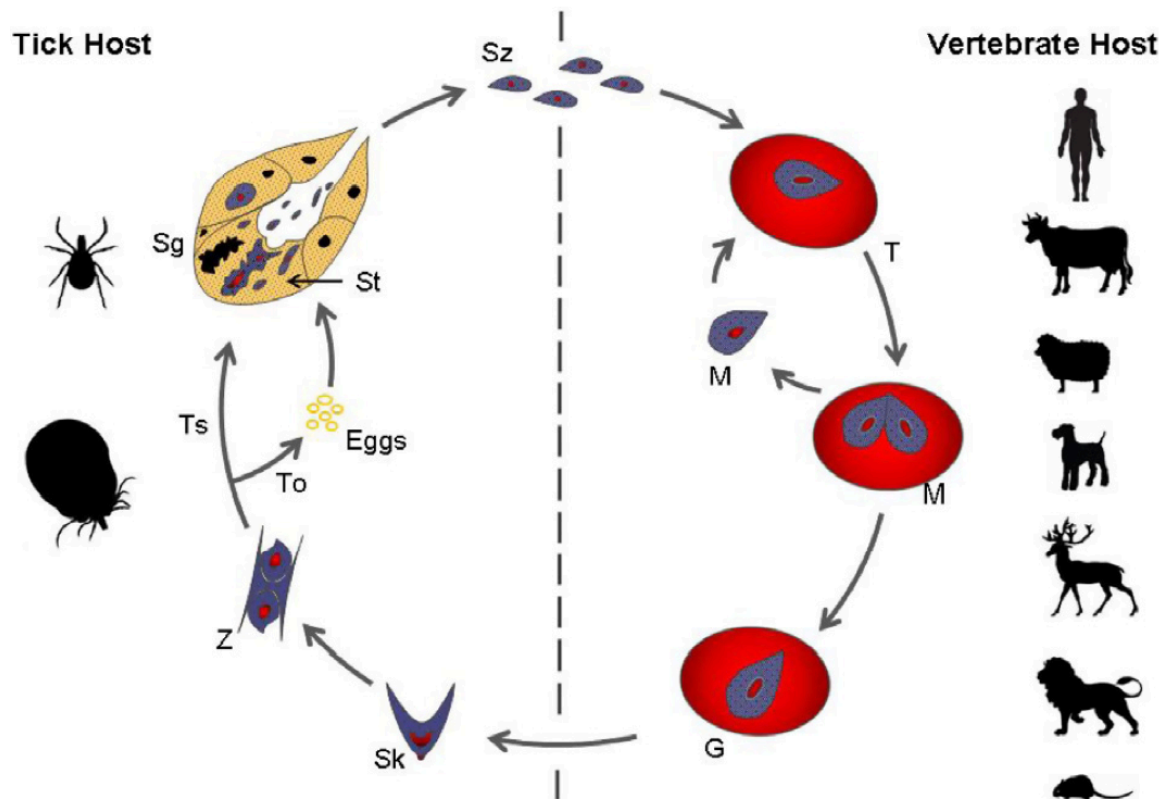
Figure 22. *Babesia* life cycle: sporozoites (Sz) differentiate into trophozoites (T) when they enter into the vertebrate host's blood stream. Later, T asexually divide into merozoites (M) which exit the erythrocyte and invade other cells and continue to replicate. Some M stop division and transform into pre-gametocytes (G). When G are taken into the invertebrate host by a tick feeding, they differentiate into Strahlenkörper (Sk); Sk fuse and form zigotes (Z), which undergo meiosis given rises to kinetes (Ts and To). To represents kinetes which go into the tick's ovaries and eggs, whereas Ts represents kinetes which transform in the salivary glands (Sg) of the tick into Sz ready to infect the next vertebrate host.[2]

(XXVIII)

(XXIX)

(XXX)

(XXXI)
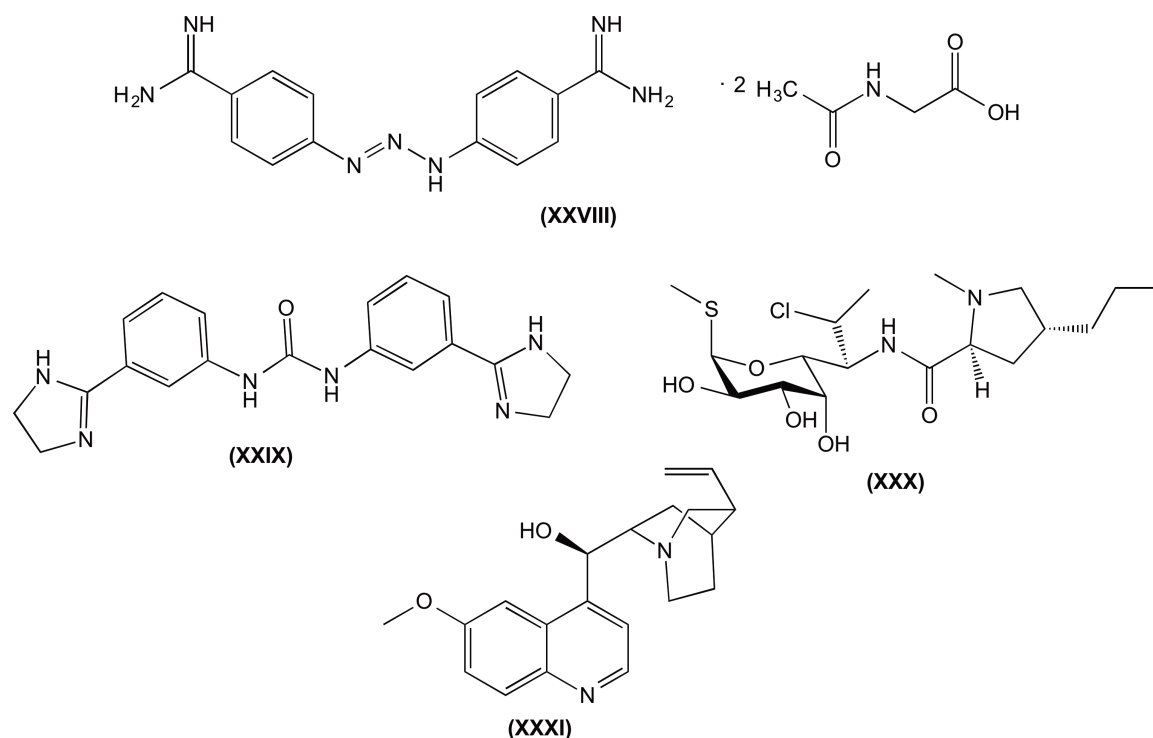
Like *Plasmodia*, *B. bigemina* is a protozoan of the *phylum Apicomplexa*.[4] The sequencing of the genome of *B. bigemina* is a project in active progress[8] and the information obtained to this point has revealed potential targets that may be useful for the development of new chemotherapy strategies against babesiosis. For instance, three cysteine proteases from *B. bigemina*, BbiCPL1 to BbiCPL3, have been identified which belong to the same cysteine protease family and share many features with papain.[9] These features include: i) 20–23 amino acid putative transmembrane domain, ii) the ERFNIN and GNFD pro-sequence motifs typical of cathepsin L-like cysteine proteases, iii) the main catalytic residues, for instance, histidine, cysteine and asparagine, and iv) six cysteine residues predicted to form disulfide bonds in the mature domain of the protease.[9]

BbiCPL1 (bbspn-1) is the first cysteine protease from a piroplasm described to possess proteolytic activity.[9] It is believed to act in the cytosol at an optimum acidic pH of 5.5, and it is inhibited by leupeptin and E64,[7, 9] known inhibitors of cysteine proteases. In this context and based on the fact that i) the roles of cysteine proteases in protozoan parasites are often associated with cell invasion and rupture[10], and ii) it has been found that modest falcipain inhibitors[11] are more potent inhibitors of bbspn-1 than of FP2,[1] some *HEDICIN*s and *HECIN*s were further evaluated against bbspn-1.

3.2. *In vitro* evaluation of HE[DI]CINs as bbspn-1 inhibitors

*HE[DI]CIN*s were evaluated following previously described methods.[1] Results obtained (Table 5) demonstrated that *HEDICIN*s and *HECIN*s are generally more efficient inhibitors of bbspn-1 (IC_{50} = 9.7-35.8 µM and IC_{50} = 9.8-48.3 µM, respectively) than of FP2 (IC_{50} = 23.1->50 µM and IC_{50} = 14.2->50 µM, respectively). Close analysis of the data shows:

- *HEDICIN*s and *HECIN*s displayed about the same range of activities IC_{50} = 9.7-35.8 µM and IC_{50} = 9.8-48.3 µM, respectively.

- Electro-donating substituents in the cinnamoyl moiety seem to be preferred in *HECIN*s series. For instance, the *p*-OMe substituted compound **2d** is more active (IC_{50} = 9.8 µM) than the *p*-Me analogue **2b** (IC_{50} = 13.4 µM), in turn more active than the unsubstituted derivative **2a** (IC_{50} = 20.3 µM). Such pattern is not observed in *HEDICIN*s series.

- *HEDICIN*s results suggest that *meta* substitution is preferred over *ortho* substitution in the cinnamoyl moiety. For instance, *m*-NO_2 derivatives **1k** (IC_{50} = 10.2 µM) was more active than *o*-NO_2 **1j** (IC_{50} = 18.6 µM). Similar results were observed against FP2.

- No significant different was observed between *meta* and *para* substitution in *HEDICIN*s series. For example, the *p*-F **1g** and the *m*-F **1f** presented IC_{50} of 28.1 µM and 29.1 µM, respectively. The same is observed in *HECIN*s series.

- Contrary to *HECIN*s results, the best inhibitor of *HEDICIN*s displayed electro-withdrawing group (*p*-Cl **1h**, IC_{50} = 9.7 µM) and the worst presented an electro-donating group (*p*-OMe **1d**, IC_{50} = 35.8 µM) in the *para* position.

- No clear correlation was found between the lipophilicity of the compounds (clog P; see table 3 in chapter 2)[12] or Charton steric parameter (v)[13] of *p*-alkyl substituent on the cinnamoyl moiety (0.0, 0.52 and 0.76 for alkyl substituents of compound **1a**, **1b**, and **1c**, respectively), and compounds' ability to inhibit babesipain-1.

Table 5. *In vitro* data on test compounds, *HEDICIN*s **1** and *HECIN*s **2**, as bbspn-1 inhibitors. Compounds' activity as FP2 inhibitors (determined as described in chapter 2) is also displayed, for better comparison.

*HEDICIN*s	R	bbspn-1 IC$_{50}$(μM)	FP2 IC$_{50}$ (μM)	*HECIN*s	R	bbspn-1 IC$_{50}$(μM)	FP2 IC$_{50}$ (μM)
1a	H	30.8 ± 12.7	19.6 ± 0.4	2a	H	20.3 ± 3.1	>50
1b	*p*-Me	31.3 ± 11.2	>50	2b	*p*-Me	13.4 ± 2.3	28.5 ± 0.3
1c	*p*-iPr	27.7 ± 10.9	>50				
1d	*p*-OMe	35.8 ± 12.2	>50	2d	*p*-OMe	9.8 ± 0.6	>50
1f	*m*-F	29.1 ± 5.7	23.1 ± 1.6	2e	*m*-F	20.9 ± 2.2	>50
1g	*p*-F	28.1 ± 7.6	50.0	2f	*p*-F	17.4 ± 1.5	>50
1h	*p*-Cl	9.7 ± 3.0	>50	2g	*p*-Cl	17.9 ± 4.2	41.3 ± 1.2
1i	*p*-Br	11.0 ± 2.3	48.3 ± 2.4	2h	*p*-Br	14.2 ± 5.2	33.1 ± 3.0
1j	o-NO$_2$	18.6 ± 8.8	>50				
1k	*m*-NO$_2$	10.2 ± 3.5	28.1 ± 3.5	2j	*m*-NO$_2$	48.3 ± 14.7	14.2 ± 0.4
E64[a]		13.7 ± 3.7	24.6 ± 1.2			13.7 ± 3.7	24.6 ± 1.2

[a] E64 values are in the nM level.

3.3. *In silico* study of bbspn-1 inhibition by *HE[DI]CIN*s

A better understanding of the distinctive features of FP2 versus bbspn-1, and of their respective interactions with compounds **1** and **2**, was pursued through an *in silico* study. This study comprised two major tasks: 1) generation of the bbspn-1 model structure by homology modeling, and 2) compound-model enzyme docking studies.

3.3.1. Generation and validation of the bbspn-1 model structure by homology modeling

The number of crystallographic structures available in Protein Data Bank (PDB) (http://www.pdb.org/pdb/home/home.do), though high, is not comparable to the huge number of sequences entries encountered in the Universal Protein Resource (Uniprot) database (http://www.uniprot.org/). The elucidation of the 3D structure of a protein by X-ray diffraction crystallography is a high-demanding and frequently unsuccessful endeavor. In addition, some proteins are too large for NMR analysis or unable to be crystallized for X-ray diffraction.[14] In those cases where the 3D structure of a protein of interest is unavailable, but the protein's sequence is known, a model structure may be predicted by *in silico* homology modeling, based on the sequence similarity to other proteins whose 3D structures are available. Homology modeling thus provides a 3D structure of the desired protein that can be used to carry out studies such as structure-based drug design, analysis of protein functions, ligand-protein interactions, and protein-protein interactions, among others.[14]

In order to build the 3D structure of bbspn-1, i) the protein's sequence was obtained, ii) a template search was carried out to identify homolog sequences using the mature site of bbspn-1, iii) the corresponding homolog structures were aligned with that of bbspn-1 to generate several model candidates, and finally, iv) the generated models were validated using a toolbox of validation techniques.

i) Obtaining the sequence of bbspn-1

The complete sequence of bbspn-1 was searched using the Uniprot database. Once the entire sequence (458 amino acids) was retrieved, the enzyme's mature site was identified based on results previously reported by Domingos *et al*., and the prodomain of the protein was cleaved off (Fig. 23).[9] Accordingly, the mature sequence contained 217 amino acids starting from residue Ser242. For simplicity purposes, the numbering of the mature sequence was started from 1 for the following studies performed. Correspondingly, Ser242 and His458 were addressed as Ser1 and His217, respectively.

```
         10          20          30          40          50          60
MSGTRSYMSN DDHHYICSDE VDRDTALIGT ARRRRTCTGN KIAICVLSLA AIGAITTGIV

         70          80          90         100         110         120
LLIVRSTKDP EPPKLMEPRK FVEPRKEMYE EPTPPHGGCL TSSDLLEELN EFYKLGGISS

        130         140         150         160         170         180
YNDEELCRFV HFKRLEKRYN RRYTDVAARH AGFLNFRRNM AIVEEHKKKA NATYTKGPNH

        190         200         210         220         230         240
FFDMDVKELA SKLLHPIDVG QNFQEYGSLG EVIVTKDNQE TYSLLKGHTD DPYAVDVGSK

        250         260         270         280         290         300
VSFENVNWRT PGAVSPVKDQ GHCGSCWAFA AIGAVESLFR MEKHQYLTFS EQELVSCDLQ

        310         320         330         340         350         360
SSGCGGGFSD FALEYIKKNG VTSSEDWNYE ASNGECSAHH GIRYYIKDYV SARGANVAST

        370         380         390         400         410         420
LLVRAPTVVY VAFTEDLFHY SGGVYNGECP EEQLNHAVLL VGEGYDATVK KRYWLIKNSW

        430         440         450
GSDWGEDGFI RLERTDKGYD KCGVLSFGFI PTGAVLAH
```

Figure 23. Sequence of bbspn-1 found in Uniprot. Amino acids 1 to 247 respresent the prodomain and Amino acids 242 to 458 represent the mature site of the enzyme according to Domingos *et al.*[9]

ii) Template search and selection

A template search using BLAST was conducted, using the sequence of the mature site of bbspn-1 and PDB as database. Based on the search results, the only homolog sequences selected were the ones which complied with the following set restrictions: a) E-value below 10^{-40}; b) query coverage > 90 % and sequence identity > 35% or query coverage > 85% and sequence identity > 40%; c) a PDB structure with a resolution < 2.5 Å without missing residues in the active site and with bound ligand (See table 6). The quality of the built model depends on the quality of the sequence alignment and structure template chosen, for instance, the closest the E value to zero the highest the level of the sequence similarity.[15] Therefore, the previous set restrictions would encourage the probability of obtaining reliable results in further studies carried to achieve the desired 3D structure of bbspn-1 through homology model.

Table 6. Homolog sequences identified with BLAST according to the established search criteria.

PDB code (chain used)	Uniprot code	Organism	Identity %	Coverage %	PDB resolution (Å)	E-value
1EWM (A)	P25779	*Trypanosoma cruzi*	43	91	2.00	1×10^{-41}
1S4V (A)	O65039	*Ricinus communis*	41	87	2.00	2×10^{-43}
2BDZ (C)	P84346	*Jacaratia mexicana*	38	95	2.10	4×10^{-43}
2OUL (A)	Q9N6S8	*Plasmodium falciparum*	41	94	2. 20	1×10^{-46}
2P7U (A)	Q95PM0	*Trypanosomo brucei rhodesiense*	43	90	1.65	2×10^{-42}
3BWK (B)	Q9NAW4	*Plasmodium falciparum*	41	94	2.42	3×10^{-45}

Multiple sequence alignment performed using *PSI-coffee*[16] of the sequence of bbspn-1 and the selected templates is presented in Figure 24. For simplicity, the numbering was started at 1 for all the alignments performed and the numbering referred in the text corresponds to bbspn-1 sequence. Based on their sequences, bbspn-1 and the six homologs are classifiable as cysteine peptidases belonging to Clan CA, subfamily C1A. These peptidases present the catalytic residues glutamine (Gln19), cysteine (Cys25), histidine (His55), and asparagine (Asn177) that follow always the same order.[17] Alignment of bbspn-1 with the corresponding homolog sequences demonstrated strict conservation of the catalytic residues, significant similarities amongst the catalytic sites of the proteins and low polymorphism in the surrounding areas (Fig. 24). For instance, the tryptophan (Trp179) and Gln (Gln19) known to form the "oxyanion hole" are preserved.[18] In addition, the 6 cysteine residues (Cys22, Cys63, Cys56, Cys95, Cys148, Cys201) predicted to form disulfide bonds are also observed. In addition, according to table 7 the selected templates present a significant number of residues in the active site as compared to bbspn-1. The proteases, which possess the highest similitude to bbspn-1, are 1S4V and 2P7U.

Table 7. Sequence similarity against the active site of bbspn-1.

bbspn-1	S1'						S1				S2					S3				
	V 130	F 132	T 133	F 137	H 155	W 179	Q 19	G 23	C 63	G 64	F 67	S 68	Y 129	L 153	F 206	Q 59	S 60	S 61	G 65	G 66
1EWM (A)	V	A	S	M	H	W	Q	G	C	S	L	M	A	L	E	T	D	S	G	G
1S4V (A)	I	A	G	Q	H	W	Q	G	C	N	L	M	A	L	E	Q	N	Q	G	G
2BDZ (C)	T	S	R	Q	H	W	Q	G	C	D	Y	Q	V	T	S	R	S	H	G	G
2OUL (A)	V	V	S	A	H	W	Q	G	C	N	L	I	S	L	D	K	N	Y	G	G
2P7U (A)	V	A	T	M	H	W	Q	G	C	G	L	M	A	L	A	I	D	F	G	G
3BWK (B)	I	A	S	A	H	W	Q	G	C	Y	Y	I	S	P	E	K	N	N	G	G

```
bbspn1     ------------------SFENVNWRTPGAVSPVKDQGHCGSCWAFAAI 31
1ewm_A     ------------------APAAVDWRARGAVTAVKDQGQCGSCWAFSAI 31
1s4v_A     T-----------------VPASVDWRKKGAVTSVKDQGQCGSCWAFSTI 32
2bdz_C     ------------------YPESIDWREKGAVTPVKNQNPCGSCWAFSTV 31
2oul_A     QMN-YEEVIKKYRGE-ENFDHAAYDWRLHSGVTPVKDQKNCGSCWAFSSI 48
2p7u_A     ------------------APAAVDWREKGAVTPVKDQGQCGSCWAFSTI 31
3bwk_B     YEANYEDVIKKYKPADAKLDRIAYDWRLHGGVTPVKDQALCGSCWAFSSV 50

bbspn1     GAVESLFRMEKHQYLTFSEQELVSCDL-QSSGCGGGFSDFALEYIKK--N 78
1EWM_A     GNVECQWFLAGHPLTNLSEQMLVSCDK-TDSGCSGGLMNNAFEWIVQENN 80
1S4V_A     VAVEGINQIKTNKLVSLSEQELVDCDTDQNQGCNGGLMDYAFEFIKQ--R 80
2BDZ_C     ATIEGINKIITGQLISLSEQELLDCER-RSHGCDGGYQTTSLQYVVD--N 78
2OUL_A     GSVESQYAIRKNKLITLSEQELVDCSF-KNYGCNGGLINNAFEDMIE--L 95
2P7U_A     GNIEGQWQVAGNPLVSLSEQMLVSCDT-IDFGCGGGLMDNAFNWIVNSNG 80
3BWK_B     GSVESQYAIRKKALFLFSEQELVDCSV-KNNGCYGGYITNAFDDMID--L 97

bbspn1     -GVTSSEDWNYEASNGE---CSAH-HGIRYYIKDYVSARGANV--ASTLL 121
1EWM_A     GAVYTEDSYPYASGEGISPPCTTSGHTVGATITGHVELPQDEAQIAAWLA 130
1S4V_A     GGITTEANYPYEAYDGT--CDVSKENAPAVSIDGHENVPENDENALLKAV 128
2BDZ_C     -GVHTEREYPYEKKQGR--CRAKDKKGPKVYITGYKYVPANDEISLIQAI 125
2OUL_A     GGICPDGDYPYVSDAPN--LCNIDRCTEKYGIKNYLSVPDNKL--KEALR 141
2P7U_A     GNVFTEASYPYVSGNGEQPQCQMNGHEIGAAITDHVDLPQDEDAIAAYLA 130
3BWK_B     GGLCSQDDYPYVSNLPE--TCNLKRCNERYTIKSYVSIPDDKF--KEALR 143

bbspn1     VRAPTVVYVAFT-EDLFHYSGGVYNGECPEEQLNHAVLLVGEGYDAT--- 167
1EWM_A     VNGPVAVAVDAS--SWMTYTGGVMTSCVS-EQLDHGVLLVGYNDSA---- 173
1S4V_A     ANQPVSVAIDAGGSDFQFYSEGVFTGSCG-TELDHGVAIVGYGTTI---- 173
2BDZ_C     ANQPVSVVTDSRGRGFQFYKGGIYEGPCG-TNTDHAVTAVGYGK------ 168
2OUL_A     FLGPISISVAVS-DDFAFYKEGIFDGECG-DQLNHAVMLVGFGMKEIVNP 189
2P7U_A     ENGPLAIAVDAT--SFMDYNGGILTSCTS-EQLDHGVLLVGYNDAS---- 173
3BWK_B     YLGPISISIAAS-DDFAFYRGGFYDGECG-AAPNHAVILVGYGMKDIYNE 191

bbspn1     -----VKKRYWLIKNSWGSDWGEDGFIRLERTDK-GYDKCGVLSFGFIPT 211
1EWM_A     ------AVPYWIIKNSWTTQWGEEGYIRIAKGS----NQCLVKEEASSAV 213
1S4V_A     -----DGTKYWTVKNSWGPEWGEKGYIRMERGISDKEGLCGIAMEASYPI 218
2BDZ_C     --------TYLLLKNSWGPNWGEKGYIRIKRASGRSKGTCGVYTSSFFPI 210
2OUL_A     LTKKGEKHYYYIIKNSWGQQWGERGFINIETDESGLMRKCGLGTDAFIPL 239
2P7U_A     ------NPPYWIIKNSWSNMWGEDGYIRIEKGT----NQCLMNQAVSSAV 213
3BWK_B     DTGRMEKFYYYIIKNSWGSDWGEGGYINLETDENGYKKTCSIGTEAYVPL 241

bbspn1     GAVLAH 217
1EWM_A     ----VG 215
1S4V_A     KKSSNN 224
2BDZ_C     ----KG 212
2OUL_A     ----IE 241
2P7U_A     ----VG 215
3BWK_B     -----L 242
```

Figure 24. Multiple sequence alignment performed with *PSI-coffee* mode of *T-Coffee* of the amino acid sequence of bbspn-1 and the selected templates. The boxes indicate the Cys25, His155, and Asn177 catalytic regions, correspondingly. The arrows show the catalytic residues glutamine (Gln19), cysteine (Cys25), histidine (His155) and asparagine (Asn177), respectively.

All these described characteristics make the selected 3D structures suitable templates to build the 3D model structure of bbspn-1. Moreover, bbspn-1 will present a higher probability to fold in the same structure of the selected template if it has a percent sequence identity above ~30% and the length of the templates sequence, individually, fall below 250 as compared to the homolog protein (See figure 25).[14] In other words, the higher the sequence similarity between the selected 3D template obtained from the PDB and bbspn-1, the more reliable will be the obtained results. However, since BLAST search only resulted proteins with identical residues to bbspn-1 closed to the limit but within the safe zone (Fig. 25), building the 3D structure of bbspn-1 through homology modeling represented a major challenge.
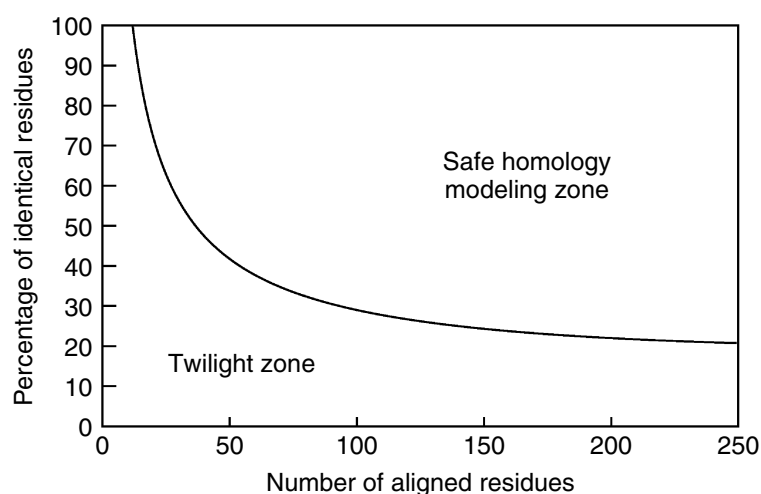
Figure 25. The safe zone defined for homology modeling.[14]

iii) Sequence alignments and homology models generation

Homology models were built by two different strategies: a) single template: using one available 3D structure homolog to bbspn-1, and b) multiple templates: combining up to three 3D structures homolog to bbspn-1. Selected templates were carefully aligned with bbspn-1 using *PSI-coffee.*[16] Results demonstrated alignment scores, reflecting the expected accuracy of the alignment, up to 93%. Homology modeling calculations were done using Modeller v.9.11 (http://salilab.org/modeller/about_modeller.html) and *PSI-coffee* alignments. One hundred models were generated for each template combination. As previous studies reported in the literature, Modeller performed best when using combinations of two or three templates as compared to a single template since it can utilize information from multiple templates.[19]

iv) Validating the built 3D structure of bbspn-1

The quality assessment basically predicts substantial errors in the built model analyzing whether energy or structural parameters of the built models are comparable to those already reported experimental 3D structures.[20] Multiple validations tools were used to assess the built 3D structures of babesipain-1 and enhance the probability to find possible errors non-detected by a single validation tool. For instance, ProSA measurement of model quality highly depends on protein size; the higher the protein size, the lowest the ProSA accuracy. Therefore, using multiple validation scores will suffice for the lack of accuracy of some validation tools. In this work, resulted homology models were assessed not only by Modeller 9.11 Z-score, but also by PROCHECK,[21] ProQ,[22] QMEAN,[20] and ProSA[17, 18] (See tables 8-9) and visualization of the biomolecular system of the different models built. In addition, all the structures presenting a Modeller Z-DOPE >-1.00 were disregarded. Accordingly, the best models were expected to present i) >90 % of the amino acids in the most favorable region of the Ramachandran plot as determined by PROCHECK; ii) a Prosa Z-score which agrees with the scores obtained for the PDB structures of the templates used to derive the corresponding model; iii) an LG score > 5 and a Maxsub score > 0.5 as determined by ProQ; and iv) a QMEAN score > 0.75. These validation score restrictions will help in the selection of the most accurate model to evaluate the interaction of *HEDICIN*s and *HECIN*s against bbspn-1. Furthermore, docking calculations of a well-known inhibitor of cysteine protease, namely E64-C, were ran to evaluate whether resulted ligand conformations would allow a possible alkylation of the cysteine residue in the active site of bbspn-1 and the different functionalities of the ligands, respectively, were to place in the corresponding reported subsite of the cavity. Detailed analysis of the results of each validation tool is provided below.

Table 8. Homology modeling validation scores obtained by Modeller 9.11.

Model	Alignment	Alignment score[a]	Modeller (Z-DOPE)
1	1EWM-1S4V-2BDZ_42	91	-1.06
2	1S4V-2BDZ_18	93	-1.06
3	1S4V-2BDZ_54	93	-1.05
4	1EWM-1S4V-2BDZ_51	91	-1.04
5	1EWM-1S4V-2BDZ_76	91	-1.04
6	2BDZ-2P7U_77	89	-1.03
7	1S4V-2BDZ_51	93	-1.01
8	1S4V-2P7U_13	89	-1.01
9	1S4V-2P7U_68	89	-1.00

[a] Alignment score by *Psi-coffee*.

Table 9. Additional scoring parameters of models built and selected according to Modeller 9.11 Z-DOPE score.

Model	ProQ		QMEAN Score	PROCHECK (%)[a]	RMSD (Å)[b]
	LGscore	MaxSub			
1	5.068	0.536	0.773	88.7; 10.2; 1.1; 0.0	1.14; 0.80; 0.64
2	5.118	0.555	0.742	91.4; 7.0;0.0;1.6	0.91; 0.65
3	5.318	0.560	0.706	91.4; 7.5; 0.0; 1.1	0.94; 0.67
4	5.091	0.508	0.720	87.6; 11.3; 0.5; 0.5	1.11; 0.74; 0.61
5	5.358	0.547	0.718	89.8; 8.1; 2.2; 0.0	1.15; 0.80; 0.67
6	5.394	0.575	0.703	82.3; 14.5; 1.6; 1.6	1.08; 0.87
7	5.384	0.565	0.751	90.8; 7.0; 1.1; 1.1;	0.79; 0.71
8	5.391	0.543	0.677	88.7; 10.2; 1.1; 0.0	0.82; 1.10
9	5.297	0.538	0.684	90.3; 8.1; 1.6; 0.0	0.61; 1.10

[a] Correspond to the percentage of residues that are located in the most favorable, additionally allowed, generously allowed, and disallowed regions, respectively according to the Ramachandran Plot. [b] RMSD values of babesipain-1 model compared to the 3D structures of the templates used for the alignment

VMD visualization

All models (1-9) built for bbspn-1 were aligned and visualized using the molecular visualization program VMD. Accordingly, most structures were quite similar since the RMSD between the built models oscillated between 0.37 and 1.20. As expected the main differences observed in the binding cavity of bbspn-1 resulted from the phenylalanine residues, specifically, Phe132, Phe67, Phe137. Generally, the rest of the residues in the main cavity displayed a significantly similar conformation.

PROCHECK

According to PROCHECK results, model 7 has more than 90% of the amino acids in the most favored regions (Table 9) and there are only two amino acids in the disallowed region (Asp199, Arg102) of the Ramachandran diagram (Fig. 26). Analysis of the 3D structure in VMD shows that these amino acids are outside of the binding pocket of bbspn-1. In fact, the closest amino acid, Asp199, is located at ~20 Å of the α–carbon of the catalytic cysteine, falling completely out of the region used for docking *HEDICIN*s and *HECIN*s against the enzyme. Therefore, these amino acids should not have impact on further docking results. Model 5 and model 9 also present ≥ 90% of the amino acids in the most favorable regions but a difference from model 7, they do not present any amino acid in the disallowed regions. However, model 7 was derived from the alignment with the highest *PSI-coffee* alignment score and it presents the lowest RMSD compared to the original structures 1S4V and 2BDZ, which increases the probability that the sequence of bbspn-1 folds correctly on the template combination used to build the structure.
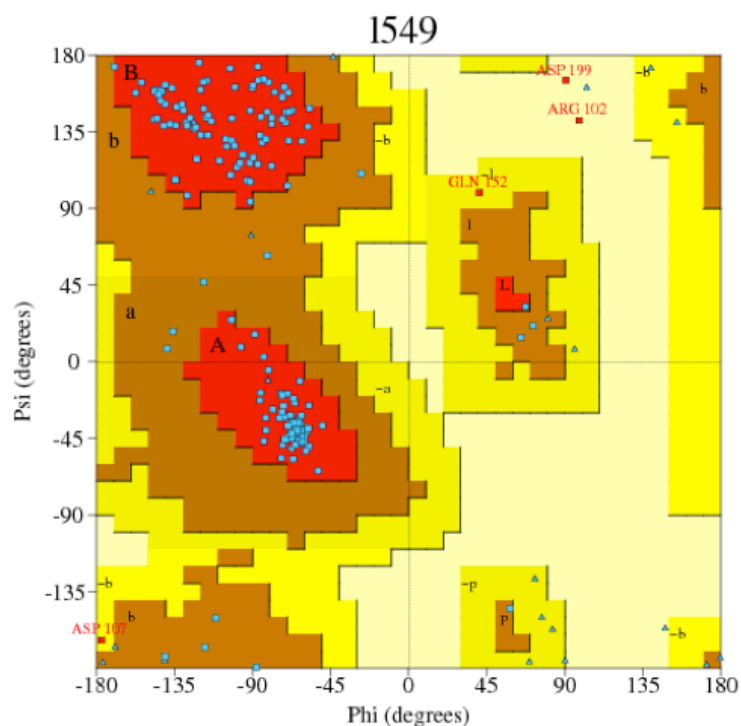
Figure 26. Ramachandran plot of built 3D structure of bbspn-1 for model 7. The different colored areas indicate ''disallowed'' (beige), ''generously allowed'' (yellow), ''additional allowed'' (brown), and ''most favored'' (red) regions.

ProSA

Additionally, ProSA, a diagnostic tool that is based on the statistical analysis of all available PDB structures, was used to reveal whether the built structures presented misfolded areas. This validation score specifically assesses whether the interactions of each residue in the built structure are favorable.[23, 24] Accordingly, ProSA Z-score resulted for each experimental structure used are presented in Table 10. Comparison of ProSA Z-scores of experimental results with those obtained for each built model indicates overall good quality of the models since they Z-score are comparable to those obtained for the corresponding used templates. The best results are obtained for models 4, 6, 7, and 9. As example, the overall model quality of model 7 is displayed in fig. 27. Z-scores are -7.98, -6.48 and –6.85 for 1S4V (A), model 7 of bbspn-1 (B) and 2BDZ (C), respectively. Results demonstrated that although the Z-score of model 7 is slightly lower than that of template 1S4V, it is in the same range of template 2BDZ and it is a perfect fit within the structures in PDB.

Table 10. ProSA Z-score of experimental structure and build model.

Model	ProSA[a]				
	Model	1EWM(A)	1S4V(A)	2BDZ(C)	2P7U(A)
1	-6.43				
2	-6.31				
3	-6.20				
4	-6.58				
5	-6.25	-6.85	-7.98	-6.85	-7.14
6	-6.60				
7	-6.48				
8	-6.39				
9	-6.64				
[a]	ProSA	determined	using		ProSA-web.
https://prosa.services.came.sbg.ac.at/prosa.php					
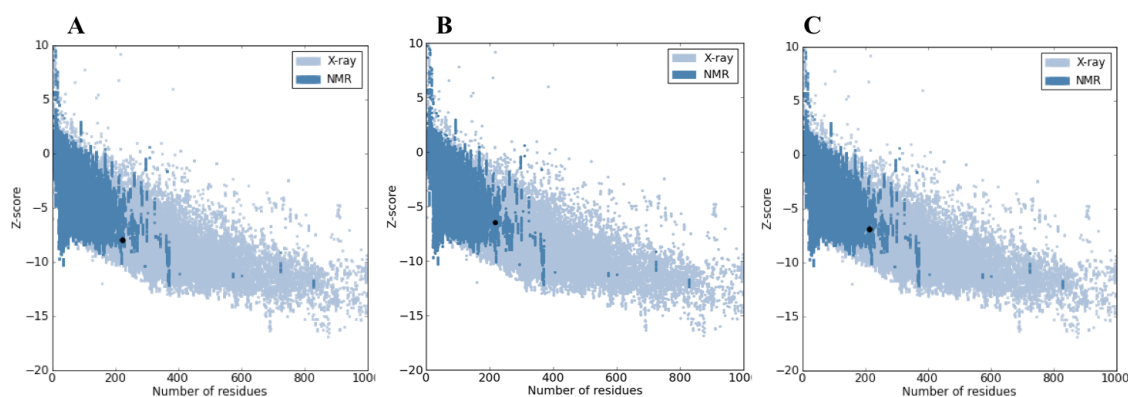
Figure 27. ProSA analysis for the model structure of bbspn-1 (B) the template structures, 1S4V (A) and 2BDZ (C).

ProQ

Models were also validated by ProQ which help to separate correct models from less correct models by finding similar fragments between a built model and a native structure. In other words, ProQ score allows to determine whether protein folds are not compatible with a protein sequence.[25] The quality is quantified taking into account indexes LGscore[22] and MaxSub.[26] A model can be qualified as appropriate if LGscore > 1.5 and MaxSub > 0.1, good if LGscore > 3 and MaxSub > 0.5, and very good if LGscore > 5 and MaxSub > 0.8.[27] Accordingly, model 6 and 7 presented the best ProQ

scores (Table 9). For instance, model 7 was evaluated as very good and good according to the LG score (5.384) and the MaxSub index (0.565), respectively.

QMEAN

QMEAN score was also used to validate the model. This score corresponds to the global score of the whole model, on the basis of a linear combination of six structural descriptors, reflecting the predicted model reliability ranging from 0 to 1 with higher scores for reliable models.[20] In contrast to other validation tools such as ProSA, QMEAN's quality score is not dependable on protein size. Accordingly, model 1 and 7 presents the best reliability, compared to the rest of the built models, with a global QMEAN score of 0.773 and 0.751, respectively (Table 9). Moreover, the quality of the model can be further compared to reference structures of high resolution obtained from X-ray crystallography analysis through QMEAN Z-score, where a value of 0 is the average value for a good model.[20] According to Benkert *et al*, QMEAN Z-score provides an estimation of the "degrees of nativeness" of the structural features observed in a model and indicates if the model has a quality comparable to experimental structures.[20] Based on results, QMEAN Z-score for babesipain-1 model 7 is -0.22 (Fig. 28), which reinforces the good quality of this derived model for babesipain-1.
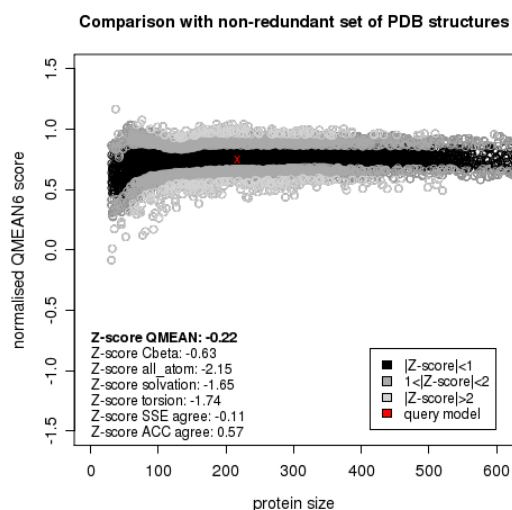
Figure 28. Graphical representation of the estimation of the absolute quality of bbspn-1 model 7 assessed by QMEAN Z-score. Good models are generally located in the dark zone. The red cross represents the positioning of model 7.

Docking known cysteine proteases inhibitors

Docking studies were carried using the docking algorithm GOLD[28] and the ligand E64-C, a known inhibitor of cysteine proteases. An active site radius of 12 Å centered in the

thiolate moiety of Cys25 was established. Docking calculation were run with flexible ligands and results obtained were compared with crystallographic structure already reported for papain (1PPP).[29] Except for results found for model 7 (Fig. 29), most docking conformations resulted for each built model located the electrophilic warhead far away from Cys25, out of the binding site and into S2 and S3 pocket, or the oxygen of the epoxide of E64-C facing the thiolate moiety of Cys25. In the case of model 7, the most frequent ligand conformations place the electrophilic warhead of E64-C, respectively, at 3.7 Å and right over the catalytic cysteine, a distance which could allow a cysteine alkylation to take place. Moreover, the docking conformation found for E64-C against model 7 significantly match the typical binding mode of the ligand against other cysteine protease such as papain (1PPP). Based on all above, model 7 is suitable to evaluate the interaction of *HEDICIN*s and *HECIN*s with bbspn-1 since it was the model that presented the best generally validation score according to PROCHECK, ProSA, ProQ, Qmean, and a known inhibitor of cysteine proteases, E64-C, docked well within the active pocket the corresponding built model. Therefore, the respective docking studies of *HEDICIN*s and *HECIN*s were carried using the 3D structure of model 7.
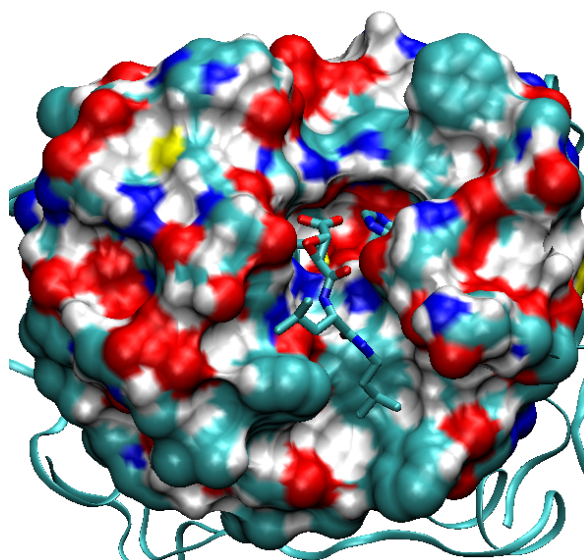
Figure 29. Most frequent docking conformation observed for E64-C against model 7, respectively. All within 15 Å of Cys25 is represented in MSMS, E64-C is represented in Licorice, and the rest of the protein in NewRibbons (cyan).

Detailed description of model 7

The overall topology of bbspn-1 structure is similar to that of other family members as it presents typical papain-like cysteine protease features (Fig. 30-31):

i)   it displays two domains, an α-helix-rich (L) domain and a β-sheet-rich (R) domain, separated by the active site of the protein (Figure 30 (A, C)); the L domain is composed of four helices and the R domain is formed by six anti-parallel β-sheets;[30]

ii)   it presents six cysteine residues forming disulfide bonds (Cys22-Cys63, Cys56-Cys95 and Cys148-Cys201) and one cysteine residue (Cys25) in the active site;

iii)   it shows Cys25 close to His155 and Asn177 which may facilitate the appropriate orientation for the thiolate/imidazolium ion pair (Fig. 30 (B));

iv)   it locates Gln19 and Trp179 as to allow the possibility of the formation of the "oxyanion hole" that stabilizes the tetrahedral adduct during the nucleophilic attack of the thiolate anion to the electrophilic warhead of the substrate (Figure 30 (A));[18]

v)   it also demonstrates the presence of a glycine-rich region, comprising mainly of Gly65 and Gly66, that has been found to provide additional stability to the complex in other papain-like cysteine proteases, by forming a constellation of hydrogen bonds with the substrates.[31]

vi)   the binding cavity of papain-like cysteine proteases are generally constituted by four pockets, S1, S1', S2 and S3, as shown in Figure 31 for bbspn-1. S1

vii)   and S1' contain Gln19 and Trp179, respectively, the amino acids which form the "oxyanion hole," S2 pocket governs ligand specificity, and S3 pocket contains the glycine rich region of the binding site.
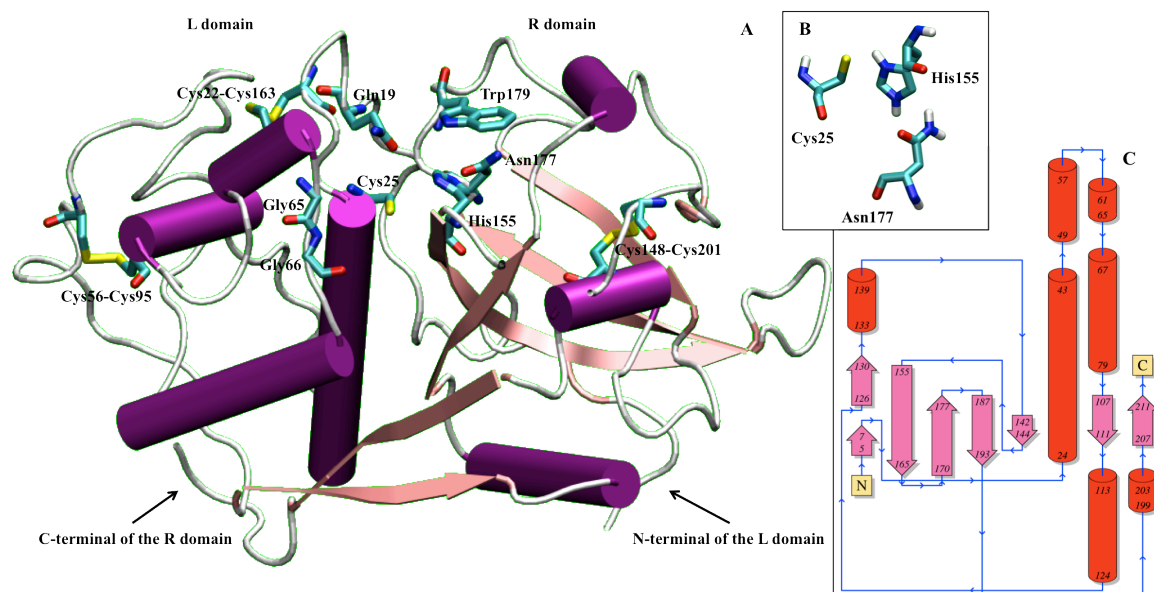
Figure 30. (A) Modeled structure of babesipain-1 represented in Cartoon, where some conserved catalytic residues and the disulfide bonds are shown. (B) Catalytic residues Cys25, His155, Asn177 of babesipain-1 in Licorice. (C) Predicted secondary structure of bbspn-1 using PDBSum server. The N-terminal domain and the C-terminal domain are constituted by α-helices (red) and anti-parallel β-sheets (pink), respectively.
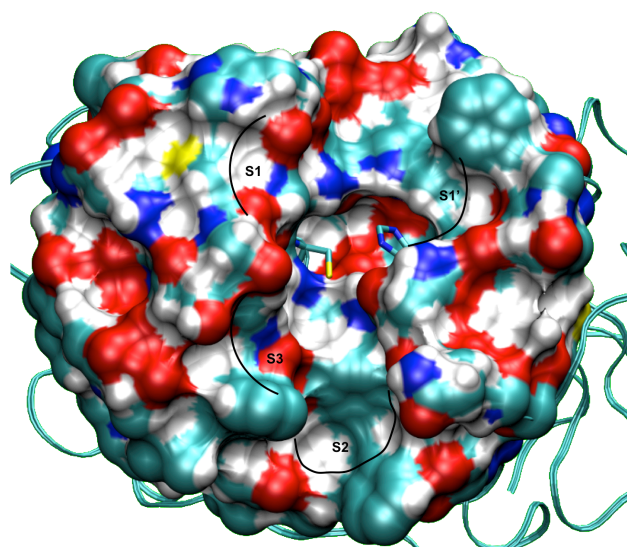
Figure 31. S1, S1', S2, and S3 site of bbspn-1. All within 15 Å of Cys25 is represented in MSMS, residue 25 and His155 are represented in licorice, and the rest of the protein in NewRibbons.

Comparing FP2 and bbspn-1 active pocket, it is possible to notice that the active pockets of bbspn-1 and FP2 are significantly different as demonstrated by table 11. The most conserved cavity is S1 and the main differences are observed in the S2 pocket which is believe to be responsible for substrate specificity.[18] Table 11 shows that S2 is more hydrophobic for bbspn-1 than for FP2. For instance, S2 cavity of bbspn-1 presents Phe206 while the S2 cavity of FP2 Asp234 instead.[7] Moreover, S2 cavity of bbspn-1 seems to be less deep due to the existence of a Tyr129 instead of Ser149 in the case of FP2 which could explain the P2 rank order reported for in bbspn-1 Val > Leu > Phe.[7] In

addition, the higher hydrophobicity of S2 cavity could justify that the highly hydrophobic *HEDICIN*s are more efficient inhibitors of bbspn-1. Furthermore, analysis of the S3 pocket shows that S3 seems to be more basic for FP2 than for bbspn-1, since the former presents polar residues and one basic residue (Lys76) and instead, bbspn-1 only presents polar residues (Gln59-Ser60-Ser61). In summary, the above-mentioned analyses indicate that the model structure is consistent with the current understanding of the protein structure.

Table 11. Active site of bbspn-1 and FP2 cysteine proteases.

Cysteine protease	S1'	S1	S2	S3
bbspn-1	Val130-**Phe132**-**Thr133**-**Phe137**-His155-Trp179	Gln19-Gly23-Cys63-**Gly64**	**Phe67**-**Ser68**-**Tyr129**-Leu153-**Phe206**	**Gln59**-**Ser60**-**Ser61**-Gly65-Gly66
Falcipain-2	Val150-**Val152**-**Ser153**-**Ala157**-His174-Trp206	Gln36-Gly40-Cys80-**Asn81**	**Leu84**-**Ile85**-**Ser149**-Leu172-**Asp234**	**Lys76**-**Asn77**-**Tyr78**-Gly82-Gly83

Bold letter highlights the main difference between the cavities

3.3.2. Docking studies

*HEDICIN*s

Model 7, the 3D structure of bbspn-1 obtained from the alignment of bbspn-1, with 1S4V, and 2BDZ, allowed to perform the respective *in silico* studies to evaluate the interactions of *HEDICIN*s and *HECIN*s with the protein and draw conclusions regarding SAR against bbspn-1. These results were compared to those previously obtained by Dr. Cátia Teixeira for falcipains. *In silico* results demonstrated that the most preferred conformation for *HEDICIN*s against bbspn1 is similar to the one previously obtained for FP2. The chloroquinoline is located in S2', and the cinnamoyl moiety, Leu, and hPhe are placed in the S2 site, S1, S1', respectively (Fig. 32). However, the steric hindrance caused by Phe137 impeded the chloroquinoline moiety to form a π-π stacking interaction with Trp179 as seen in FP2. Instead, in FP2, there is Ala in place of Phe, thus such a steric impediment does not occur. Moreover, docking results against bbspn-1 suggest strong hydrophobic interactions between the aromatic ring of the cinnamoyl functionality and residues Phe67 and Tyr129 placing the beta carbon between 3.8 and 5.8 Å of the cysteine residue which makes possible in some cases that a covalent interaction takes place. However, since the cinnamoyl moiety is too rigid, the approximation of the β-carbon is impeded. In addition, *h*Phe forms a π–π stacking

interaction with Phe 137 and other non-covalent interactions with residues Asn154, His155, and Gln19 are also observed. Furthermore, S2 cavity seems to accommodate better apolar groups due to the hydrophobic side chains of the residues Phe67, Leu153 and Phe206. The latter is in agreement with *in vitro* data since the polar *p*-OMe cinnamoyl derivative **1d** displayed the worst activity of the series (IC$_{50}$ = 35.8 µM).
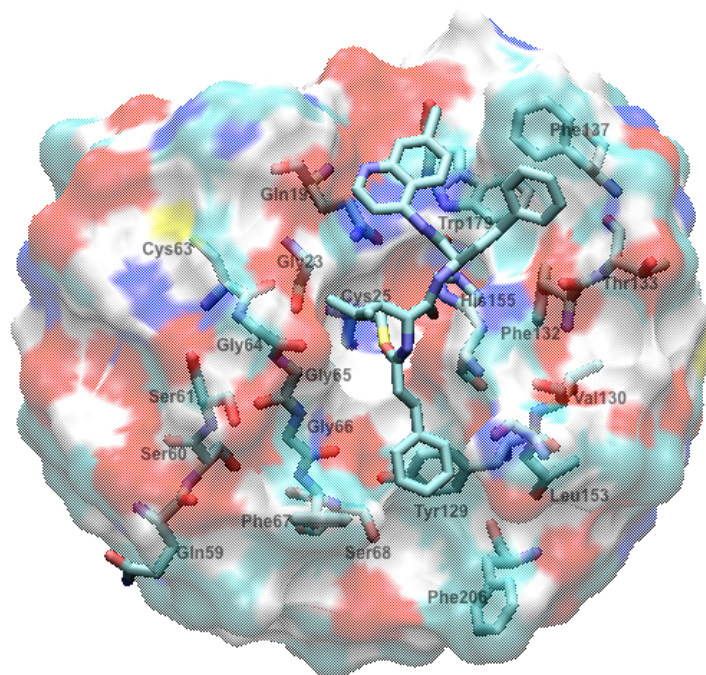
Figure 32. Most frequent conformation of ligand **1a** against bbspn1. All within 15 Å of Cys25 is represented in MSMS, Ligand **1a** is represented in Licorice, the residues of the S1, S1', S2, and S3 pocket are represented in CPK.

HECINs

In the case of *HECIN*s, all ligands, except the *m*-NO$_2$ analogue **2j**, displayed the same preferred conformation (Fig. 33). This result is in agreement with *in vitro* data which shows that compound **2j** (IC$_{50}$ = 48.3 µM) is at least two times less active than the rest of the compounds of the series (IC$_{50}$ = 9.8-20.9 µM). Docking results of compounds **2a-b** and **2d-h** indicate that the chloroquinoline ring is located between the S2 and S3 pockets building non-covalent interactions with residues Phe67, Tyr129, Phe206 and Leu153. Further results suggest that the amide functionality of the respective ligands interact with residues Ser205 and His155 except for *p*-OMe conjugate **2d** which only interacts with the former residue. The beta carbon of the vinyl bond of the cinnamoyl functionality is located within ~4.5 Å from Cys25. Additional trends observed regarding

the electrondonating properties of cinnamoyl substituent could be explained by atomic Fukui indices for *HECIN*s calculated by Dr. Teixeira. These fukui indices were used as a measure of the electrophilicity of the β-carbon of the vinyl bond. Accordingly, electron-donating substituent favors electron-delocalization towards the carbonyl group, consequently, promoting the alkylation of the β-carbon by the catalytic cysteine and explaining that the best inhibitor of the series was the *p*-OMe (IC$_{50}$ = 9.8 μM).
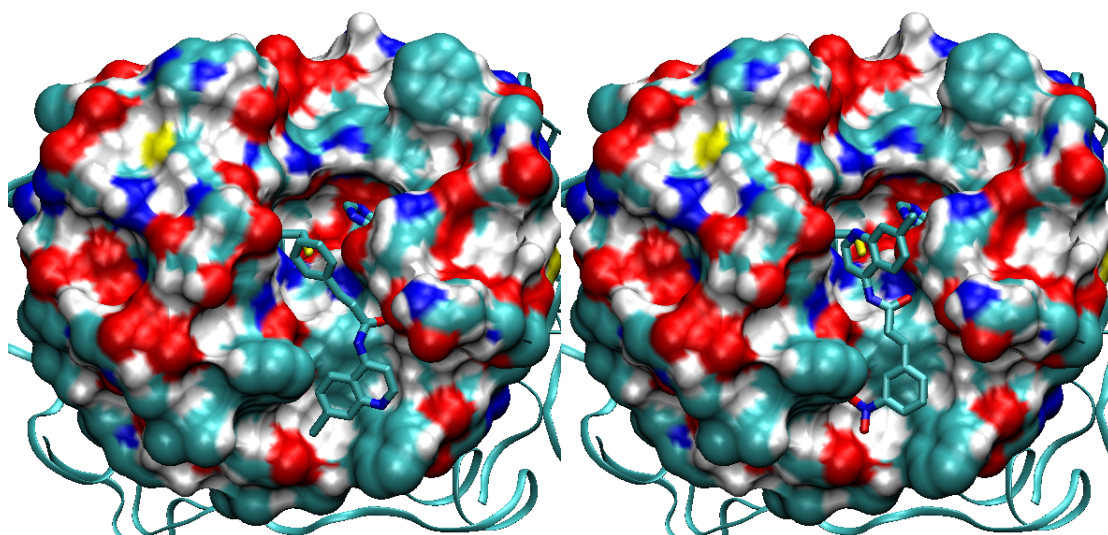
Figure 33. Most frequent conformation of ligand **2a** and **2j** against bbspn-1, respectively. All within 15 Å of Cys25 is represented in MSMS, ligand **2a** and **2j** are represented in Licorice, residue Cys25 and His155 are displayed in CPK, and the rest of the protein in NewRibbons (cyan).

3.4. *In silico* protocol

Homology modeling

The bbspn-1 sequence was obtained from Uniprot database. Only the mature sequence from residue 242 to 458 was considered to do the homology model studies. Templates search was performed on BLAST using default parameters. Templates matching the following requirements: i) E-value below 10^{-40}; ii) query coverage > 90 % and sequence identity > 35% or query coverage > 85% and sequence identity > 40%; iii) PDB structure with a resolution < 2.5 Å, without missing residues in the active site, and with bounded ligand were chosen for these analysis. PDB structures were downloaded from www.pdb.org. The templates and the target sequences were aligned using the *PSI-coffee* mode of *T-Coffee* v.9.03.[32] The bbspn-1 models were constructed based on different alignments, single and multiple. For each alignment, 100 models were generated using the standard "automodel" routine of Modeller v.9.11.[33] The best built models were validated by PROCHECK, ProQ, ProSA, and QMEAN, and by docking a known inhibitor of papain-like cysteine proteases.

Docking of the inhibitors

Dockings were performed using GOLD[28] version 5.01 allowing the full flexibility of the ligand but keeping the protein fixed. The built 3D structure of bbspn-1 (model 7) was prepared and used for docking. Basically, the acid and basic residues of the protein were protonated at pH=5.5. The protein was then minimized with the AMBER 11 program[34] by 500 steps of steepest descent followed by 2000 steps of conjugate gradient to remove bad contacts using a generalized-Born solvent model. The biomolecular force field ff03 was used.[35] On the other hand, the inhibitors were minimized using gaff force field and Born solvation. The active site was established as 15 Å from the Cys 25 while the docking exploration consisted of 500 conformation runs independent for each inhibitor based on the default genetic algorithm (GA) search parameters, which were then ranked according to the GOLDScore scoring function.

3.5. References

1. Martins, T. M.; Goncalves, L. M.; Capela, R.; Moreira, R.; do Rosário, V. E.; Domingos, A. Effect of synthesized inhibitors on babesipain-1, a new cysteine protease from the bovine piroplasm Babesia bigemina. *Transbound Emerg Dis* **2010,** 57, 68-9.

2. Schnittger, L.; Rodriguez, A. E.; Florin-Christensen, M.; Morrison, D. A. Babesia: a world emerging. *Infect Genet Evol* **2012,** 12, 1788-809.

3. Mosqueda, J.; Olvera-Ramirez, A.; Aguilar-Tipacamu, G.; Canto, G. J. Current advances in detection and treatment of babesiosis. *Curr Med Chem* **2012,** 19, 1504-18.

4. Vial, H. J.; Gorenflot, A. Chemotherapy against babesiosis. *Vet Parasitol* **2006,** 138, 147-60.

5. de Waal, D. T.; Combrink, M. P. Live vaccines against bovine babesiosis. *Vet Parasitol* **2006,** 138, 88-96.

6. Fish, L.; Leibovich, B.; Krigel, Y.; McElwain, T.; Shkap, V. Vaccination of cattle against B. bovis infection with live attenuated parasites and non-viable immunogens. *Vaccine* **2008,** 26, Supplement 6, G29-G33.

7. Martins, T. M.; do Rosário, V. E.; Domingos, A. Expression and characterization of the Babesia bigemina cysteine protease BbiCPL1. *Acta Trop* **2012,** 121, 1-5.

8. http://www.sanger.ac.uk/resources/downloads/protozoa/babesia-bigemina.html

9. Martins, T. M.; do Rosário, V. E.; Domingos, A. Identification of papain-like cysteine proteases from the bovine piroplasm Babesia bigemina and evolutionary relationship of piroplasms C1 family of cysteine proteases. *Exp Parasitol* **2011,** 127, 184-94.

10. Rosenthal, P. J. Cysteine proteases of malaria parasites. *Int J Parasitol* **2004,** 34, 1489-99.

11. Capela, R.; Oliveira, R.; Goncalves, L. M.; Domingos, A.; Gut, J.; Rosenthal, P. J.; Lopes, F.; Moreira, R. Artemisinin-dipeptidyl vinyl sulfone hybrid molecules: design, synthesis and preliminary SAR for antiplasmodial activity and falcipain-2 inhibition. *Bioorg Med Chem Lett* **2009,** 19, 3229-32.

12. ChemAxon. MarvinSketch 5.2.2. http://www.chemaxon.com. **2009**.

13. Charton, M. Steric effects. I. Esterification and acid-catalyzed hydrolysis of esters. *J Am Chem Soc* **1975,** 97, 1552-1556.

14. Elmar Krieger, S. B. N., Gert Vriend. Homology Modeling. In *Structural Bioinformatics*, Wiley-Liss, I., Ed. 2003; pp 507-521.

15. Ippoliti, E. Homology Modeling Tutorial. **2012**.

16.   Notredame, C.; Higgins, D. G.; Heringa, J. T-Coffee: A novel method for fast and accurate multiple sequence alignment. *J Mol Biol* **2000,** 302, 205-17.

17.   Rawlings, N. D.; Barrett, A. J.; Bateman, A. MEROPS: the peptidase database. *Nucleic Acids Res* **2010,** 38, D227-33.

18.   Sajid, M.; McKerrow, J. H. Cysteine proteases of parasitic organisms. *Mol Biochem Parasitol* **2002,** 120, 1-21.

19.   Larsson, P.; Wallner, B.; Lindahl, E.; Elofsson, A. Using multiple templates to improve quality of homology models in automated homology modeling. *Protein Sci* **2008,** 17, 990-1002.

20.   Benkert, P.; Biasini, M.; Schwede, T. Toward the estimation of the absolute quality of individual protein structure models. *Bioinformatics* **2011,** 27, 343-50.

21.   Laskowski, R. A.; MacArthur, M. W.; Moss, D. S.; Thornton, J. M. PROCHECK: a program to check the stereochemical quality of protein structures. *J Appl Crystallogr* **1993,** 26, 283-291.

22.   Cristobal, S.; Zemla, A.; Fischer, D.; Rychlewski, L.; Elofsson, A. A study of quality measures for protein threading models. *BMC Bioinformatics* **2001,** 2, 5.

23.   Sippl, M. J. Recognition of errors in three-dimensional structures of proteins. *Proteins* **1993,** 17, 355-62.

24.   Wiederstein, M.; Sippl, M. J. ProSA-web: interactive web service for the recognition of errors in three-dimensional structures of proteins. *Nucleic Acids Res* **2007,** 35, W407-10.

25.   Wallner, B.; Elofsson, A. Can correct protein models be identified? *Protein Science* **2003,** 12, 1073-1086.

26.   Siew, N.; Elofsson, A.; Rychlewski, L.; Fischer, D. MaxSub: an automated measure for the assessment of protein structure prediction quality. *Bioinformatics* **2000,** 16, 776-85.

27.   SBC Stockholm Bioinformatics Center. ProQ - Protein Quality Predictor. http://www.sbc.su.se/~bjornw/ProQ/ProQ.html

28.   Jones, G.; Willett, P.; Glen, R. C.; Leach, A. R.; Taylor, R. Development and validation of a genetic algorithm for flexible docking. *J Mol Biol* **1997,** 267, 727-48.

29.   Kim, M. J.; Yamamoto, D.; Matsumoto, K.; Inoue, M.; Ishida, T.; Mizuno, H.; Sumiya, S.; Kitamura, K. Crystal structure of papain-E64-c complex. Binding diversity of E64-c to papain S2 and S3 subsites. *Biochem J* **1992,** 287 (Pt 3), 797-803.

30.   Drenth, J.; Jansonius, J. N.; Koekoek, R.; Swen, H. M.; Wolthers, B. G. Structure of papain. *Nature* **1968,** 218, 929-32.

31.   Brinen, L. S.; Hansell, E.; Cheng, J.; Roush, W. R.; McKerrow, J. H.; Fletterick, R. J. A target within the target: probing cruzain's P1' site to define structural determinants for the Chagas' disease protease. *Structure* **2000,** 8, 831-40.

32.   Di Tommaso, P.; Moretti, S.; Xenarios, I.; Orobitg, M.; Montanyola, A.; Chang, J. M.; Taly, J. F.; Notredame, C. T-Coffee: a web server for the multiple sequence alignment of protein and RNA sequences using structural information and homology extension. *Nucleic Acids Res* **2011,** 39, W13-7.

33.   Sali, A.; Blundell, T. L. Comparative protein modelling by satisfaction of spatial restraints. *J Mol Biol* **1993,** 234, 779-815.

34.   Case DA, D. T., Cheatham TE, Simmerling CLI, Wang J, Duke RE, Luo R, Crowley M, Walker RC, Zhang W, Merz KM, Wang B, Hayik S, Roitberg A, Seabra G, Kolossváry KF, Wong KF, Paesani F, Vanicek F, Wu X, Brozell SR, Steinbrecher T, Gohlke H, Yang L, Tan C, Mongan J, Hornak V, Cui G, Mathews DH, Seetin MG, Sagui C, Babin V, Kollman PA. AMBER 10, University of California, San Francisco; 2008.

35.   Duan, Y.; Wu, C.; Chowdhury, S.; Lee, M. C.; Xiong, G.; Zhang, W.; Yang, R.; Cieplak, P.; Luo, R.; Lee, T.; Caldwell, J.; Wang, J.; Kollman, P. A point-charge force field for molecular mechanics simulations of proteins based on condensed-phase quantum mechanical calculations. *J Comput Chem* **2003,** 24, 1999-2012.

Chapter 4

*HEFLECIN*s

Second generation of heterocyclic-cinnamic acid conjugates

4.0. Rationale

Following synthesis, *in vitro* and *in silico* evaluation of *HEDICIN*s and *HECIN*s, as described in the previous chapters, a second generation of potential dual-action antimalarials was envisioned. Second generation compounds, called *HEFLECIN*s (*HE*terocyclic-*FLE*xible spacer-*CIN*namic acid conjugates), were designed to also join in the same molecular construct a heterocyclic core from a classical antimalarial drug and a cinnamoyl moiety, but this time linked together through a flexible alkyl chain (Fig. 34). The choice of this spacer was based on earlier reports on the favorable role of alkyl chains linked to the heterocyclic core of antimalarial aminoquinolines.[1] The substitution of the rigid dipeptide spacer in *HEDICIN*s by the flexible and more lipophilic ones in *HEFLECIN*s might improve antimalarial properties of the corresponding compounds. Finally, *HEFLECIN*s were predicted to have a basicity closer to that of reference antimalarial drug chloroquine (pKa~7) than *HEDICIN*s (pKa~4),[2] which might favor their accumulation in the FV of intraerythrocytic *Pf* .
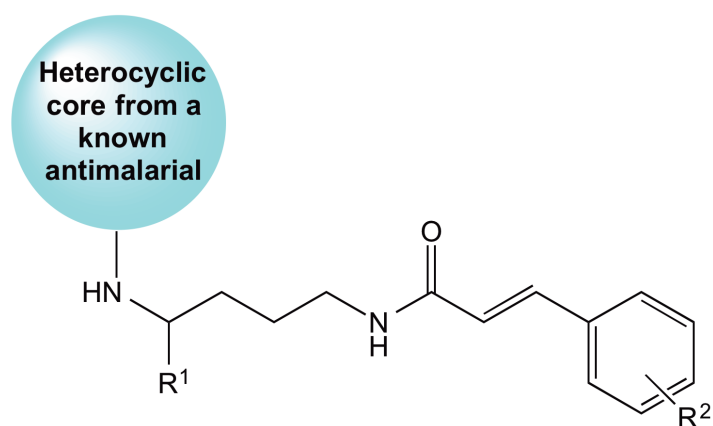
Figure 34. General structure of *HEFLECIN*s.

As in the case of *HE[DI]CIN*s the doctoral candidate was in charge of the chemical synthesis and characterization of *HEFLECIN*s and their evaluation as inhibitors of β-H formation, whereas assessment of their inhibitory activity against both falcipains (*in vitro*) and development of blood-stage *Pf* parasites (*in vitro* and *in vivo*) was carried out by Prof. Philip J. Rosenthal's team. The experimental research work was developed alongside an *in silico* study carried out by the thesis co-supervisor, Dr. Cátia Teixeira. Further evaluation of *HEFLECIN*s against liver-stage *P. berghei* parasites and *Leishmania* was carried out by Dr. Miguel Prudêncio's team at Instituto de Medicina Molecular, Faculdade de Medicina, Universidade de Lisboa and Dr. M. S. Gomes's team

in IBMC (Instituto de Biologia Molecular e Celular) in Universidade do Porto, respectively.

4.1. Chloroquinoline-based *HEFLECINs*

According to previous results found for *HEDICIN*s, *N*-alkylcinnamoylated/chloroquine analogues were synthesized to evaluate the influence of the alkyl chain instead of the dipeptide chain in the antimalarial properties of the chloroquinoline derivatives here reported.

4.1.1. Synthesis and characterization of *HEFLECIN*s

*Synthesis of HEFLECINs **13-15, 20-21**, and **24-25***

Chloroquinoline-based *HEFLECIN*s **13-15** were synthesized in two steps, starting with an S$_N$*Ar* reaction between the appropriate alkanediamine and 4,7-dichloroquinoline, which was followed by condensation of the resulting 4-(*N*-aminoalkyl)amino-7-chloroquinoline with the relevant cinnamic acid (Scheme 11). In order to form the amide bond, the respective carboxylic acid was activated using TBTU and DIEA as coupling reagents, and the amine **16-18** was added to reaction. The main challenge found in the synthetic procedure was that most cinnamoyl/chloroquinoline derivatives were only partially soluble in DCM turning difficult the extraction of the desired product from reaction mixture. The same solubility issue appeared when using other polar organic solvent as ethyl acetate, known to extract electron donor solutes.[3] Nonetheless, all reactions afforded the cinnamoyl derivatives from low to good yields (8-67%).
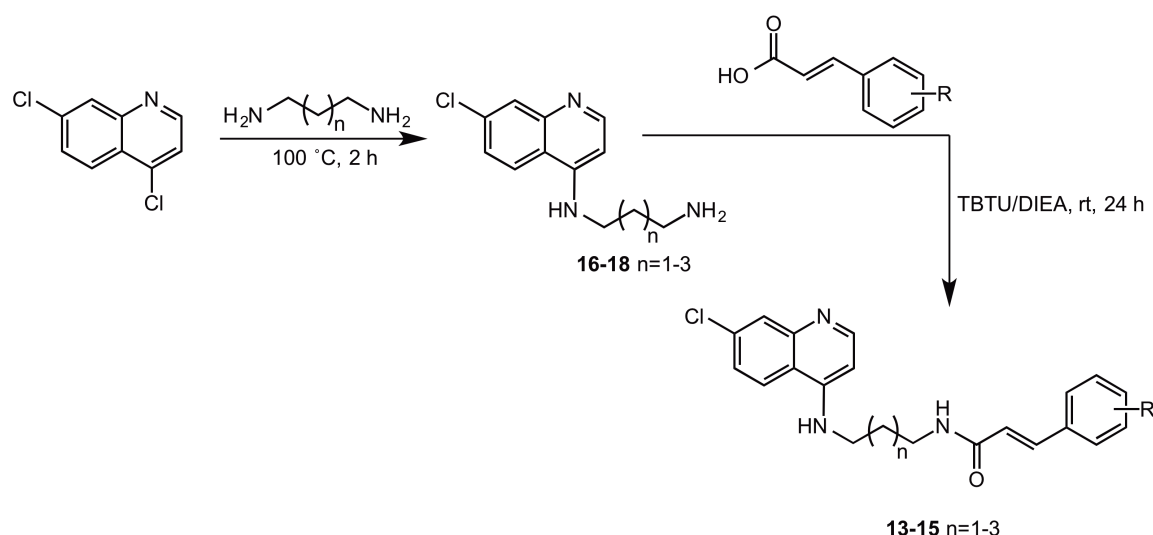
Scheme 11. Synthetic pathway of *HEFLECIN*s (**13-15**).

As in *HEDICIN*s and *HECIN*s, the *p*-NO_2 derivative of series **13** presented significantly lower yield than the other compounds of the series. However, experimental observations suggested that there was no difference behavior between the reactions. For instance, for each cinnamic acid, once its activation started, a solid began to appear and stopped forming at around half the activation time suggesting that this activation step was straightforward. Moreover, this solid disappeared when the corresponding amine was added to the reaction to obtain the desired amide bond. Calculation of the atomic Fukui indices (f+), derived from Natural Bond Order population analysis of the neutral compound and its respective anion,[4] was done to quantify the electrophilicity of the carbonyl moiety for the activated unsubstituted cinnamic acid **19a** and *p*-nitrocinnamic acid **19b,** which correspond to the best (%yield = 52) and the worst (%yield = 8) yields for compounds **13**, respectively. The Fukui indices obtained (f+**19a** = 0.08; f+**19b** = 0.04) suggested that the greater the magnitude of f+, the greater the change in electron density near the atoms of interest, and thus the higher reactivity of a molecule at that atomic site towards nucleophilic attack. The latter explains the higher yield obtained for the generation of the unsubstituted compound as compared to the *p*-nitro substituted derivative.
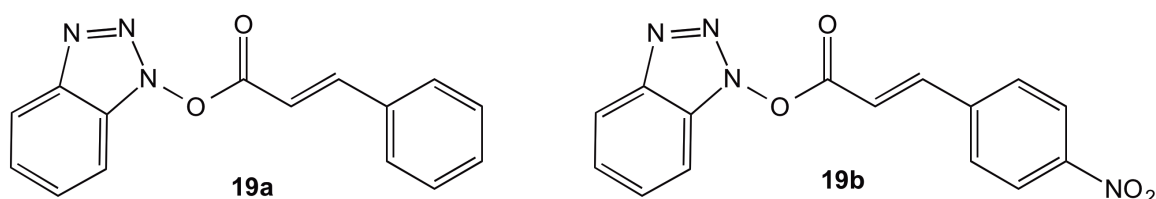
Furthermore, compounds **20-21** were synthesized, following similar procedures as the above described (Scheme 12), to assess the influence of the ester bond and chlorine substituent in position seven of the quinoline ring on the antimalarial activity. Briefly, the convenient amine **22** and alcohol **23** derivatives were synthesized. The amine **22** was further coupled to cinnamic acids using TBTU and DIEA, whereas the cinnamoylated product **21** was obtained through reaction of alcohol **23** with the adequate cinnamoyl chloride, in the presence of Et₃N. Accordingly, compounds **20-21** were obtained in low yields (11-21%).
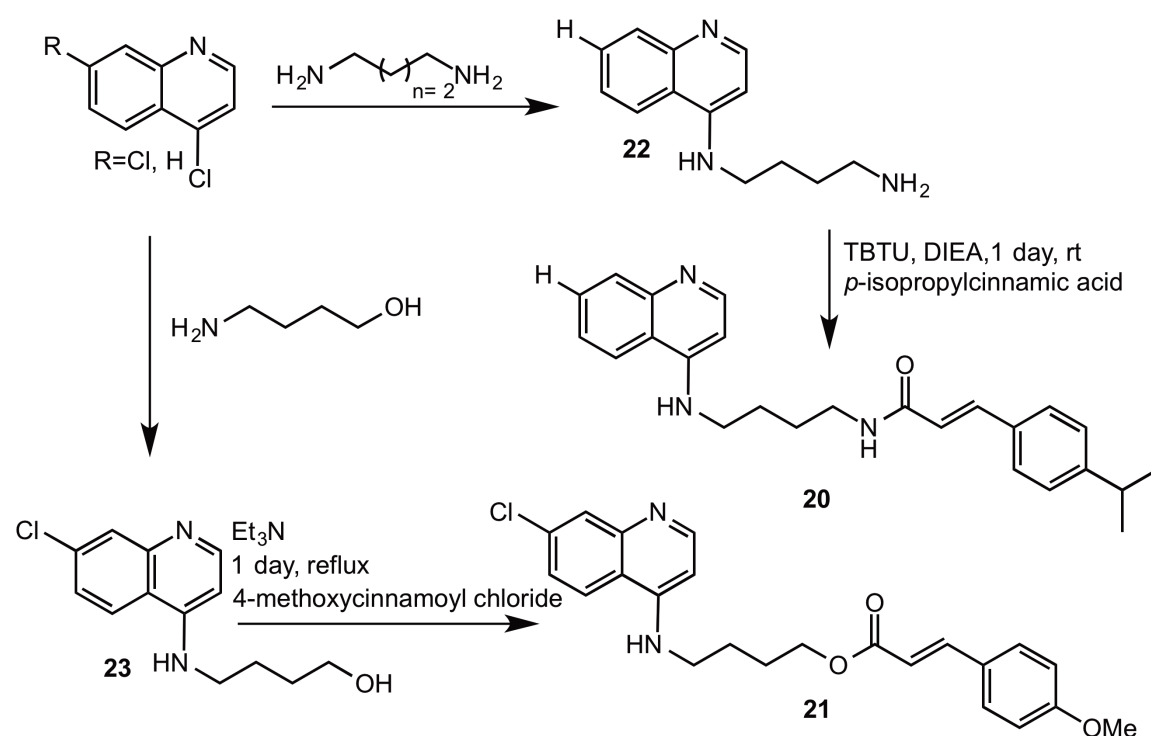
Scheme 12. Synthetic pathway to obtain cinnamoylated derivatives **20-21**.

Moreover, in order to assess the influence of the quinoline moiety on the antimalarial activity, two additional *N*-cinnamoylated compounds were synthesized, the pyridine derivative **24** and the morpholine derivative **25**. Compound **24** was synthesized following the procedure previously used to achieve the CQ analogues **13**-**15**. Initially, it was obtained the corresponding amine **26** that was later coupled to *p*-methoxy cinnamic acid (Scheme 13). To yield the morpholine derivative **24**, first an *N*-alkylation with *N*-bromobutylphthalimide was carried, followed by the removal of the phthalimide protecting group; subsequently, *p*-isopropyl cinnamic acid was coupled to the resulting amine **27** using TBTU and DIEA (Scheme 13). Both compounds **24** and **25** were obtained in fairly good yields (30-61%).
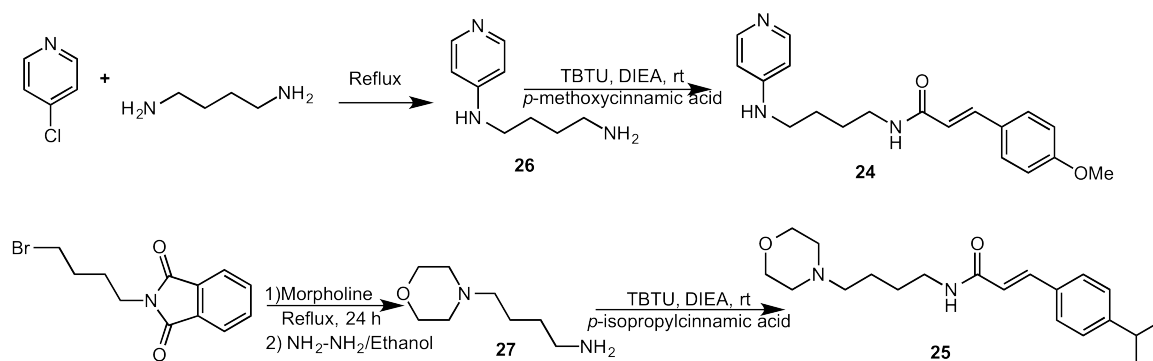
Scheme 13. Synthetic route to yield cinnamoylated derivatives **24-25**.

Characterization of HEFLECINs *13-15* and *20-21* and *24-25*

All compounds **13a-l, 14a-l, 15a-c**, **20, 21, 24** and **25** were characterized by 1H-NMR, 13C-NMR, ESI-IT MS, and HPLC, and the data obtained agreed with the desired compounds. As an example, the NMR spectra of compound **13i** is shown (Fig. 35-36). Accordingly, figure 35 displays the characteristic signals of compound **13i**, for instance, the shielded region below 4 ppm shows the 4 protons corresponding to the methylene groups at 3.36 ppm overlapped with the protons of water from the use of DMSO-d_6 as a solvent to run the NMR spectra, and the 4 protons of the most shielded methylene groups in **13i** at 1.64 ppm. The α-vinyl proton is observed at 6.64 ppm with J= 15.6 Hz, a coupling characteristic of a *trans*-vinyl proton. The deshielded aromatic protons are also visible. For example, in the downfield region, the 1H-NMR spectrum shows the characteristic signal of the proton at position 3 of the quinoline ring at 6.47 ppm, the protons of the position 8 in the quinoline ring at 7.77 ppm with a small coupling constant J= 2 Hz, and the triplet of one of the proton bound to a nitrogen atom at 8.17 ppm. The 13C-NMR (Fig. 36) displays the number of signals in agreement with the structure of the desired compounds: 16 signals in the downfield region and four signals in the upfield region, the most deshielded signal corresponding to the carbonyl functionality. For more detailed analysis of the NMR data, please refer to the experimental section of this chapter. In the mass spectrum, two signals were expected since bromine atom has two isotopes approximately equally abundant. Interestingly, instead of displaying two peaks associated to two different molecules, containing different isotope ^{79}Br and ^{81}Br, respectively, the m/z peak showed only one peak corresponding to the compound containing the isotope of ^{81}Br (Fig. 37).
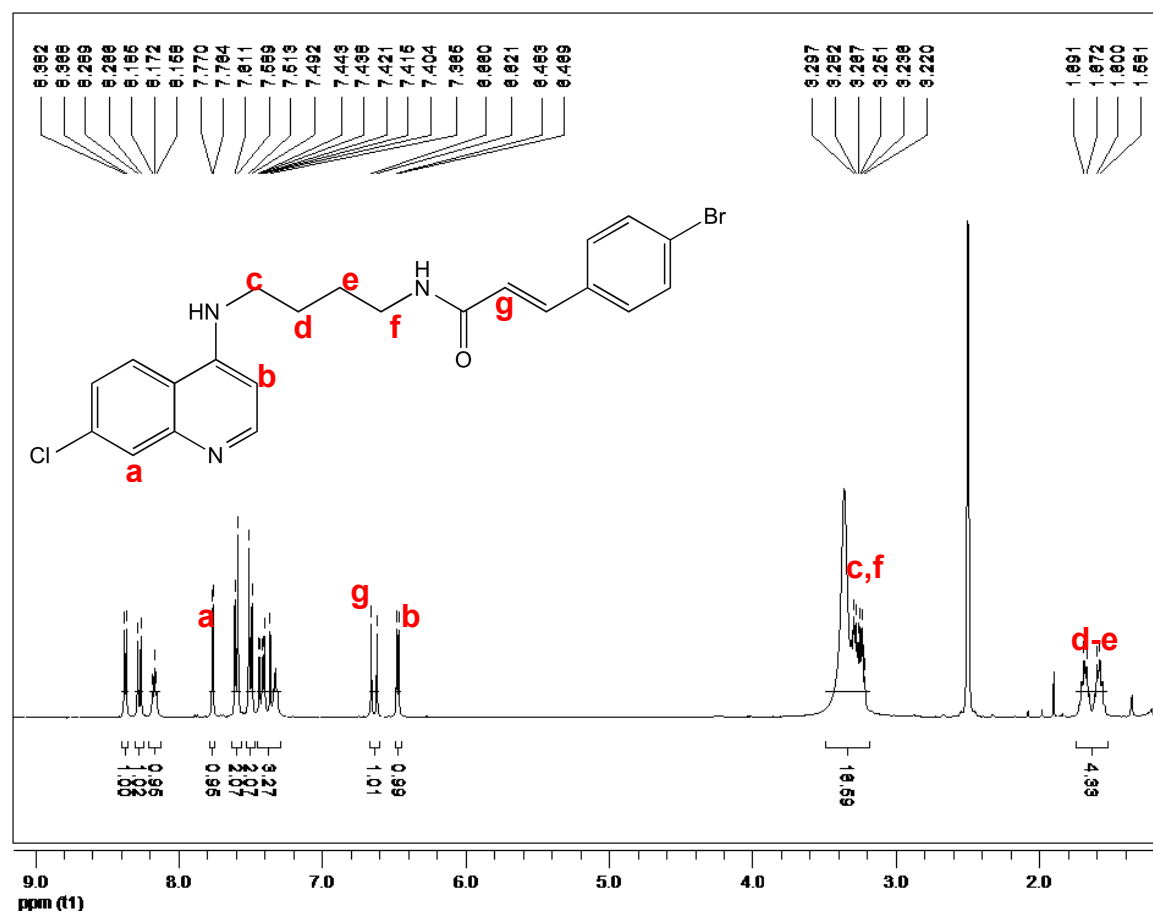
Figure 35. 1H-NMR (400 MHz, DMSO-d$_6$) of compound **13i**.
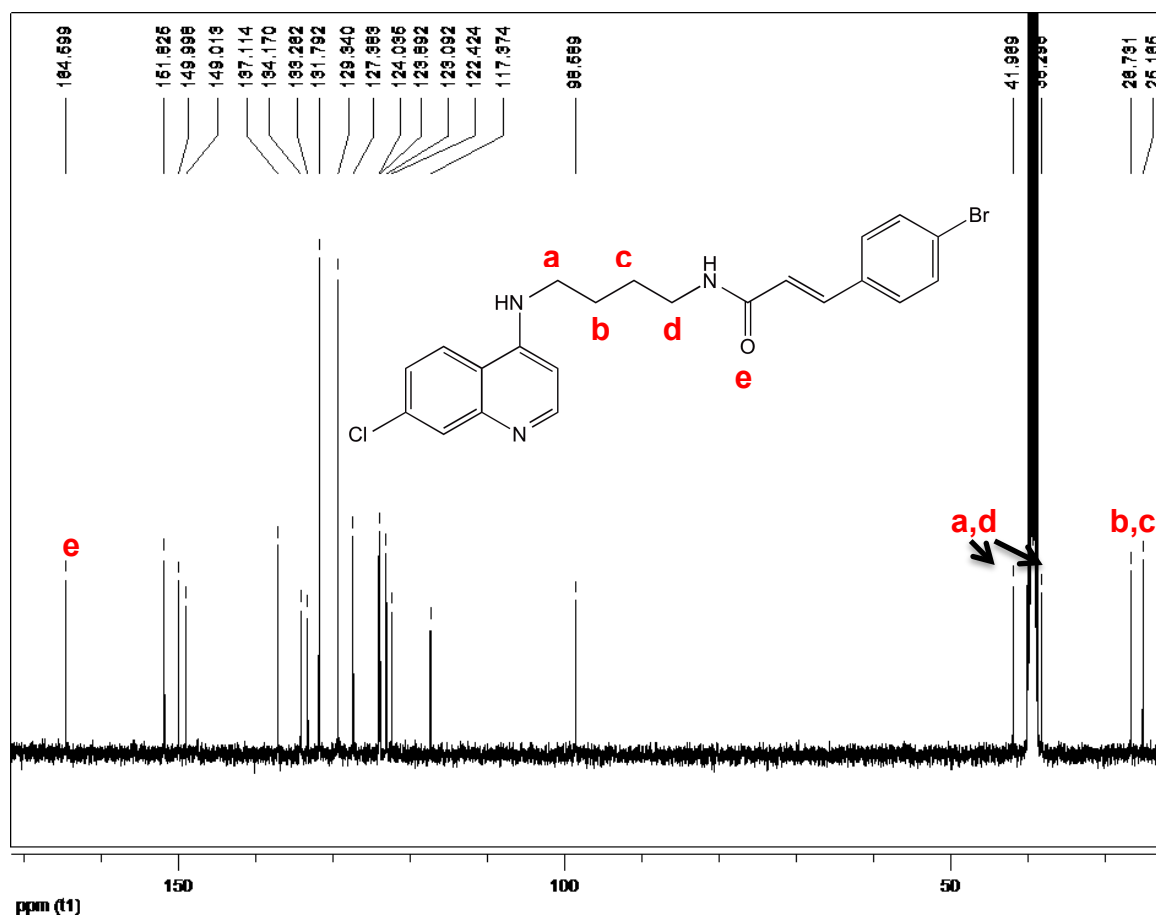
Figure 36. 13C-NMR (100 MHz, DMSO-d6) of compound **13i**.

Chemical Formula: $C_{22}H_{21}BrClN_3O$
Exact Mass: 457.06
Molecular Weight: 458.78
m/z: 459.05 (100.0%), 457.06 (77.4%), 461.05 (24.3%), 460.06 (24.1%),
458.06 (18.6%), 462.05 (6.0%), 461.06 (3.0%), 459.06 (2.5%), 460.05 (1.1%)
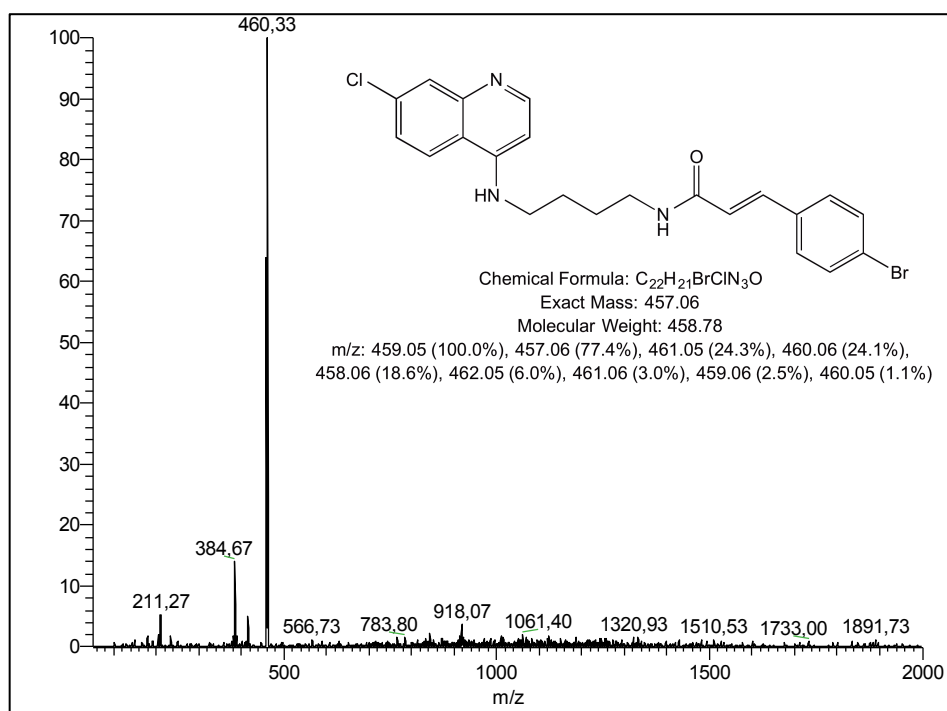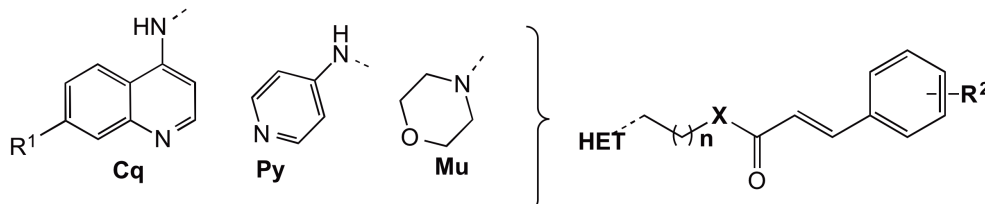
Figure 37. ESI-MS of the compound **13i**.

4.1.2. *In vitro* assays of *HEFLECIN*s

Once all compounds were obtained they were evaluated as inhibitors of blood stage *Plasmodia*. Compounds were tested *in vitro* against a CQ-resistant strain (P*f* W2) and some of them were also tested against a CQ-sensitive strain (P*f* 3D7). As shown in table 12, most tested chloroquinoline derivatives resulted more active against the blood stage *Pf* 3D7 parasites than the parent drug, CQ. More importantly, all compounds displayed activity higher than CQ against CQ-resistant *Pf* W2 parasites. Compound **13c** (IC_{50} (*Pf* 3D7) = 15.6 nM and IC_{50} (*Pf* W2) = 11.0 nM) and **13h** (IC_{50} (*Pf* 3D7) = 26.2 nM and IC_{50} (*Pf* W2) = 11.6 nM) were the most active of the series against *Pf* 3D7 and *Pf* W2, respectively, displaying activity comparable to ART, the key component of artemisinin combination therapies (ACT) which is currently recommended by the WHO as first-line treatment against CQ-resistant malaria.

Table 12. *In vitro* data of *HEFLECIN*s against *Pf* W2 and *Pf* 3D7. clog P of the series of compounds **13** are also shown.

Compound	HET	n	X	R^2	*Pf* W2 IC$_{50}$ (nM)[b]	*Pf* 3D7 IC$_{50}$ (nM)[b]	clogP[e]
13a				H	46.6 ± 5.5	62.9 ± 3.5	4.51
13b				*p*-Me	16.9 ± 1.2	24.2 ± 0.2	4.90
13c				*p*-^{i}Pr[a]	11.0 ± 6.2	15.6 ± 5.4	5.72
13d				*p*-OMe[a]	20.0 ± 2.6	30.6 ± 9.5	4.45
13e				*p*-NH$_2$	58.8 ± 1.5	78.1 ± 2.2	3.77
13f				*m*-F	34.1 ± 4.2	50.9 ± 1.0	4.68
13g	Cq	3	N	*p*-F	19.7 ± 0.4	39.9 ± 3.5	4.69
13h	R^1= Cl			*p*-Cl[a]	11.6 ± 0.4	26.2 ± 2.0	5.12
13i				*p*-Br	18.2 ± 2.8	28.8 ± 6.3	5.26
13j				*o*-NO$_2$	38.3 ± 4.2	56.9 ± 5.1	4.37
13k				*m*-NO$_2$	26.2 ± 2.1	42.1 ± 7.1	4.41
13l				*p*-NO$_2$	23.5 ± 1.3	48.9 ± 3.2	4.43
13m				*p*-NMe$_2$	25.8 ± 2.1	ND	
13n				*m,p*-diOMe	110.8 ± 13.0	ND	
14a				H	74.8 ± 2.0	141 ± 9.3	
14b				*p*-Me	47.4 ± 1.2	55.9 ± 5.1	
14c				*p*-iPr	38.0 ± 11.2	50.2 ± 50.3	
14d				*p*-OMe	55.1 ± 2.3	49.5 ± 5.8	
14e				*p*-NH$_2$	79.8 ± 2.0	135 ± 5.4	
14f	Cq	2	N	*m*-F	73.3 ± 6.8	138 ± 1.2	
14g	R^1= Cl			*p*-F	46.7 ± 3.3	47.7 ± 1.3	
14h				*p*-Cl	41.6 ± 2.9	46.5 ± 4.5	ND
14i				*p*-Br	38.2 ± 6.9	50.0 ± 3.5	
14j				*o*-NO$_2$	52.1 ± 4.0	64.2 ± 6.7	
14k				*m*-NO$_2$	50.3 ± 1.3	52.7 ± 5.3	
14l				*p*-NO$_2$	23.7 ± 2.1	52.5 ±10.8	
15a				*p*-^{i}Pr	31.5 ± 3.8		
15b	Cq R^1= Cl	4	N	*p*-OMe	50.3 ± 2.6		
15c				*p*-Cl	25.1 ± 0.2		
20	Cq R^1= Cl	3	O	*p*-OMe	122 ± 6	ND[d]	
21	Cq R^1= H	3	N	*p*-^{i}Pr	115 ± 3		
24	Py	3	N	*p*-OMe	>10000		
25	Mu	3	N	*p*-^{i}Pr	>10000		
ART					9.5	23.5	2.86 (2.90)[f]
CQ					138[c]	52.5	4.49 (4.63)[f]

[a] Tested *in vivo*; [b] blood-stage antiplasmodial activity against *Pf* strain W2 and strain 3D7; [c] Value taken from Ref[5]; [d] Not determined; [e] clogP was calculated using ALOGPS 2.1 (http://www.vcclab.org/lab/alogps/). [f] Experimental values for artemisinin and CQ are given in parentheses;

Results demonstrate that the cinnamoyl moiety seems to have a key role in reversing parasite resistance to CQ. *In vitro* data in table 12 show that tested quinoline-based *HEFLECIN*s are generally more active against *Pf* W2 (IC_{50} = 11.0-79.8 nM) than against *Pf* 3D7 (IC_{50} = 15.6-141 nM). Similar trends were observed against both strains. For instance, compounds **13** (IC_{50} (*Pf* 3D7) = 15.6-62.9 nM and IC_{50} (*Pf* W2) = 11.0-111 nM) are mostly more active than compounds **14** (IC_{50} (*Pf* 3D7) = 46.5-141 nM and IC_{50} (*Pf* W2) = 23.7-79.8 nM). Detailed inspection of the data shows the following:

- Compounds **13**, **14**, and **15** are highly active against *Pf* W2 (IC_{50} = 11.0-79.8 nM) except for compound **13n**. Comparison between the homologues, which differ only on the length of the polymethylene spacer, shows that a butyl spacer is preferred over the pentyl and propyl spacers. For instance, compound **13c** (IC_{50} = 11.0 nM) is more active than compounds **14c** (IC_{50} = 38.0 nM) and **15a** (IC_{50} = 31.5 nM).

- Removal of the chlorine in position 7 of the quinoline ring leads to a 10-fold decrease in the activity, as demonstrated by compound **21** (IC_{50} = 115 nM) that was ten times less active than compound **13c** (IC_{50} = 11.0 nM).

- Substitution of the amide bond by an ester functionality negatively influences the activity of the compounds. For example, compound **20** (IC_{50} = 122 nM) was 6 times less active than compound **13d** (IC_{50} = 20.0 nM).

- Replacement of the quinoline ring by pyridine or by a non-aromatic heterocyclic ring, such as morpholine, leads to complete loss of activity as shown by compounds **24** and **25**, which were both inactive (IC_{50} > 10000 nM).

- *In vitro* data of compounds **13** and **14** suggest that the electro-donating or electro-withdrawing character of the substituent on the cinnamoyl ring seems to have not significant effect on the activity of the compounds. Still, there seems to be a preference for substituents in the *para* position over the *meta* one as demonstrated by the *p*-F derivative **13g** (IC_{50} = 19.7 nM) *vs* the *m*-F substituted compound **13f** (IC_{50} = 34.1 nM), and the *p*-NO$_2$ derivative **13l** (IC_{50} = 23.5 nM) over the *m*-NO$_2$ substituted compound **13k** (IC_{50} = 26.2 nM). In addition, as shown in table 12 and fig. 38, there seems to exist some correlation between antiplasmodial activity and the lipophilicity of the compounds, as estimated by calculating log*P* values.
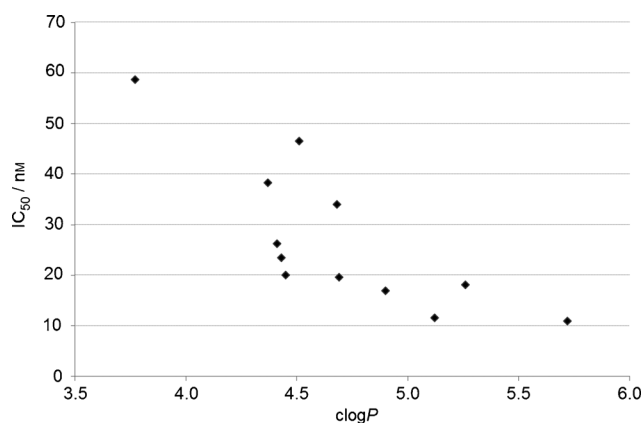
Figure 38. Plot of IC_{50} vs clogP values.

- Results also show some correlation of the antiplasmodial activity of the compounds with the Charton's steric parameter values[6] of *p*-alkyl substituent on the aryl ring of compounds **13-14**, with values of 0.0, 0.52 and 0.76 for the unsubstituted, *p*-Me, and *p*-*i*Pr substituents, respectively. For instance, compound **13a** (IC_{50} = 46.6 nM) is about 2 times less active than compound **13b** (IC_{50} = 16.9 nM), and three times less active than compound **13c** (IC_{50} = 11.0 nM). However, this trend is not clearly observed in the halogen substituted cinnamoyl derivatives.

4.1.3. Treatment of *P. berghei*-infected mice

For the most promising compounds, namely, the two most active compounds **13c** and **13h,** which had activity comparable to ART, and compound **13d,** the most active compound which complied with the Lipinski,[7] Veber,[8] and leadlikeness filters,[9] were further studied *in vivo* using the *P. berghei* mouse model. Briefly, mice were infected intraperitoneally (ip) with *P. berghei* and treated twice a day with intraperitoneal (ip) injections of 100 mg/kg, 30 mg/kg and 10 mg/kg. CQ was used as a positive control at concentrations of 30 mg/kg, 10 mg/kg and 3mg/kg, and was ip administered twice daily. In order to compare compounds efficacy, survival rate over time was analyzed (Fig. 39). According to fig. 39, compound **13d** was active *in vivo* at the highest concentration tested (100 mg/kg) while compounds **13c** and **13h** were highly toxic at this concentration. At 30 mg/kg and 10 mg/kg, compound **13h** extended survival compared to untreated control, contrary to compound **13c**. Finally, compound **13d** did not appear to have deadly toxic effect at any tested concentration. *In vivo* studies in rodent malaria model confirm that compounds **13d** and **13h** have *in vivo* antimalarial activity. The lack of activity of compound **13c** might be attributed to its high lipophilicity (logP > 5),[7] still compound **13d** and **13h** are only slightly less

lipophilic (logP ≈ 5). In addition, compounds' *in vivo* activities were significantly lower compared to the *in vitro* result, this could be explained by: i) the compounds' limited bioavailability, ii) biological difference between *P. berghei* and *Pf*, and/or iii) extensive binding to plasma proteins. Further studies need to be carried out to assess the bioavailability properties of the compounds to proceed with any needed structural modifications in order to improve the correlation between the *in vitro* and *in vivo* displayed activities.
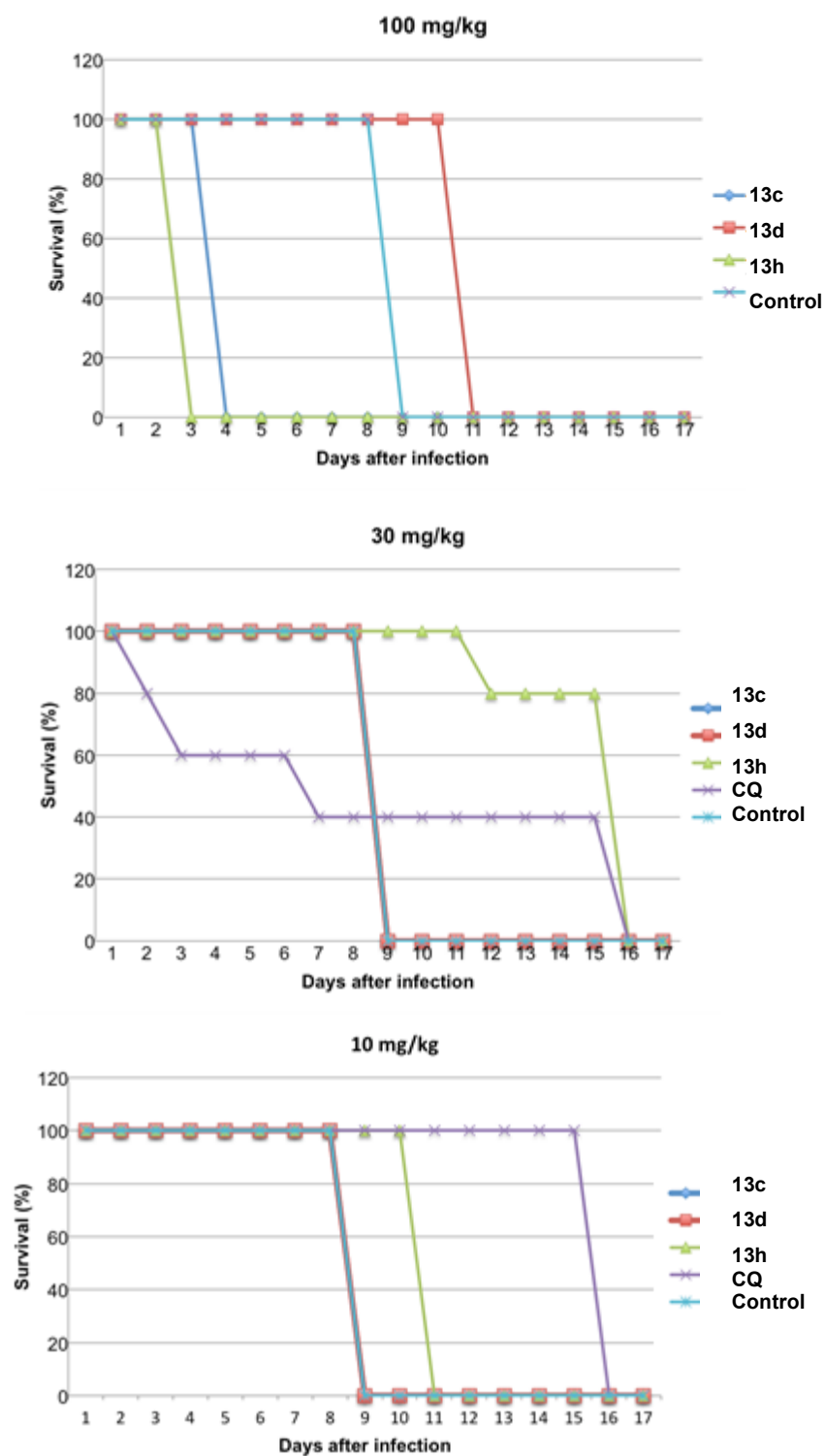
Figure 39. Survival curves for *P.berghei*-infected mice treated with compounds **13c**, **13d** and **13h**, and CQ.

4.1.4. Mechanism of action of *N-cinnamoylated derivatives*

Inhibition of falcipain activity and of β-hematin formation

Docking calculations showed that CQ-derived *HEFLECINs* could fit well into the active pocket of falcipain-2, making electrostatic and Van der Waals interactions with the residues in the cavity of the protease. However, further MD demonstrated that the ligand moves away from the binding pocket. Possibly, the non-covalent interactions that the ligand establishes with the residues of the active site are not strong enough to keep it within the cavity. These last results suggest that the α,β-unsaturated portion of the ligand will not be able to alkylate the catalytic Cys. However, since the docked conformations of compounds **13-14** place the vinyl within ~3.5 Å from the thiolate, we still envisaged that, if favoured by its kinetics, the reaction could occur and the ligand could form a covalent interaction with Cys before being expulse of the active cavity of falcipain. In this context, compounds **13-14** were evaluated as inhibitors of falcipain-2 by Rosenthal's team.[10] In addition, *in vitro* assays against β-H formation (Table 13) were carried following the procedure described in the experimental section of chapter 2.

Although none of the compounds exhibited activity against FP2, most of them showed to be active *in vitro* against β-H formation. Accordingly, results suggest that inhibition of the β-H formation seems to be one of the mechanisms contributing to the antiplasmodial activities of the compounds since variation of inhibition of β-H formation follows the same trend of activities against CQ-resistant strain *Pf* W2, as shown by compounds **13c** *vs* **14c** *vs* **15a**. Also, the chlorine in position 7 of the chloroquinoline aromatic ring is once again shown to be essential for the activity of CQ and its analogues against the β-H formation.[11, 12] However, since the most active compounds inhibiting the parasite development, namely, the *p*-iPr and *p*-Cl derivatives **13c** (IC$_{50}$ = 11.0 nM) and **13h** (IC$_{50}$ = 11.6 nM), were not the most active inhibitors of β-H formation, results suggest the existence of an additional mechanism through which *HEFLECIN*s exert their activities.

Table 13. *In vitro* assays against β-hematin formation.
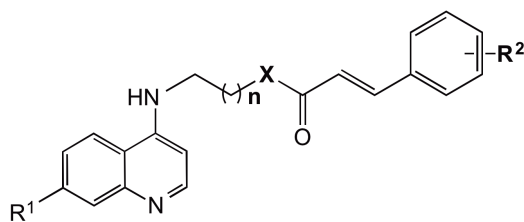
Compound	R^1	n	X	R^2	β-H[a]
13a				H	-
13b				*p*-Me	-
13c				*p*-*i*Pr[c]	+
13d				*p*-OMe[c]	+
13e				*p*-NH$_2$	-
13f				*m*-F	+
13g		3	N	*p*-F	+
13h				*p*-Cl[d]	+
13i				*p*-Br	++
13j				*o*-NO$_2$	+
13k				*m*-NO$_2$	-
13l				*p*-NO$_2$	++
13m				*p*-NMe$_2$	+
13n				*m,p*-diOMe	-
14a	Cl			H	-
14b				*p*-Me	-
14c				*p*-iPr	-
14d				*p*-OMe	-
14e				*p*-NH$_2$	-
14f		2	N	*m*-F	-
14g				*p*-F	-
14h				*p*-Cl	+
14i				*p*-Br	-
14j				*o*-NO$_2$	+
14k				*m*-NO$_2$	+
14l				*p*-NO$_2$	+
15a				*p*-*i*Pr	+
15b		4	N	*p*-OMe	-
15c				*p*-Cl	-
20		3	O	*p*-OMe	+
21	H	3	N	*p*-*i*Pr	-
CQ					++

[a] β-H inhibition was determined and ranked as shown in chapter 2; test compounds were ranked as follows: <50%, not active (-); between 50 and 75%, moderately active (+); ≥75%, highly active (++).

Inhibition of New Permeability Pathways in Pf-infected erythrocytes

One possible additional mechanism underlying the activity of *HEFLECINs* against blood-stage *Pf* could be inhibition of intraerythrocytic parasite's nourishment: the growth of *Pf* within RBC relies on the uptake of certain nutrients from the extracellular medium; during the intraerythrocytic development of the parasite, the RBC show increased permeability to a wide range of structurally unrelated low molecular weight solutes, through the so-called "New Permeability Pathways" (NPP), whose nature is still elusive and may comprehend one or several host-encoded channels, or a single parasite-encoded channel also known as plasmodial surface anion channel (PSAC).[13, 14] Some inhibitors of these NPP include furosemide (**XXXII**), 5-nitro-2-(3-phenylpropylamino) benzoic acid (NPPB, **XXXIII**)[15] and dantrolene (**XXXIV**).[13] The latter nitro-substituted compound (**XXXIV**) was found not to have any measurable effect on other anion channels previously identified, consequently, addressing the concern of designing inhibitors with specificity towards this relatively new antimalarial target.[13]

(XXXII)

(XXXIII)

(XXXIV)
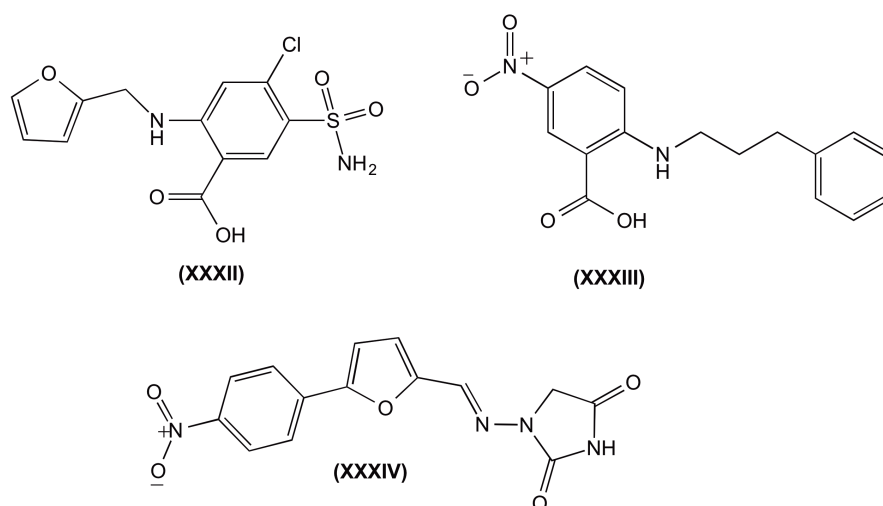
Remarkably, the nitro substituted *HEFLECIN*s are highly active as compared with most of the other substituted derivatives. Additionally, Kanaani and co-workers found that cinnamic acid derivatives inhibit NPP.[16] Interestingly, they found that the antiplasmodial activity correlated with the hydrophobic character of the molecules evaluated. In addition, Kirk's team found, through the study of a series of arylaminobenzoates,[17] analogues of the anion channel blocker 5-nitro-2-(3-phenylpropylamino)benzoic acid (NPPB), that the antimalarial activity of the derivatives increase with the length and lipophilicity of the hydrophobic tail. These findings are comparable to the results obtained for *HEFLECINs,* which might suggest that NPP could be the additional mechanism of action through

which the cinnamoyl derivatives here presented exert their activity. In order to test this hypothesis, preliminary NPP-inhibition assays were carried out by sorbitol-induced hemolysis assays, as following described.

The erythrocyte membrane is normally impermeant to sorbitol, but NPP appearance in the infected RBC membrane allows the passage of sorbitol and, when mature parasitized erythrocytes are suspended in an isosmotic sorbitol solution, there is a net uptake of sorbitol and water into the erythrocyte, resulting in cell swelling and hemolysis.[18] The rate of hemolysis can be correlated with the influx of sorbitol, hence, can be used as a good indicator of NPP inhibitory activity. In this context, the rate of hemolysis of *p*-isopropyl cinnamic derivatives **13c** and **1c** was evaluated since the *p*-isopropyl derivatives were the compounds which generally presented the highest activity among the series (Fig. 40). These *in vitro* assays were performed by Egée's team at *Université Pierre et Marie Curie*, France. Compound **13c** was shown to display (at 1 µM) significant NPP-inhibition activity as it markedly delayed sorbitol-induced hemolysis in *Pf* infected RBC, whereas **1c** did not. These results correlate with *in vitro* antiplasmodial data since *HEFLECIN* **13c** (IC_{50} = 11 nM) was more active than *HEDICIN* **1c** (IC_{50} = 830 nM) against *Pf* W2. However, these are only preliminary results and additional experiments are already scheduled to test all *HEFLECINs* using the patch-clamp technique, which is today the most precise way to decipher subtle changes in channel activity.[19]
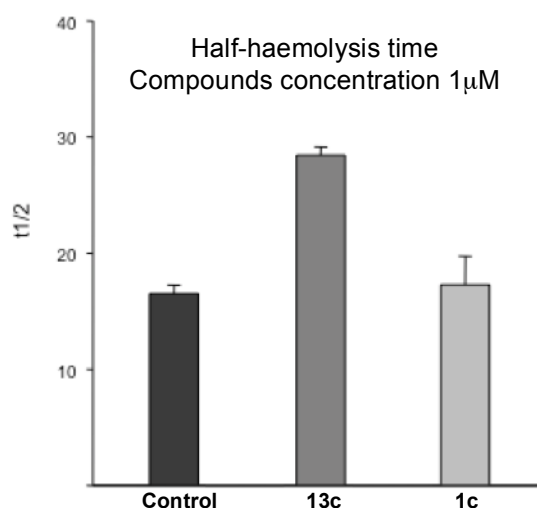
Figure 40. Half-haemolysis time of *p*-isopropyl cinnamic derivatives **13c** and **1c**.

Although the results here presented reinforce the idea that *HEFLECINs* might exert their antimalarial action through inhibition of NPP, other MOA cannot be ruled out. For instance, inhibition of plasmodial cytosolic proteases[20, 21] like aminopeptidases *Pf*A-M1 and *Pf*A-M17[22] or CQ-chemosensitization.[23] It has been shown that resistance to chloroquine is due to mutations in a putative transmembrane chloroquine transporter, *Pf*CRT, which seems to allow the drug to rapidly efflux from the parasite digestive vacuole, preventing sufficient inhibition of heme polymerization to block parasite development.[24] Chloroquine chemosensitizers are thought to interact with *Pf*CRT in such a way that drug efflux is impeded.[23] *HEFLECINs* described here match relevant structural factors of chloroquine-chemosensiziting agents recently reported by Kelly[25] and Lavrado[26] such as a hydrogen bond acceptor (nitrogen) or aminobutyl chains between the heterocyclic core of the compound and its *N*-substituted terminal amine. Therefore, we cannot rule out that *HEFLECINs* might (also) through this mechanism, and future investigations should be undertaken to pursue this hypothesis.

4.1.5. Antiplasmodial assays against liver-stage *P. berghei* parasites

Motivated by the fact that preliminary studies suggest *HEFLECINs* to be capable of inhibiting NPP (see previous section), and since similar anion channel enhanced activity has been described for *P. berghei*-infected liver cells,[27] we decided to further evaluate the *in vitro* activity of *HEFLECIN*s against liver stage malaria. *In vitro* assays were carried out following procedure previously reported.[28] Remarkably, all CQ-derived *HEFLECIN*s were active against liver stage parasites (Fig. 41 and Table 14), displaying activity in the low micromolar range (IC_{50} = 1.1-6.5 μM). These are unprecedented results since CQ has been reported to be inactive against liver stage malaria[29] and, to the best of our knowledge, *HEFLECINs* were the first CQ analogues with dual-stage antimalarial activity. As shown in table 14, compounds present IC_{50} 5 to 15 times lower than CQ and 3-7 times lower than those of the reference drug for liver stage malaria, PQ. Some preliminary SAR could be devised from the liver stage inhibition results:

- As observed for blood stage activity, the butyl spacer is preferred over the propyl and pentyl spacers, for instance, activity displayed by **13c-d,h** *vs* **14c-d,h** and **15a-c**.

- Contrary to results against blood stage malaria, substitution on the cinnamoyl moiety leads to a decrease in the activity, as the most active compound was the unsubstituted derivative **13a** (IC_{50} = 1.1 μM).

- The presence of electro-withdrawing groups in the *para* position of the cinnamoyl ring leads to a slight increase on the activity, as demonstrated by **13b-d** (IC_{50} = 2.4-2.9 μM) and **13g-i** (IC_{50} = 1.1-1.4 μM).

- Similar to blood stage results, removal of the chlorine in position 7 of the quinoline ring or substitution of the amide bond by an ester functionality lead to a decrease in the activity (Fig. 41).

- Substitution of the chloroquinoline core by a non-aromatic ring or pyridine is also detrimental for liver-stage activity, as shown by compound **13c** (IC_{50} = 2.5 μM) vs **25** (IC_{50} > 10 μM) and **13d** (IC_{50} = 2.9 μM) vs **24** (IC_{50} = >10 μM).

The mechanism of *HEFLECIN*s against liver stage *Plasmodia* remains to be elucidated, and work is currently in course that aims at investigating whether the compounds are also able to inhibit anion channel activity in *P. berghei*-infected hepatocytes. Based on the antiplasmodial results against both liver and blood stage parasite, compound **13d** and **13h** were evaluated *in vivo* against the liver stage form of malaria. *In vivo* assays were carried out by Prudêncio's team at Universidade de Lisboa. However, none of the compounds displayed *in vivo* activity against this stage. The latter might be explained by the fact that the liver is responsible for most drug metabolism, since the liver has the most drug metabolising enzymes relative to other organs.[30, 31] Thus *HEFLECIN*s might be metabolized into inactive compounds. Nonetheless, compounds here presented represent new leads towards the discovery of multistage antimalarials.
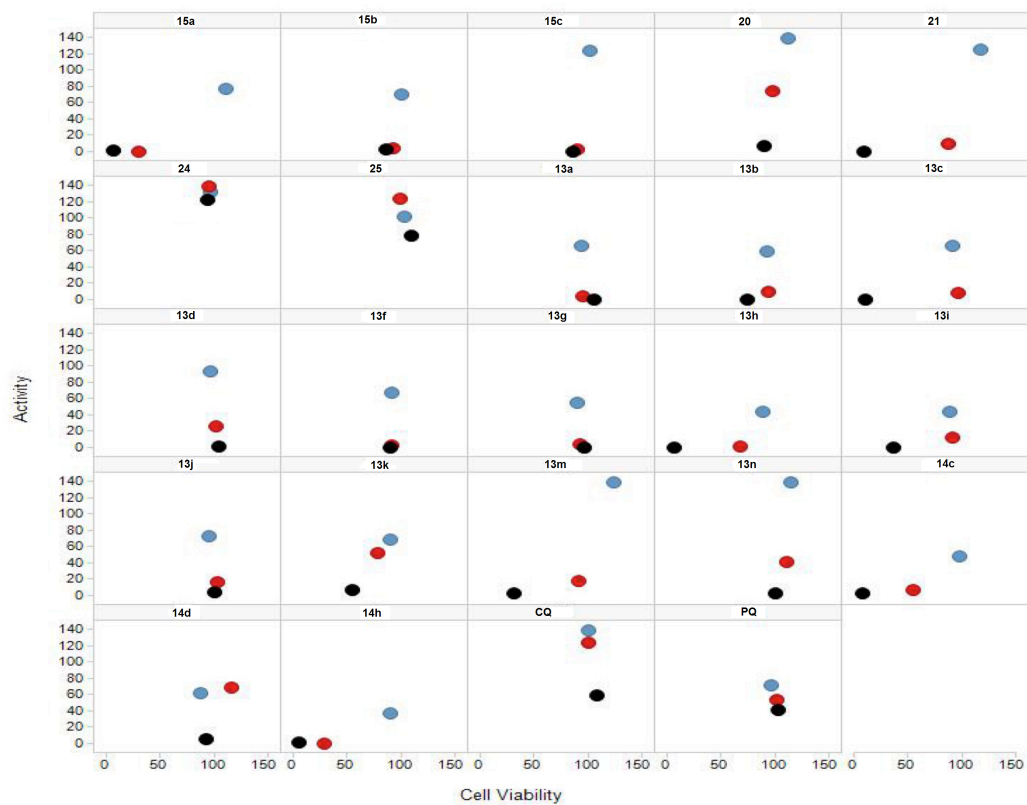
Figure 41. Anti-infective activity vs toxicity to hepatoma cells plot. PQ and CQ were included for comparison. The black, red, and blue circles represent results for the tested compounds at 10, 5, and 1 µM, respectively. Infection loads of Huh7 cells, from a human hepatoma cell line, were determined by bioluminescence measurements of cell lysates 48 h after infection with luciferase-expressing *P. berghei* parasites by Prudêncio's team.

Table 14. *In vitro* assays of *N*-cinnamoylated derivatives **13-14**, **20-21**, and **24-25** against *P. berghei* liver stage malaria.
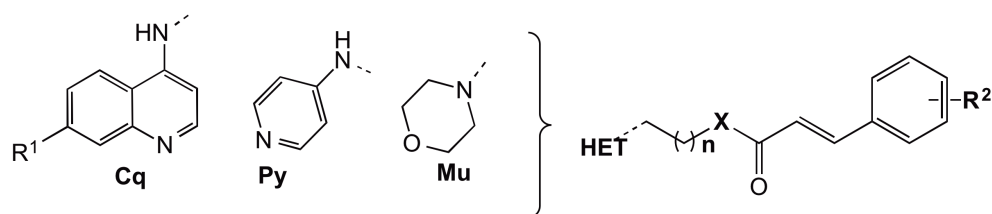
Compound	HET	n	X	R²	Liver Stage IC$_{50}$ (µM)[a]
13a				H	1.1 ± 0.1
13b				*p*-Me	2.4 ± 0.5
13c				*p*-^{i}Pr[c]	2.5 ± 0.2
13d				*p*-OMe[c]	2.9 ± 0.4
13e				*p*-NH$_2$	ND
13f				*m*-F	1.1 ± 0.2
13g	Cq	3	N	*p*-F	1.4 ± 0.2
13h	R¹= Cl			*p*-Cl[d]	1.4 ± 0.3
13i				*p*-Br	2.3 ± 0.6
13j				*o*-NO$_2$	1.1 ± 0.2
13k				*m*-NO$_2$	
13l				*p*-NO$_2$	ND
13m				*p*-NMe$_2$	
13n				*m,p*-diOMe	4.1 ± 0.2
14a				H	
14b				*p*-Me	ND
14c				*p*-iPr	
14d				*p*-OMe	4.0 ± 0.6
14e				*p*-NH$_2$	
14f	Cq	2	N	*m*-F	
14g	R¹= Cl			*p*-F	
14h				*p*-Cl	
14i				*p*-Br	ND
14j				*o*-NO$_2$	
14k				*m*-NO$_2$	
14l				*p*-NO$_2$	
15a	Cq			*p*-^{i}Pr	
15b	R¹= Cl	4	N	*p*-OMe	2.3 ± 0.6
15c				*p*-Cl	1.6 ± 0.1
20	Cq R¹= Cl	3	O	*p*-OMe	6.5 ± 0.9
21	Cq R¹= H	3	N	*p*-^{i}Pr	ND
24	Py	3	N	*p*-OMe	>10
25	Mu	3	N	*p*-^{i}Pr	>10
ART					ND
CQ					15.9
PQ					7.5

[a] IC$_{50}$ of the most active compounds against liver stage.

4.2. PQ-based *HEFLECIN*s

Given the rather promising findings made with *N*-cinnamoylated analogues of CQ, especially in what concerns the display of activity against liver forms of *Plasmodia*, further studies were carried to evaluate whether *N*-cinnamoylation would also enhance the activity of PQ against liver stage malaria. Any advance towards development of liver-stage malaria drugs is of particular importance, not only because liver parasites silently open the doorway for establishment of the malarial infection, but also due to the fact that drugs acting against liver forms of *Plasmodia* are scarce, and PQ is the only drug in clinical use worldwide. In this view, a series of PQ-cinnamic acid conjugates (**28**) was synthesized and characterized following a similar procedure to that previously used for compound **13-15.**

4.2.1. Synthesis and characterization of PQ-based *HEFLECIN*s

Synthesis of PQ-based HEFLECINs

The synthetic procedure to obtain PQ-based *HEFLECINs* was straightforward. Initially, cinnamic acids were activated using TBTU as coupling reagent and DIEA. After this activation step, a solution of PQ in DMF was added and the reaction allowed to proceed (Scheme 14) to finally yield the desired conjugate.

R= H; *p*-Me; *p*-iPr, *p*-OMe; *p*-NHBOC;
m-F; *p*-F; *p*-Cl; *p*-Br; *o*-NO$_2$; *m*-NO$_2$; *p*-NO$_2$
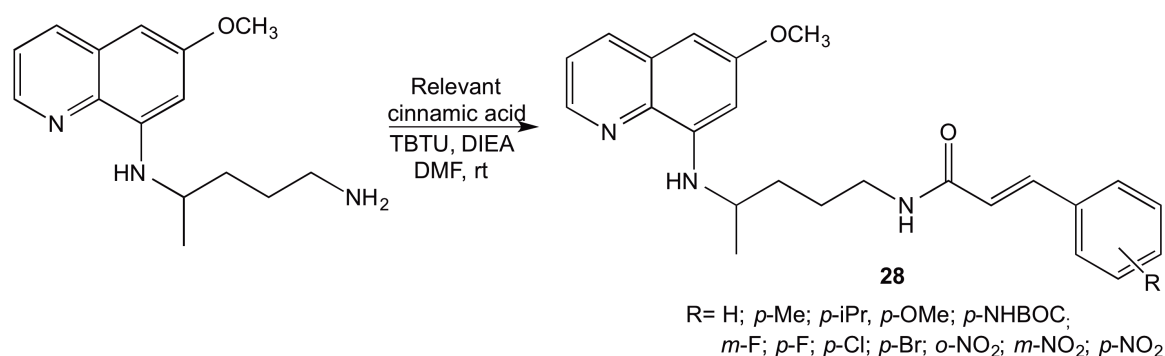
Scheme 14. Synthetic pathway of PQ-based *HEFLECIN*s (**28**).

Characterization of PQ-based HEFLECINs

All PQ-based *HEFLECINs* obtained were characterized by 1H-NMR and 13C-NMR, ESI-IT MS, and HPLC. Obtained data were in agreement with structure of PQ-based *HEFLECINs*. Figures 42-43 display an example of the NMR results for PQ-based *HEFLECIN* **28f**. As shown, the 1H-NMR of compound **28f** displays the expected signals

of the methyl and methylene groups in the upfield region: i) a doublet at 1.30 ppm of the protons of the methyl group attached to the alkyl spacer, ii) a singlet at 3.86 ppm corresponding to the protons of the methoxy group, and iii) the signal of the 3 methylene groups of the alkyl chain at 1.73 and 3.40 ppm respectively. The 1H-NMR spectrum also displayed in the downfield region the characteristic signals of the aromatic protons present in quinoline ring such as the doublets with small coupling constants at 6.34 ppm and 6.30 ppm, which belong to protons at position 5 and 7 of the heterocycle, respectively. Regarding the cinnamoyl functionality, the 1H-NMR spectrum (Fig. 42) shows the α,β-unsaturated vinyl protons at 6.18 ppm and 7.53 ppm. In the 1H-NMR, it is also displayed the deshielded protons attached to a nitrogen atom at 5.86 and 7.31 ppm. Furthermore, the 13C-NMR (Fig. 43) shows the signals related to *PRIMACIN* **28f**, for instance, it displays the deshielded signal of the carbonyl group at 165.7 and 6 signals in the shielded region. Moreover, in the ESI-IT MS (Fig. 44) is observed i) one strong peak at 408.33 which is associated with the desired compound, ii) a peak at 837 that might suggest that the compound forms a dimer, and iii) a peak at 1243.13 which suggest the formation of a trimer.
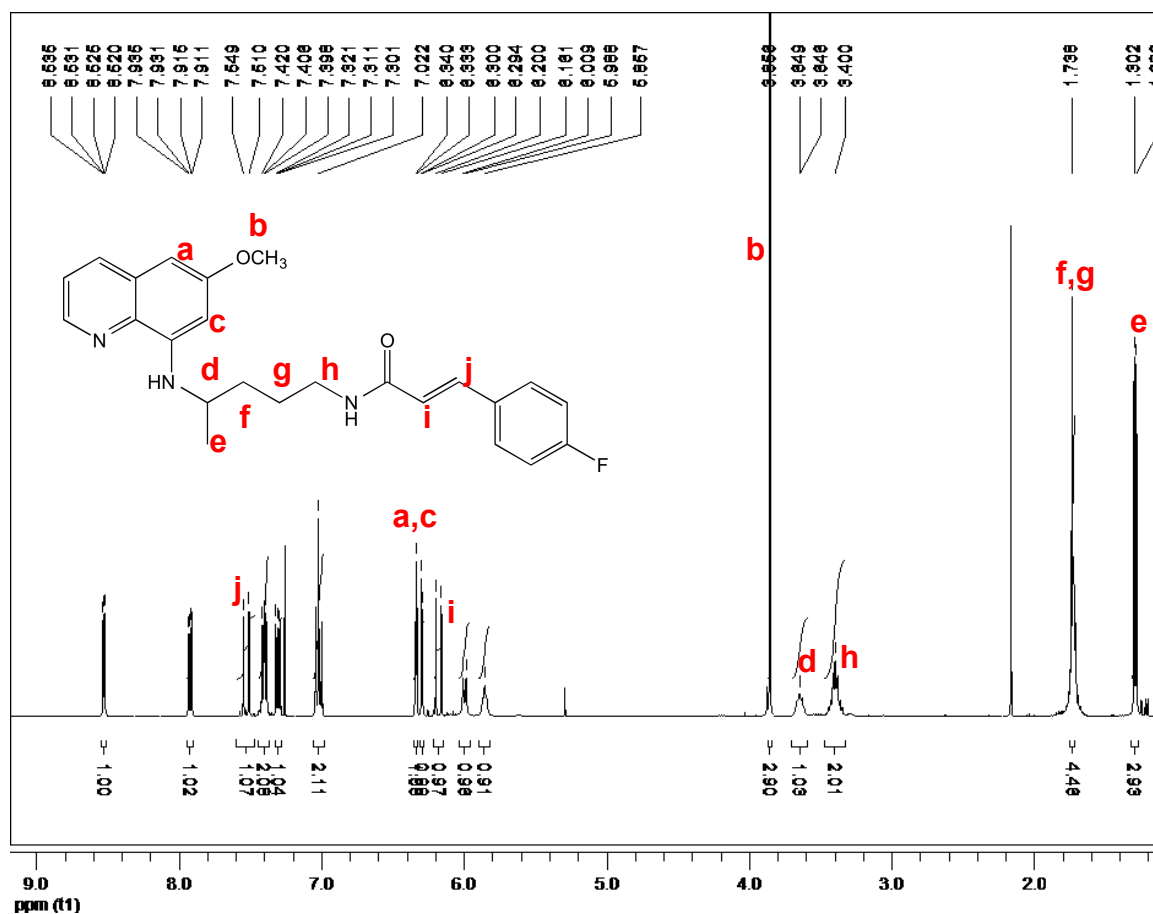
Figure 42. 1H-NMR (400 MHz, CDCl₃) of compound **28f**.
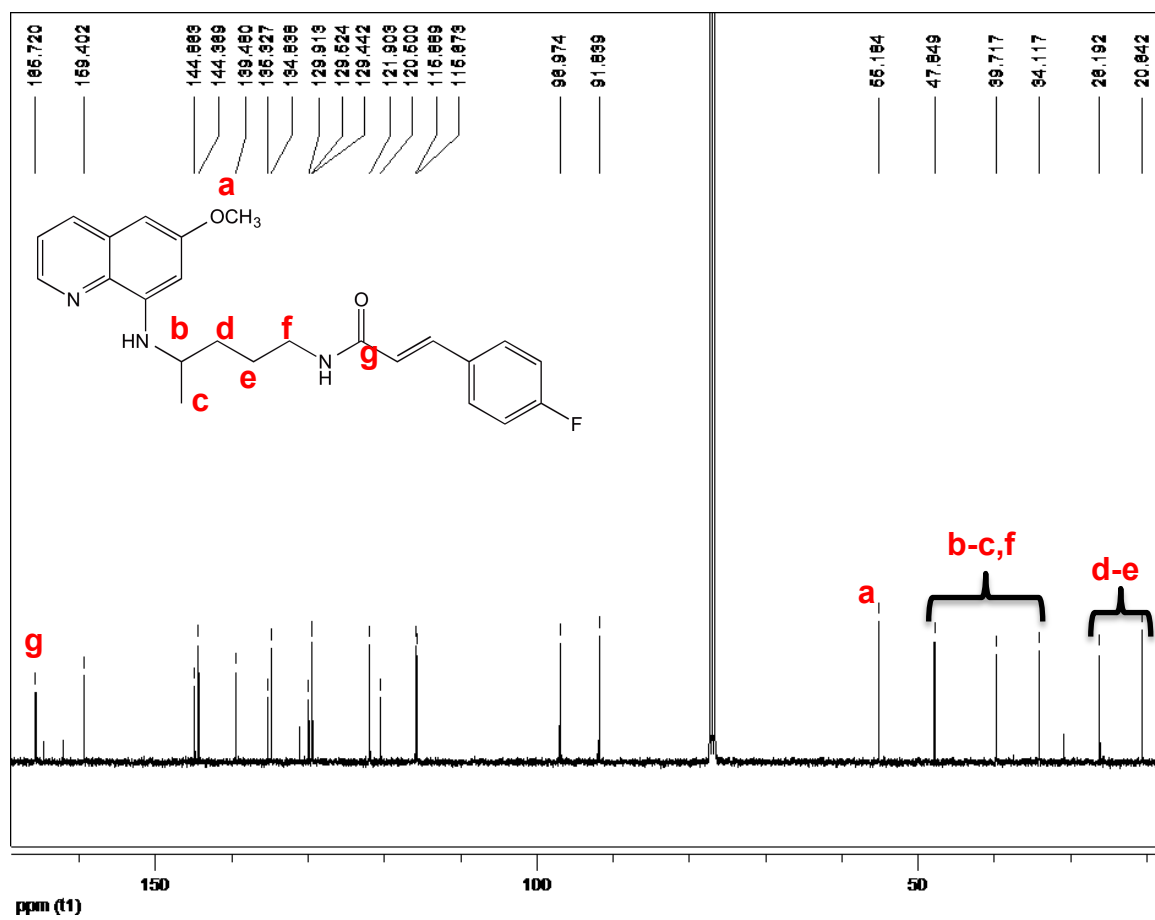
Figure 43. 13C-NMR (100 MHz, CDCl$_3$) of compound **28f**.
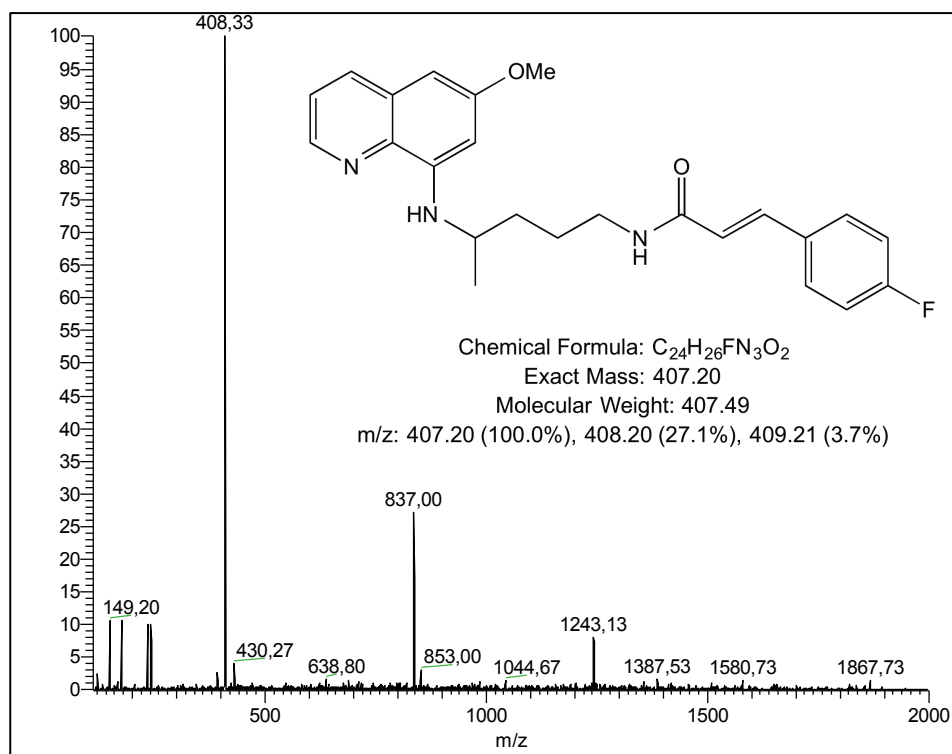
Figure 44. ES-IT MS of compound **28f**.

4.2.2. Antiplasmodial assays of PQ-based *HEFLECINs*

Once the desired PQ-based *HEFLECINs* were obtained, they were evaluated against liver stage malaria following procedures previously reported.[32] Accordingly, all cinnamoyl derivatives **28** were found to inhibit the parasite activity in the micromolar range (IC_{50} = 1.29 - 3.33 µM) with IC_{50} values lower than those presented by PQ (IC_{50} = 7.5 µM), the reference drug for liver stage malaria (Table 15). Although results present a relative short activity range, it seems that the electro-donating or electro-withdrawing properties of the substituent in the *para* position of the cinnamoyl ring do not have an effect on the activity against liver stage parasites. In addition, though it seems that the meta substitution is preferred over the para substitution for both the fluoro- and nitro-substituted derivatives such detailed conclusion cannot be made since compounds presented a range of activity significantly short. Furthermore, as observed in fig. 45, compounds resulted non-toxic to Huh7 human hepatoma cells *in vitro*.

 PQ-based *HEFLECINs* were also evaluated against blood stage parasite to assess other quinoline moiety against this stage. Except for compound **28c** (IC_{50} = 4.84 µM) that was modestly active, none of PQ-based *HEFLECINs* resulted active (IC_{50} = ≥ 10 µM). This result is in agreement with the fact that PQ-based structures are not efficient blood-Schizontocidals. The latter could be explained by the findings that suggest that the 8-amino-6-methoxyquinoline core is not an efficient inhibitor of hemozoin formation

because it forms a weak binding with heme that does not interfere with hemozoin formation.[33, 34] Consequently, results from PQ-based *HEFLECIN*s' blood-stage activity reinforce our previous findings regarding the essential role of the chloroquine core for the activity of *HEFLECIN*s **28** against intraerythrocytic parasites. Moreover, based on the fact that PQ-based *HEFLECIN*s presented a short range of activity and cytotoxicity and the *p*-methoxy chloroquine-based *HEFLECIN* **13d** did not present deathly toxicity when assessed *in vivo* against blood stage parasite at any of the tested concentrations, PQ derivative **28d** was further evaluated *in vivo* against liver stage. However, compound **28d** did not display *in vivo* activity against liver stage parasite.
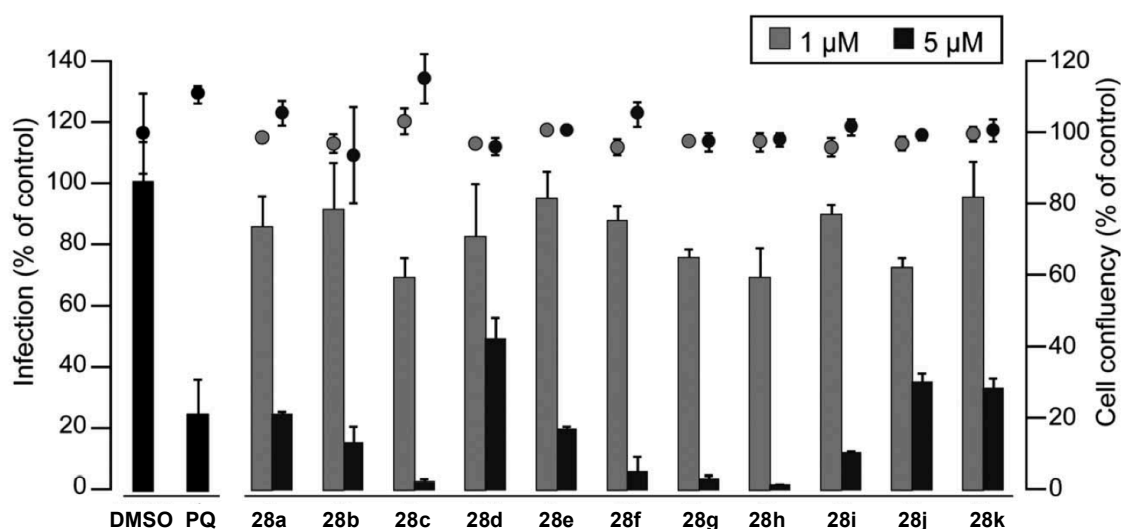
Figure 45. *P. berghei* liver stages activities of PQ-based *HEFLECIN*s **28**. Data shown are for the screening of anti-infective activity (infection scale, bars) and toxicity to human hepatoma Huh-7 cells (cell confluency scale, dotted lines with round markers).

Table 15. Antiplamosdial activity of compounds against liver stage malaria.
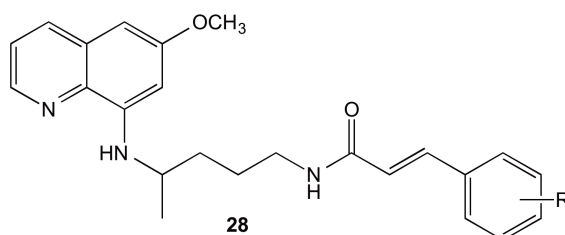
Compound	R	IC$_{50}$ (μM) against liver-stage *P. berghei*	IC$_{50}$ (μM) against blood-stage *Pf*[a]
Reference drug[b]	-	7.50 (PQ)	5.64 ± 0.04 nM (ART)
28a	H	2.01 ± 0.27	≥ 10
28b	*p*-Me	2.13 ± 0.58	
28c	*p*-*i*Pr	1.54 ± 0.35	4.84 ± 0.98
28d	*p*-OMe	2.35 ± 0.19	
28e	*m*-F	1.63 ± 0.16	
28f	*p*-F	2.33 ± 0.47	
28g	*p*-Cl	2.39 ± 0.19	≥ 10
28h	*p*-Br	1.38 ± 0.33	
28i	*o*-NO$_2$	2.36 ± 0.58	
28j	*m*-NO$_2$	2.12 ± 0.49	
28k	*p*-NO$_2$ (0.78)	2.24 ± 0.27	

[a] CQ-resistance *Pf* W2; [b] reference drug for liver stage (PQ: Primaquine (**III**)) and blood stage malaria (ART). Highlighted in blue the most active compound against liver stage malaria.

4.3. Acridine-based *HEFLECIN*s

Other heteroaromatic cores such as acridine have demonstrated to display activity against malaria.[35] For instance, acridine analogue of CQ (**XXXV**) presented nanomolar activity against *Pf* CQ-sensitive strain 3D7 (EC$_{50}$ = 720 nM; Molecule ChEMBL ID: CHEMBL532286). Accordingly, we decided to evaluate whether a similar effect to that displayed by the *N*-cinnamoylation of the PQ and CQ will be observed by the *N*-cinnamoylation of the AQ core. In this context, the chloroquine core was substituted by an acridine nucleus to evaluate the antiplasmodial activity of the resulted compounds. Compound **29a-g** were synthesized following previous synthetic procedure used for chloroquinoline-based *HEFLECIN*s (Scheme 15).

(**XXXV**)
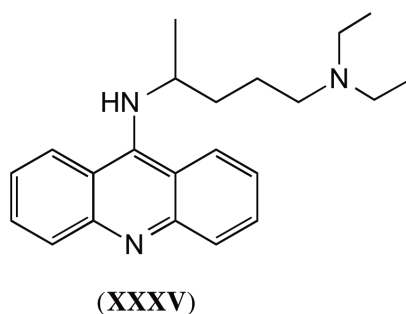
4.3.1. Synthesis and characterization of acridine-based *HEFLECIN*s

Synthesis of acridine-based HEFLECINs (29)

Acridine-based *HEFLECIN*s were synthesized following procedure depicted in Scheme 15. Significant challenges were encountered when trying to synthesize compound **29** due to the low purity of the intermediate compound **30** that was used in the coupling reaction. Although different attempts were carried out in order to purify compound **30**, this was not achieved. Consequently, the oily mixture containing compound **30** as major component was used in the following coupling reaction with cinnamic acids. Accordingly, *N*-alkylcinnamoylated acridine derivatives were obtained in low yields but the procedure allowed fast generation of the compounds **29** for *in vitro* screening.
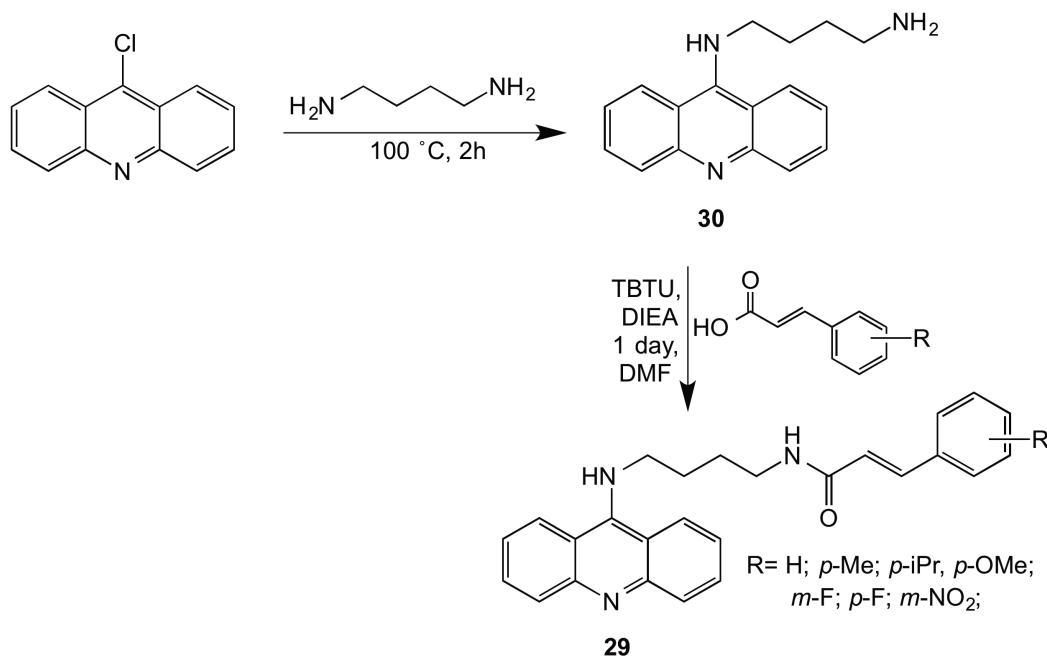
Scheme 15. Synthetic pathway of acridine derivatives **29**.

Interestingly, in spite of the fact that similar coupling conditions were used for the synthesis of *HEFLECINs* **13**, **28** *and* **29**, significant yield differences were observed in between series. Yields globally decreased in the following order: PQ-based *HEFLECINs* **28** > CQ-based *HEFLECIN*s **13** > Acridine-based *HEFLECINs* **29**. Knowing that the nucleophiles constitute the main difference between the reactions, the corresponding structures were analyzed to better understand why yield decreases in the previously stated order. Since the three relevant nucleophiles PQ, **16**, and **30** consisted in a primary amine linked to a butyl chain placing the amino group at the same distance from the heteroaromatic core, the nucleophilic power of the primary amine should not be influencing the reactivity of the respective compounds. In fact, the main difference between those three nucleophiles is their heteroaromatic cores. Accordingly, pKa value of the heteroaromatic nitrogen was estimated for each of the three structures, using MarvinSketch (Fig. 46). Remarkably, results show that the lowest the pKa of the heterocyclic nitrogen in the nucleophile, the highest the yield of its condensation with cinnamic acids. Therefore, one possible explanation is that as the pKa of the heteroaromatic nitrogen increases, so does the organization of molecules in solution, through formation of intermolecular hydrogen bonds. The latter may turn the amino group less available to perform the nucleophilic attack to the activated cinnamic acid. However, this is just a hypothesis and further studies should be done to confirm such premise.
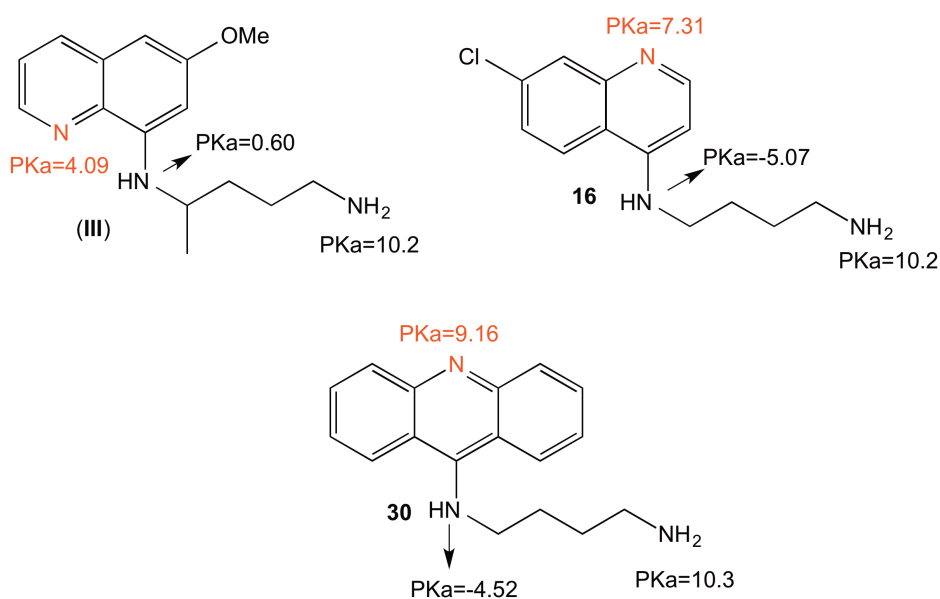
Figure 46. Nucleophiles and estimated pKa values for their nitrogen-based groups.

Characterization of acridine-based HEFLECINs

All acridine-based derivatives were characterized through NMR, ESI-IT MS, and HPLC. Data resulted in agreement with the structure of the target compounds. Compounds presented 1H-NMR spectra similar to those of compounds **13**, with major differences located at the deshielded region. As an example, fig. 47-48 display the downfield region of the NMR spectra of compound **29c**, where such distinctive signals are observed. For instance, fig. 47 shows the deshielded protons of the acridine ring at 8.05 ppm, 7.60 ppm, 7.29 ppm, and 7.00 ppm, the characteristic signals of the α,β-unsaturated carbons at 6.58 ppm and 7.60 ppm, and the signals of the cinnamoyl ring protons at 7.17 ppm and 7.40 ppm. Furthermore, fig. 48 displays the 14 signals associated to the deshielded carbons of compound **29c** in the downfield region, including the signal of the carbonyl group at 178.0 ppm. In addition, the ESI-IT MS (Fig. 49) shows the base peak at m/z 438.53 which matches the expected value for the *quasi*-molecular ion of the desired compound **29c**.
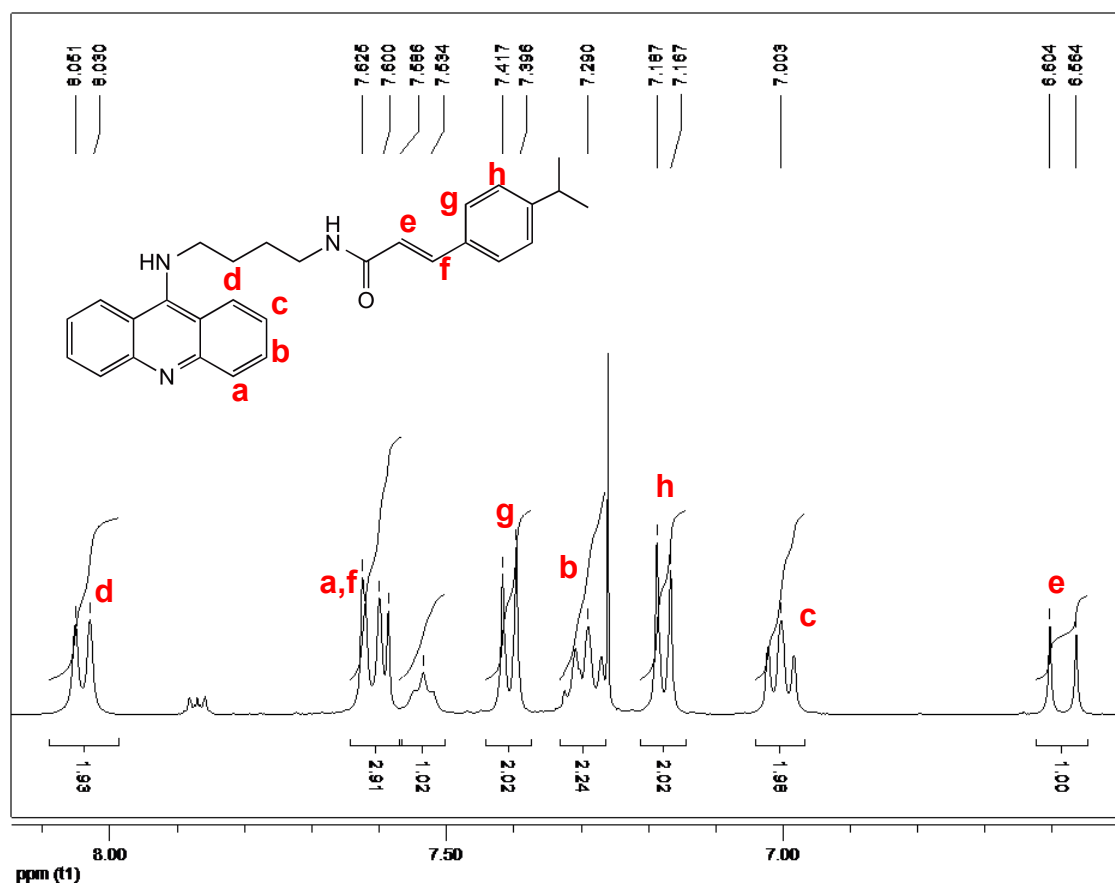
Figure 47. 1H-NMR (400 MHz, CDCl₃) of compound **29c**.
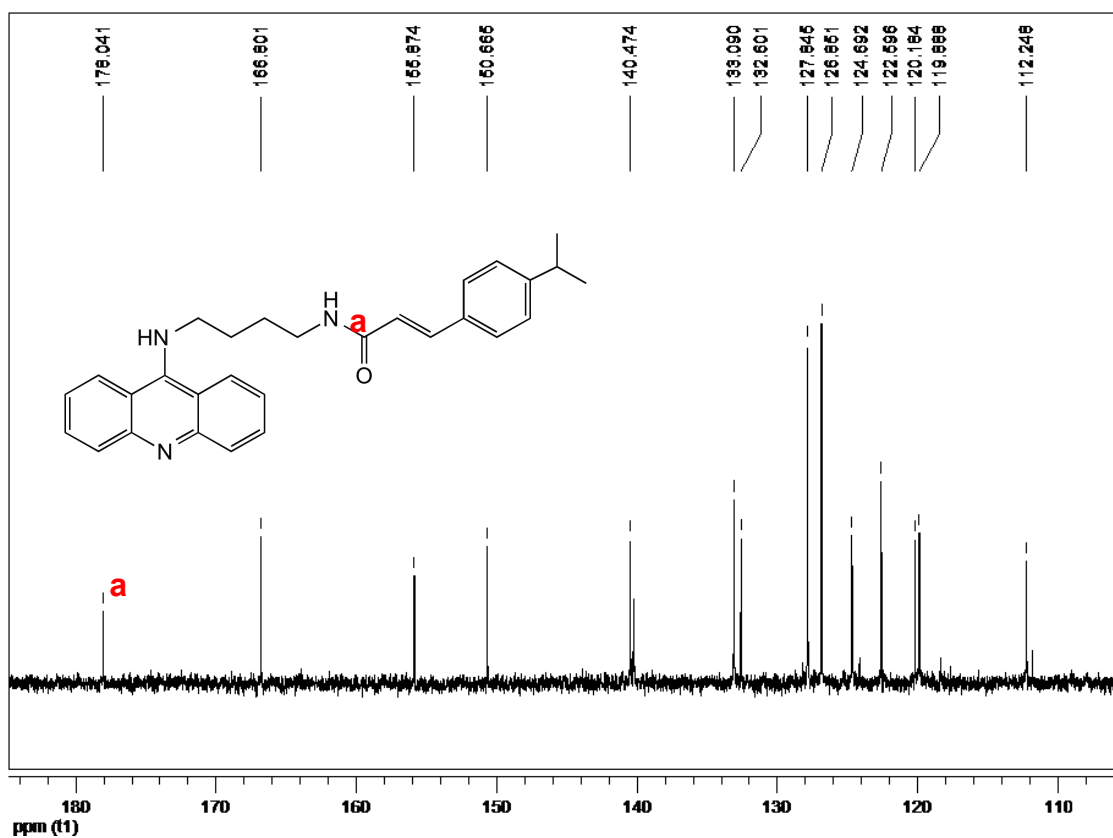
Figure 48. 13C-NMR (100 MHz, CDCl$_3$) of compound **29c**.

Chemical Formula: C$_{29}$H$_{31}$N$_3$O
Exact Mass: 437.25
Molecular Weight: 437.59
m/z: 437.25 (100.0%), 438.25 (31.8%),
439.25 (5.3%), 438.24 (1.1%)
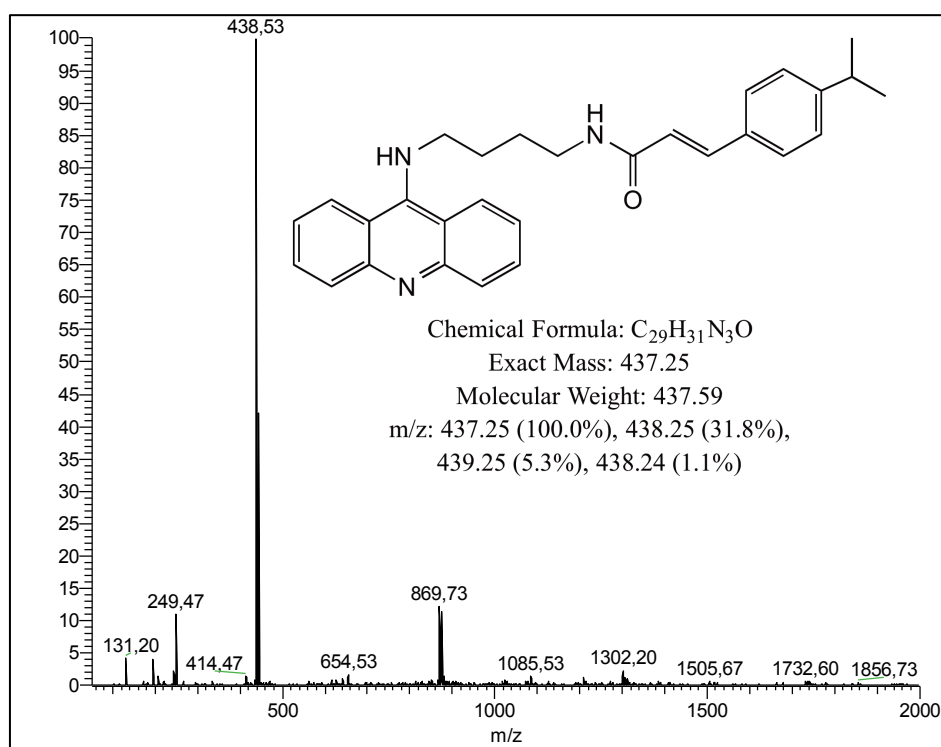
Figure 49. ES-IT MS of compound **29c**.

4.3.2. *In vitro* assays of acridine-based *HEFLECIN*s

All acridine derivatives **29** were evaluated against blood stage parasites and β-H formation *in vitro* (Table 16), and three of the compounds were further assessed against liver stage parasites. Accordingly, compounds **29** presented blood-stage activity activity in the mid-nanomolar range, with compounds **29c-d** and **29f-g** exhibiting activity in the same order of magnitude than reference CQ. The most active compound of the series was the *p*-isopropyl cinnamoyl derivative **29c** was significantly more active than the unsubstituted cinnamoyl derivative **29a**, demonstrating the importance of substituent on the cinnamoyl moiety. A similar effect had already been observed for CQ-based *HEFLECINs*, where the *p-^{i}Pr* cinnamoyl and the unsubstituted derivatives were amongst the best and worst, respectively, against blood-stage *Plasmodia*. In addition, the *para*-fluoro derivative **29f** shows activity (IC_{50} = 145 nM) almost 3-fold higher than the *meta*-fluoro derivative **29e** (IC_{50} = 345 nM), suggesting a preference for *para* over *meta* substitution in the cinnamoyl moiety.

The mechanism of antimalarial action of acridine-based compounds remains to be elucidated.[35] Still, some authors have reported that acridine derivatives were able to inhibit β-H formation.[36] Hence, compounds **29** were also tested *in vitro* for their ability to inhibit β-H formation *in vitro*, but none resulted active, indicating that an alternative MOA underlies their activity against blood-stage malaria parasites.

Compounds **29c**, **29d** and **29e** were taken further to *in vitro* liver-stage activity assays. Compound selection was made according to: i) highest blood-stage activity (**29c**), ii) highest drug-likeness, compound **29d** being the most active compound which best complied with the Veber filter,[8] Lipinski's rules,[7] and lead-likeness[9] properties, iii) the likelihood to present good stability, solubility, and bioavailability, properties expectedly enhanced in derivatives bearing a fluorinated cinnamoyl ring (**29f**).[37] Accordingly, the three selected compounds displayed higher liver-stage activity than the reference drug, PQ, and were non-toxic to Huh7 human hepatoma cells at 10 μM (Fig. 50). Compound **29d** presented the best activity/citotoxicity profile, so its IC_{50} value was determined (3.2 μM), and found to be approximately 2 times lower than that of PQ (IC_{50} = 7.5 μM).

Table 16. *In vitro* efficiency of acridine derivatives **29** against CQ-resistant *Pf* W2 and IC$_{50}$ of compound **29d** against liver stage parasite.

29
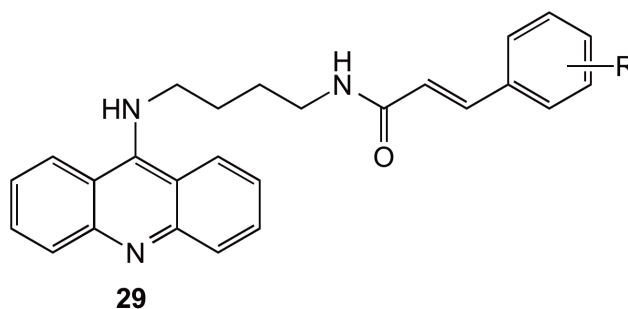
Compound	R	β-H[a]	*Pf* W2 IC$_{50}$ (nM)[b]	Liver Stage IC$_{50}$ (μM)[c]
29a	H	-	892 ± 152	
29b	*p*-Me	-	225 ± 3	ND
29c	*p*-iPr	-	126 ± 2	
29d	*p*-OMe	-	138 ± 2	3.2
29e	*m*-F	-	345 ± 32	
29f	*p*-F	-	145 ± 6	ND
29g	*m*-NO$_2$	-	142 ± 2	
ART			9.5	ND
CQ		++	138[d]	15.9
PQ			ND	7.5

[a] Inhibition of β-H formation calculated and ranked as shown in previous chapters; [b] blood-stage antiplasmodial activity against *Pf* strain W2; [c] IC$_{50}$ of the most active compounds against liver stage; [d] Value taken from Ref;[5]
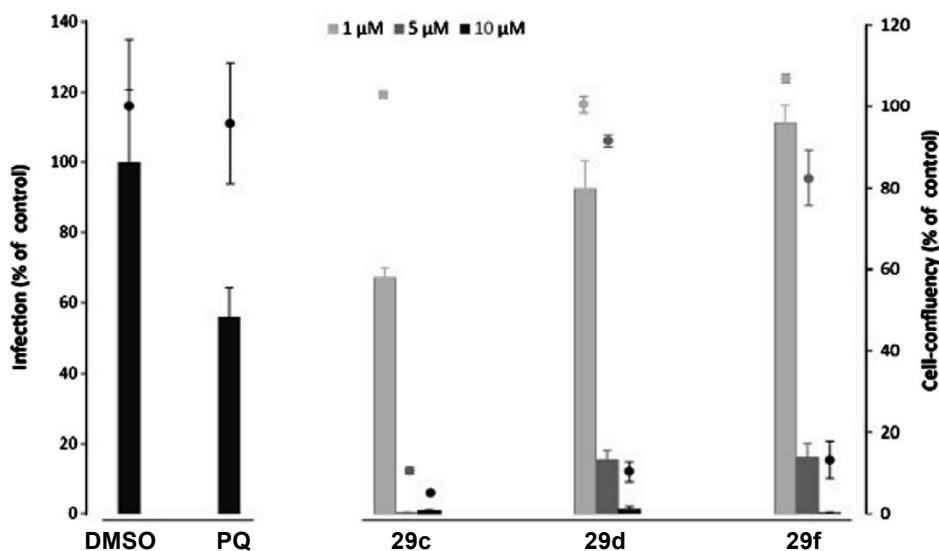
Figure 50. *In vitro* results of acridine-based *HEFLECIN*s **29** against liver stage malaria.

4.4. Quinoline-based *HEFLECIN*s as antileishmanial agents

Leishmaniasis is a neglected disease that affects mainly tropical countries.[38] There are three different clinical forms of leishmaniasis: visceral, cutaneous, and mucocutaneous.[39] Visceral leishmaniasis (VL) is caused by *Leishmania dovani* and *Leishamania infantum* and if untreated, it can lead to death.[40] Phlebotomine insects, also known as sand fly, are the insects responsible for transmitting the disease. *Leishmania* parasites life cycle alternates between the promastigotes and amastigotes form of *Leishmania*.[41] During a blood meal a sand fly injects promastigotes (Fig. 51) which subsequently are phagocytized and released. These promastigotes transform into amastigotes inside macrophages and continue to multiply in cells. When ingested by another sand fly, amastigotes eventually transform into promastigotes within the sand fly midgut and as such, the *Leishmania* life cycle continues.
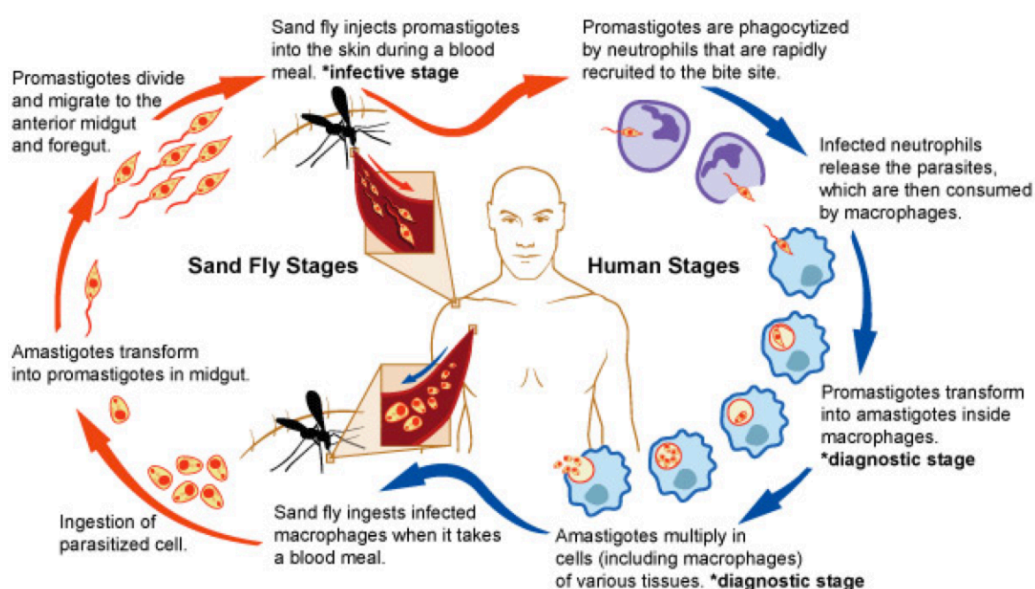
Figure 51. Life cycle of *Leishmania* retrieved from NIAID website.[41]

The conventional chemotherapy to treat against leishmaniasis such as antimonials and liposomal amphotericin B are either too toxic or expensive for routine use. In addition, miltefosine (**XXXVI**), an anticancer agent, which has become a first-choice therapy by oral route for leishmaniasis, has a median long terminal half-life that can promote developing resistance.[42] Also, there are side effects and drawback related to treatment with miltefosine. Another drug with acceptable efficacy as an oral VL therapy in clinical trials is sitamaquine (**XXXVII**).[42, 43] However, there are still unanswered question

regarding sitamaquine's potential toxicity. Therefore, there is a need for safer, cheaper, and more effective antileishmanial drugs. In view of the above and encouraged by i) PQ and other 8-aminoquinoline analogues activity against other protozoan species such as *Leishmania,*[44] and ii) the fact that *N*-cinnamoylation of heterocyclic aromatic antimalarial cores enhances the antiplasmodial activity of the corresponding compounds against both blood and liver stage malaria; the most potent *HEFLECIN*s and PQ-based *HEFLECIN*s were further evaluated *in vitro* against *Leishmania*.

(**XXXVI**)

(**XXXVII**)
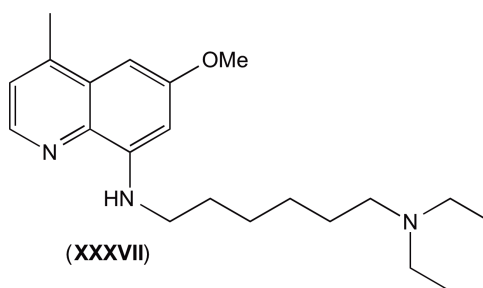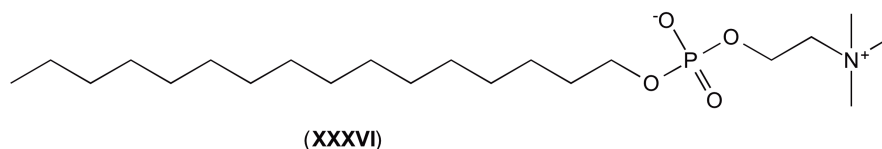
Compounds **13** and **28** were assessed *in vitro* against the promastigote forms of *Leishmania infantum* (Table 17-18). Those compounds which resulted highly active against *L. infantum promastigotes* were further evaluated against the intramacrophagic amastigote forms of *L. infantum*. *In vitro* assays against *L. infantum* promastigotes and amastigotes and cytotoxicity assays on mouse bone marrow-derived macrophages were carried out following procedures previously reported.[45] Synthesis of the corresponding compounds was carried following before presented procedures (Scheme 11 and 14).

Most of the *N*-cinnamoylated CQ derivatives presented higher activities than miltefosine against promastigote. However, there seems to not be any clear correlation between the electro-withdrawing properties of the substituents in the cynnamoyl ring and the antileishmanial activity. In addition, the compounds lipophilicity did not correlate with the corresponding activities against *L. infantum*, contrary to antiplasmodial results. In the case of PQ-based *HEFLECIN*s, cinnamoyl derivatives with a *p*-Me, *p*-iPr, *p*-OMe or *m*-NO$_2$ substituent, (**28b**, **28c**, **28d**, **28j**) respectively, present moderately higher activity (IC$_{50}$ = 16.0-24.7 μM) than PQ (IC$_{50}$ = 33.5 μM). However, the remaining compounds had not significant effect on the activity of the compounds as shown in table 17.
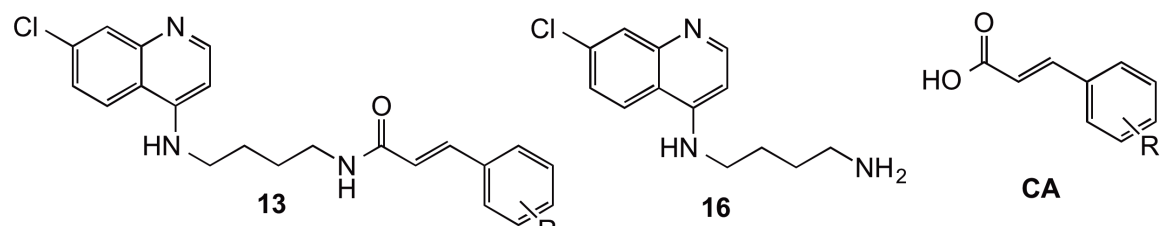
On the contrary, choroquinoline derivatives **13** presented about the same range of activity against promastigotes forms as CQ. Conjugation of cinnamic acid (CA) with compound **16** through an amide bond demonstrated to enhance activity against the promastigotes and amastigotes since compound **13a** was more active than the cinnamic acid alone, compound **16** alone, or the 1:1 mixture of the cinnamic acid and compound **16**. Moreover, the CQ analogues **13** which presented the lowest IC_{50} against promastigotes were also evaluated *in vitro* against amastigotes. All of the selected compounds were more active against amastigotes (IC_{50} = 1.2-9.3 μM) than CQ (IC_{50} = 23.0 μM), whose *in vitro* properties have been reported against VL,[46, 47] and presented activity comparable to miltefosine (IC_{50} = 1.7μM). Contrary to antiplasmodial results against blood stage of CQ analogues **13,** the most active compound against *L. infantum* amastigotes was the unsubstituted compound **13a**.

Regarding the cytotoxicity assays all compounds resulted more cytotoxic than CQ which could explain their higher activity against intramacrophagic amastigotes as compared to CQ. Nonetheless, except for compound **13h**, all *N*-cinnamoylated analogues presented the same range of cytotoxicity against macrophages than mitelfosine. Furthermore, as shown in table 18, compound **13a** represents a hit identification according to the World Health Organization's criteria[48] against *Leishmania* intramacrophagic amastigotes (IC_{50} < 1-2 µg/mL) and a selectivity index (SI) > 20). However, these results are only preliminary and further work is needed in order to elucidate the MOA of the *N*-cinnamoylated compounds **13** evaluated against *L. infantum*.

Table 17. *In vitro* data of PQ-based *HEFLECIN*s against *L. infantum* promastigotes (PM)
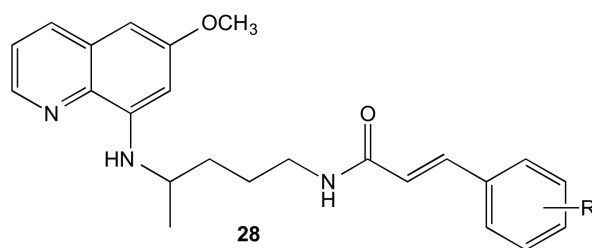
Compound	R	IC$_{50}$ (µM)PM[a]
28a	H	39.0 ± 4.5
28b	*p*-Me	18.3 ± 1.3
28c	*p*-iPr	16.0 ± 3.0
28d	*p*-OMe	22.3 ± 1.8
28e	*m*-F	52.9 ± 17.4
28f	*p*-F	35.7 ± 11.2
29g	*p*-Cl	35.1 ± 6.3
28h	*p*-Br	30.1 ± 9.0
28i	*o*-NO$_2$	35.4 ± 5.2
28j	*m*-NO$_2$	24.7 ± 2.9
28k	*p*-NO$_2$	>160
PQ		33.5 ± 8.7
Miltefosine		19.6 ± 4.3

[a] IC$_{50}$ (µM) on *L. infantum* promastigotes at 72h (mean ± SD)

Table 18. *In vitro* data of CQ-based *HEFLECIN*s against *L. infantum* promastigotes (PM) and amastigotes (AM) and cytotoxicity results on mouse bone marrow-derived macrophages (MP).

Compound	R	IC$_{50}$ (µM) PM[a]	IC$_{50}$ (µM) AM[b]	IC$_{50}$ (µg/mL) AM[c]	CC$_{50}$ (µM) MP[d]	CC$_{50}$ (µg/mL) MP[e]	SI[f]
13a	H	3.1 ± 1.8	1.2 ± 0.8	0.5 ± 0.3	25.4 ± 6.7	9.6 ± 2.5	21.2
16	-	18.8 ± 2.9	43.9 ± 5.8	11.0 ± 1.4	74.5 ± 1.8	18.6 ± 0.4	1.7
Cinnamic Acid (CA)	-	> 80	47.1 ± 16.1	7.0 ± 2.4	> 80	> 11.9	> 1.7
16 + CA		18 ± 5.0	65.5 ± 34.5	-	34.1 ± 16.9	-	-
13b	*p*-Me	21.8 ± 15.4			ND[g]		
13c	*p*-iPr	2.6 ± 0.4	4.0 ± 0.9	1.7 ± 0.4	13.5 ± 6.2	5.7 ± 2.6	3.4
13d	*p*-OMe	3.9 ± 2.0	9.3 ± 1.9	3.8 ± 0.8	61.9 ± 26.5	25.4 ± 10.9	6.7
13f	*m*-F	3.3 ± 1.4	4.2 ± 2.9	1.7 ± 1.2	17.6 ± 0.6	7.0 ± 0.2	4.2
13g	*p*-F	5.5 ± 2.1	5.7 ± 2.7	2.3 ± 1.1	22.2 ± 5.9	8.8 ± 2.3	3.9
13h	*p*-Cl	3.1 ± 0.9	6.6 ± 2.3	2.7 ± 1.0	7.7 ± 2.1	3.2 ± 0.9	1.2
13i	*p*-Br	10.8 ± 1.6					
13j	*o*-NO$_2$	7.3 ± 0.4			ND[g]		
CQ		1.3 ± 0.2	23.0 ± 12.1	11.9 ± 6.9	71.3 ± 2.7	36.8 ± 1.4	3.1
PQ		33.5 ± 8.7			ND		
Miltefosine		19.6 ± 4.3	4.1 ± 3.3	1.7 ± 1.3	25.5 ± 4.5	10.4 ± 1.8	6.2

[a] IC$_{50}$ (µM) on *L. infantum* promastigotes at 72h (mean ± SD); [b] IC$_{50}$ (µM) on *L. infantum* intramacrophagic amastigotes at 72h (mean ± SD); [c] IC$_{50}$ (µg/mL) on *L. infantum* intramacrophagic amastigotes at 72h (mean ± SD); [d] CC$_{50}$ (µM) on mouse bone marrow-derived macrophages (MP) at 72h (mean ± SD); [e] CC$_{50}$ (µg/mL) on mouse bone marrow-derived macrophages at 72h (mean ± SD); [f] SI – selectivity index calculated as the ratio between CC$_{50}$ and IC$_{50}$.; [g] Not Determined.

4.5. Experimental section

4.5.1. Chemistry

4.5.1.1. Chemicals and Instrumentation. All solvents and common chemicals were from Sigma-Aldrich (Spain) and the coupling agent TBTU was from Bachem (Switzerland). NMR spectra were acquired on a Bruker Avance III 400 spectrometer from solutions in either deuterated chloroform or deuterated dimethylsulfoxide (DMSO-d_6) containing tetramethylsilane as internal reference. Mass spectrometry (MS) analyses were run on a Thermo Finnigan LCQ Deca XP Max LC/MSn instrument operating with electrospray ionization and ion-trap (ESI-IT) quadrupole detection. The target compounds were confirmed to have at least 85% purity, based on peak areas obtained through HPLC analyses that were run using the following conditions: 10-70% for chloroquinoline-based *HEFLECIN*s and 30−100% for PQ-based *HEFLECINs* of B in A (A = H_2O with 0.05% of trifluoroacetic acid; B = acetonitrile) in 22 min with a flow rate of 1 mL/min on a Merck-Hitachi Lachrom Elite instrument equipped with a diode array detector (DAD) and thermostated (Peltier effect) autosampler, using a Purospher STAR RP-18e column (150 mm × 4.0 mm; particle size, 5 µm).

4.5.1.2. Synthesis of 4-(N-aminobutyl)amino-7-chloroquinoline (16)
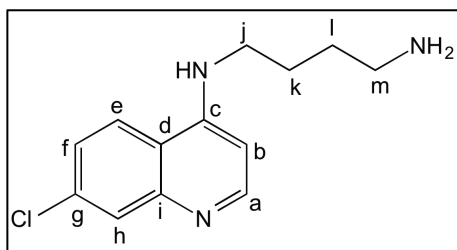
1,4-Diaminobutane (10 eq) and 4,7-dichloroquinoline (1 eq) were stirred at 100°C for 3h. After cooling to RT, the mixture was diluted with CH_2Cl_2 (25 mL), and the solution was washed with 5 % aq Na_2CO_3. The organic layer was separated and dried over anhydrous Na_2SO_4, filtered, and concentrated to yield the title compound. Further purification was not required. Desired compound resulted a white solid (198 mg, 64%); mp 62-65°C; δ_H (400 MHz, DMSO-d_6) 8.37 (d, J= 5.6 Hz, 1H, Ha), 8.27 (d, J= 8.8 Hz, 1H, He), 7.77 (d, J= 2.4 Hz, 1H, Hh), 7.46-7.30 (m, 2H, Hf, -NH), 6.45 (d, J= 5.6 Hz, 1H, Hb), 3.27-3.17 (m, 4H, Hj, -NH$_2$), 2.64-2.55 (m, 2H, Hm), 1.77-1.43 (m, 4H, Hk-l); δ_C (100 MHz, DMSO-d_6) 151.8, 150.0, 133.2, 127.4, 124.1, 123.9 (Ca, Cc, Ce-i), 117.4 (Cd), 98.5 (Cb), 42.3 (Cj), 41.1 (Cm), 30.4, 25.2 (Ck-l); ESI-IT MS: m/z (M+H$^+$) 249.10 ($C_{13}H_{16}ClN_3$) requires 250.27.

4.5.1.3. Synthesis of chloroquinoline-based *HEFLECIN*s 13.

A solution of substituted cinnamic acid (1.1 eq), TBTU (1.1 eq) and DIEA; 2.2 eq in DMF (5 mL) was stirred at 0°C for 10 min. Then, a solution of compound **16** (1.1 eq) in DMF was added, and the reaction proceeded at RT for an additional 24 h. The mixture was diluted with CH_2Cl_2 (25 mL), and the solution was washed with 5 % aq Na_2CO_3. The organic layer was separated, dried over anhydrous Na_2SO_4, filtered, and concentrated. The crude product was purified by column chromatography (EtOAc/MeOH, 4:1 v/v) to give the desired compound **13**.

4-(*N*-cinnamoylaminobutyl)amino-7-chloroquinoline (13a).
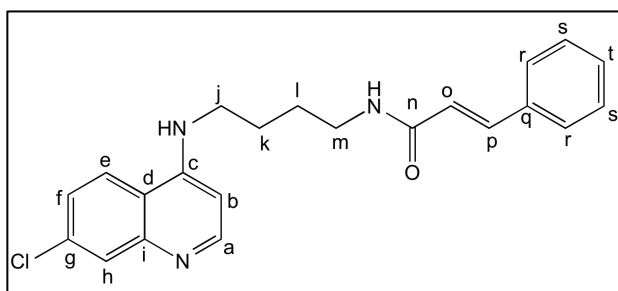
White solid (39.5 mg, 52%); mp 194-198°C; R_F (DCM/MeOH 8:2) 0.44; δ_H (400 MHz, DMSO-d_6) 8.38 (d, J= 5.2 Hz, 1H, Ha), 8.28 (d, J= 9.2 Hz, 1H, He), 8.16 (t, J= 5.6 Hz, 1H, -NH), 7.77 (d, J= 2 Hz, 1H, Hh), 7.56-7.54 (m, 2H, Hr), 7.44-7.32 (m, 6H, Hf, Hp, Hs-t, -NH), 6.63 (d, J= 15.6 Hz, 1H, Ho), 6.48 (d, J= 5.6 Hz, 1H, Hb), 3.33-3.23 (m, 4H, Hj-m), 1.73-1.55 (m, 4H, Hk-l); δ_C (100 MHz, DMSO-d_6) 164.8 (Cn), 151.8, 150.0, 149.0, 138.4, 134.9, 133.3, 129.3, 128.8, 127.4, 124.0, 123.9, 122.2, 117.4 (Ca, Cc-i, Co-t), 98.6 (Cb), 42.0, 38.3 (Cj, Cm), 26.7, 25.2 (Ck-l); ESI-IT MS: m/z 380.47 (M+H$^+$); ($C_{22}H_{22}ClN_3O$ requires 379.15); HPLC-DAD: rt = 13.25 min (% Area = 100).

4-[*N*-(*p*-methyl)cinnamoylaminobutyl]amino-7-chloroquinoline (13b).
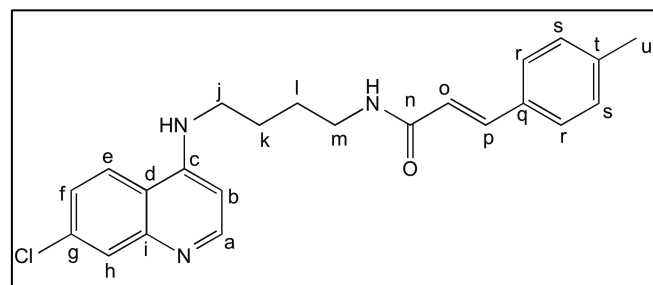
White solid (24.8 mg, 32%); mp 200-203°C; R_F (DCM/MeOH 8:2) 0.44; δ_H (400 MHz, DMSO-d_6) 8.38 (d, J= 5.6 Hz, 1H, Ha), 8.29 (d, J= 9.2 Hz, 1H, He), 8.10 (t, J= 5.2 Hz, 1H, -NH), 7.77 (d, J= 1.6 Hz, 1H, Hh), 7.52-7.28 (m, 5H, Hf, Hp, Hr, -NH), 7.20 (d, J= 7.6 Hz, 2H, Hs), 6.56 (d, J= 15.6 Hz, 1H, Ho), 6.47 (d, J= 5.6 Hz, 1H, Hb), 3.36-3.16 (m, 4H, Hj, Hm), 2.31 (s, 3H, Hu), 1.74-1.54 (m, 4H, Hk-l); δ_C (100 MHz, DMSO-d_6) 165.0 (Cn), 151.8, 150.0, 149.0, 139.0, 133.3, 132.1, 129.4, 128.8, 127.4, 124.0, 123.9, 121.2, 117.4 (Ca, Cc-i, Co-t), 98.6 (Cb), 42.0, 38.3 (Cj,Cm), 26.8, 25.2, 20.1 (Ck-l, Cu); ESI-IT MS (M+H$^+$) 394.40 ($C_{23}H_{24}ClN_3O$ requires 393.16); HPLC-DAD: rt= 14.14 (% Area = 100).

4-[*N*-(*p*-isopropyl)cinnamoylaminobutyl]amino-7-chloroquinoline (13c).
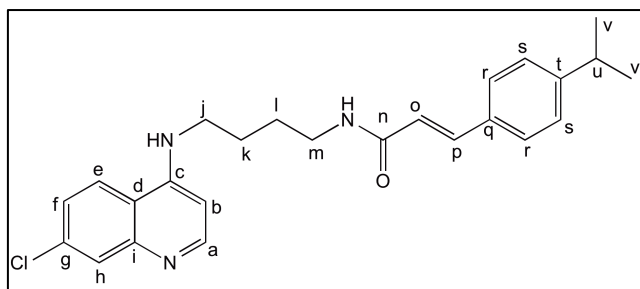
White solid (24 mg, 28%); mp 179-184°C; R_F (DCM/MeOH 8:2) 0.44; δ_H (400 MHz, DMSO-d$_6$) 8.38 (d, J= 5.6 Hz, 1H, Ha), 8.28 (d, J= 9.2 Hz, 1H, He), 8.12 (t, J= 5.6 Hz, 1H, -NH), 7.77 (d, J= 2.4 Hz, 1H, Hh), 7.47-7.22 (m, 7H, Hf, Hp, Hr-s, -NH), 6.57 (d, J= 15.6 Hz, 1H, Ho), 6.48 (d, J= 5.6 Hz, 1H, Hb), 3.30-3.22 (m, 4H, Hj, Hm), 2.94-2.84 (m, 1H, Hu), 1.77-1.51 (m, 4H, Hk-l), 1.19 (d, J= 5.8 Hz, 6H, Hv); δ_C (100 MHz, DMSO-d$_6$) 165.0 (Cn), 151.8, 150.0, 149.9, 149.0, 138.3, 133.3, 132.5, 127.5, 127.4, 126.8, 124.0, 123.9, 121.2, 117.4 (Ca, Cc-i, Co-t), 98.6 (Cb), 42.0, 38.3 (Cj, Cm), 33.2, 26.8, 25.2, 23.6 (Ck-l, Cu-v); ESI-IT MS: m/z (M+H$^+$) 422.40 (C$_{25}$H$_{28}$ClN$_3$O requires 421.19); HPLC-DAD: rt = 16.01 min; (% Area = 99.16).

4-[*N*-(*p*-methoxy)cinnamoylaminobutyl]amino-7-chloroquinoline (13d).
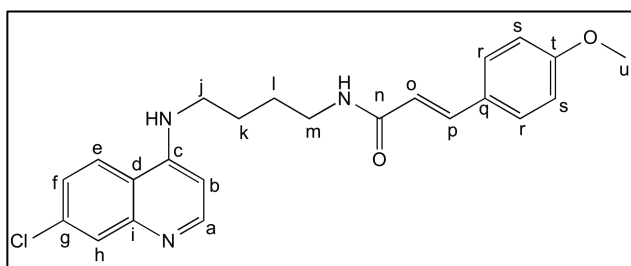
White solid (24.7 mg, 30%); mp 176-178°C; R_F (DCM/MeOH 8:2) 0.44; δ_H (400 MHz, DMSO-d$_6$) 8.38 (d, J= 5.2 Hz, 1H, Ha), 8.28 (d, J= 8.8 Hz, 1H, He), 8.04 (t, J= 5.6 Hz, 1H, -NH), 7.77 (d, J= 2.4 Hz, 1H, Hh), 7.50-7.32 (m, 5H, Hf, Hp, Hr, -NH), 6.96 (d, J= 8.8 Hz, 2H, Hs), 6.52-6.42 (m, 2H, Hb, Ho), 3.77 (s, 3H, Hu), 3.30-3.21 (m, 4H, Hj, Hm), 1.72-1.54 (m, 4H, Hk-l); δ_C (100 MHz, DMSO-d$_6$) 165.1 (Cn), 160.2, 151.8, 150.0, 149.0, 138.1, 133.2, 128.9, 127.4, 124.0, 123.9, 119.7, 117.4, 114.3 (Ca, Cc-i, Co-t), 98.6 (Cb), 55.1 (Cu), 42.0, 38.2 (Cj, Cm), 26.8, 25.2 (Ck-l); ESI-IT MS: m/z (M+H$^+$) 410.52 (C$_{23}$H$_{24}$ClN$_3$O$_2$) requires 409.16; HPLC-DAD: rt = 13.25 min; (% Area = 100).

4-[*N*-(*p*-(*N*-tert-butoxycarbonyl)amino)cinnamoylaminobutyl]amino-7-chloroquinoline (13e').
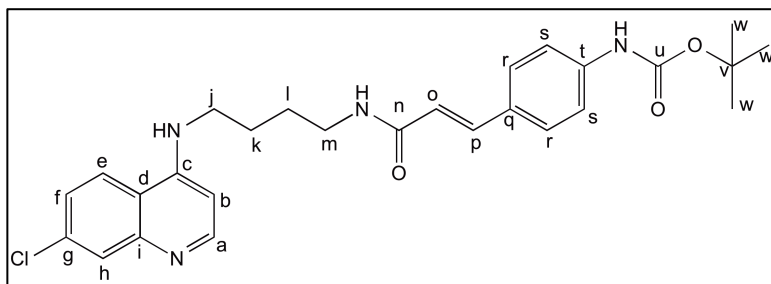
White solid (67.1mg, 57%); mp 178-182 °C; R_F (EtOAc/MeOH 8:2) 0.25; δ_H (400 MHz, DMSOd$_6$) 9.53 (s, 1H, -NH), 8.38 (d, J= 5.6 Hz, 1H, Ha), 8.28 (d, J= 8.8 Hz, 1H, He), 8.05 (t, J= 5.6 Hz, 1H, -NH), 7.77 (d, J= 2 Hz, 1H, Hh), 7.50 -7.42(m,

5H), 7.35-7.30 (m, 2H) (Hf, Hp, -NH, Hr-s), 6.50-6.46 (m, 2H, Ho, Hb), 3.32-3.20 (m, 4H, Hj, Hm), 1.74-1.52 (m, 4H, Hk-l), 1.45 (s, 9H, Hw); δ_C (100 MHz, DMSOd$_6$) 165.1 (Cn), 152.5, 151.8, 150.0, 149.0, 140.6, 138.1, 133.2, 128.6, 128.0, 127.4, 124.0, 123.9, 120.0, 118.0 (Ca, Cc-i, Co-u), 98.6 (Cb), 79.2 (Cv), 42.0, 38.2 (Cj, Cm), 28.0, 26.7, 25.2 (Ck-l, Cw); ESI-IT MS: m/z (M+H$^+$) 495.33 (C$_{27}$H$_{31}$ClN$_4$O$_3$) requires 494.21; HPLC-DAD rt = 15.09 (% Area = 99).

4-[*N*-(*p*-amino)cinnamoylaminobutyl]amino-7-chloroquinoline (13e).
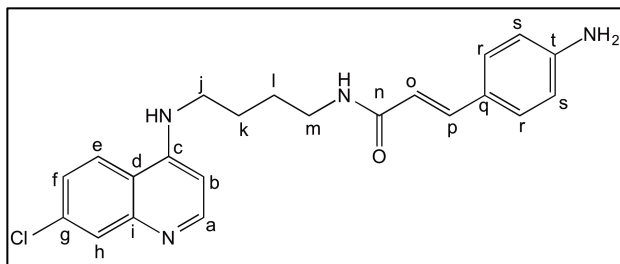
White solid (8 mg, 18%); mp 134-139°C; R$_F$ (DCM/MeOH 8:2) 0.44; δ_H (400 MHz, DMSO-d$_6$) 8.37 (d, J= 5.2 Hz, 1H, Ha), 8.28 (d, J= 9.2 Hz, 1H, He), 7.88 (t, J= 5.6 Hz, 1H, -NH), 7.77 (d, J= 2.4 Hz, 1H, Hh), 7.43 (dd, J= 8.6 Hz, J= 2.4 Hz, 1H, Hf), 7,33 (t, J= 5.2 Hz, 1H, -NH), 7.26-7.18 (m, 3H, Hp, Hr), 6.54 (d, J= 8.4 Hz, 2H, Hs), 6.47 (d, J= 5.2 Hz, 1H, Hb), 6.27 (d, J= 15.6 Hz, 1H, Ho), 5.54 (b, 2H, -NH$_2$), 3.32-3.16 (m, 4H, Hj, Hm), 1.63-1.55 (m, 4H, Hk-l); δ_C (100 MHz, DMSO-d$_6$) 165.7 (Cn), 151.8, 150.3, 149.0, 139.2, 133.2, 128.9, 127.4, 124.0, 123.9, 122.1, 117.4, 115.9, 113.6 (Ca, Cc-i, Co-t), 98.6 (Cb), 42.0, 38.1 (Cj, Cm), 26.9, 25.2 (Ck-l); ESI-IT MS: m/z (M+H$^+$) 395.47 (C$_{22}$H$_{23}$ClN$_4$O requires 394.16); HPLC-DAD: rt = 9.21min (% Area = 86.38).

4-[*N*-(*m*-fluoro)cinnamoylaminobutyl]amino-7-chloroquinoline (13f).
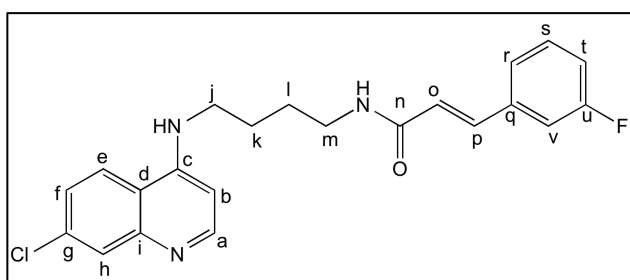
White solid (37.3 mg, 52%); mp 195-200°C; R$_F$ (DCM/MeOH 8:2) 0.44; δ_H (400 MHz, DMSO-d$_6$) 8.38 (d, J= 5.2 Hz, 1H, Ha), 8.28 (d, J= 9.2 Hz, 1H, He), 8.18 (t, J= 5.6 Hz, 1H, -NH), 7.77 (d, J= 2.4 Hz, 1H, Hh), 7.49-7.32 (m, 5H, Hf, Hp, Hr, Ht, Hv), 7.33 (t, J= 5.6 Hz, 1H, -NH), 7.20 (t, J= 7.2 Hz, 1H, Hs), 6.67 (d, J= 16 Hz, 1H, Ho), 6.47 (d, J= 5.6 Hz, 1H, Hb), 3.32-3.20 (m, 4H, Hj, Hm), 1.66-1.58 (m, 4H, Hk-l); δ_C (100 MHz, DMSO-d$_6$) 164.5 (Cn), 163.6, 161.2, 151.8, 150.0, 149.0, 137.5, 137.1, 133.3, 130.8, 127.4, 123.8, 123.5, 117.4, 116.6, 113.9 (Ca, Cc-i, Co-v), 98.6 (Cb), 42.0, 38.3 (Cj, Cm), 26.7, 25.2 (Ck-l); ESI-IT MS: m/z (M+H$^+$) 398.40 (C$_{22}$H$_{21}$ClFN$_3$O requires 397.14); HPLC-DAD: rt = 13.53 min (% Area = 99.23).

4-[*N*-(*p*-fluoro)cinnamoylaminobutyl]amino-7-chloroquinoline (13g).
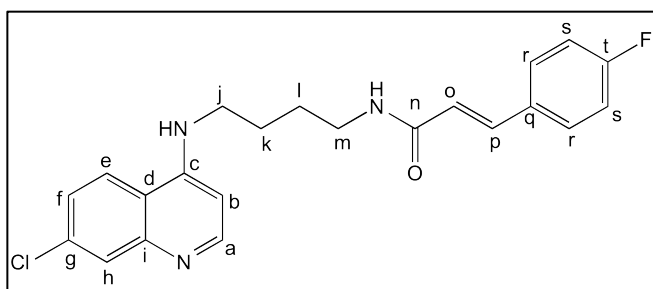
White solid (24.1 mg, 34%); mp 195-200°C; R_F (DCM/MeOH 8:2) 0.44; δ_H (400 MHz, DMSO-d_6) 8.38 (d, J= 5.2 Hz, 1H, Ha), 8.28 (d, J= 9.2 Hz, 1H, He), 8.14 (t, J= 5.6 Hz, 1H, -NH), 7.77 (d, J= 1.6 Hz, 1H, Hh), 7.60 (dd, J= 8.8 Hz, J= 5.6 Hz, 2H, Hr), 7.46-7.39 (m, 2H, Hf, Hp), 7.33 (t, J= 5.2 Hz, 1H, -NH), 7.24 (t, J= 8.8 Hz, 2H, Hs), 6.57 (d, J= 15.6 Hz, 1H, Ho), 6.47 (d, J= 5.6 Hz, 1H, Hb), 3.32-3.20 (m, 4H, Hj, Hm), 1.68-1.60 (m, 4H, Hk-l); δ_C (100 MHz, DMSO-d_6) 164.7 (Cn), 151.8, 150.0, 149.0, 137.2, 133.3, 131.5, 129.5, 127.4, 124.0, 123.9, 122.1, 117.4, 115.9 (Ca, Cc-i, Co-t), 98.6 (Cb), 42.0, 38.3 (Cj, Cm), 26.8, 25.2 (Ck-l); ESI-IT MS: m/z (M+H$^+$) 398.40 ($C_{22}H_{21}ClFN_3O$ requires 397.14); HPLC-DAD: rt = 13.46 min (% Area = 100)

## 4-[*N*-(*p*-chloro)cinnamoylaminobutyl]amino-7-chloroquinoline (13h).
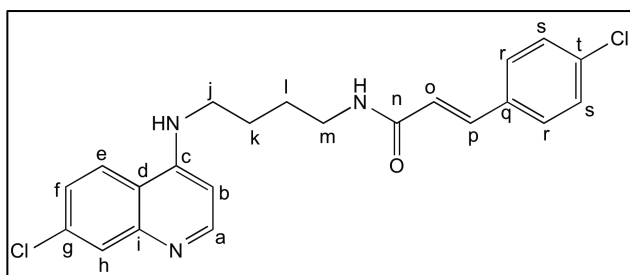
White solid (13 mg, 16%); mp 194-196°C; R_F (DCM/MeOH 8:2) 0.44; δ_H (400 MHz, DMSO-d_6) 8.38 (d, J= 5.2 Hz, 1H, Ha), 8.28 (d, J= 9.2 Hz, 1H, He), 8.17 (t, J= 5.6 Hz, 1H, -NH), 7.77 (d, J= 2 Hz, 1H, Hh), 7.57 (d, J= 8.4 Hz, 2H), 7.48-7.37 (m, 4H) (Hf, Hp, Hr-s), 7.33 (t, J= 5.6 Hz, 1H, -NH), 6.66 (d, J= 16 Hz, 1H, Ho), 6.47 (d, J= 5.6 Hz, 1H, Hb), 3.32-3.20 (m, 4H, Hj, Hm), 1.68-1.60 (m, 4H, Hk-l); δ_C (100 MHz, DMSO-d_6) 164.6 (Cn), 151.8, 150.0, 149.0, 137.2, 133.8, 133.3, 129.1, 128.9, 127.4, 124.0, 123.9, 123.0, 117.4, 115.9 (Ca, Cc-i, Co-t), 98.6 (Cb), 42.0, 38.3 (Cj, Cm), 26.7, 25.2 (Ck-l); m/z (ESI-IT MS) 414.47 (M+H$^+$); M+ $C_{22}H_{21}Cl_2N_3O$ requires 413.11; HPLC-DAD: rt = 14.51 min (% Area = 99.71).

4-[*N*-(*p*-bromo)cinnamoylaminobutyl]amino-7-chloroquinoline (13i).
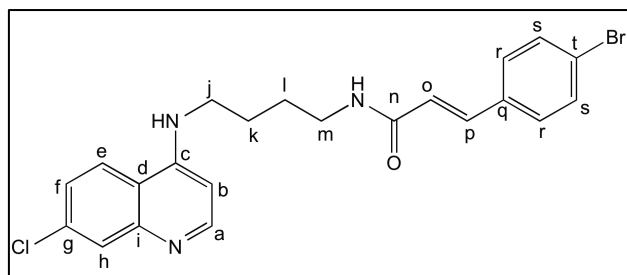
White solid (13 mg, 16%); mp 194-196°C; R_F (DCM/MeOH 8:2) 0.44; δ_H (400 MHz, DMSO-d_6) 8.38 (d, J= 5.2 Hz, 1H, Ha), 8.28 (d, J= 9.2 Hz, 1H, He), 8.17 (t, J= 5.2 Hz, 1H, -NH), 7.77 (d, J= 1.6 Hz, 1H, Hh), 7.60 (d, J= 8.4 Hz, 2H), 7.50 (d, J= 8.4 Hz, 2H) (Hr-s), 7.44-7.30 (m, 3H, Hf, Hp, -NH), 6.64 (d, J= 15.6 Hz, 1H, Ho), 6.47 (d, J= 5.6 Hz, 1H, Hb), 3.32-3.20 (m, 4H, Hj, Hm), 1.68-1.60 (m, 4H, Hk-l); δ_C (100 MHz, DMSO-d6) 164.6 (Cn), 151.8, 150.0, 149.0, 137.1, 134.2, 133.3, 131.8, 129.3, 127.4, 124.0, 123.9, 123,1, 122.4, 117.4 (Ca, C-i, Co-t), 98.6 (Cb), 42.0, 38.3 (Cj, Cm), 26.7, 25.2 (Ck-l); ESI-IT MS: m/z (M+H$^+$) 460.33 ($C_{22}H_{21}ClBrN_3O$ requires 457.06); HPLC-DAD: rt = 14.81 min (% Area = 98.62).

### 4-[*N*-(*o*-nitro)cinnamoylaminobutyl]amino-7-chloroquinoline (13j).
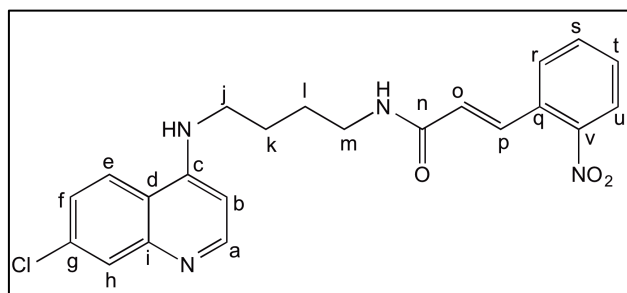
Yellow solid (56.7 mg, 67%); mp 114-116°C; R_F (DCM/MeOH 8:2) 0.44; δ_H (400 MHz, DMSO-d_6) 8.38 (d, J= 5.6 Hz, 1H, Ha), 8.32-8.27 (m, 2H, He, -NH), 8.04 (d, J= 8 Hz, 1H, Hu), 7.78-7.60 (m, 5H, Hh, Hp, Hr-t), 7.42 (d, J= 9 Hz, J= 2 Hz, 1H, Hf), 7.34 (t, J= 5.2 Hz, 1H, -NH), 6.62 (d, J= 15.6 Hz, 1H, Ho), 6.47 (d, J= 5.6 Hz, 1H, Hb), 3.33-3.21 (m, 4H, Hj, Hm), 1.68-1.60 (m, 4H, Hk-l); δ_C (100 MHz, DMSO-d_6) 172.0 (Cn), 164.0, 151.8, 150.0, 149.0, 148.2, 133.7, 133.3, 130.1, 130.0, 128.5, 127.4, 126.9, 124.4, 124.0, 123.9, 117.4 (Ca, Cc-i, Co-v), 98.6 (Cb), 42.0, 38.4 (Cj, Cm), 26.7, 25.2 (Ck-l); ESI-IT MS: m/z (M+H$^+$) 425.40 ($C_{22}H_{21}ClN_4O_3$ requires 424.13); HPLC-DAD: rt = 13.20 min (% Area = 100).

4-[*N*-(*m*-nitro)cinnamoylaminobutyl]amino-7-chloroquinoline (13k).
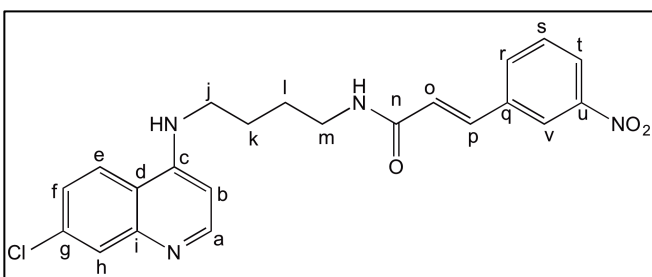
Yellow solid (31 mg, 36%); mp 195-200 °C; R_F (DCM/MeOH 8:2) 0.44; δ_H (400 MHz, DMSO-d_6) 8.39-8.35 (m, 2H, Ha, Hv), 8.30-8.18 (m, 3H, He, Ht, -NH), 8.00 (d, J= 8 Hz, 1H, Hr), 7.77 (d, J= 2.4 Hz, 1H, Hh), 7.70 (t, J= 8 Hz, 1H, Hs), 7.54 (d, J= 16 Hz, 1H, Hp), 7.44 (dd, J= 9.2 Hz, J= 2.4 Hz, 1H, Hf), 7.34 (t, J= 5.2 Hz, 1H, -NH), 6.82 (d, J= 15.6 Hz, 1H, Ho), 6.47 (d, J= 5.2 Hz, 1H,

Hb), 3.33-3.21 (m, 4H, Hj, Hm), 1.68-1.60 (m, 4H, Hk-l); δ_C (100 MHz, DMSO-d_6) 164.3 (Cn), 151.8, 150.0, 148.2, 136.8, 136.1, 133.8, 133.3, 130.4, 127.4, 125.1, 124.0, 123.9, 123.6, 121.4, 117.4 (Ca, Cc-i, Co-v), 98.6 (Cb), 42.0, 38.4 (Cj, Cm), 26.7, 25.2 (Ck-l); ESI-IT MS: m/z (M+H$^+$) 425.47 ($C_{22}H_{21}ClN_4O_3$ requires 424.13); HPLC-DAD: rt = 13.41 min (% Area = 95.93).

4-[*N*-(*p*-nitro)cinnamoylaminobutyl]amino-7-chloroquinoline (13l).
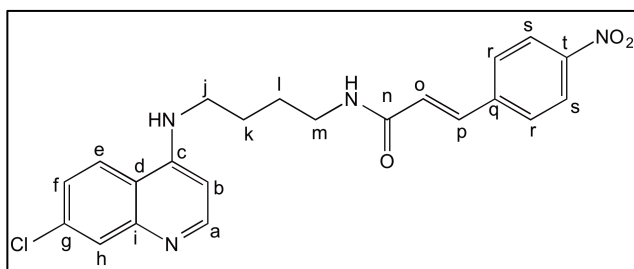
Yellow solid (13 mg, 8%); mp 178-182 ^{o}C; R_F (DCM/MeOH 8:2) 0.44; δ_H (400 MHz, DMSO-d_6) 8.38 (d, J= 5.2 Hz, 1H, Ha), 8.30-8.18 (m, 4H, He, Hs, -NH), 7.82-7.74 (m, 3H, Hh, Hr), 7.52 (d, J= 16 Hz, 1H, Hp), 7.44 (dd, J= 9

Hz, J= 2 Hz, 1H, Hf), 7.35 (t, J= 5.2 Hz, 1H, -NH), 6.81 (d, J= 15.6 Hz, 1H, Ho), 6.47 (d, J= 5.2 Hz, 1H, Hb), 3.34-2.22 (m, 4H, Hj, Hm), 1.71-1.63 (m, 4H, Hk-l); δ_C (100 MHz, DMSO-d_6) 164.1 (Cn), 151.7, 150.0, 148.9, 147.4, 141.5, 136.1, 133.3, 128.5, 127.3, 126.5, 124.0, 123.9, 117.4 (Ca, Cc-i, Co-t), 98.6 (Cb), 42.0, 38.4 (Cj, Cm), 26.7, 25.2 (Ck-l); ESI-IT MS: m/z (M+H$^+$) 425.35 ($C_{22}H_{21}ClN_4O_3$ requires 424.13); HPLC-DAD: rt = 13.94 min (% Area = 85.94).

4-[*N*-(*p*-dimethylamino)cinnamoylaminobutyl]amino-7-chloroquinoline (13m)
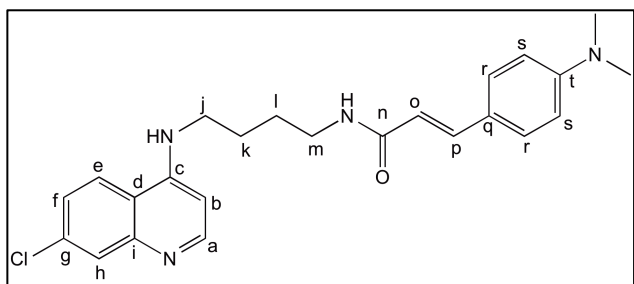
White solid (14 mg, 8%); mp=176-180°C; R_F (DCM/MeOH 8:2) 0.44; δ_H (400 MHz, DMSO-d_6) 8.39 (d, J= 5.6 Hz, 1H, Ha), 8.32 (d, J= 8.8 Hz, 1H, He), 7.95 (t, J= 5.6 Hz, 1H, -NH), 7.79 (d, J= 2 Hz, 1H, Hh), 7.62 (t, J= 5.2

Hz, 1H, -NH), 7.47 (dd, J= 8.8 Hz, J= 2.4 Hz, 1H, Hf), 7.36 (d, J= 8.8 Hz, 2H, Hr), 7.29 (d, J= 16 Hz, 1H, Hp), 6.70 (d, J= 8.8 Hz, 2H, Hs), 6.53 (d, J= 5.6 Hz, 1H, Hb), 6.35 (d, J= 16 Hz, 1H, Ho), 3.36-3.30 (m, 2H), 3.25-3.19 (m, 2H) (Hj, Hm), 2.94 (s, 6H, -NMe$_2$), 1.72-1.64 (m, 2H), 1.60-1.54 (m, 2H) (Hk-Hl); δ_C (100 MHz, DMSO-d_6) 165.6 (Cn), 150.9, 150.7, 150.6, 147.6, 138.8, 133.9, 128.7, 126.3, 124.3, 122.3, 117.1, 116.7, 111.9 (Ca, Cc-i, Co-t), 98.6 (Cb), 42.1, 38.1 (Cj, Cm) 26.9, 25.1 (Ck-l); ESI-IT MS: m/z (M+H$^+$) 423.47 ($C_{24}H_{27}ClN_4O$ requires 422.19); HPLC-DAD: rt = 11.7 min, (% Area = 93.0).

4-[*N*-(*m,p*-dimethoxy)cinnamoylaminopropyl]amino-7-chloroquinoline (13n)
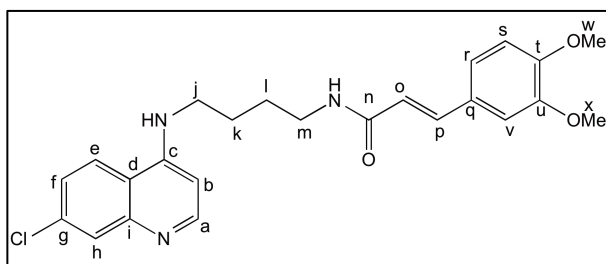
White solid (29 mg, 17%); mp=168-172 °C; R_F (DCM/MeOH 8:2) 0.44; δ_H (400 MHz, DMSO-d$_6$) 8.44-8.35 (d, J= 5.6 Hz, 1H, Ha), 8.36 (d, J= 9.2 Hz, 1H, He), 8.06 (t, J= 5.6 Hz, 1H, -NH), 7.84-7.81 (m, 2H, Hh, -NH); 7.50 (dd, J= 9.4 Hz, J= 2.4 Hz, 1H, Hf), 7.34 (d, J= 16 Hz, 1H, Hp), 7.13-7.08 (m, 2H), 6.96 (d, J= 8.4 Hz, 1H) (Hr-s, Hv), 6.60-6.46 (d, J= 5.6 Hz, 1H, Hb), 6.51 (d, J= 16 Hz, 1H, Ho), 3.78 (s, 3H), 3.77 (s, 3H) (Hw-x), 3.37-3.31 (m, 2H), 3.26-3.21 (m, 2H) (Hj, Hm), 1.77-1.66 (m, 2H), 1.63-1.52 (m, 2H) (Hk-Hl); δ_C (100 MHz, DMSO-d$_6$) 165.2 (Cn), 151.2, 150.0, 149.8, 148.8, 146.6, 138.4,134.3, 127.6, 125.5, 124.5, 124.4, 121.2, 119.9, 116.9, 111.7, 109.9 (Ca, Cc-i, Co-v), 98.6 (Cb), 55.4, 55.3 (Cw-x), 42.2, 38.2 (Cj, Cm), 26.7, 25.1 (Ck-l); ESI-IT MS: m/z (M+H$^+$) 440.40 ($C_{24}H_{26}ClN_3O_3$ requires 439.17); HPLC-DAD: rt = 12.5 min (% Area = 100).

4.5.1.4. Synthesis of compounds 14-15.

Compounds **14** and **15** were synthesized by methods similar to those previously described for compounds **13**. Briefly, 4,7-dichloroquinoline (1 eq, 1.2 mmol) was reacted with the appropriate diaminoalkane (10 eq, 12 mmol) at 100 °C for 3 h; the mixture was brought to room temperature and then diluted with DCM, and the resulting solution was washed with 5% aqueous Na_2CO_3. The organic layer was isolated and dried over anhydrous Na_2SO_4, filtered and evaporated to dryness to afford the desired 4-(N-aminoalkyl)amino-7-chloroquinoline (**17-18**). Each compound was then coupled to the respective cinnamic acid in DMF, using TBTU and DIEA: a solution of cinnamic acid (1.1 eq, 0.2 mmol), TBTU (1.1 eq, 0.22 mmol), and 2.2eq of DIEA (68 μL) in DMF was stirred at 0 °C for 10 min; a solution of the appropriate compound **17-18** (1.1 eq, 0.2 mmol) in DMF was then added, and the reaction allowed to proceed at room temperature for 24 h. The mixture was diluted with DCM and the resulting solution was washed with 5% aqueous Na_2CO_3. The organic layer was separated, dried over anhydrous Na_2SO_4, filtered and evaporated to dryness, and the crude product was purified by liquid chromatography on silica using EtOAc/MeOH, 8:2 (v/v) to give the desired compounds **14**, **15**. In the particular case of **14e**, 4-(N-aminopropyl)amino-7-chloroquinoline was first coupled to *p*-(*N*-tert-butoxycarbonyl)aminocinnamic acid as above, to yield the *N*-tert-butoxycarbonyl (Boc) protected precursor (**14e'**), followed by removal of Boc through acidolysis with neat trifluoroacetic acid (TFA). Spectral/analytical data on compounds **14-15** follows.

4-(*N*-cinnamoylaminopropyl)amino-7-chloroquinoline (14a)
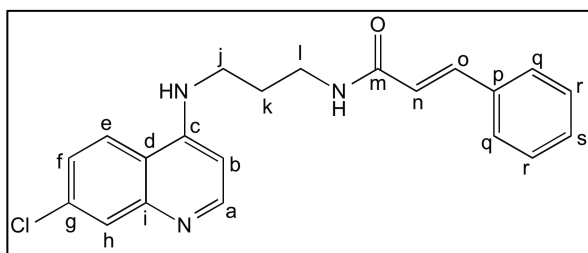
White solid (32 mg, 42%); mp 174-192 °C; R_F (EtOAc/MeOH 8:2) 0.25; δ_H (400 MHz, DMSO-d_6) 8.39 (d, J= 5.6 Hz, 1H, Ha), 8.29-8.25 (m, 2H, He, -NH), 7.79 (d, J= 2.4 Hz, 1H, Hh), 7.57-7.35 (m, 8H, Hf, Ho, Hq-s, -NH), 6.67 (d, J= 15.6 Hz, 1H, Hn), 6.49 (d, J= 5.6 Hz, 1H, Hb), 3.34-3.30 (m, 4H, Hj, Hl), 193-1.84 (m, 2H, Hk); δ_C (100 MHz, DMSO-d_6) 172.0, (Cm), 165.1, 151.9, 150.0, 149.0, 138.5, 134.8, 133.3, 129.3, 128.8, 127.4, 127.4, 124.0, 122.1, 117.4 (Ca, Cc-i, Cn-s), 98.6 (Cb), 40.0, 36.6 (Cj, Cl), 27.8 (Ck); ESI-IT MS: m/z (M+H$^+$) 366.47 ($C_{21}H_{20}ClN_3O$ requires 365.13); HPLC-DAD: rt = 13.0 min (% Area = 100).

4-[*N*-(*p*-methyl)cinnamoylaminopropyl]amino-7-chloroquinoline (14b)
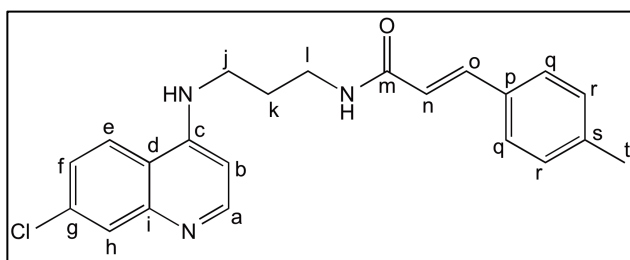
White solid (53 mg, 68%); mp 204-209 °C; R_F (EtOAc/MeOH 8:2) 0.25; δ_H (400 MHz, DMSO-d_6) 8.39 (d, J= 5.6 Hz, 1H, Ha), 8.27 (d, J= 9.2 Hz, 1H, He), 8.22 (t, J= 5.6 Hz, 1H, -NH), 7.79 (d, J= 2.4 Hz, 1H, Hh), 7.46-7.34 (m, 5H, -NH, Hf, Ho, Hq), 7.20 (d, J= 8 Hz, 2H, Hr), 6.60 (d, J= 16 Hz, 1H, Hn), 6.48 (d, J= 5.6 Hz, 1H, Hb), 3.34-3.30 (m, 4H, Hj, Hl), 2.30 (s, 3H, Ht), 1.90-1.84 (m, 2H, Hk); δ_C (100 MHz, DMSO-d_6) 165.2 (Cm), 151.8, 149.9, 149.0, 139.1, 138.5, 133.3, 132.1, 129.4, 127.4, 127.4, 124.0, 121.0, 117.4 (Ca, Cc-i, Cn-s), 98.6 (Cb), 39.4, 36.6 (Cj, Cl), 27.8, 20.8 (Ck, Ct); ESI-IT MS: m/z (M+H$^+$) 380.4 ($C_{22}H_{22}ClN_3O$ requires 379.15); HPLC-DAD: rt = 14.0 min (% Area =100).

4-[*N*-(*p*-isopropyl)cinnamoylaminopropyl]amino-7-chloroquinoline (14c)
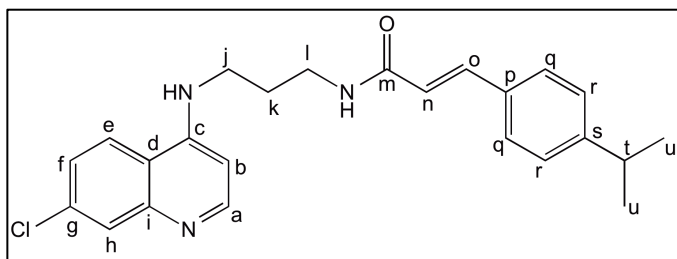
White solid (28.7 mg, 33%); mp 173-178°C; R_F (EtOAc/MeOH 8:2) 0.25; δ_H (400 MHz, DMSO-d_6) 8.39 (d, J= 5.2 Hz, 1H, Ha), 8.27 (d, J= 9.2 Hz, =1H, He), 8.22 (t, J= 5.6 Hz, 1H, -NH), 7.79 (d, J= 2.4 Hz, 1H, Hh), 7.49-7.23 (m, 5H, -NH, Hf, Ho, Hq), 7.27 (d, J= 8 Hz, 2H, Hr), 6.59 (d, J= 15.6 Hz, 1H, Hn), 6.49 (d, J= 5.6 Hz, 1H, Hb), 3.35-3.29 (m, 4H, Hj, Hl), 2.92-2.85 (m, 1H, Ht), 1.90-1.81 (m, 2H, Hk), 1.19 (d, J= 6.8 Hz, 6H, Hu); δ_C (100 MHz, DMSO-d_6)

165.2 (Cm), 151.8, 150.0, 149.9, 149.0, 138.5, 133.3, 132.5, 127.5, 127.5, 126.8, 124.0, 121.1, 117.4 (Ca, Cc-i, Cn-s), 98.6 (Cb), 40.0, 36.6 (Cj, Cl), 33.2, 27.8, 23.6 (Ck, Ct-u); ESI-IT: m/z (M+H$^+$) 408.47 (C$_{24}$H$_{26}$ClN$_3$O requires 407.18); HPLC-DAD: rt = 16.0 min (% Area =90.9).

4-[*N*-(*p*-methoxy)cinnamoylaminopropyl]amino-7-chloroquinoline (14d)
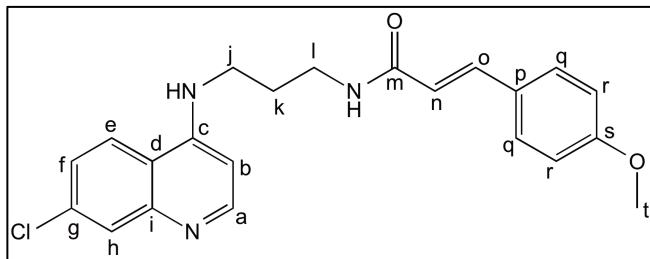
White solid (15 mg, 7%); mp 178-180°C; R$_F$ (EtOAc/MeOH 8:2) 0.25; δ$_H$ (400 MHz, DMSO-d$_6$) 8.39 (d, J= 5.6 Hz, 1H, Ha), 8.28 (d, J= 9.2 Hz, =1H, He), 8.18 (t, J= 5.6 Hz, 1H, -NH), 7.79 (d, J= 2.4 Hz, 1H, Hh),

7.54-7.36 (m, 5H, -NH, Hf, Ho, Hq), 6.97 (d, J= 8.8 Hz, 2H, Hr), 6.51-6.47 (m, 2H, Hb, Hn), 3.78 (s, 3H, Ht), 3.36-3.28 (m, 4H, Hj, Hl), 1.90-1.80 (m, 2H, Hk); δ$_C$ (100 MHz, DMSO-d$_6$) 172.0 (Cm), 165.4, 160.2, 151.6, 150.1, 148.7, 138.2, 133.4, 129.0, 127.4, 127.2, 124.0, 119.6, 117.4, 114.2 (Ca, Cc-i, Cn-s), 98.6 (Cb), 55.2 (Ct), 40.0, 36.5 (Cj, Cl), 27.8 (Ck); ESI-IT MS: m/z (M+H$^+$) 396.53 (C$_{22}$H$_{22}$ClN$_3$O$_2$ requires 395.14); HPLC-DAD: rt = 13.1 min (% Area = 98.0).

4-[*N*-(*p*-(*N*-*tert*-butoxycarbonyl)amino)cinnamoylaminopropyl]amino-7-chloroquinoline (14e')
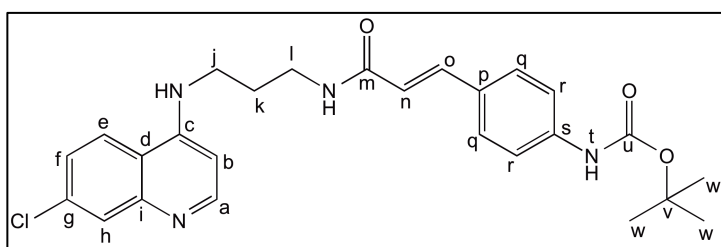
White solid (124.5 mg, 41%); mp 218-220 °C; R$_F$ (EtOAc/MeOH 8:2) 0.1; δ$_H$ (400 MHz, DMSO-d$_6$) 9.54 (s, 1H, -NHBoc), 8.39 (d, J= 5.6 Hz, 1H, Ha), 8.27 (d, J= 8.8 Hz,

1H, He), 8.15 (t, J= 5.6 Hz, 1H, -NH), 7.78 (d, J= 2.4 Hz, 1H, Hh), 7.51-7.44 (m, 5H, Hf, Hq-r), 7.37-7.32 (m, 2H, Ho, -NH), 6.52-6.48 (m, 2H, Hb, Hn), 3.36-3.28 (m, 4H, Hj, Hl), 1.88-1.82 (m, 2H, Hk), 1.48 (s, 9H, Hw); δ$_C$ (100 MHz, DMSO-d$_6$) 165.3 (Cm), 152.5, 151.8, 149.9, 149.0, 140.7, 138.3, 133.3, 128.5, 128.1, 127.4, 124.0, 123.9, 119.9, 118.0, 98.6 (Ca-I, Cn-s, Cu), 79.3 (Cv), 40.0, 36.5 (Cj, Cl), 28.0, 27.8 (Ck, Cw); ESI-IT: m/z (M+H$^+$) 481.33 (C$_{26}$H$_{29}$ClN$_4$O$_3$ requires 480.19); HPLC-DAD: rt = 15.0 min (% Area = 100).

4-[*N*-(*p*-amino)cinnamoylaminopropyl]amino-7-chloroquinoline (14e).
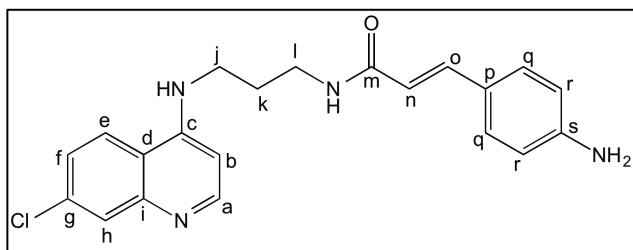
White solid (28.8 mg, 73%); mp 103-105 °C; R_F (EtOAc/MeOH 8:2) 0.1; δ_H (400 MHz, DMSO-d_6) 8.39 (d, J= 5.2 Hz, 1H, Ha), 8.27 (d, J= 9.2 Hz, 1H, He), 8.0 (t, J= 5.6 Hz, 1H, -NH), 7.79 (d, J= 2 Hz, 1H, Hh), 7.44 (dd, J= 8.8 Hz, J=2Hz, 1H, Hf), 7.36-7.22 (m, 4H, Ho, Hq, -NH), 6.56 (d, J= 8.4Hz, 2H, Hr), 6.48 (d, J= 5.6 Hz, 1H, Hb), 6.29 (d, J= 15.6 Hz, 1H, Ho), 5.55 (b, 2H, -NH$_2$), 3.31-3.27 (m, 4H, Hj, Hl), 1.87-1.81 (m, 2H, Hk); δ_C (100 MHz, DMSO-d_6) 166.0 (Cm), 151.8, 150.4, 150.0, 149.0, 139.4, 133.3, 129.0, 127.4, 124.0, 122.1, 117.4, 115.7, 113.6 (Ca, Cc-I, Cn-s), 98.6 (Cb), 40.0, 36.5 (Cj, Cm), 27.9 (Ck); ESI-IT MS: m/z (M+H$^+$) 381.40 (C$_{21}$H$_{21}$ClN$_4$O requires 380.14); HPLC-DAD: rt = 8.65 min (% Area = 96.0).

4-[*N*-(*m*-fluoro)cinnamoylaminopropyl]amino-7-chloroquinoline (14f)
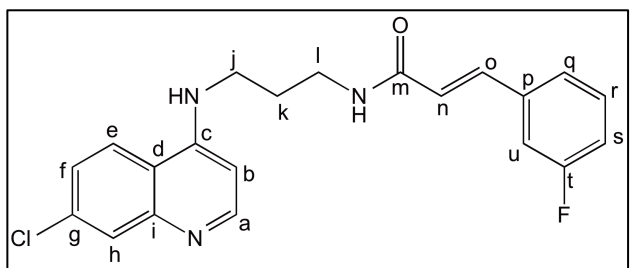
White solid (36 mg, 45%); mp 185-190 °C; R_F (EtOAc/MeOH 8:2) 0.25; δ_H (400 MHz, DMSO-d_6) 8.39 (d, J= 5.2 Hz, 1H, Ha), 8.30-8.24 (m, 2H, He, -NH), 7.79 (d, J= 2Hz, 1H, Hh), 7.47-7.35 (m, 6H, Hf, Ho, Hq, Hs, Hu, -NH), 7.20 (t, J= 8.8 Hz, 1H, Hr), 6.67 (d, J= 16 Hz, 1H, Hn), 6.48 (d, J= 5.6 Hz, 1H, Hb), 3.36-3.30 (m, 4H, Hj, Hl), 1.90-1.84 (m, 2H, Hk); δ_C (100 MHz, DMSO-d_6) 172.7 (Cm), 164.8, 163.6, 161.2, 151.8, 150.0, 149.0, 137.4, 137.2, 133.3, 130.7, 127.4, 124.0, 123.6, 117.4, 115.9, 113.8 (Ca, Cc-i, Cn-u), 98.6 (Cb), 40.0, 36.7 (Cj, Cl), 27.7 (Ck); ESI-IT MS: m/z (M+H$^+$) 384.40 (C$_{21}$H$_{19}$ClFN$_3$O requires 383.12); HPLC-DAD: rt = 13.4 min (% Area = 100).

4-[*N*-(*p*-fluoro)cinnamoylaminopropyl]amino-7-chloroquinoline (14g)
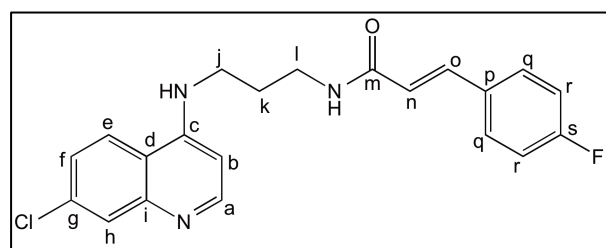
White solid (27 mg, 34%); mp 187-193 °C; R_F (EtOAc/MeOH 8:2) 0.25; δ_H (400 MHz, DMSO-d_6) 8.39 (d, J= 5.2 Hz, 1H, Ha), 8.30-8.26 (m, 2H, He, -NH), 7.78 (d, J= 2.4 Hz, 1H, Hh), 7.61 (dd, J= 8.6 Hz, J= 5.6 Hz, 2H, Hq), 7.46-7.35 (m, 2H, Hf, Ho), 7.36 (t, J= 5.2 Hz, 1H, -NH), 7.24 (t, J= 8.8 Hz, 2H, Hr), 6.59 (d, J= 16 Hz, 1H, Hn), 6.48 (d, J= 4.8 Hz, 1H, Hb), 3.34-3.30 (m, 4H, Hj, Hl), 1.91-1.83 (m, 2H, Hk); δ_C

(100 MHz, DMSO-d_6) 172.1 (Cm), 165.0, 163.8, 161.3, 151.8, 150.0, 149.0, 137.4, 133.3, 129.6, 127.4, 124.0, 122.0, 117.4, 115.9 (Ca, Cc-i, Cn-s), 98.6 (Cb), 40.0, 36.6 (Cj, Cl), 27.8 (Ck); ESI-IT MS: m/z (M+H+) 384.47 ($C_{21}H_{19}ClFN_3O$ requires 383.12); HPLC-DAD: rt = 13.3 min (% Area = 100).

## 4-[*N*-(*p*-chloro)cinnamoylaminopropyl]amino-7-chloroquinoline (14h)
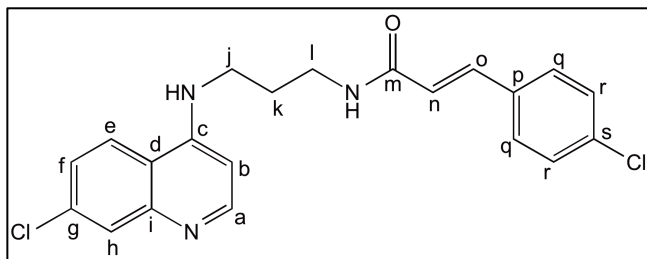
White solid (39 mg, 46%); mp 191-195 °C; R_F (EtOAc/MeOH 8:2) 0.25; δ_H (400 MHz, DMSO-d_6) 8.39 (d, J= 5.6 Hz, 1H, Ha), 8.28 (m, 2H, He, -NH), 7.78 (d, J= 2.4 Hz, 1H, Hh), 7.58 (d, J= 8.4 Hz, 2H), 7.49-7,37

(m, 5H) (Hf, Ho, -NH, Hq-r), 6.63 (d, J= 15.6 Hz, 1H, Hn), 6.49 (d, J= 5.6 Hz, 1H, Hb), 3.34-3.30 (m, 4H, Hj, Hl), 1.90-1.83 (m, 2H, Hk); δ_C (100 MHz, DMSO-d_6) 164.9 (Cm), 151.7, 150.1, 148.8, 137.2, 133.8, 133.4, 129.1, 128.9, 127.3, 124.1, 124.0, 122.9, 117.4 (Ca, Cc-i, Cn-s), 98.6 (Cb), 40.0, 36.6 (Cj, Cl), 27.8 (Ck); ESI-IT MS: m/z (M+H$^+$) 400.40 ($C_{21}H_{19}Cl_2N_3O$ requires 399.09); HPLC-DAD: rt = 13.4 min (% Area = 96.2).

4-[*N*-(*p*-bromo)cinnamoylaminopropyl]amino-7-chloroquinoline (14i)
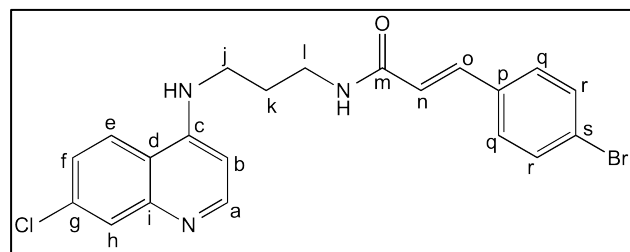
White solid (22 mg, 39%); mp 214-219°C; R_F (EtOAc/MeOH 8:2) 0.25; δ_H (400 MHz, DMSO-d_6) 8.39 (d, J= 5.2 Hz, 1H, Ha), 8.32-8.26 (m, 2H, He, -NH), 7.78 (d, J= 2 Hz, 1H, Hh), 7.60 (d, J= 8.4 Hz, 2H), 7.51 (d, J= 8.8 Hz, 2H) (Hq-r), 7.46-7.34 (m, 3H, -NH, Hf, Ho), 6.65 (d, J= 16 Hz, 1H, Hn), 6.48 (d, J= 5.6 Hz, 1H, Hb), 3.34-3.30 (m, 4H, Hj, Hl), 1.89-1.82 (m, 2H, Hk); δ_C (100 MHz, DMSO-d_6) 164.9 (Cm), 151.8, 150.0, 149.0, 137.3, 134.1, 133.3, 131.8, 129.4, 127.4, 124.0, 123.0, 122.5, 117.4 (Ca, Cc-i, Cn-s), 98.6 (Cb), 40.0, 36.6 (Cj, Cl), 27.7 (Ck); ESI-IT MS: m/z (M+H$^+$) 446.20 ($C_{21}H1_9ClBrN_3O$ requires 443.04); HPLC-DAD: rt = 14.7 (% Area = 100).

(4-[*N*-(*o*-nitro)cinnamoylaminopropyl]amino-7-chloroquinoline (14j).
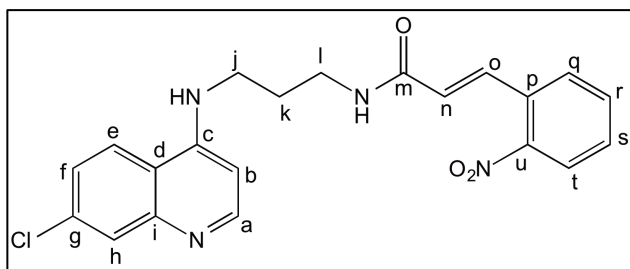
White solid (61.7 mg, 72%); mp 190-195°C; R_F (EtOAc/MeOH 8:2) 0.25; δ_H (400 MHz, DMSO-d_6) 8.41-8.39 (m, 2H, Ha, -NH), 8.29 (d, J= 9.2 Hz, 1H, He), 8.03 (d, J= 8 Hz, 1H, Ht), 7.79-7.58 (m, 5H, Hh, Ho, Hq-s), 7.44 (dd, J= 9 Hz, J=2Hz, 1H, Hf), 7.33 (t, J= 5.2 Hz, 1H, -NH), 6.63 (d, J= 15.6 Hz, 1H, Hn), 6.49 (d, J= 5.2 Hz, 1H, Hb), 3.35-3.31 (m, 4H, Hj, Hl), 1.94-1.85 (m, 2H, Hk); δ_C (100 MHz, DMSO-d_6) 164.2 (Cm), 151.8, 149.9, 149.0, 148.2, 133.7, 133.5, 133.3, 130.1, 130.0, 128.6, 127.4, 126.8, 124.5, 124.0, 117.4 (Ca, Cc-i, Cn-u), 98.6 6 (Cb), 40.0, 36.7 (Cj, Cl), 27.7 (Ck); ESI-IT MS: m/z (M+H$^+$) 411.47 ($C_{21}H_{19}ClN_4O_3$ requires 410.11); HPLC-DAD: rt = 13.0 min (% Area = 100).

4-[*N*-(*m*-nitro)cinnamoylaminopropyl]amino-7-chloroquinoline (14k)
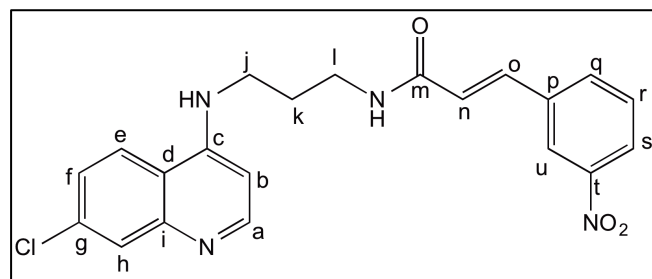
Yellow solid (22 mg, 25%); mp 209-214°C; R_F (EtOAc/MeOH 8:2) 0.25; δ_H (400 MHz, DMSO-d_6) 8.40-8.38 (m, 2H, Ha, Hu), 8.35-8.26 (m, 2H, He, -NH), 8.20 (dd, J= 8 Hz, J= 1.6 Hz, 1H, Hs), 8.01 (d, J= 7.6 Hz, 1H, Hq), 7.77 (d, J= 2 Hz, 1H, Hh), 7.70 (t, J= 8 Hz, 1H, Hr), 7.55 (d, J= 15.6 Hz, 1H, Ho), 7.44 (dd, J= 8.8 Hz, J= 2.4Hz, 1H, Hf), 7.34 (t, J= 5.2 Hz, 1H, -NH), 6.82 (d, J= 15.6 Hz, 1H, Hn), 6.49 (d, J= 5.6 Hz, 1H, Hb), 3.36-3.32 (m, 4H, Hj, Hl), 1.93-1.85 (m, 2H, Hk); δ_C (100 MHz, DMSO-d_6) 164.5 (Hm), 151.8, 149.9, 149.0, 148.2, 136.7, 136.2, 133.8, 133.3, 130.4, 127.4, 125.0, 123.8, 123.6, 121.4, 117.4 (Ca, Cc-i, Cn-u), 98.6 (Cb), 36.7 (Cl), 27.7 (Ck); ESI-IT MS: m/z (M+H$^+$) 411.40 ($C_{21}H_{19}ClN_4O_3$ requires 410.11); HPLC-DAD: rt = 13.2 min (% Area = 93.2).

4-[*N*-(*p*-nitro)cinnamoylaminopropyl]amino-7-chloroquinoline (14l)
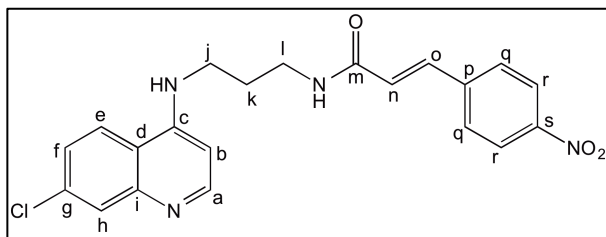
Yellow solid (42 mg, 49%); mp 200-205°C; RF (EtOAc/MeOH 8:2) 0.25; δ_H (400 MHz, DMSO-d_6) 8.39 (m, 2H, Ha, -NH), 8.26 (m, 3H, He, Hr), 7.81 (m, 3H, Hh, Hq), 7.53 (d, J= 15.6 Hz, 1H, Ho), 7.45 (d, J= 9 Hz, J= 2.4 Hz, 1H, Hf), 7.35 (t, J= 5.6 Hz, 1H, -NH), 6.81 (d, J= 16 Hz, 1H, Hn), 6.49 (d, J= 5.6 Hz, 1H, Hb),

3.36-3.32 (m, 4H, Hj, Hl), 1.92-1.84 (m, 2H, Hk); δ_C (100 MHz, DMSO-d_6) 164.4 (Cm), 151.7, 150.0, 149.0, 147.4, 141.5, 136.2, 133.4, 128.5, 127.3, 126.4, 124.0, 124.0, 117.4 (Ca, Cc-i, Cn-s), 98.6 (Cb), 36.8 (Cl), 27.8 (Ck); ESI-IT MS: m/z (M+H$^+$) 411.40 ($C_{21}H_{19}ClN_4O_3$ requires 410.11); HPLC-DAD: rt = 13.2 min (% Area = 94.0).

## 4-[*N*-(*p*-isopropyl)cinnamoylaminopentyl]amino-7-chloroquinoline (15a)
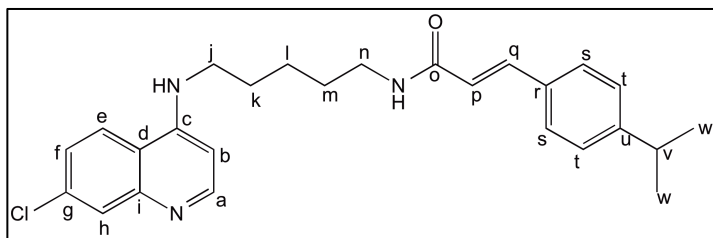
White solid (190 mg, 50%); mp=152-155°C; R$_F$ (DCM/MeOH 8:2) 0.58; δ_H (400 MHz, DMSO-d_6) 8.38 (d, J= 5.6 Hz, 1H, Ha), 8.28 (d, J= 9.5 Hz, 1H, He), 8.07 (t, J= 5.6 Hz, 1H, -NH), 7.77 (d, J= 2 Hz, 1H, Hh), 7.47-7.39 (m, 4H, Hf, Hq, Hs), 7.30-7.26 (m, 3H, Ht, -NH), 6.56 (d, J= 16 Hz, 1H, Hp), 6.46 (d, J= 5.6 Hz, 1H, Hb), 3.27-3.17 (m, 4H, Hj, Hn), 2.92-2.86 (m, 1H, Hv), 1.73-1.65 (m, 2H), 1.56-1.36 (m, 4H) (Hk-m), 1.19 (d, J=6.8Hz, 6H, Hw); δ_C (100 MHz, DMSO-d_6) 164.9 (Co), 151.8, 150.0, 149.8, 148.9, 138.2, 133.3, 132.5, 127.4, 127.3, 126.8, 124.0, 123.9, 121.3, 117.3 (Ca, Cc-i, Cp-u), 98.5 (Cb), 42.3, 38.5 (Cj, Cn), 33.2, 28.9, 27.4, 24.0, 23.6 (Ck-l, Cv-w); ESI-IT MS: m/z (M+H+) 436.47 ($C_{26}H_{30}ClN_3O$ requires 435.21); HPLC-DAD: rt = 16.3 min (% Area = 98.0).

4-[*N*-(*p*-methoxy)cinnamoylaminopentyl]amino-7-chloroquinoline (15b)
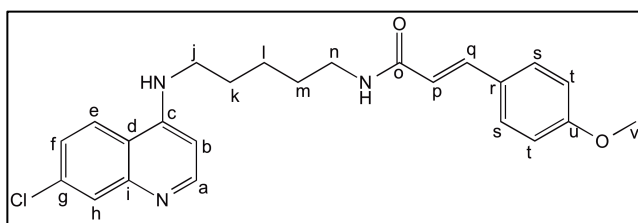
White solid (100 mg, 27%); mp=142.144°C; R$_F$ (DCM/MeOH 8:2) 0.58; δ_H (400 MHz, DMSO-d_6) 8.38 (d, J= 5.6 Hz, 1H, Ha), 8.28 (d, J=9.2 Hz, 1H, He), 8.01 (t, J= 5.6 Hz, 1H, -NH), 7.77 (d, J= 2 Hz, 1H, Hh), 7.50-7.25 (m, 4H, Hf, Hq, Hs), 7.29 (t, J= 5.2 Hz, 1H, -NH), 6.96 (d, J= 8.8 Hz, 2H, Ht), 6.48-6.45 (m, 2H, Hb, Hp), 3.78 (s, 3H, Hv), 3.27-3.17 (m, 4H, Hj, Hn), 1.76-1.62 (m, 2H), 1.56-1.39 (m, 4H) (Hk-m); δ_C (100 MHz, DMSO-d_6) 165.1 (Co), 160.1, 151.7, 150.0, 148.9, 138.0, 133.3, 128.9, 127.4, 127.3, 124.0, 123.9, 119.8, 117.3, 114.3 (Ca, Cc-i, Cp-u), 98.5 (Cb), 55.1 (Cv), 42.3, 38.4 (Cj, Cn), 28.9, 27.4, 24.0 (Ck-m); ESI-IT MS: m/z (M+H+) 424.40 ($C_{24}H_{26}ClN_3O_2$ requires 423.17); HPLC-DAD: rt = 13.7 min (% Area = 100).

(4-[*N*-(*p*-chloro)cinnamoylaminopentyl]amino-7-chloroquinoline (15c)
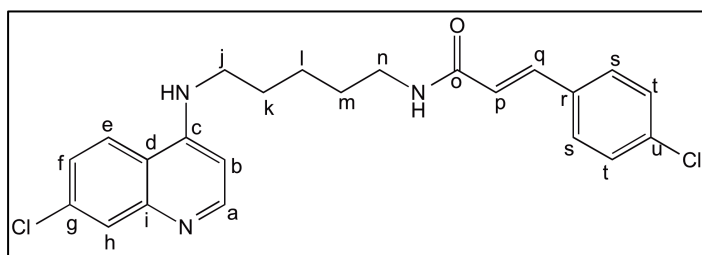
Yellowish solid (65 mg, 17%); mp=164-168°C; R_F (DCM/MeOH 8:2) 0.58; δ_H (400 MHz, DMSO-d_6) 8.38 (d, J= 5.2 Hz, 1H, Ha), 8.29 (d, J= 8.8 Hz, 1H, He), 8.16 (t, J= 5.6 Hz, 1H, -NH), 7.77 (d, J= 2 Hz, 1H, Hh), 7.56 (d, J= 8.8 Hz, 2H), 7.46-7.38 (m, 4H) (Hs-t, Hf, Hq), 7.32 (t, J= 4.8 Hz, 1H, -NH), 6.64 (d, J= 16 Hz, 1H, Hp), 6.44 (d, J= 5.2 Hz, 1H, Hb), 3.26-3.18 (m, 4H, Hj, Hn), 1.71-1.65 (m, 2H), 1.56-1.38 (m, 4H, Hk-m); δ_C (100 MHz, DMSO-d_6) 164.6 (Co), 151.7, 150.1, 148.8, 136.9, 133.8, 133.7, 133.3, 129.0, 128.8, 127.2, 124.1, 123.9, 123.1, 117.3 (Ca, Cc-i, Cp-u), 98.5 (Cb); 42.3, 38.5 (Cj, Cn), 28.9, 27.4, 24.0 (Ck-m); ESI-IT MS: m/z (M+H$^+$) 428.53 (C$_{23}$H$_{23}$Cl$_2$N$_3$O requires 427.12); HPLC-DAD: rt = 14.9, (% Area = 100).

4-[(7-chloroquinolin-4-yl)amino]butan-1-ol (16)
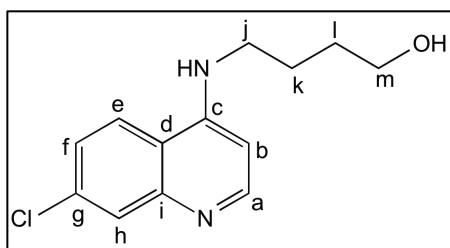
1 eq of 4,7-dichloroquinoline (0.5g, 2.5mmol) was mixed with 4 eq of 4-aminobutan-1-ol (0.9g, 10mmol) in a round bottom flask, and reaction was allowed to proceed at 100°C for 4 h. Then, DCM (25 mL) was added, followed by addition of 30% aqueous Na$_2$CO$_3$ (25 mL), with concomitant precipitation of a light pink solid; the solid was submitted to column chromatography on silica, using DCM:MeOH (8:2 v/v) as eluent, and pure **18** was obtained as a white solid (0.49 g, 78%); mp=171-174°C; R_F=0.26 (DCM/MeOH 8:2); δ_H (400 MHz, DMSO-d_6); 8.38 (d, J= 5.2 Hz, 1H, Ha), 8.27 (d, J= 9.2 Hz, 1H, He), 7.77 (d, J= 2.4 Hz, 1H, Hh), 7.42 (dd, J= 9.2 Hz, 2.4 Hz, 1H, Hf), 7.32 (t, J= 5.2 Hz, 1H, -NH), 6.44 (d, J= 5.6 Hz, 1H, Hb), 4.51 (b, 1H, -OH), 3.47-3.44 (m, 2H, Hm), 3.28-3.24 (m, 2H, Hj), 1.78-1.66 (m, 2H), 1.57-1.50 (m, 2H) (Hk-l); δ_C (100 MHz, DMSO-d_6) 151.8, 150.0, 149.0, 133.2, 127.4, 124.0, 123.9 (Ca, Cc-i), 117.4, 98.5 (Cb), 60.4 (Cm), 42.2 (Cj), 30.0, 24.4 (Ck-l); ESI-IT MS: m/z (M+H$^+$) 251.33 (C$_{13}$H$_{15}$ClN$_2$O requires 250.09).

4-[*N*-(*p*-methoxy)cinnamoyloxypropyl]amino-7-chloroquinoline (20)
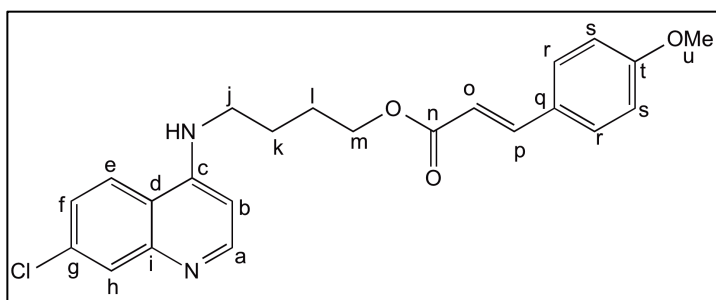
1 eq of p-methoxycinnamoyl chloride (0.08 g, 0.4 mmol) was reacted with 4 eq of **22** in refluxing DCM (2 mL), in the presence of 2 eq of triethylamine (112 µL); the solution turned yellow after 10 min and the reaction ran for 24 h. The organic layer was washed with 5% aqueous Na_2CO_3 (3 × 2 mL), dried with anhydrous Na_2SO_4, filtered, and led to dryness on a rotary evaporator. The residue was submitted to column chromatography on silica, using DCM:Me_2CO (1:1 v/v) as eluent, to yield **20** as a white solid (34 mg, 21%); mp=129-134°C; R_F (DCM/Me_2CO 1:1) 0.26; $δ_H$ (400 MHz, $CDCl_3$) 8.49 (d, J= 5.2 Hz, 1H, Ha), 7.93 (d, J= 2 Hz, 1H, Hh), 7.71 (d, J= 9.2 Hz, 1H, He), 7.63 (d, J= 16 Hz, 1H, Hp), 7.43 (d, J= 8.4 Hz, 2H, Hr), 7.31 (dd, J= 8.8 Hz, J= 2 Hz, 1H, Hf), 6.88 (d, J= 8.4 Hz, 2H, Hs), 6.39 (d, J= 5.2 Hz, 1H, Hb), 6.28 (d, J= 16 Hz, 1H, Ho), 5.38 (b, 1H, -NH), 4.28-4.26 (m, 2H, Hm), 3.82 (s, 3H, Hu), 3.37-3.36 (m, 2H, Hj), 1.90-1.84 (m, 4H, Hk-l); $δ_C$ (100 MHz, $CDCl_3$) 167.3 (Cn), 161.4, 151.7, 149.8, 148.8, 144.7, 134.9, 129.7, 128.4, 126.9, 125.3, 121.1, 117.1, 115.1, 114.3 (Ca, Cc-Ci, Co-t), 99.0 (Cb), 63.7 (Cm), 55.3 (Cu), 42.9 (Cj), 26.5, 25.3 (Ck-l); ESI-IT MS: m/z (M+H+) 411.33 ($C_{23}H_{23}ClN_2O_3$ requires 410.14); HPLC-DAD: rt = 15.4 min (% Area = 97).

4-[*N*-(*p*-isopropyl)cinnamoylaminopropyl]aminoquinoline (21)
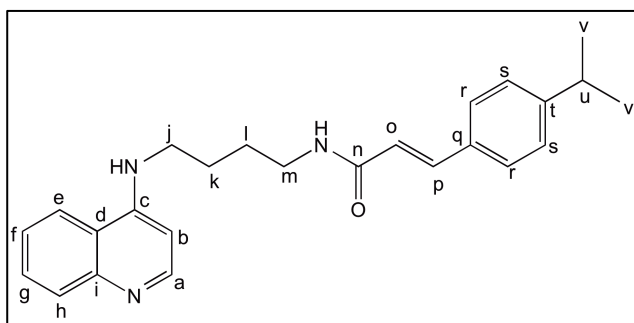
Following the experimental procedure previously described for compounds **16** and **17**-**18**, and starting from 4-chloroquinoline (0.25 g, 1.5 mmol) instead of 4,7-dichloroquinoline, compound **21** was obtained as a beige solid (55 mg, 11%); mp=73-78°C; R_F (DCM/MeOH 8:2) 0.30; $δ_H$ (400 MHz, $CDCl_3$) 8.41 (d, J= 5.6 Hz, 1H, Ha), 8.02 (d, J= 8.4 Hz, 1H, He), 7.95 (d, J= 8.4 Hz, 1H, Hh), 7.67-7.57 (m, 2H), 7.42-7.39 (m, 3H) (Hf-g, Hp, Hr), 7.18 (d, J= 8 Hz, 2H, Hs), 6.52 (t, J= 5.6 Hz, 1H, -NH), 6.46 (d, J= 16 Hz, 1H, Ho), 6.34 (d, J= 5.6 Hz, 1H, Hb), 6.15 (b, 1H, -NH), 3.49-3.42 (m, 2H), 3.40-3.30 (m, 2H) (Hj, Hm), 2.95-2.83 (m, 1H, Hu), 1.78-1.70 (m, 4H, Hk-l), 1.22 (d, J= 6.8 Hz, 6H, Hv); $δ_C$ (100 MHz, $CDCl_3$) 166.7 (Cn), 150.9, 149.2, 146.6, 141.0, 132.4, 129.7, 128.0, 127.9, 126.9, 125.0, 120.5, 119.7, 118.5 (Ca, Cc-i, Co-t), 98.4 (Cb), 43.1, 39.1 (Cj, Cm), 34.0

(Cu), 27.8, 25.5, 23.8 (Ck-l, Cv); ESI-IT MS: m/z (M+H$^+$) 388.27 (C$_{25}$H$_{29}$N$_3$O requires 387.23); HPLC-DAD: rt = 15.2 min (% Area = 99).

4.5.1.5. Synthesis of pyridine and morpholine derivatives

N^1-(pyridin-4-yl)butane-1,4-diamine (26)

1 eq of 4-chloropyridine (0.5 g, 3.3 mmol) was reacted with 10 eq of butane-1,4-diamine (2.9 g, 33 mmol) in a round bottom flask put under reflux for 2 hours; after cooling the reaction mixture to room temperature, 25 mL of distilled water were added, and the desired product was extracted with DCM (3 × 25 mL); the organic layer was dried over anhydrous Na$_2$SO$_4$, filtered, and led to dryness on a rotary evaporator; this afforded **26** as a yellow oil (0.22 g, 40%); ESI-IT MS: m/z (M+H$^+$) 166.33 (C$_9$H$_{15}$N$_3$ requires 165.13). Compound **26** was used without further purification in the synthesis of **24**

4-[N-(p-methoxy)cinnamoylbutyl]aminopyridine (24)
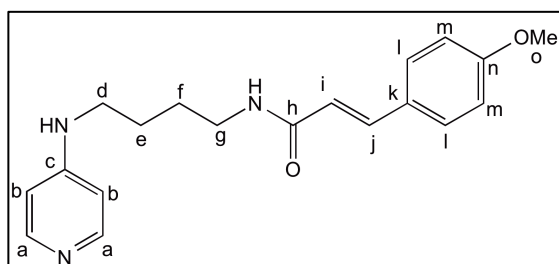
In a round bottom flask put at 0 °C, 1.1 eq of p-methoxycinnamic acid (0.29 g, 1.5 mmol) was dissolved in DMF (2.5 mL) and activated by addition of 1.1 eq of TBTU (0.47 g, 1.5 mmol) and 2 eq of DIEA (454 µL); after 10 min, a solution of 1 eq of **26** (0.22 g, 1.3 mmol) in DMF (2.5 mL) was added to the previous mixture and the reaction allowed to proceed for 24 h. Water (25 mL) was added to the reaction mixture and the desired product was extracted with DCM (3 × 25 mL); the organic extract was then washed with 5% aqueous Na$_2$CO$_3$ (3 × 25mL), dried over anhydrous Na$_2$SO$_4$, filtered, and taken to dryness on a rotary evaporator. The residue was submitted to column chromatography on silica, using DCM/MeOH 8:2 (v/v) as eluent, to afford **24** as a white solid (0.13 g, 30%); mp= 132-136 °C; R$_F$ (DCM/MeOH 8:2) 0.13; δ$_H$ (400 MHz, CDCl$_3$) 8.04 (b, 2H, Ha), 7.54 (d, J= 16 Hz, 1H, Hj), 7.33 (d, J= 8.8 Hz, 2H, Hl), 7.29-7.26 (m, 1H, -NH), 6.77 (d, J= 8.8 Hz, 2H, Hm), 6.38-6.34 (m, 3H, Hb, Hi), 5.14 (t, J= 4.8 Hz, 1H, -NH), 3.73 (s, 3H, Ho), 3.36-3.34 (m, 2H), 3.07-3.05 (m, 2H) (Hd, Hg), 1.61-1.59 (m, 4H, He-f); δ$_C$ (100 MHz, CDCl$_3$) 166.8 (Ch), 160.6, 153.7, 149.0, 140.0, 129.1, 127.4, 118.5, 114.1, 107.4 (Ca-c, Ci-n), 55.2 (Co), 42.1, 39.1 (Cd, Cg), 27.2, 26.0 (Ce-f); ESI-IT MS: m/z (M+H$^+$) 326.33 (C$_{19}$H$_{23}$N$_3$O$_2$ requires 325.18); HPLC-DAD: rt = 11.6 min, (% Area = 100).

N-(N-phthaloyl)aminobutylmorpholine (27')
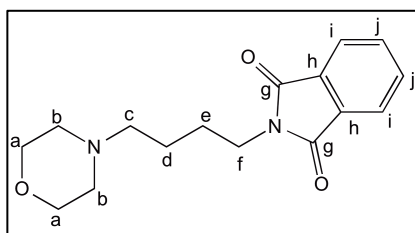
2 eq of morpholine (0.5g, 5.7 mmol) were reacted with 1 eq of 1-(N-phthaloyl)amino-4-bromobutane (0.8 g, 2.9 mmol) in refluxing DCM for 24 h, after which the reaction mixture was washed three times with 5% aqueous Na_2CO_3, dried over anhydrous Na_2SO_4, filtered, and led to dryness in a rotary evaporator; the residue was submitted to column chromatography on silica, using as eluent DCM:MeOH (8:2 v/v), to afford **27'** as a white solid (0.53 g, 64%); mp=61-63°C; R_F (DCM/MeOH 8:2) 0.67; δ_H (400 MHz, $CDCl_3$) 7.84-7.76 (m, 2H), 7.74-7.66 (m, 2H) (Hi-j), 3.67-3.64 (m, 6H, Ha, Hf), 2.46-2.32 (m, 6H, Hb-c), 1.70-1.66 (m, 2H), 1.56-1.47 (m, 2H) (Hd-e); δ_C (100 MHz, $CDCl_3$) 168.4 (Cg), 133.8, 132.1, 123.1 (Ch-j), 66.9 (Ha), 58.3 (Cf), 53.6 (Cb), 37.8, 26.4, 23.8 (Hc-e); ESI-IT MS: m/z (M+H$^+$) 289.40 ($C_{16}H_{20}N_2O_3$ requires 288.15).

N-aminobutylmorpholine (27).

N-aminobutylmorpholine (27). 1 eq of **27'** (100 mg, 0.30 mmol) was reacted with 50% ethanolic hydrazine (0.40 mL) for 2 h at room temperature, for removal of the phthaloyl N-protecting group; water was then added to the reaction mixture and the desired product was extracted with DCM (3 × 25 mL), the organic layer was dried over anhydrous sodium sulfate, filtered, and led to dryness on the rotary evaporator to afford **27** as a yellowish oil (25 mg, 45%); ESI-IT MS: m/z (M+H$^+$) 159.27 ($C_8H_{18}N_2O$ requires 158.14). Compound **27** was used without further purification in the synthesis of **25**.

N-(p-isopropyl)cinnamoylaminobutylmorpholine (25)
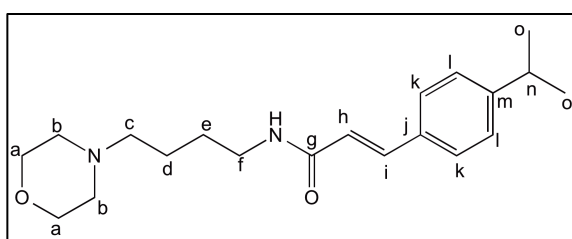
1 eq of N-aminobutylmorpholine (0.025 g, 0.16 mmol) was immediately used in the coupling with p-isopropylcinnamic acid (0.032 g, 0.17 mmol) carried out as above described for **24** but using PyBOP (0.088 g, 0.17 mmol) instead of TBTU as coupling reagent, and DCM as a solvent; this yielded **25** as a white solid (32 mg, 61%); mp=92-94°C; RF (DCM/MeOH 8:2) 0.52; δ_H (400 MHz, $CDCl_3$) 7.59 (d, J= 15.6 Hz, 1H, Hi), 7.40 (d, J= 8.4 Hz, 2H, Hk), 7.20 (d, J= 8.4 Hz, 2H, Hl), 6.36-6.33 (m, 2H, Hh, -NH), 3.73-3.71 (m, 4H, Ha), 3.40-3.36 (m, 2H, Hf), 2.95-2.85 (m, 1H, Hn), 2.44-2.42 (m, 4H, Hb), 2.38-2.34 (m, 2H, Hc), 1,60 (m, 4H, Hd-e), 1.23 (d, J= 6.8 Hz, 6H, Ho); δ_C (100 MHz, $CDCl_3$); 160.1 (Cg), 150.7, 140.7, 132.5, 127.7, 126.9, 119.8 (Ch-m), 66.9 (Ca), 58.3 (Cf), 53.6 (Cb), 39.5 (Cc), 34.0, 27.4, 24.0, 23.8 (Cd-e, Cn-o); ESI-IT MS: m/z (M+H$^+$) 331.40 ($C_{20}H_{30}N_2O_2$ requires 330.23); HPLC-DAD: rt = 13.2 min (% Area = 100).

4.5.1.6. Synthesis of PQ-based *HEFLECINs* (28).

In a round bottom flask, the relevant cinnamic acid (1.1 eq., 0.6 mmol) was solubilized in DMF (2.5 mL) and the solution put in an ice bath; then, TBTU (1.1 eq., 0.6 mmol) and DIEA (2 eq., 1.0 mmol) were added and the mixture stirred at 0 °C for 10 minutes. A solution of primaquine biphosphate in DMF (2.5mL) was then added to the mixture, which was left under stirring for one day at room temperature. Following 50 mL of DCM were added to the reaction mixture and the organic layer was washed with 5% aqueous Na_2CO_3. Finally, the organic layer was dried over anhydrous Na_2SO_4, filtered, and evaporated under reduced pressure. The residue was submitted to column liquid chromatography on silica, using dichloromethane:acetone (6:1 v/v) as eluent. All target compounds were isolated in high purity degrees and presented correct analytical and spectral data, as given below.

N-cinnamoylprimaquine (28a).
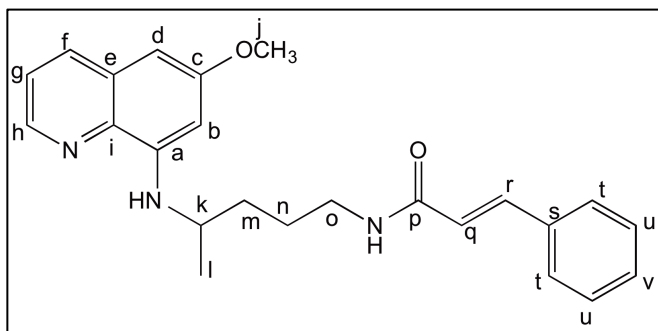
Yellow oil (0.13 g, 58%); R_F (DCM/Me$_2$CO 6:1) 0.49; δ_H (400 MHz, DMSO-d$_6$) 8.53 (dd, J= 4 Hz, J= 1.6 Hz, 1H, Hh), 7.91 (dd, J= 8.4 Hz, J= 1.6 Hz, 1H, Hf), 7.58 (d, J= 15.6 Hz, 1H, Hr), 7.44-7.42 (m, 2H, Ht), 7.35-7.28 (m, 4H, Hg, Hu-v),

6.35-6.27 (m, 3H, Hb, Hd, Hq), 6.01-5.95 (m, 2H, -NH-QN, -NH-C=O), 3.85 (s, 3H, Hj), 3.67-3.59 (m, 1H, Hk), 3.44-3.34 (m, 2H, Ho), 1.76-1.66 (m, 4H, Hm-n), 1.28 (d, J= 6.3Hz, 3H, Hl); δ_C (100 MHz, DMSO-d$_6$) 165.9 (Cp), 159.4, 144.8, 144.3, 140.7, 135.3, 134.9, 134.8, 129.9, 129.5, 128.7, 127.7, 121.9, 120.8 (Ca, Cc, Ce-i, Cq-v), 96.9, 91.7 (Cb, Cd), 55.1 (Cj), 47.8, 39.7 (Ck, Co), 34.1, 26.1, 20.1 (Cl-n); ESI-IT MS: m/z (M+H$^+$) 390.33 ($C_{24}H_{27}N_3O_2$ requires 389.21); HPLC-DAD: rt = 16.8 min (% Area =99.5%).

N-(4-methylphenyl)cinnamoylprimaquine (28b).
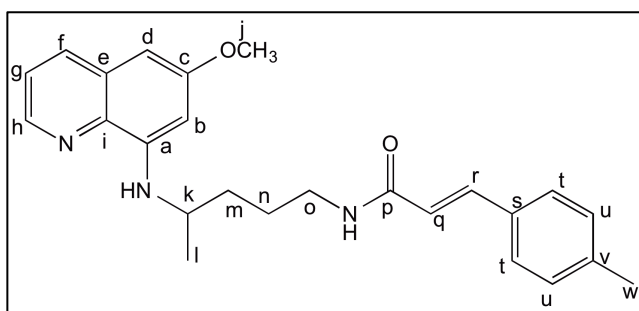
Yellow oil (0.08 g, 36%); R_F (DCM/Me$_2$CO 6:1) 0.49; δ_H (400 MHz, DMSO-d$_6$) 8.53 (dd, J= 4 Hz, J= 1.6 Hz, 1H, Hh), 7.92 (dd, J= 8.4, J= 1.6 Hz, 1H, Hf), 7.55 (d, J= 15.6 Hz, 1H, Hq), 7.35-7.28 (m, 3H, Ht, Hg), 7.15 (d, J= 8 Hz, 2H, Hu), 6.34

(d, J= 2.8 Hz, 1H), 6.30 (d, J= 2.4 Hz, 1H) (Hb, Hd), 6.23 (d, J= 15.6 Hz, 1H, Hq), 6.00

(d, J= 8.4 Hz, 1H, -NH-QN), 5.80 (t, J= 5.2 Hz, 1H, -NH-C=O), 3.86 (s, 3H, Hj), 3.67-3.63 (m, 1H, Hk), 3.45-3.34 (m, 2H, Ho), 2.35 (s, 3H, Hw), 1.78-1.69 (m, 4H, Hm-n), 1.30 (d, J= 6.4 Hz, 3H, Hl); δ_C (100 MHz, DMSO-d$_6$) 166.1 (Cp), 159.4, 144.9, 144.3, 140.7, 135.3, 134.9, 132.1, 129.9, 129.4, 127.7, 121.9, 119.7 (Ca, Cc, Ce-i, Cq-v), 96.9, 91.8 (Cb, Cd), 55.2 (Cj), 47.9, 39.7 (Ck, Co), 34.1, 26.1, 21.4, 20.1 (Cl-n, Cw); ESI-IT MS: m/z (M+H$^+$) 404.27 (C$_{25}$H$_{29}$N$_3$O$_2$ requires 403.23); HPLC-DAD: rt = 17.6 min (% Area = 99.9%).

N-(4-isopropylphenyl)cinnamoylprimaquine (28c).
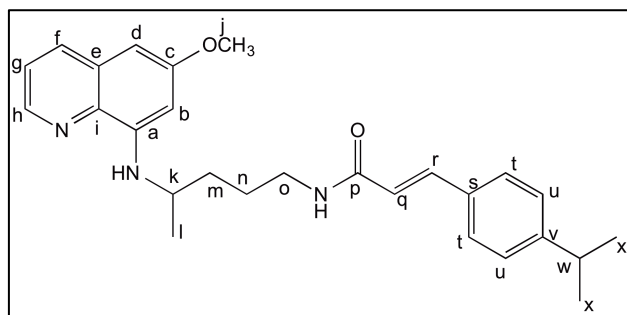
Yellow oil (0.18 g, 78%); R$_F$ (DCM/Me$_2$CO 6:1) 0.49; δ_H (400 MHz, DMSO-d$_6$) 8.53 (dd, J=4.4 Hz, J= 1.6 Hz, 1H, Hh), 7.92 (dd, J= 8 Hz, J= 1.6 Hz, 1H, Hf), 7.56 (d, J= 15.6 Hz, 1H, Hr), 7.37 (d, J= 8 Hz, 2H, Ht), 7.30 (dd, J= 8 Hz, J= 4 Hz, 1H, Hg), 7.19 (d, J= 8 Hz, 2H, Hu), 6.36-6.23 (m, 3H, Hb, Hd, Hq), 6.00 (d, J= 8.4 Hz, 1H, -NH-QN), 5.83 (t, J= 5.2 Hz, 1H, -NH-C=O), 3.86 (s, 3H, Hj), 3.68-3.32 (m, 1H, Hk), 3.45-3.33 (m, 2H, Ho), 2.94-2.86 (m, 1H, Hw), 1.76-1.70 (m, 4H, Hm-n), 1.30 (d, J= 6.4 Hz, 3H, Hl), 1.24 (d, J= 6.8 Hz, 6H, Hx); δ_C (100 MHz, DMSO-d$_6$) 166.1 (Cp), 159.4, 150.7, 144.9, 144.3, 140.7, 135.3, 134.8, 132.5, 129.9, 127.8, 126.8, 121.9, 119.8 (Ca, Cc, Ce-i, Cq-v), 96.9, 91.8 (Cb, Cd), 55.2 (Cj), 47.8, 39.7 (Ck, Co), 34.1, 34.0, 26.3, 23.7, 20.6 (Cl-n, Cw-x); m/z (ESI-IT MS) (M+H$^+$) 432.33 (C$_{22}$H$_{21}$ClN$_4$O$_3$ requires 431.26); HPLC-DAD: rt = 19.00 min (% Area = 99.90).

N-(4-methoxyphenyl)cinnamoylprimaquine (28d).
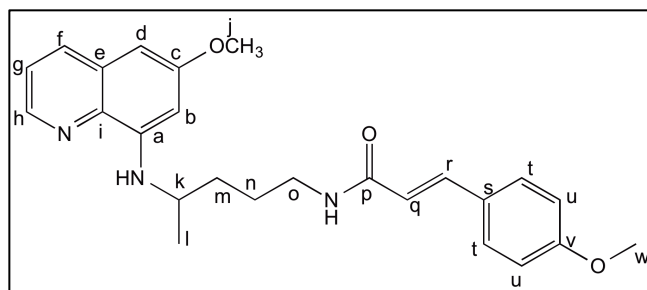
Yellow oil (0.19 g, 79%); R$_F$ (DCM/Me$_2$CO 6:1) 0.49; δ_H (400 MHz, DMSO-d$_6$) 8.53 (dd, J= 4.2 Hz, J= 2 Hz, 1H, Hh), 7.92 (dd, J= 8.4 Hz, J= 2 Hz, 1H, Hf), 7.53 (d, J= 15.6 Hz, 1H, Hr), 7.38 (d, J= 8.8 Hz, 2H, Ht), 7.29 (dd, J= 8 Hz, J= 2 Hz, 1H, Hg), 6.86 (d, J= 8.8 Hz, 2H, Hu), 6.33 (d, J= 2.4 Hz, 1H), 6.29 (d, J= 2.4 Hz, 1H) (Hb, Hd), 6.15 (d, J= 15.2 Hz, 1H, Hq), 6.00 (d, J= 8.4 Hz, 1H, -NH-QN), 5.78 (t, J= 5.6 Hz, 1H, -NH-C=O), 3.86 (s, 3H, Hj), 3.81 (s, 3H, Hw), 3.68-3.60 (m, 1H, Hk), 3.46-3.34 (m, 2H, Ho), 1.79-1.67 (m, 4H, Hm-n), 1.30 (d, J= 6.4 Hz, 3H, Hl); δ_C (100 MHz, DMSO-d$_6$)

166.2 (Cp), 160.7, 159.4, 144.9, 144.3, 140.3, 135.3, 134.8, 129.9, 129.3, 127.6, 121.9, 118.4, 114.1 (Ca, Cc, Ce-i, Cq-v), 96.9, 91.8 (Cb, Cd), 55.3, 55.2 (Cj, Cw), 47.8, 39.6 (Ck, Co), 34.1, 26.3, 20.6 (Cl-n); ESI-IT MS: m/z (M+H$^+$) 420.30 (C$_{25}$H$_{29}$N$_3$O$_3$ requires 419.22); HPLC-DAD: rt = 16.7 min (% Area = 99.9%).

_N_-(3-fluorophenyl)cinnamoylprimaquine (28e).
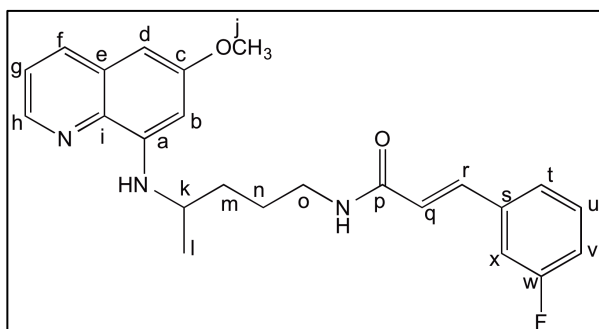
Yellow oil (0.13 g, 60%); R$_F$ (DCM/Me$_2$CO 6:1) 0.49; δ$_H$ (400 MHz, DMSO-d$_6$) 8.53 (dd, J= 4.4 Hz, J= 1.6 Hz, 1H, Hh), 7.93 (dd, J= 8.4 Hz, J= 1.6 Hz, 1H, Hf), 7.51 (d, J= 15.6 Hz, 1H, Hr), 7.34-7.26 (m, 2H, Hx, Hg), 7.18 (d, J= 7.6 Hz, 1H, Ht), 7.11-6.99 (m, 2H, Hu-v), 6.34 (d, J= 2.4 Hz, 1H), 6.30 (d, J= 2.4 Hz, 1H) (Hb, Hd), 6.15 (d, J= 15.6 Hz, 1H, Hq), 6.00 (d, J= 8.4 Hz, 1H, -NH-QN), 5.91 (t, J= 4.8 Hz, 1H, -NH-C=O), 3.85 (s, 3H, Hj), 3.70-3.60 (m, 1H, Hk), 3.45-3.35 (m, 2H, Ho), 1.80-1.68 (m, 4H, Hm-n), 1.29 (d, J= 6.4 Hz, 3H, Hl); δ$_C$ (100 MHz, DMSO-d$_6$) 165.4 (Cp), 164.2, 161.7, 159.4, 144.8, 144.4, 139.4, 137.2, 135.3, 134.9, 130.2, 129.9, 123.9, 122.0, 116.3, 113.7 (Ca, Cc, Ce-i, Cq-x), 97.0, 91.9 (Cb, Cd), 55.2 (Cj), 47.8, 39.8 (Ck, Co), 34.1, 26.1, 20.7 (Cl-n); ESI-IT MS: m/z (M+H$^+$) 408.33 (C$_{24}$H$_{26}$FN$_3$O$_2$ requires 407.20); HPLC-DAD: rt = 17.2 min (% Area = 100%).

_N_-(4-fluorophenyl)cinnamoylprimaquine (28f).
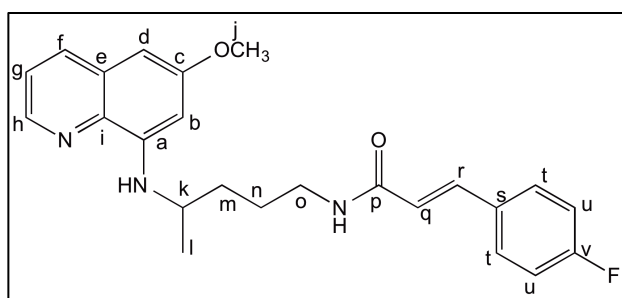
Yellow oil (0.17 g, 77%); R$_F$ (DCM/Me$_2$CO 6:1) 0.49; δ$_H$ (400 MHz, DMSO-d$_6$) 8.53 (dd, J= 4.2 Hz, J= 2Hz, 1H, Hh), 7.92 (dd, J= 8 Hz, J= 1.6 Hz, 1H, Hf), 7.53 (d, J= 15.6 Hz, 1H, Hr), 7.40 (dd, J= 8.6 Hz, J= 5.4 Hz, 2H, Ht), 7.31 (dd, J= 8 Hz, J= 4 Hz, 1H, Hg), 7.02 (t, J= 8.8 Hz, 2H, Hu), 6.34 (d, J= 2.8 Hz, 2H), 6.30 (d, J= 2.4 Hz, 2H) (Hb, Hd), 6.18 (d, J= 15.6 Hz, 1H, Hq), 6.00 (d, J= 8.4 Hz, 1H, -NH-QN), 5.86 (t, J= 5.2 Hz, 1H, -NH-C=O), 3.86 (s, 3H, Hj), 3.68-3.61 (m, 1H, Hk), 3.45-3.32 (m, 2H, Ho), 1.79-1.67 (m, 4H, Hm-n), 1.29 (d, J= 6.4 Hz, 3H, Hl); δ$_C$ (100 MHz, DMSO-d$_6$) 165.7 (Cp), 159.4, 144.9, 144.4, 139.5, 135.3, 134.8, 129.9, 129.5, 129.4, 121.9, 120.5, 115.8, 115.7 (Ca, Cc, Ce-i, Cq-v), 97.0, 91.8 (Cb, Cd), 55.2 (Cj), 47.8, 39.7 (Ck, Co), 34.1, 26.2,

20.6 (Cl-n); ESI-IT MS: m/z (M+H$^+$) 408.33 (C$_{24}$H$_{26}$FN$_3$O$_2$ requires 407.20); HPLC-DAD: rt = 17.1 min (% Area = 100%).

N-(4-chlorophenyl)cinnamoylprimaquine (28g).
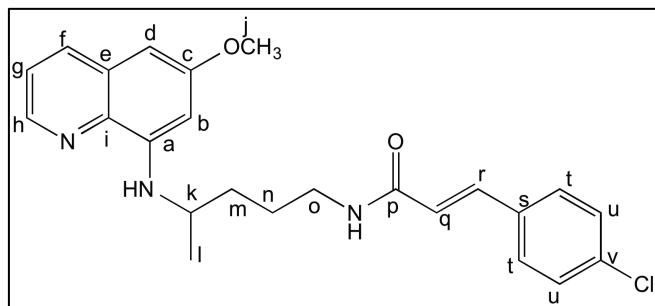
Yellow oil (0.15 g, 59%); R$_F$ (DCM/Me$_2$CO 6:1) 0.49; δ$_H$ (400 MHz, DMSO-d$_6$) 8.53 (dd, J= 4.2 Hz, J= 1.6 Hz, 1H, Hh), 7.92 (dd, J= 8.4 Hz, J= 1.6 Hz, 1H, Hf), 7.50 (d, J= 15.6 Hz, 1H, Hr), 7.35-7.29 (m, 5H, Hg, Ht-u), 6.34 (d, J= 2.8 Hz, 1H, Hd), 6.30 (d, J= 2.4 Hz, 1H, Hb), 6.22 (d, J= 15.6 Hz, 1H, Hq), 5.99 (d, J= 8.4 Hz, 1H, -NH-QN), 5.88 (t, J= 5.2 Hz, 1H, -NH-C=O), 3.86 (s, 3H, Hj), 3.67-3.63 (m,1H, Hk), 3.45-3.35 (m, 2H, Ho), 1.79-1.67 (m, 4H, Hm-n), 1.29 (d, J= 6.4 Hz, 3H, Hl); δ$_C$ (100 MHz, DMSO-d$_6$) 165.6 (Cp), 159.4, 144.9, 144.4, 139.4, 135.3, 135.3, 134.8, 133.4, 129.9, 128.9, 128.9, 121.9, 121.3 (Ca, Cc, Ce-i, Cq-v), 97.0, 91.9 (Cb, Cd), 55.2 (Cj), 47.8, 39.7 (Ck, Co), 34.1, 26.2, 20.7 (Cl-n); ESI-IT MS: m/z (M+H$^+$) 424.33 (C$_{24}$H$_{26}$ClN$_3$O$_2$ requires 423.17); HPLC-DAD: rt = 18.0 min (% Area = 100%).

N-(4-bromophenyl)cinnamoylprimaquine (28h).
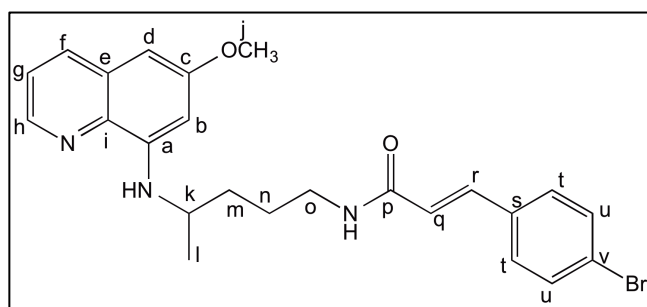
Yellow solid (0.19 g, 73%); mp 110-112°C, R$_F$ (DCM/Me$_2$CO 6:1) 0.49; δ$_H$ (400 MHz, DMSO-d$_6$) 8.53 (dd, J= 4.4, J= 1.6 Hz, 1H, Hh), 7.92 (dd, J= 8.2 Hz, J= 1.2 Hz, 1H, Hf), 7.54-7.43 (m, 3H), 7.34-7.27 (m, 3H, Hg, Hr, Ht-u), 6.34 (d, J= 2.8 Hz, 1H), 6.30 (d, J= 2.4 Hz, 1H) (Hb, Hd), 6.22 (d, J= 15.6 Hz, 1H, Hq), 6.00 (d, J= 8.8 Hz, 1H, -NH-QN), 5.86 (t, J= 4.8 Hz, 1H, -NH-C=O), 3.86 (s, 3H, Hj), 3.67-3.63 (m, 1H, Hk), 3.45-3.35 (m, 2H, Ho), 1.79-1.67 (m, 4H, Hm-n), 1.30 (d, J= 6.4 Hz, 3H, Hl); δ$_C$ (100 MHz, DMSO-d$_6$) 165.5 (Cp), 159.4, 144.9, 144.4, 139.4, 135.3, 134.8, 133.8, 131.9, 129.9, 129.1, 123.6, 121.9, 121.4 (Ca, Cc, Ce-i, Cq-v), 97.0, 91.9 (Cb, Cd), 55.2 (Cj), 47.8, 39.7 (Ck, Co), 34.1, 26.2, 20.7 (Cl-n); ESI-IT MS: m/z (M+H$^+$) 468.37 (C$_{24}$H$_{26}$BrN$_3$O$_2$ requires 467.12); HPLC-DAD: rt = 18.2 min (% Area = 100%).

N-(2-nitrophenyl)cinnamoylprimaquine (28i).
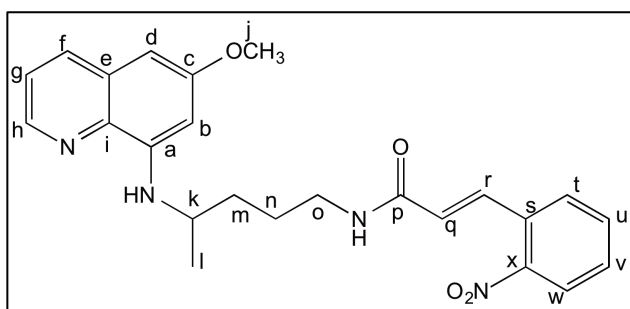
Orange oil (0.18 g, 75%); R_F (DCM/Me$_2$CO 6:1) 0.49; δ_H (400 MHz, DMSO-d$_6$) 8.51 (dd, J= 4.4 Hz, J= 1.6 Hz, 1H, Hh), 7.97 (dd, J= 8 Hz, J= 1.2 Hz, 1H, Hf), 7.92-7.88 (m, 2H, Hr, Hw), 7.59-7.44 (m, 3H, Ht-v), 7.28 (dd, J= 8.4 Hz, J= 4.4 Hz, 1H, Hg), 6.31 (d, J= 2.4 Hz, 1H), 6.29 (J= 2.4 Hz, 1H) (Hb, Hd), 6.20 (d, J= 15.2 Hz, 1H, Hq), 6.07 (t, J= 5.6 Hz, 1H, -NH-C=O), 5.98 (d, J= 8.4 Hz, 1H, -NH-QN), 3.85 (s, 3H, Hj), 3.65-3.61 (m,1H, Hk), 3.45-3.35 (m, 2H, Ho), 1.78-1.66 (m, 4H, Hm-n), 1.29 (d, J= 6.4 Hz, 3H, Hl); δ_C (100 MHz, DMSO-d$_6$) 164.9 (Cp), 159.4, 148.2, 144.8, 144.3, 135.7, 135.3, 134.8, 133.2, 131.1, 129.9, 129.6, 129.1, 126.2, 124.7, 121.9 (Ca, Cc, Ce-i, Cq-x), 96.9, 91.8 (Cb, Cd), 55.2 (Cj), 47.8, 39.8 (Ck, Co), 34.1, 26.1, 20.6 (Cl-n); ESI-IT MS: m/z (M+H$^+$) 435.40 (C$_{24}$H$_{26}$N$_4$O$_4$ requires 434.20); HPLC-DAD: rt = 16.7 min (% Area = 100%).

N-(3-nitrophenyl)cinnamoylprimaquine (28j).
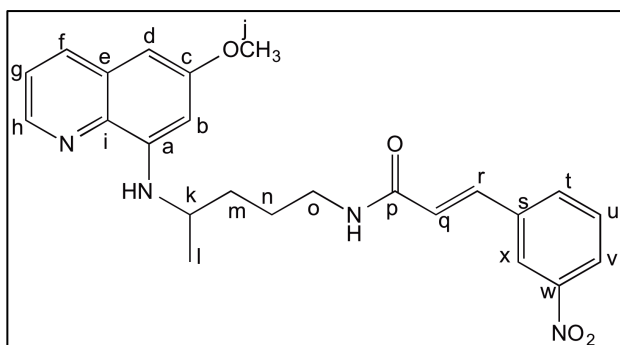
Orange oil (0.16 g, 65%); R_F (DCM/Me$_2$CO 6:1) 0.49; δ_H (400 MHz, DMSO-d$_6$) 8.53 (dd, J= 4.4 Hz, J= 1.6 Hz, 1H, Hh), 8.26 (t, J= 1.8 Hz, 1H, Hx), 8.15 (ddd, J= 8.4 Hz, J= 2.4 Hz, J= 1.2 Hz, 1H, Hv), 7.92 (dd, J= 8 Hz, J= 1.6 Hz, 1H, Hf), 7.68 (d, J= 7.6 Hz, 1H, Ht), 7.58 (d, J= 15.6 Hz, 1H, Hr), 7.50 (t, J= 8 Hz, 1H, Hu), 7.30 (dd, J= 8.4 Hz, J= 4.4 Hz, 1H, Hg), 6.36-6.29 (m, 3H, Hb, Hd, Hq), 6.10-5.99 (m, 2H, -NH-QN, -NH-C=O), 3.84 (s, 3H, Hj), 3.67-3.63 (m, 1H, Hk), 3.47-3.37 (m, 2H, Ho), 1.79-1.67 (m, 4H, Hm-n), 1.29 (d, J= 6.4Hz, 3H, Hl); δ_C (100 MHz, DMSO-d$_6$) 164.9 (Cp), 159.4, 148.5, 144.8, 144.4, 138.0, 136.7, 135.3, 134.9, 134.0, 129.9, 129.8, 123.8, 123.8, 121.9, 121.5 (Ca, Cc, Ce-i, Cq-x), 97.0, 91.9 (Cb, Cd), 55.2 (Cj), 47.8, 39.8 (Ck, Co), 34.1, 26.0, 20.6 (Cl-n); ESI-IT MS: m/z (M+H$^+$) 435.27 (C$_{24}$H$_{26}$N$_4$O$_4$ requires 434.20); HPLC-DAD: rt = 17.1 min (% Area = 99.8%).

N-(4-nitrophenyl)cinnamoylprimaquine (28k).
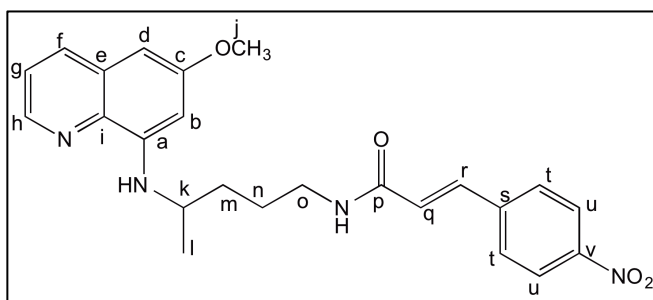
Orange oil (0.17 g, 69%); R_F (DCM/Me$_2$CO 6:1) 0.49; δ_H (400 MHz, DMSO-d$_6$) 8.52 (dd, J= 4.4 Hz, J= 1.6 Hz, 1H, Hh), 8.16 (d, J= 8.8 Hz, 2H, Hu), 7.92 (dd, J= 8.4 Hz, J= 1.6 Hz, 1H, Hf), 7.60-7.49 (m, 3H, Hr, Ht), 7.30 (dd, J= 8 Hz, J= 2 Hz, 1H, Hg), 6.37-6.27 (m, 3H, Hb, Hd, Hq), 6.01 (t, J= 5.6 Hz, 1H, -NH-C=O), 5.98 (d, J= 8.4 Hz, 1H, -NH-QN), 3.85 (s, 3H, Hj), 3.67-3.63 (m, 1H, Hk), 3.45-3.35 (m, 2H, Ho), 1.80-1.68 (m, 4H, Hm-n), 1.29 (d, J= 6.4 Hz, 3H, Hl); δ_C (100 MHz, DMSO-d$_6$) 164.8 (Cp), 159.4, 148.0, 144.8, 144.4, 141.2, 138.0, 135.3, 134.9, 129.9, 128.2, 125.0, 124.0, 122.0 (Ca, Cc, Ce-i, Cq-v), 97.1, 91.9 (Cb, Cd), 55.2 (Cj), 47.9, 39.9 (Ck, Co), 34.2, 26.0, 20.6 (Cl-n); ESI-IT MS: m/z (M+H$^+$) 435.26 (C$_{24}$H$_{26}$N$_4$O$_4$ requires 434.20); HPLC-DAD: rt = 17.1 min (% Area = 100%).

4.5.1.7. Synthesis of acridine derivatives

9-(N-aminobutyl)aminoacridine (30)

10 eq of butane-1,4-diamine (414 mg, 4.7 mmol) and 1 eq of 9-chloroacridine (100 mg, 0.47 mmol) were added in a round bottom flask and put in an oil bath. The temperature was raised to 100°C and let it react for two hours. The reaction mixture was allowed to reach room temperature, and 25 mL of water were added; the desired product **30** was extracted three times with DCM. The organic layer was dried with anhydrous Na$_2$SO$_4$, filtered, and evaporated to yield an orange oil. The resulted oil was analyzed by ESI-IT MS and used without further purification in the synthesis of compound **29**. ESI-IT MS: m/z (M+H$^+$) 266.33 (C$_{17}$H$_{19}$N$_3$ requires 265.16).

4.5.1.7.1. Synthesis of compounds 9-(N-cinnamoylaminobutyl)acridines (29)

The relevant cinnamic acid (1.1 eq), TBTU (1.1 eq), DIEA (2 eq.) and DMF (1 mL) were mixed in a round bottom flask and put under stirring for 20 minutes. Then, a solution of **30** (1 eq) in DMF (1 mL) was added and the reaction allowed to proceed for one day, after which DCM (25 mL) was added to the reaction mixture. The mixture was washed with 5% aqueous Na$_2$CO$_3$ (3×25mL), dried over anhydrous Na$_2$SO$_4$ and evaporated to yield a crude product that was purified by liquid column chromatography on silica using DCM:MeOH (8:2 v/v) as eluent.

9-(*N*-cinnamoylaminobutyl)aminoacridine (29a)
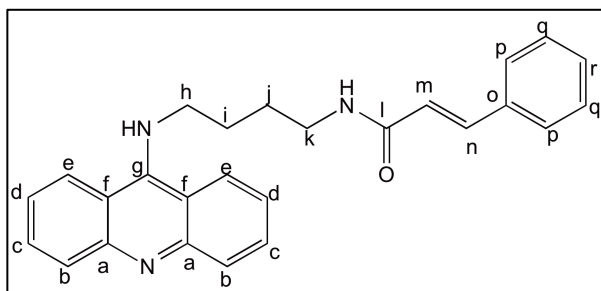
Yellow oil (8 mg, 6%); R_F (DCM/MeOH 8:2) 0.4; δ_H (400 MHz, CDCl$_3$) 8.01 (d, J= 8.4Hz, 2H, He), 7.64-7.53 (m, 4H, Hb, -NH, Hn), 7.50-7.47 (m, 2H, Hp), 7.37-7.26 (m, 6H) (-NH, Hc, Hq-r), 7.00 (t, J= 7.6 Hz, 2H, Hd), 6.64 (d, J= 16 Hz, 1H, Hm), 3.91-3.83 (m, 2H), 3.48-3.45 (m, 2H) (Hh, Hk), 2.05-1.97 (m, 2H), 1.76-1.70 (m, 2H) (Hi-j); δ_C (100 MHz, CDCl$_3$) 166.7 (Cl), 156.1, 140.4, 139.7, 135.0, 133.4, 129.5, 128.7, 127.8, 124.7, 122.7, 121.2, 119.4, 112.0 (Ca-g, Cm-r), 48.4, 38.9 (Ch, Ck), 27.3, 26.6 (Ci-j); ESI-IT MS: m/z (M+H$^+$) 396.40 (C$_{26}$H$_{25}$N$_3$O requires 395.20); HPLC-DAD: rt = 14.12 min; (% Area = 85).

9-[*N*-(*p*-methylcinnamoyl)aminobutyl]aminoacridine (29b)
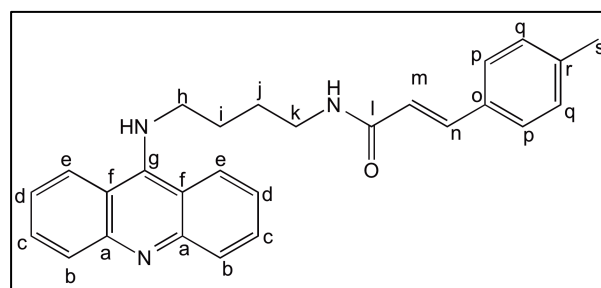
Yellow oil (7 mg, 5%); R_F (DCM/MeOH 8:2) 0.4; δ_H (400 MHz, CDCl$_3$) 8.03 (d, J= 8.4 Hz, 2H, He), 7.61-7.47 (m, 4H, Hb, Hn, -NH), 7.37 (d, J= 8 Hz, 2H, Hp), 7.34-7.27 (m, 2H, Hc), 7.12 (d, J= 8 Hz, 2H, Hq), 7.01 (t, J= 8 Hz, 2H, Hd), 6.58 (d, J= 16 Hz, 1H, Hm), 3.89-3.83 (m, 2H), 3.48-3.45 (m, 2H) (Hh, Hk), 2.33 (s, 3H, Hs), 2.06-1.96 (m, 2H), 1.78-1.71 (m, 2H) (Hi Hj);

δ_C (100 MHz, CDCl$_3$) 166.8 (Cl), 156.0, 140.4, 140.0, 139.7, 133.2, 132.3, 129.5, 127.7, 124.7, 122.6, 120.1, 119.7, 112.1 (Ca-g, Cm-r), 48.4, 38.9 (Ch, Ck), 27.4 (Cs), 26.7, 21.4 (Ci-j); ESI-IT MS: m/z (M+H$^+$) 410.6 (C$_{27}$H$_{27}$N$_3$O requires 409.22); HPLC-DAD: rt = 15.15 min; (% Area = 93).

9-[*N*-(*p*-isopropylcinnamoyl)aminobutyl]aminoacridine (29c)
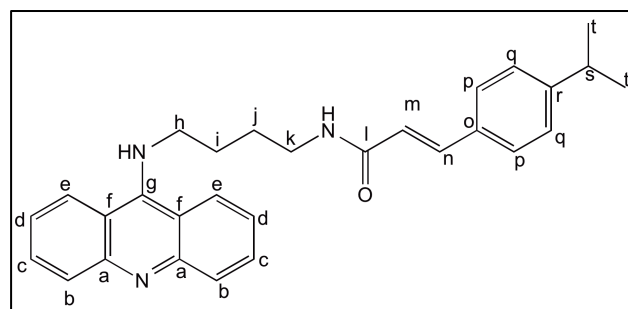
Orange solid (37 mg, 18%); mp = 49-52 °C; R_F (DCM/MeOH 8:2) 0.4; δ_H (400 MHz, CDCl$_3$) 8.04 (d, J= 8.4 Hz, 2H, He), 7.63-7.59 (m, 3H, Hn, Hb), 7.53 (t, J= 5.2 Hz, 1H, -NH), 7.40 (d, J= 8.4 Hz, 2H, Hp), 7.32-7.27 (m, 2H, Hc), 7.17 (d, J= 8 Hz, 2H, Hq), 7.0 (t, J= 7.6 Hz, 2H, Hd), 6.58 (d, J= 16 Hz, 1H, Hm), 3.88-3.83 (m, 2H), 3.48-3.42 (m, 2H) (Hh, Hk), 2.91-2.85 (m, 1H, Hs), 2.05-1.96 (m, 2H), 1.81-1.69 (m, 2H) (Hi-j), 1.22 (d, J= 7.2 Hz, 6H, Ht); δ_C (100 MHz, CDCl$_3$) 178.0 (Cl), 166.8, 155.9, 150.7, 140.5, 133.1,

132.6, 127.8, 126.9, 124.7, 122.6, 120.2, 119.9, 112.2 (Ca-g, Cm-r), 48.4, 38.9 (Ch, Ck), 34.0 (Cs), 27.4, 26.7 (Ci-j), 23.8 (Ct); ESI-IT MS: m/z (M+H$^+$) 438.53 ($C_{29}H_{31}N_3O$ requires 437.25); HPLC-DAD: rt = 17.03 min; (% Area = 98).

9-[*N*-(*p*-methoxycinnamoyl)aminobutyl]aminoacridine (29d)
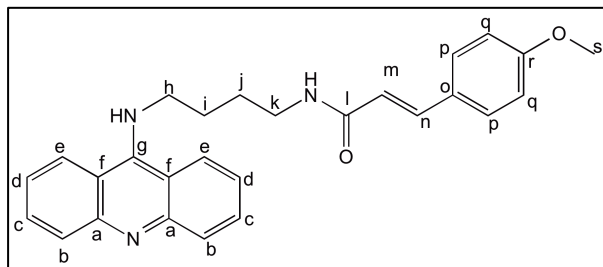
Yellow oil (5 mg, 2%); R_F (DCM/MeOH 8:2) 0.4; δ_H (400 MHz, CDCl$_3$) 8.07 (d, J= 8.4 Hz, 2H, He), 7.92 (d, J= 8.4 Hz, 2H, Hb), 7.62-7.50 (m, 4H, -NH, Hn, Hc), 7.42 (d, J= 8.8 Hz, 2H, Hp), 7.30-7.24 (m, 2H, Hd), 6.87 (d, J= 8.8 Hz, 2H, Hq), 6.31 (d, J= 16 Hz, 2H, Hm, -NH), 3.85 (m, 2H), 3.86-3.81 (s, 3H), 3.49-3.41 (m, 2H) (Hh, Hk, Hs), 1.93.1.83 (m, 2H), 1.78-1.68 (m, 2H) (Hi-j); δ_C (100 MHz, CDCl$_3$) 166.8 (Cl), 160.9, 140.6, 130.8, 129.3, 127.7, 127.5, 125.9, 124.8, 123.8, 123.3, 123.0, 118.3, 114.2 (Ca-g, Cm-r), 55.3 (Cs), 49.9, 39.1 (Ch, Ck), 28.5, 27.1 (Ci-j); ESI-IT MS: m/z (M+H$^+$) 426.47 ($C_{27}H_{27}N_3O_2$ requires 425.21); HPLC-DAD: rt = 14.17 min (% Area = 92).

9-[*N*-(*m*-fluorocinnamoyl)aminobutyl]aminoacridine (29e)
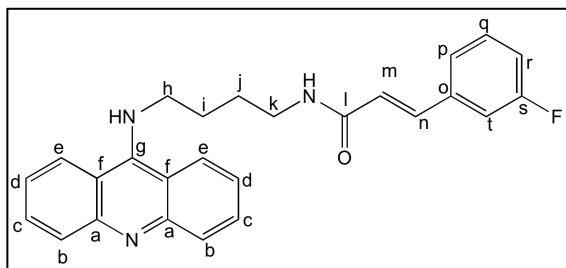
Orange oil (7.4 mg, 3%); RF (DCM/MeOH 8:2) 0.4; δ_H (400 MHz, CDCl$_3$) 8.10 (d, J= 8 Hz, 2H, He), 7.98-7.90 (m, 3H, Hb, Hp), 7.64-7.44 (m, 4H, Hc, Hn, -NH), 7.35-7.22 (m, 3H, Hd, Ht), 7.16 (d, J= 9.6 Hz, 1H, Hr), 7.04-6.97 (m, 1H, Hq), 6.65 (b, 1H, -NH), 6.49 (d, J= 16 Hz, 1H, Hm), 3.91-3.85 (m, 2H), 3.49-3.45 (m, 2H) (Hh, Hk), 1.98-1.88 (m, 2H), 1.80-1.71 (m, 2H) (Hi-j); δ_C (100 MHz, CDCl$_3$) 165.9 (Cl), 164.2, 161.7, 139.6, 137.1, 131.1, 130.5, 130.3, 129.8, 125.9, 123.5, 123.0, 122.2, 116.3, 115.4, 113.8 (Ca-g, Cm-t), 49.8, 39.1 (Ch, Ck), 28.4, 26.9 (Ci-j); ESI-IT MS: m/z (M+H$^+$) 414.40 ($C_{26}H_{24}FN_3O$ requires 413.19); HPLC-DAD: rt = 14.6 min (% area = 88).

9-[*N*-(*p*-fluorocinnamoyl)aminobutyl]aminoacridine (29f)
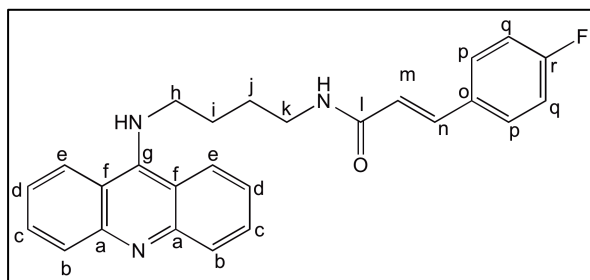
Orange oil (6.8 mg, 3%); R_F (DCM/MeOH 8:2) 0.4; δ_H (400 MHz, CDCl$_3$); 8.08 (d, J= 8.8 Hz, 2H, He), 7.92 (d, J= 8.4 Hz, 2H, Hb), 7.62-7.42 (m, 5H, Hc, Hn, Hp, -NH), 7.31-7.23 (m, 2H, Hd), 7.03 (t, J= 8.4 Hz, 2H, Hq), 6.35 (d, J= 15.6 Hz, 1H, Hm), 6.29 (b, 1H, -NH), 3.90-3.83 (m, 2H), 3.48-3.41 (m, 2H) (Hh, Hk), 1.95-1.85 (m, 2H), 1.78-1.70 (m, 2H) (Hi-j); δ_C (100 MHz, CDCl$_3$) 166.1 (Cl), 139.8, 130.8, 130.6, 129.8, 129.6, 129.5, 126.0, 123.8, 123.3, 123.0, 120.4, 116.0, 115.8 (Cm-r), 49.9, 39.1 (Ch, Ck), 28.5, 27.0 (Ci-j); ESI-IT MS: m/z (M+H$^+$) 414.53 (C$_{26}$H$_{24}$FN$_3$O requires 413.19); HPLC-DAD: rt = 14.4 min (% Area = 90).

9-[*N*-(*m*-nitrocinnamoyl)aminobutyl]aminoacridine (29g)
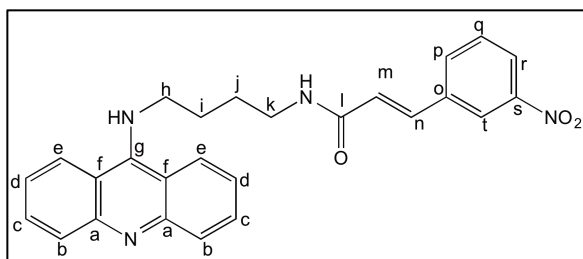
Orange solid (3 mg, 1%); mp=65-70°C; R_F (DCM/MeOH 8:2) 0.4; δ_H (400 MHz, CDCl$_3$) 8.40 (s, 1H, Ht), 8.28-8.24 (m, 1H, Hr), 8.17 (dd, J= 8.4 Hz, 1.6Hz, 1H, Hp), 8.05 (d, J= 8.8 Hz, 2H, He), 7.81-7.75 (m, 1H, Hq), 7.69-7.49 (m, 4H, Hb, Hn, -NH), 7.32 (t, J= 7.6 Hz, 2H, Hc), 7.06 (t, J= 7.6 Hz, 2H, Hd), 6.80 (d, J= 16 Hz, 1H, Hm), 6.79 (b, 1H, -NH), 3.93-3.88 (m, 2H), 3.55-3.49 (m, 2H) (Hh, Hk), 2.11-2.02 (m, 2H), 1.88-1.78 (m, 2H) (Hi-j); δ_C (100 MHz, CDCl$_3$) 165.5 (Cl), 155.5, 148.6, 137.7, 136.9, 134.0, 132.7, 130.7, 129.9, 126.2, 124.4, 123.8, 122.6, 121.7, 120.8, 112.8 (Ca-g, Cm-t), 48.5, 39.1 (Ch, Ck), 27.7, 26.5 (Ci-j); ESI-IT MS: m/z (M+H$^+$) 441.47 (C$_{26}$H$_{24}$N$_4$O$_3$ requires 440.18); HPLC-DAD: rt = 14.4 min; (% Area = 92).

4.5.2. In silico studies

Fukui indices

The local fukui indices were calculated to obtain information regarding the electrophilicity of the carbonyl group of compound **19a**-**19b** using the following equation:

$$f_A^+ = P_A(N+1) - P_A(N)$$

where f_A^+ represents the electrophilicity of atom A in a molecule and P the population of atom A (with N electrons) in a neutral (N) or anionic molecule (N+1). N and N+1 species were obtained from Natural Bond Order population analysis[49] for the optimized structures of the compounds in the gaseous phase. The calculations took into account the hybrid density functional B3LYP[50, 51] approach and the 6-31+G(d) basis set as included in the Gaussian 03 suite.[52]

4.6. References

1. Hocart, S. J.; Liu, H.; Deng, H.; De, D.; Krogstad, F. M.; Krogstad, D. J. 4-aminoquinolines active against chloroquine-resistant Plasmodium falciparum: basis of antiparasite activity and quantitative structure-activity relationship analyses. *Antimicrob Agents Ch* **2011,** 55, 2233-44.

2. ChemAxon. MarvinSketch 5.2.2. http://www.chemaxon.com. **2009**.

3. Siek, T. J. Effective use of organic solvents to remove drugs from biologic specimens. *Clin Toxicol* **1978,** 13, 205-30.

4. Mineva, T.; Parvanov, V.; Petrov, I.; Neshev, N.; Russo, N. Fukui Indices from Perturbed Kohn−Sham Orbitals and Regional Softness from Mayer Atomic Valences. *J Phys Chem A* **2001,** 105, 1959-1967.

5. Lavrado, J.; Gani, K.; Nobre, P. A.; Santos, S. A.; Figueiredo, P.; Lopes, D.; Rosário, V.; Gut, J.; Rosenthal, P. J.; Moreira, R.; Paulo, A. Bis-alkylamine quindolone derivatives as new antimalarial leads. *Bioorg Med Chem Lett* **2010,** 20, 5634-7.

6. Charton, M. Steric effects. I. Esterification and acid-catalyzed hydrolysis of esters. *J Am Chem Soc* **1975,** 97, 1552-1556.

7. Lipinski, C. A.; Lombardo, F.; Dominy, B. W.; Feeney, P. J. Experimental and computational approaches to estimate solubility and permeability in drug discovery and development settings. *Adv Drug Deliv Rev* **2001,** 46, 3-26.

8. Veber, D. F.; Johnson, S. R.; Cheng, H. Y.; Smith, B. R.; Ward, K. W.; Kopple, K. D. Molecular properties that influence the oral bioavailability of drug candidates. *J Med Chem* **2002,** 45, 2615-23.

9. Oprea, T. I.; Davis, A. M.; Teague, S. J.; Leeson, P. D. Is There a Difference between Leads and Drugs? A Historical Perspective. *J Chem Inf Comp Sci* **2001,** 41, 1308-1315.

10. Shenai, B. R.; Lee, B. J.; Alvarez-Hernandez, A.; Chong, P. Y.; Emal, C. D.; Neitz, R. J.; Roush, W. R.; Rosenthal, P. J. Structure-Activity Relationships for Inhibition of Cysteine Protease Activity and Development of Plasmodium falciparum by Peptidyl Vinyl Sulfones. *Antimicrob Agents Ch* **2003,** 47, 154-160.

11. Vippagunta, S. R.; Dorn, A.; Matile, H.; Bhattacharjee, A. K.; Karle, J. M.; Ellis, W. Y.; Ridley, R. G.; Vennerstrom, J. L. Structural Specificity of Chloroquine−Hematin Binding Related to Inhibition of Hematin Polymerization and Parasite Growth. *J Med Chem* **1999,** 42, 4630-4639.

12.   Portela, C.; Afonso, C. M. M.; Pinto, M. M. M.; João Ramos, M. Definition of an electronic profile of compounds with inhibitory activity against hematin aggregation in malaria parasite. *Bioorg Med Chem* **2004,** 12, 3313-3321.

13.   Lisk, G.; Kang, M.; Cohn, J. V.; Desai, S. A. Specific inhibition of the plasmodial surface anion channel by dantrolene. *Eukaryot Cell* **2006,** 5, 1882-93.

14.   Lisk, G.; Pain, M.; Sellers, M.; Gurnev, P. A.; Pillai, A. D.; Bezrukov, S. M.; Desai, S. A. Altered plasmodial surface anion channel activity and in vitro resistance to permeating antimalarial compounds. *BBA-Biomembranes* **2010,** 1798, 1679-1688.

15.   Kirk, K. Membrane transport in the malaria-infected erythrocyte. *Physiol Rev* **2001,** 81, 495-537.

16.   Kanaani, J.; Ginsburg, H. Effects of cinnamic acid derivatives on in vitro growth of Plasmodium falciparum and on the permeability of the membrane of malaria-infected erythrocytes. *Antimicrob Agents Ch* **1992,** 36, 1102-1108.

17.   Kirk, K.; Horner, H. A. In search of a selective inhibitor of the induced transport of small solutes in Plasmodium falciparum-infected erythrocytes: effects of arylaminobenzoates. *Biochem J* **1995,** 311, 761-0.

18.   Ginsburg, H.; Krugliak, M.; Eidelman, O.; Ioav Cabantchik, Z. New permeability pathways induced in membranes of Plasmodium falciparum infected erythrocytes. *Mol Biochem Parasitol* **1983,** 8, 177-190.

19.   Pillai, A. D.; Pain, M.; Solomon, T.; Bokhari, A. A.; Desai, S. A. A cell-based high-throughput screen validates the plasmodial surface anion channel as an antimalarial target. *Mol Pharmacol* **2010,** 77, 724-33.

20.   Naughton, J. A.; Nasizadeh, S.; Bell, A. Downstream effects of haemoglobinase inhibition in Plasmodium falciparum-infected erythrocytes. *Mol Biochem Parasitol* **2010,** 173, 81-7.

21.   McGowan, S.; Oellig, C. A.; Birru, W. A.; Caradoc-Davies, T. T.; Stack, C. M.; Lowther, J.; Skinner-Adams, T.; Mucha, A.; Kafarski, P.; Grembecka, J.; Trenholme, K. R.; Buckle, A. M.; Gardiner, D. L.; Dalton, J. P.; Whisstock, J. C. Structure of the Plasmodium falciparum M17 aminopeptidase and significance for the design of drugs targeting the neutral exopeptidases. *P Natl Acad Sci USA* **2010**.

22.   Deprez-Poulain R.; Flipo M.; Piveteau C.; Leroux F.; Dassonneville S.; Florent I.; Maes L.; Cos P.; Deprez B. Structure–Activity Relationships and Blood Distribution of Antiplasmodial Aminopeptidase-1 Inhibitors. *J Med Chem* **2012**, *55*, 10909-17.

23. Martin, R. E.; Butterworth, A. S.; Gardiner, D. L.; Kirk, K.; McCarthy, J. S.; Skinner-Adams, T. S. Saquinavir inhibits the malaria parasite's chloroquine resistance transporter. *Antimicrob Agents Ch* **2012,** 56, 2283-9.

24. Sidhu, A. B.; Verdier-Pinard, D.; Fidock, D. A. Chloroquine resistance in Plasmodium falciparum malaria parasites conferred by pfcrt mutations. *Science* **2002,** 298, 210-3.

25. Kelly, J. X.; Smilkstein, M. J.; Brun, R.; Wittlin, S.; Cooper, R. A.; Lane, K. D.; Janowsky, A.; Johnson, R. A.; Dodean, R. A.; Winter, R.; Hinrichs, D. J.; Riscoe, M. K. Discovery of dual function acridones as a new antimalarial chemotype. *Nature* **2009,** 459, 270-3.

26. Lavrado, J.; Cabal, G. G.; Prudêncio, M.; Mota, M. M.; Gut, J.; Rosenthal, P. J.; Diaz, C.; Guedes, R. C.; dos Santos, D. J.; Bichenkova, E.; Douglas, K. T.; Moreira, R.; Paulo, A. Incorporation of basic side chains into cryptolepine scaffold: structure-antimalarial activity relationships and mechanistic studies. *J Med Chem* **2011,** 54, 734-50.

27. Prudêncio, M.; Derbyshire, E. T.; Marques, C. A.; Krishna, S.; Mota, M. M.; Staines, H. M. Plasmodium berghei-infection induces volume-regulated anion channel-like activity in human hepatoma cells. *Cell Microbiol* **2009,** 11, 1492-501.

28. Matos, J.; da Cruz, F. P.; Cabrita, E.; Gut, J.; Nogueira, F.; do Rosário, V. E.; Moreira, R.; Rosenthal, P. J.; Prudêncio, M.; Gomes, P. Novel potent metallocenes against liver stage malaria. *Antimicrob Agents Ch* **2012,** 56, 1564-70.

29. Derbyshire, E. R.; Mota, M. M.; Clardy, J. The Next Opportunity in Anti-Malaria Drug Discovery: The Liver Stage. *PLoS Pathog* **2011,** 7, e1002178.

30. Remmer, H. The role of the liver in drug metabolism. *Am J Med* **1970,** 49, 617-629.

31. Schonborn, J. L. The role of the liver in drug metabolism. *Anaesthesia Tutorial of the Week* **2010**.

32. Vale, N.; Prudêncio, M.; Marques, C. A.; Collins, M. S.; Gut, J.; Nogueira, F.; Matos, J.; Rosenthal, P. J.; Cushion, M. T.; do Rosário, V. E.; Mota, M. M.; Moreira, R.; Gomes, P. Imidazoquines as antimalarial and antipneumocystis agents. *J Med Chem* **2009,** 52, 7800-7.

33. Dorn, A.; Vippagunta, S. R.; Matile, H.; Jaquet, C.; Vennerstrom, J. L.; Ridley, R. G. An Assessment of Drug-Haematin Binding as a Mechanism for Inhibition of Haematin Polymerisation by Quinoline Antimalarials. *Biochem Pharmacol* **1998,** 55, 727-736.

34. Parapini, S.; Basilico, N.; Pasini, E.; Egan, T. J.; Olliaro, P.; Taramelli, D.; Monti, D. Standardization of the physicochemical parameters to assess in vitro the beta-hematin inhibitory activity of antimalarial drugs. *Exp Parasitol* **2000,** 96, 249-56.

35. Valdes, A. F. Acridine and acridinones: old and new structures with antimalarial activity. *Open Med Chem J* **2011,** 5, 11-20.

36. Guetzoyan, L.; Yu, X. M.; Ramiandrasoa, F.; Pethe, S.; Rogier, C.; Pradines, B.; Cresteil, T.; Perree-Fauvet, M.; Mahy, J. P. Antimalarial acridines: synthesis, in vitro activity against P. falciparum and interaction with hematin. *Bioorg Med Chem* **2009,** 17, 8032-9.

37. Watson, D. A.; Su, M.; Teverovskiy, G.; Zhang, Y.; García-Fortanet, J.; Kinzel, T.; Buchwald, S. L. Formation of ArF from LPdAr(F): Catalytic Conversion of Aryl Triflates to Aryl Fluorides. *Science* **2009,** 325, 1661-1664.

38. Hotez, P. J.; Molyneux, D. H.; Fenwick, A.; Kumaresan, J.; Sachs, S. E.; Sachs, J. D.; Savioli, L. Control of Neglected Tropical Diseases. *New Engl J Med* **2007,** 357, 1018-1027.

39. Fernandes Rodrigues, J. C.; Concepcion, J. L.; Rodrigues, C.; Caldera, A.; Urbina, J. A.; de Souza, W. In vitro activities of ER-119884 and E5700, two potent squalene synthase inhibitors, against Leishmania amazonensis: antiproliferative, biochemical, and ultrastructural effects. *Antimicrob Agents Ch* **2008,** 52, 4098-4114.

40. Marrapu, V. K.; Mittal, M.; Shivahare, R.; Gupta, S.; Bhandari, K. Synthesis and evaluation of new furanyl and thiophenyl azoles as antileishmanial agents. *Eur J Med Chem* **2011,** 46, 1694-1700.

41. National Institute of Allergy and Infectious Diseases (NIAID). http://www.niaid.nih.gov/topics/leishmaniasis/pages/lifecycle.aspx. .

42. Vieira, N. C.; Herrenknecht, C.; Vacus, J.; Fournet, A.; Bories, C.; Figadère, B.; Espindola, L. S.; Loiseau, P. M. Selection of the most promising 2-substituted quinoline as antileishmanial candidate for clinical trials. *Biomed Pharmacother* **2008,** 62, 684-689.

43. Sundar, S.; Sinha, P. K.; Dixon, S. A.; Buckley, R.; Miller, A. K.; Mohamed, K.; Al-Banna, M. Pharmacokinetics of oral sitamaquine taken with or without food and safety and efficacy for treatment of visceral leishmaniais: a randomized study in Bihar, India. *Am J Trop Med Hyg* **2011,** 84, 892-900.

44. Carvalho, L.; Luque-Ortega, J. R.; Manzano, J. I.; Castanys, S.; Rivas, L.; Gamarro, F. Tafenoquine, an antiplasmodial 8-aminoquinoline, targets

leishmania respiratory complex III and induces apoptosis. *Antimicrob Agents Ch* **2010,** 54, 5344-51.

45. Vale-Costa, S.; Vale, N.; Matos, J.; Tom·s, A.; Moreira, R.; Gomes, P.; Gomes, M. S. Peptidomimetic and organometallic derivatives of primaquine active against Leishmania infantum. *Antimicrob Agents Ch* **2012,** 56, 5774-5781.

46. Pomel, S.; Biot, C.; Bories, C.; Loiseau, P. M. Antiprotozoal activity of ferroquine. *Parasitol Res* **2013,** 112, 665-669.

47. Castanys-Muñoz, E.; Pérez-Victoria, J. M.; Gamarro, F.; Castanys, S. Characterization of an ABCG-like transporter from the protozoan parasite Leishmania with a role in drug resistance and transbilayer lipid movement. *Antimicrob Agents Ch* **2008,** 52, 3573-3579.

48. Nwaka, S.; Ramirez, B.; Brun, R.; Maes, L.; Douglas, F.; Ridley, R. Advancing Drug Innovation for Neglected Diseases Criteria for Lead Progression. *PLoS Neglect Trop D* **2009,** 3.

49. Alan, E. R.; Robert, B. W. f. f.; Frank, W. Natural population analysis@f@f. *J Chem Phys* **1985**.

50. Becke, A. D. Density-functional thermochemistry. III. The role of exact exchange. *J Chem Phys* **1993,** 98, 5648-5652.

51. Stephens, P. J.; Devlin, F. J.; Chabalowski, C. F.; Frisch, M. J. Ab Initio Calculation of Vibrational Absorption and Circular Dichroism Spectra Using Density Functional Force Fields. *J Phys Chem* **1994,** 98, 11623-11627.

52. M.J.T. Frisch, G. W. T., H.B. Schlegel, G.E. Scuseria, M.A. Robb, J.R. Cheeseman, J.A. Montgomery Jr., T. Vreven, K.N. Kudin, J.C. Burant, J.M. Millam, S.S. Iyengar, J. Tomasi, V. Barone, B. Mennucci, M. Cossi, G. Scalmani, N. Rega, G.A. Petersson, H. Nakatsuji, M. Hada, M. Ehara, K. Toyota, R. Fukuda, J. Hasegawa, M. Ishida, T. Nakajima, Y. Honda, O. Kitao, H. Nakai, M. Klene, X. Li, J.E. Knox, H.P. Hratchian, J.B. Cross, C. Adamo, J. Jaramillo, R. Gomperts, R.E. Stratmann, O. Yazyev,; A.J. Austin, R. C., C. Pomelli, J.W. Ochterski, P.Y. Ayala, K. Morokuma, G.A. Voth, P. Salvador, J.J. Dannenberg, V.G. Zakrzewski, S. Dapprich, A.D. Daniels, M.C. Strain, O. Farkas, D.K. Malick, A.D. Rabuck, K. Raghavachari, J.B. Foresman, J.V. Ortiz, Q. Cui, A.G. Baboul, S. Clifford, J. Cioslowski, B.B. Stefanov, G. Liu, A. Liashenko, P. Piskorz, I. Komaromi, R.L. Martin, D.J. Fox, T. Keith, M.A. Al-Laham, C.Y. Peng, A. Nanayakkara, M. Challacombe, P.M.W. Gill, B. Johnson, W. Chen, M.W. Wong, C. Gonzalez, J.A. Pople, Gaussian 03, Gaussian, Inc., Pittsburgh PA, 2003.

Chapter 5

Looking beyond malaria chemotherapy

Understanding vaccine-induced antibody responses against malaria

5.0. Preamble

Malaria chemotherapy control strategy relies on the use of safe and highly effective drugs to impair the parasite development.[1] Chemotherapy combined with other strategies such as a preventive vaccination could be a sustainable way to fight against malaria. A malaria vaccine should protect not only semi-immune adults but also pregnant women and children.[2] The latter two groups are the most susceptible to die from the disease. In one hand, in infants, the predominance of parasitemia significantly increases at 20 weeks of age.[3] Children usually start to be more susceptible to fever and severe malaria when they become 6 months old although the risk of presenting clinical malaria is also dependent on the transmission level.[4] On the other hand, pregnant women are especially susceptible to malaria, because *Pf*-infected erythrocytes adhere to the placenta.[5]

Nowadays, there is not a licensed vaccine that prevents against malaria.[6] Most vaccine candidates target a single stage of the malaria life cycle and the most efficacious vaccines have demonstrated to be those which target the pre-erythrocytic stage of the malaria parasite. One example of a pre-erythrocytic vaccine constitute RTS,S, formulated as a recombinant protein in an adjuvant, which has shown partial efficacy in human trials.[7] Still a malaria pre-erythrocytic vaccine should be 100% effective since the escape of one liver stage form will lead to a thousand of merozoites.[6, 8] However, the inadequate understanding of the mechanism of action of RTS,S has hindered its subsequent efficacy improvement. In addition, the development of a more efficacious vaccine has mainly been impaired by the parasite complexity, the failure to completely understand naturally acquired immunity (NAI) to malaria parasites, and the poor understanding of the antigenic targets to induce protective immunity.[3, 7, 9]

In this context, a three and a half month study was carried out to contribute to the understanding of the immune response to *Pf* in RTS,S-vaccinated children and the effect of the intensity of exposure on IgG levels, thus providing input in the development of future attempts to improve vaccine efficacy against malaria. The antibody (Ab) responses were measured by Luminex assays, which permit the detection of IgG responses against multiple antigenic targets. The corresponding experimental procedure was carried out at the Barcelona Centre for International Health Research (CRESIB) under the direction of Dr. Carlota Dobaño and the laboratory supervision of Joseph J. Campo, who also performed the statistical analysis of the data obtained.

5.1. Protective immunity to Malaria

NAI has been observed to be i) effective in adults continuously and heavily exposed to the parasite, ii) species-specific, since protection against one parasite species does not confer protection against others, but not necessarily strain-specific since strain-transcendent immunity can be acquired after few infections, and iii) acquired at a rate dependent upon the degree of exposure.[3] Acquired immunity may be active, a result of the immune response of the host due to previous exposure to the parasite, or passive, by the transfer of prenatal or postnatal protective immune factors (e.g. antibodies) to the child.[3] Acquired, or adaptive, immunity against *Plasmodium* can be generally classified in i) anti-disease immunity: decrease the risk of death associated to a given parasite density, ii) anti-parasite immunity: influences the density of parasites circulating in the body, and iii) premunition: the absence of symptomatic malaria but low burden of parasitemia. For instance, most semi-immune adults reside across sub-Saharan Africa without experiencing the disease, but with a parasite density in their blood that could prove fatal in a person who has never been exposed to the parasite. This last immunity takes longer to develop and it might be of shorter duration.[3] However, other studies in transmigrants have shown adults to acquire clinical immunity rather quickly.[10] This incomplete immunity is a consequence of *Pf*'s ability to avoid protective immune effects while coexisting with the human host. The slow development of this type of immunity is mostly due to the parasite's ability to evade the host's immune response by antigenic polymorphism.[3] Thus, to be superior to this slowly gained exposure-dependent NAI, a vaccine is needed to insure long lasting protection.

Pre-erythrocytic immunity has been achieved by the infection of volunteers with irradiated sporozoites. These attenuated sporozoites are capable of liver cell invasion but can not complete hepatocyte development or progression to the blood stage.[11, 12] Although immunization by irradiated sporozoites has been proved to be safe and last for at least 42 weeks, it requires a minimum of 1000 bites of irradiated mosquitoes in order to induce sterile immunity in human,[13] a type of immunity that exists after the malaria parasite has disappeared from the host. Moreover, the efficacy of this methodology was lower compared to the one achieved in rodent models.[14] Pre-erythrocytic immunity can also be generated by inoculating intact sporozoites while treating with CQ, a drug known to impair erythrocytic parasite development but that has no effect on the pre-erythrocytic stage of the malaria life cycle, as explained in previous chapters of this dissertation.[15] This model was recently tested in volunteers who have not been previously exposed to malaria.[16] The study proved to induce immunity in humans by presenting the host immune system with a broader range of pre-erythrocytic as well as erythrocytic

antigens.[16] Strategies for human immunization with whole *Pf* parasites (attenuated or with CQ veil) are presently being actively pursued by many research groups.[17]

Antigens generated by recombinant or synthetic peptide chemistry have been other methodology used to develop a malaria vaccine. However, these efforts have been hindered by the difficulty to identify the target antigens and a specific immune response which protects against malaria.[18] For instance, the brevity of Ab response and the heterogeneity of exposure to malaria are two factors which can hinder individual immune responses against malaria related to protection[18] and, consequently, make difficult the discovery of antigens which could be used towards the development of vaccines. High Ab levels are usually associated with high transmission and Abs tend to be higher in those individuals who present parasitemia than those who do not. These types of responses are generally observed in children contrary to adults whose Ab responses are higher and take more time to wane even in the absence of infection.

Longitudinal studies where Ab responses drop rapidly over time suggest that Ab response to specific antigens might be short-lived.[19] For instance, studies done by Kinyanjui and co-workers demonstrated the brevity of IgG responses to merozoite antigens such as EBA-175 (Erythrocyte binding antigen 175), MSP-1 (Merozoite surface protein), and AMA-1 (Apical Membrane Antigen 1) in children from Kenya who were recovering from malaria over a period of 12 weeks.[19] Accordingly, the majority of the Ab responses reached a high peak and then dropped rapidly to low levels in less than eight weeks. However, Kinyanjui et al were unable to explain whether this short-lived response was characteristic to the antigen and they observed that re-infection seemed to not significantly improve the Ab responses. Therefore, it becomes necessary to take into account the longevity of the Ab response and transmission heterogeneity for the design of serological studies and selection of antigens to develop a vaccine that induces specific Ab responses against malaria. In addition, in a study by Greenhouse et al, Ab responses were measured against AMA-1, MSP1- and 3 and the results showed that stronger immune responses to these antigens were not associated with blood stage protection when taking into account prior exposure. Therefore, when analyzing mechanisms of protective immune response, the study design should integrate information regarding prior exposure, and ideally assess multiple immune responses.[20]

Up today, numerous antigens have been identified as potential candidates for the development of a malaria vaccine. For instance, a malaria vaccine based on the AMA-1 antigen has shown to be well-tolerated and induce high and sustained Ab levels in children exposed to malaria.[21] Other antigens which have shown to be potential candidates for a malaria vaccine include CelTOS (Cell-traversal protein for ookinetes and sporozoites),[22] EBA-175,[23] LSA-1 (Liver stage antigen-1),[24] and VAR2CSA DBL

(Duffy binding-like)[25] and SSP2 (Second sporozoite surface protein).[26] However, today the most studied and developed candidate is the CSP (Circumsporozoite surface protein).

5.2. RTS,S malaria vaccine candidate

RTS,S, the most clinically advanced malarial vaccine candidate in the world, contains a portion of the CSP.[27] The role of CSP in the development of immunity against sporozoites has been described.[28] CSP is the most prominent protein in the surface of sporozoites and is involved in the liver stage invasion of the *Pf* parasite. CSP promotes binding to liver cells, and it is vital for the sporozoite development in the mosquito.[29] Epitopes of CSP are found to react with Abs that inhibit hepatocytic cell invasion and also promote an immune response that eliminates the sporozoites from inside liver cells. The CSP antigen contains a major B cell epitope composed of repeat amino acid sequences Asn-Ala-Asn-Pro (NANP) and Asn-Val-Asp-Pro (NVDP), and CD4+ and CD8+ T cell epitopes at the C-terminal end (Fig. 52).[30]
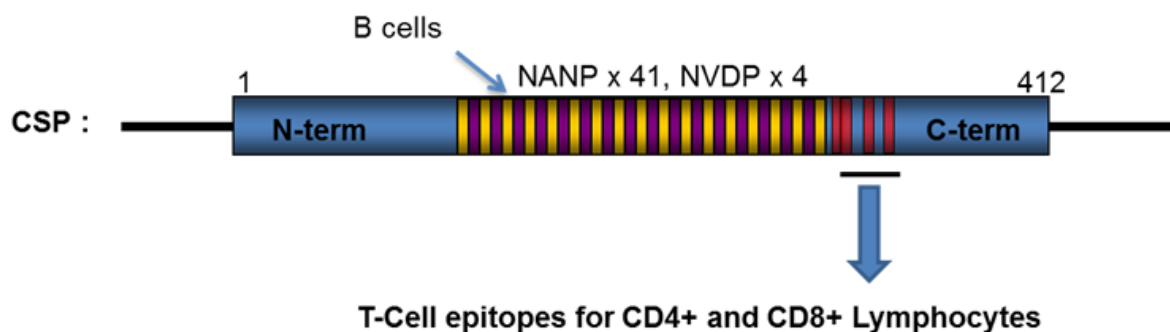
Figure 52. CSP including its major B cell epitope, CD4+ and CD8+ T cell epitopes at the C-terminal end.

In the RTS,S vaccine, the central repeat and C-terminal portion of the *Pf* CSP "R" and major "T" cell epitopes were combined with the hepatitis B virus surface antigen "S". Subsequently, these fused proteins were auto-assembled as a virus-like particle which also includes non-combined "S."[31] RTS,S does not seem to induce strain-specific immune responses.[32] In addition, CSP itself is poorly immunogenic and therefore, an adjuvant needs to be incorporated in the vaccine formulation in order to promote the immune response.

In early clinical trials of RTS,S in adults, the adjuvant which displayed the best results was AS02[33] which consists of an oil-in-water emulsion combined with two

immunostimulants, monophosphoryl Lipid A (MPL), and *Quillaja saponaria* fraction 21 known as QS21, with mercury based reagents (thymerosal) used as preservatives. RTS,S/AS02 demonstrated to be safe, immunogenic, and partially protective in naïve U.S. volunteers and semi-immune adults living in malaria endemic regions,[34] which required two to three standard 50 μg doses for best efficacy.[35] Although thyromerosal has proven to be safe, concerns regarding potential neurotoxicity led to its removal from AS02 resulting in the new adjuvant AS02A, an oil-in-water emulsion containing the same immune stimulants MPL and QS21 but using lactose instead as cryopreservant.[27]

In a Phase I trial, RTS,S/AS02A was evaluated for safety and immunogenicity at three different doses: 10 μg (10 μg RTS,S in 0.1 mL AS02A), 25 μg (25 μg RTS,S in 0.25 mL AS02A) and finally a 50 μg (50 μg RTS,S in 0.5 mL AS02A).[36] One hundred and thirty five children were enrolled in this study. Based on the results obtained, the 10 μg dose displayed lower anti-CSP Ab response than the 50 μg and 25 μg doses. In addition, it was demonstrated that the higher the concentration, the lower the safety of the vaccine. Accordingly, the 25 μg dose was selected for posterior studies in the pediatric population.

In a Phase IIb trial in Mozambique, children between 1-4 years old were divided in two cohorts: cohort 1 (C1) included 1,605 children from Manhiça who were followed by passive case detection (PCD), and cohort 2 (C2) constituted by 407 children from Ilha Josina followed during the first 6 months post vaccination (M8.5) by active case detection and subsequently by PCD.[37] More than 92% of the children followed the entire protocol receiving all three doses. The results of this trial suggested that RTS,S/AS02A was safe and well tolerated, and that malaria transmission was higher in C2 than in C1. In addition, the anti-CSP Ab response increased after the third dose, but dropped to a quarter of the initial values after six months (M8.5) from the last vaccination, but still remaining above baseline values. In C1 RTS,S/AS02A conferred protection of 29.9% (95% confidence interval (CI), 11.0%–44.8%; *P* = 0.004) against the first clinical episode and 57.7% (95% CI, 16.2%–80.6%; *P* = 0.019) against severe malaria. In C2, vaccine efficacy was 45% (95%), 31.4%–55.9%; *P* = 0.001) against infection.[37]

An extended follow-up showed that C1 continued to present anti-CSP Ab units 50% higher than in the control vaccine group at month 21 (M21).[38] The prevalence of asexual *Pf* parasitemia in C2 was similar in the control vaccine group, in contrast with C1, where the prevalence of parasitemia was 29% lower than in the control vaccine group. However, C2 differs from C1, because C2 was drug-treated to clear parasitemia after the final dose, and children from C2 were given treatment if a new infection was detected from month 2.5 to M8.5. The latter could account for C2 interrupted exposure to the

malaria parasite, and consequently, affecting the development of NAI. The efficacy for the extended follow-up period from the third dose to M21 was 35.3% (95% CI, 21.6%–48.6%; P = 0.001) against clinical malaria and 48.6% (95% CI, 12.3%–71.0%; P= 0.02) against severe malaria.

Subsequently, the efficacy of the vaccine was evaluated at month 45 (M45).[39] A limitation of the clinical trials is the difficulty to estimate the efficacy of a vaccine over time against malaria, when immunity is age and exposure dependent. From the 2,022 children, a total of 1,465 completed the follow-up to study month 45. The prevalence of parasitemia was lower in RTS,S/AS02A vaccinated children and vaccine efficacy over the entire follow-up was 30.5% (95% CI, 18.9%–40.4%) against clinical malaria and 38.3% (95% CI, 3.4%–61.3%) against severe malaria.[39]

In the Phase IIb trial, the difference in naturally acquired Ab responses between children vaccinated with RTS,S and control has been evaluated at M8.5 in C1 and C2;[40] the time when waning efficacy was observed in C2 but not C1. Campo et al. hypothesized that since C1 children were exposed to low burden of blood stage parasitemia because they were not actively followed and treated, a higher difference of immune response against erythrocytic stage antigens between RTS,S and control group should be observed in C1 compared to C2 at M8.5. However, at month M8.5 there was not a difference between groups against all the antigens tested in this study in children ≥ 2 years old (AMA-1-3D7, AMA-1-FVO, MSP-1_{42}-3D7, MSP-1_{42}-FVO, EBA-175) suggesting neither enhancement nor impairment of acquired immune response against these antigens. Results were unable to explain the waning efficacy in one cohort and not the other. Recent finding suggests that waning efficacy in C2 might be due to the fact that higher transmission regions presented the lowest RTS,S efficacy.[41] Nonetheless, further longitudinal studies against blood stage malaria antigens might help to understand whether RTS,S vaccination might facilitate a more effective blood stage immune response, consequently, generating a long lasting protection against clinical malaria.

Recently, RTS,S/AS01 is being evaluated in a Phase III trial. In this trial, 15,460 children were enrolled in two age categories: i) 6,537 infants between 6 to 12 week of age and ii) 8,923 children between 5 to 17 months of age. Preliminary results during 12 months of follow-up in the first 6,000 children between 5 to 17 months of age who received the three RTS,S/AS01 doses demonstrated that the vaccine has an efficacy of 55.8% and 47.3% against clinical and severe malaria, respectively.[42] In this trial, further results,[7] using as primary end point clinical malaria, suggests that the efficacy reported was lower for infants from 6 to 12 week of age than that previously found for children of 5-17 months of age. WHO will review the results of the RTS,S/AS01 vaccine in 2015 and

make a policy recommendation depending on the complete data obtained in Phase III trial by 2014.[43]

Up to now, it has been demonstrated that anti-CSP IgG response correlate with protection against *Pf* infection[44] but not consistently with clinical[40] or severe malaria. Vaccinated children are still partially protected against clinical and severe malaria after 43 months of follow-up (with stable efficacy) in some studies[37-39] but not in others.[45] Also, it is known that strong acquired immunity against CSP is not naturally developed. However, the interaction between RTS,S vaccination and the development of naturally acquired immunity to malaria at different ages and under different transmission intensities remains to be established.

5.3. Aim and Scope

This work aimed to determine naturally acquired IgG Ab acquisition against seven *Pf* antigens in RTS,S-vaccinated and control-vaccinated children at seven different time points over a period of 60 months post-vaccination. For this study, 401 among 1,605 children from Manhiça, Mozambique, who had completed the entire follow-up period (5 years), were randomly selected from C1. Specifically, the study aims to:

i.   Estimate the rate of Ab acquisition in the RTS,S and control groups.

ii.   Describe the Ab kinetics after parasite exposure.

iii.   Describe the influence of age and transmission co-variates in the Ab responses.

The antigens selected for this longitudinal study are well characterized and known to have important roles in parasite invasion and development in the human host. These antigens are being developed as potential vaccine candidates. The antigens are the following:

i.   <u>AMA-1</u> (3D7 and FVO), the polymorphic form expressed in merozoites which is involved in erythrocyte invasion.[46]

ii.   <u>MSP-1$_{42}$</u> (3D7 and FVO), the major merozoite surface protein which binds to erythrocyte and has a role in its invasion.[47]

iii.   <u>EBA-175</u>, promotes *Pf* binding to erythrocytes.[48]

iv.   <u>DBL-alpha</u>, involved in the formation of rosettes, or healthy erythrocytes surrounding infected erythrocytes.[49]

v.   <u>SSP2</u>, presents in the surface of the sporozoite.[50]

vi.   <u>LSA-1</u>, accumulates in the parasitophorous vacuole of infected hepatocytes around the merozoites.[51]

vii.   <u>CelTOS</u>, mediates malaria invasion into the host.[52]

viii.   BSA (bovine serum albumin), a non-*Pf* malaria antigen used as negative control in this study.

Children were divided into two age groups: < 2 years old and ≥ 2 years old since these two groups received different control vaccines. Older children received three doses of hepatitis B vaccine (Engerix; GSK) and younger children received 7-valent pneumococcal conjugate vaccine (Prevenar;Wyeth LederleVaccines) in the first and third vaccination, and in the second vaccination they were administered *Haemophilus influenzae* type B vaccine (Hiberix; GSK Biologicals). The seven different times points included for this study were pre-vaccine (D0), month 3 (M3), M8.5, M21, M33, M45, and M63, resulting in a total number of 2,807 samples analyzed by Luminex.

5.4. Results and Discussion

There were only 821 children out of the 1,605 from cohort 1 who had completed the 60 months of follow-up. Therefore, to test whether a bias was introduced by randomly selecting 401 samples from the 821 children instead of making a random selection from the 1,605 of entire cohort, the baseline levels of Ab responses against the malaria parasite of the 401 children, were measured by immunofluorescence antibody test (IFAT), and analyzed at D0, pre-vaccination (Fig. 53). Accordingly, if there were bias in the sample selection, a significant difference ($p < 0.05$) will be observed between the Ab responses of RTS,S and control group at D0 meaning imbalance between the Ab responses among groups before vaccination. However, such a difference was not observed concluding that bias was not introduced in the sample selection.
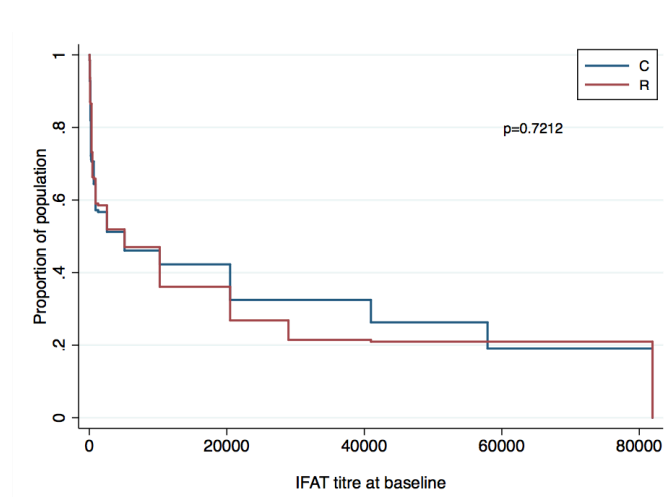
Figure 53. IFAT titre at baseline for RTS,S (R) and control (C) groups.

The non-bias of the selection permitted further analysis of the samples by Luminex. Luminex was used for the study because it reduces labor and cost compared to ELISA assays.[53] Luminex is a fluorescence-based assay using a flow cytometer, which allows the quantification of Ab responses against up to 100 proteins in one assay-plate. Since the microspheres, also known as beads, are coded with a fluorescent signature, it is possible to use a multiple suspension array technology (SAT) to distinguish Ab responses to multiple antigens at once.

The multiplex SAT used included the 9 pre-erythrocytic and erythrocytic antigens and the BSA as a negative control. Initially, the beads were coupled to the respective antigens using EDC (1-Ethyl-3-(3-dimethylaminopropyl)carbodiimide) and Sulfo-NHS (N-hydroxysulfosuccinimide) as coupling reagents (Scheme 16). Sulfo-NHS is a water soluble reagent which allows to run the reaction at physiological conditions and significantly increases the efficacy of amide bond formation/or coupling reaction since it generates a very amine-reactive intermediate which is stable and hydrolyzed relatively slowly in water.[54] In contrast, EDC alone fails to quickly react, permitting the hydrolysis of the corresponding ester intermediate resulting isourea and the inactivation of EDC, and consequently, obtainment of the original carboxylic acid, in this case, the uncoupled bead.
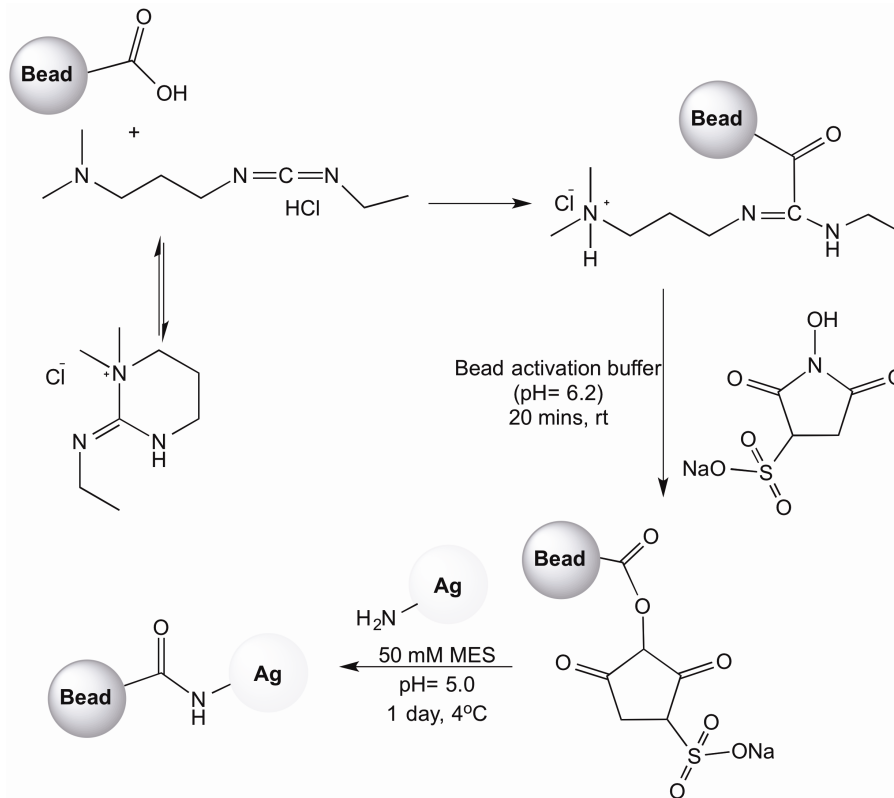
Scheme 16. Microspheres coupling.

The Luminex assay was designed to include in each plate the following: i) all time points (M0, M3, M8.5, M21, M33, M45, M63) on the same plate for a child; ii) duplicate readings; iii) 2 dilutions of serum or plasma samples (1:500 and 1:20000); iv) positive-hyperimmune control plasma (adults who were exposed to the parasite and present a high Ab response) in two 2 dilutions (1:500 and 1:15000); and v) negative European adult control plasma samples. All samples were analyzed following the same protocol previously published,[40] where the microspheres were initially incubated with the test plasma to allow the interaction of the IgG with the different antigens in the multiplex SAT, followed by an anti-IgG Ab conjugated to biotin. Finally, a streptavidin-conjugated fluorocrome (R-phycoerythrin) was incubated with the bead-antigen-Ab complexes to permit the detection and quantification of fluorescence intensity when read in the Luminex (Fig. 54).
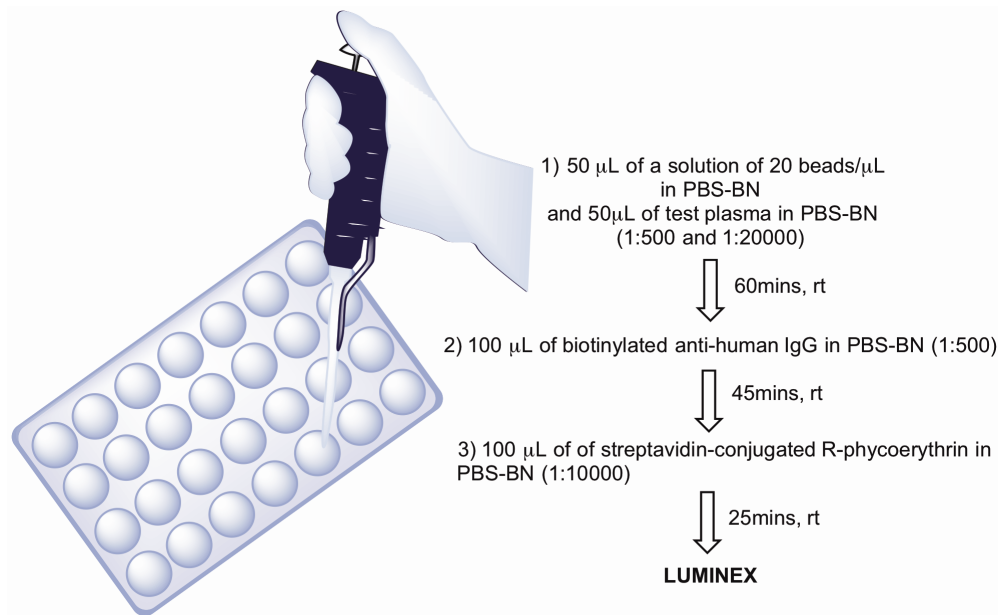
Figure 54. Luminex assays to evaluate the IgG response of each selected child. PBS-BN: 1% BSA/0.05% sodium azide in PBS.

A total of 138 Luminex assays were run, 4 of which were repeats, to analyze the 401 children from C1 and each of the corresponding 7 time points of this longitudinal study. Accordingly, there were only four plates from the entire study whose positive control did not follow the same trends as the Ab response of positive-hyperimmune controls from the rest of the assays, since the Ab responses were lower. Those plates were repeated and the new results did follow the desired pattern of Ab response as seen in fig. 55; the results of the old 4 plates were discarded. Accordingly, the MFI (median fluorescence intensity) results for each sample were normalized using the positive hyperimmune control responses as a reference curve for MFI values. To do this, MFI for each analyte at each concentration were fit to expected concentrations using a 4-parameter logistic regression, as specified:

$$y = A + \frac{D - A}{(1 + (^x/_C)^B)}$$

where *A* and *D* are the maximum and minimum asymptotes of the sigmoidal curve, respectively, *C* is the concentration at point of inflection, and *B* is the slope at point *C*. Using the fit of the positive controls in each plate, MFI values for test samples were interpolated and expressed as arbitrary units per mL. For each sample analyzed, there were two dilutions. Those MFI results that were too high or low and fell out of the range of the positive hyperimmune response were assigned a fixed value correspondingly

above or below the asymptotes. Those values where the duplicates resulted in a CV (coefficient of variation) greater than 30% were omitted from analysis.
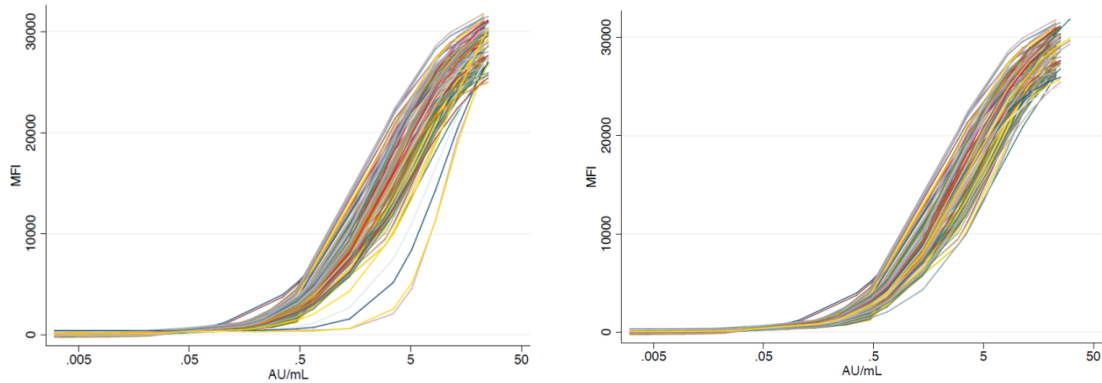
Figure 55. Ab responses of positive hyperimmune controls: In the left are all initial assays Ab responses. In the right corner are the results once the four assays were repeated.

Evaluation of the Ab units or MFI over time for RTS,S and control group allowed the validation of the study since it demonstrated:

i) Both groups, RTS,S and control, presented low non-specific Ab response against the antigen BSA (Fig. 56) and these responses were not significantly different from one another. These Ab responses + 2 standard deviations (SD) were used as a threshold for seropositivity in this study (a child is considered seropositive if he/she presents Ab units over the threshold established using anti-BSA Ab units).
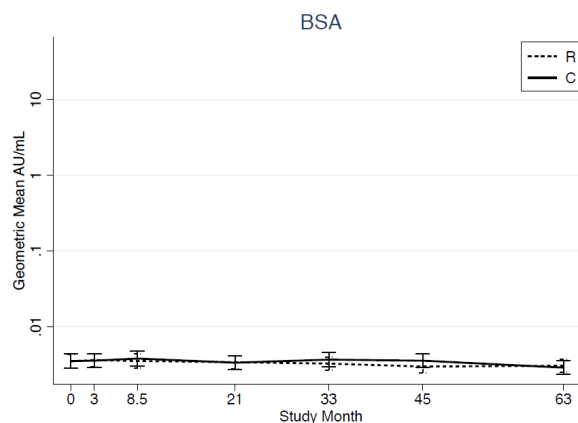
Figure 56. Geometric mean of anti-BSA Ab units of both control (C) and RTS,S (R) group.

ii) Older children (≥ 2 years) presented higher level of Ab units than younger children as observed in the Ab breadth over time. Ab breadth is a score calculated by the sum of

seropositive antibody responses at the individual level (Fig. 57). These results are in agreement with previously reported data.[40]
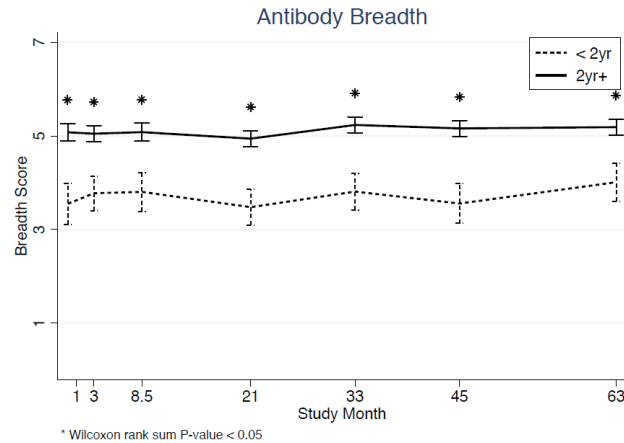
Figure 57. Ab breadth representation by age.

iii) Cross-strain recognition was evaluated by plotting Ab responses against 3D7 versus Ab responses against FVO for AMA-1 and MSP-1$_{42}$, correspondingly. Correlation of the Ab responses between strains was assessed using Pearson's correlation coefficient (ρ), where values of ρ between 0.5 and 1 are considered strong correlation (the closer the ρ value is to one, the stronger the correlation). Accordingly, ρ values obtained of 0.945 for AMA-1 and of 0.835 for MSP-1$_{42}$ show strong correlation between the anti-AMA-1 or anti-MSP-1$_{42}$ Ab response against the 3D7 and FVO strains. Therefore, high level of Ab units were observed against antigen AMA-1 and MSP-1$_{42}$ regardless of the strain tested (3D7 and FVO) demonstrating high level of cross-strain recognition which is in agreement with previously reported data (Fig. 58).[40]
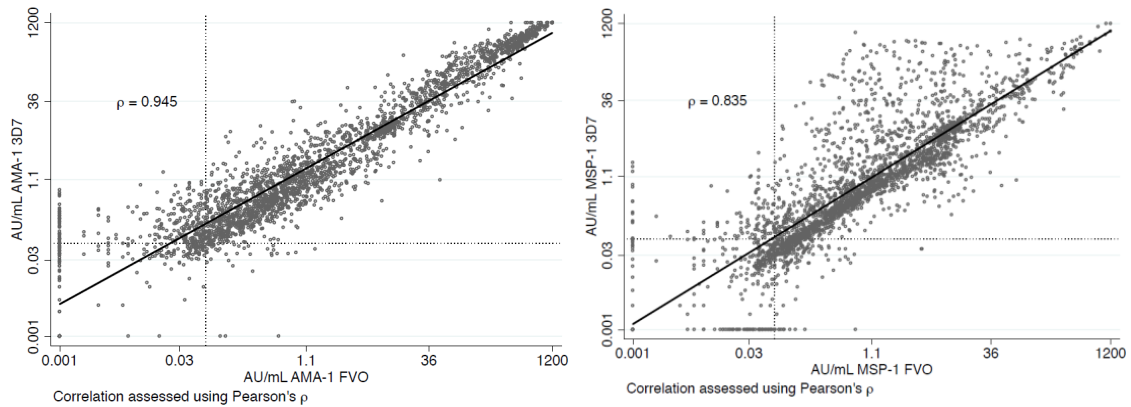
Figure 58. Anti-AMA-1 (left) and anti-MSP-142 (Right) Ab responses against both strains 3D7 in the "Y" axis and FVO in the "X" axis, respectively. Dash lines defines the anti-BSA Ab units + 2SD.

Analysis of the Ab units over time of all results together (Control and RTS,S group responses) by geographical area, high Ab units were identified as possible markers of areas with higher malaria exposure as observed in the Ab response against AMA-1 3D7 and the prevalence of parasitemia (% of children with infection) by region (Fig. 59). Accordingly, regions 1, 4, 7, 9, 14, 15, and 21, 23, and 24 (See map of Manhiça, Mozambique divided by region in Appendix F) represent areas of high malaria transmission intensity. This finding might help to monitor trends of the prevalence of malaria in certain regions and, consequently, help in the obtainment of information regarding the effectiveness of malaria control programs in those areas. Also, these results confirm previous findings[20, 55] that immunoepidemiology studies need to take into account prior exposure in order to better understand mechanism of immune protection.

Geoarea	M8.5	M21	M33	M45	M63
1	0.27	0.36	0.55	0.41	0.59
2	0.05	0.05	0.11	0.05	0.05
3	0.08	0.00	0.04	0.08	0.08
4	0.33	0.33	0.44	0.30	0.30
5	0.05	0.05	0.05	0.00	0.05
6	0.02	0.04	0.08	0.04	0.08
7	0.15	0.24	0.22	0.22	0.20
9	0.27	0.18	0.27	0.45	0.27
14	0.25	0.50	0.25	0.25	0.38
15	0.17	0.09	0.17	0.09	0.13
16	0.06	0.00	0.11	0.06	0.06
17	0.00	0.00	0.00	0.04	0.00
19	0.00	0.04	0.04	0.04	0.00
21	0.00	0.25	0.25	0.00	0.25
22	0.33	0.00	0.00	0.00	0.00
23	0.22	0.33	0.44	0.56	0.44
24	0.41	0.34	0.36	0.30	0.14
25	0.13	0.00	0.00	0.00	0.00
27	0.00	0.00	0.11	0.11	0.00

Parasitemia

Geoarea	M8.5	M21	M33	M45	M63
1	156.4	107.8	249.5	161.6	169.2
2	29.3	8.4	34.7	10.4	72.9
3	22.5	14.0	49.4	51.8	67.1
4	89.6	125.9	226.7	197.6	139.4
5	8.9	1.7	2.6	24.8	60.0
6	8.9	8.8	17.0	5.2	70.5
7	69.8	79.7	95.9	108.1	48.7
9	202.5	194.7	296.5	258.7	148.3
14	330.2	327.6	331.9	334.9	262.3
15	66.7	60.0	95.7	81.0	71.7
16	60.1	6.4	69.1	11.6	2.6
17	3.3	1.6	1.7	0.9	24.3
19	9.8	2.1	69.2	2.5	1.1
21	77.2	178.2	175.1	157.7	292.9
22	117.3	15.3	15.9	7.5	2.4
23	232.4	193.9	295.1	267.6	183.8
24	329.3	244.7	229.4	221.9	141.0
25	0.3	0.4	0.5	0.2	136.6
27	18.7	5.9	5.1	9.1	6.2

AMA-1 3D7

Figure 59. Parasitemia, shown as proportion of children with *Pf* infection (left), and anti-AMA-1 3D7 Ab units (right). The red color indicated the highest prevalence or Ab responses and the yellow the lowest.

5.4.1. Difference between RTS,S and control group

The *Pf* parasitemia was examined in both groups (Control and RTS,S) from pre-vaccination to M63 after vaccination. Data suggest that there is no difference between these two groups at M63 which may imply that the efficacy of RTS,S vaccine completely disappears after 5 years of the follow-up (Fig. 60). Although the anti-CSP Ab response for the 401 samples at M63 was not measured, these data was available for a subset of children from the entire cohort. Correspondingly, it could be estimated that at M63 Ab levels seemed to continue to drop over time, although the sample size at M63 (n= 220) might be too small to draw definite conclusions (Fig. 60).
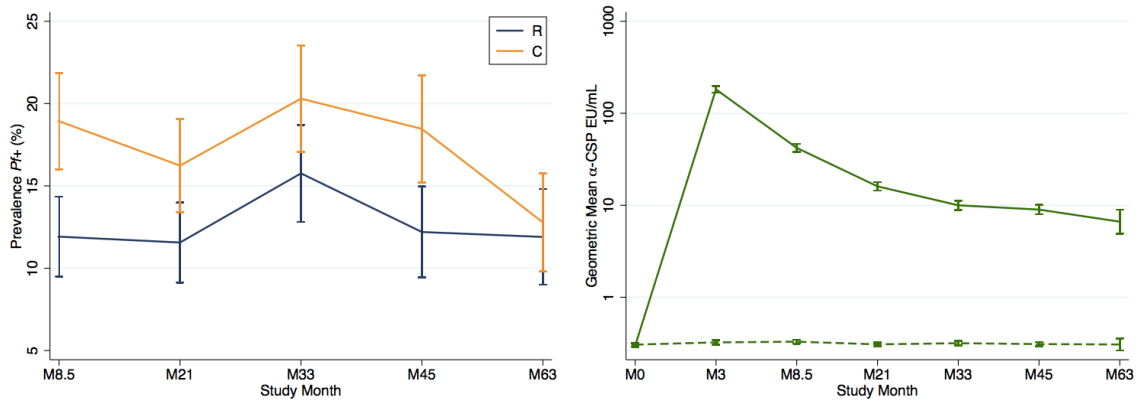
Figure 60. RTS,S (R) and control (C) groups difference in terms of parasitemia (left) and anti-CSP Ab response (right).

Furthermore, the difference between the RTS,S and control groups was examined using a reverse cumulative distribution of Ab units (See results summarized in table 19). In this type of graphic, the proportion of children in each group who presented Ab units at a given level are plotted *versus* Ab units. The difference previously observed in the Ab response of older and younger children should not impact the results of this analysis because age groups were equally divided between RTS,S and Control vaccinated children. Kolmogorov-Smirnov equality-of-distributions test, used to evaluate whether the distribution across the two groups of data set is the same, was used to compare distributions of Ab units between RTS,S and control group, and only *P*-values below 0.05 representing a significant difference between groups are shown in Table 19. Accordingly, it was found that the control group seemed to present higher Ab response than the RTS,S group for tested antigens (except for AMA-1 FVO) at months 8.5, and/or 21, and/or 33, and/or 45.

Table 19. Statistically significant difference found (*p* values lower than 0.05).

Antigen	Month	*P* values		
		RandC (all)	RandC (<2 years)	RandC (≥2 years)
AMA-1 3D7	33	0.0249	0.0226	0.4757
AMA-1 FVO	NO[a]			
CelTOS	8.5	0.01	0.4196	0.0801
	33	0.0617	0.8617	0.0418
DBL-alpha	45	0.0086	0.1064	0.1069
EBA-175	8.5	0.0068	0.6393	0.0147
LSA-1	33	0.047	0.5142	0.0212
MSP-1$_{42}$ 3D7	21	0.0277	0.9904	0.0323
	33	0.0015	0.0126	0.0219
	45	0.0372	0.2094	0.0777
MSP-1$_{42}$ FVO	8.5	0.0016	0.4119	0.014
	21	0.0243	0.77	0.0163
	33	0.0336	0.1841	0.0761
SPP2	63	0.3406	0.0399	0.9327

NO: No difference was observed for antigen AMA1-FVO at any time point. *P* values were estimated using Kolmogorov-Smirnov equality-of-distributions test.

By examining the Ab responses stratified by age in the RTS,S and control groups, the difference becomes less obvious and in some cases it disappears. The latter can be observed in the Ab responses against CelTOS at M8.5, DBL-alpha at M45, MSP-1$_{42}$ 3D7 at M45, MSP-1$_{42}$ FVO at M33. These results could be explained by the fact that the total sample size including both age groups has higher statistical power than the sample sizes of each age group, separately. Ab response with group-wise differences in the younger children but not in the total cohort could be explained by the fact that the sample size of children ≥ 2 year-old (n=311) is bigger than the < 2 year-old children (n=90). Therefore, it could be inferred that older children should have more impact in the outcomes of the analysis (anti-SSP2 Ab responses at M63). Results reflecting differences in RTS,S and control groups as a whole and in age group <2 year-old, such as Ab responses against AMA-1 at M33, independent of strain, are mostly related to the <2 year-old age group. In contrast, data which shows difference between RTS,S and control vaccinated children as a whole and in group age >2 year-old, such as Ab responses against EBA-175 at M8.5

and LSA-1 at M33, are exclusively associated to children ≥ 2 year-old. These findings suggest: i) differences in Ab responses between RTS,S and control groups from month 8.5 on, and ii) Ab responses to studied antigens are age-dependent.

Ab kinetics after malaria exposure

To estimate the time since last exposure to malaria at each study visit, the PCD follow-up to identify cases occurring before sampling was used. The pattern of Ab levels against time since last exposure to the malaria parasite was evaluated using lowess regression, which produced a "smooth" set of predictions for Ab units at small windows (bandwidth) of time (since exposure). These graphics represent the Ab responses of children measured in one of the studied time points against a specific antigen *vs* the number of days between a scheduled visit (M3, M8.5, M21, M33, M45) and the last malaria episode or parasitemia reported before that visit (See fig. 61). Children who were parasitemic at time of sample collection were given a value of 0 for time since last documented exposure and M63 was not included in this study due to a break in follow-up for clinical malaria. As observed, in general, children show a high peak of Ab responses against all antigens immediately after a malaria case or parasitemia, especially for AMA-1 and MSP-1. This high Ab response drops rapidly over time after a malaria event, largely disappearing within a 90-days range. After about 180 days had passed from the last malaria episode or parasitemia, Ab units continued to decrease, but at a lower rate compared to the beginning. In addition, examining the other Ab responses against the other antigens from this study, it is possible to notice that most Ab responses stay close to the seropositivity threshold.
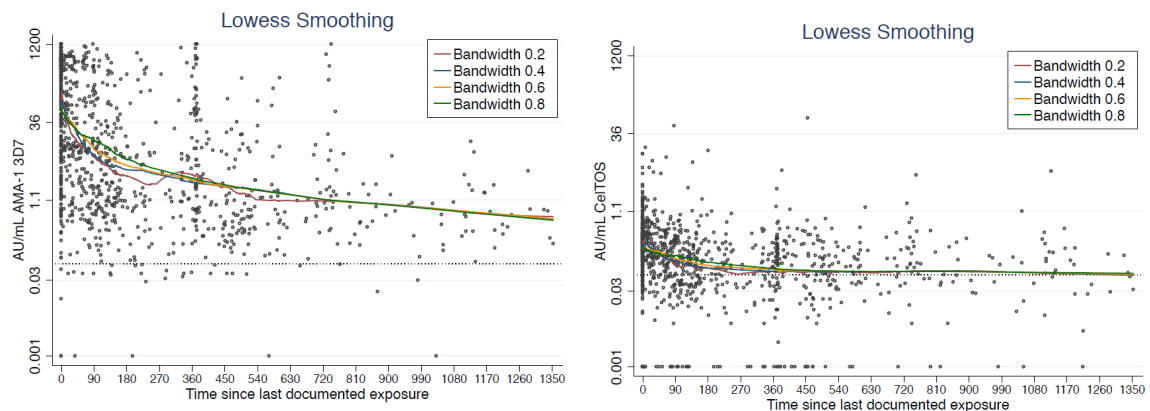
Figure 61. Anti-AMA-1 Ab response (3D7 and FVO) versus time since last exposure (in days) to a malaria episode or parasitemia by lowess smoothing analysis. Dot line represents the seropositivity threshold.

In addition, when analyzing Ab units over time (in days) until month 43 of the follow-up after the third vaccine dose (M45), there seems to be no difference between RTS,S and control, as observed in Fig. 62 where the blue and the dark-red dots representing the control and RTS,S group, respectively, are equally distributed through time.
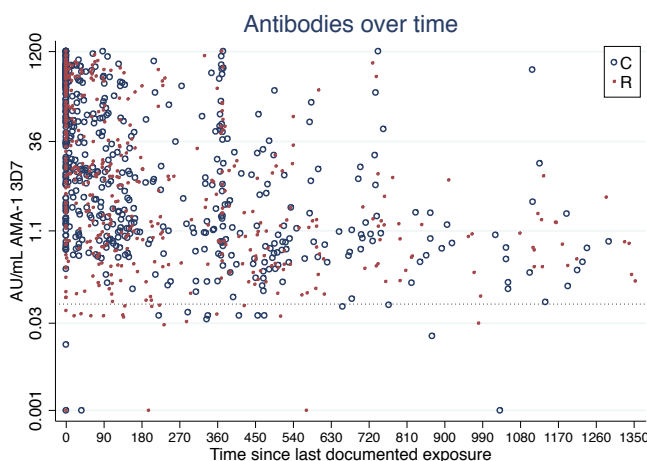
Figure 62. Anti-AMA-1 and anti-MSP-1 ab responses, respectively, vs time since last exposure (in days). Control (C) and RTS,S (R) group.

Qualitative analysis

Further qualitative analyses were carried and different patterns at the individual level were identified. In this analysis, M63 was not considered also due to a break in follow-up for clinical malaria. After M33, some children who have previously presented a malaria episode later present only parasitemia and high Ab response, but no symptomatic malaria, regardless of age and of being from the control or RTS,S group, suggesting a level of clinical immunity and maintenance of immune response (ID 347 and 1654 in the lattice plot shown below, fig. 63). These children were generally from higher transmission regions previously identified (Regions 1,4, 9, 15, 21, 23, 24). Other children did not present any Ab responses or malaria episodes during the entire follow up, as in the case of subject 1,604, likely due to lack of exposure, which could be justified by the fact that Manhiça started with a moderate transmission rate that dropped over time. In addition, a small group of children who presented intermediate Ab responses, but one or no malaria episodes during the entire follow up, as in subject 928, could indicate low/non-detected parasitemia exposure but protection from disease, and/or possible control of parasitemia at subpatent levels. Furthermore, some children such as subject 1,371 presented with only Ab units against SSP2, which could represent false positives or parasites that never made it to the liver. Finally, some other children, probably immune to the disease,

presented high Ab units after one malaria episode at the beginning of the follow up but no parasitemia or malaria clinical thereafter (ID 318). These data highlight the heterogeneity of malaria exposure in Manhiça, Mozambique.
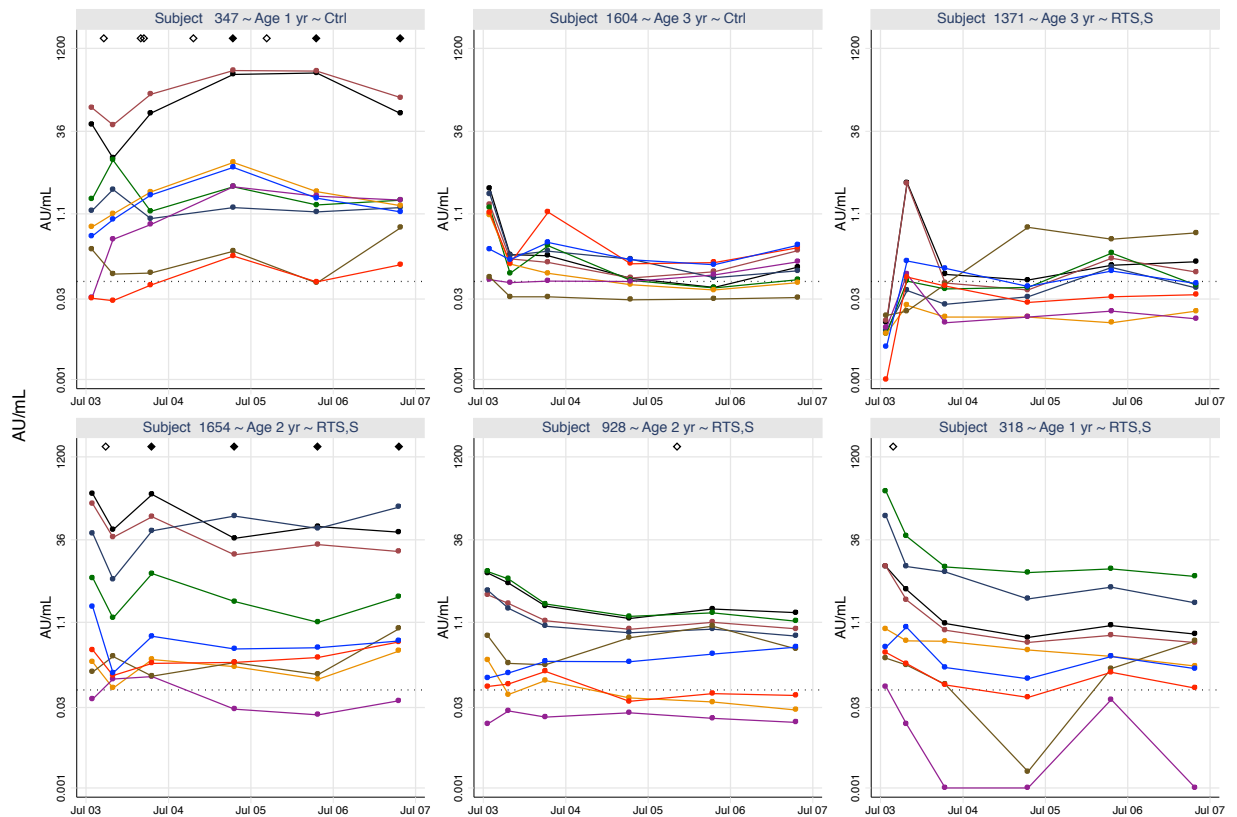
Figure 63. Lattice plot of individuals' antibody levels over time. Each subplot represents a randomly selected individual. The title box contains the subject ID for this study, his/her age in years, and which vaccination group the individual belongs to (RTS,S or Control). The Ab response against specific antigens is represented in colored lines: AMA-1 3D7, black; AMA-1 FVO, maroon; MSP-1$_{42}$ 3D7, navy; MSP-1$_{42}$ FVO, green; EBA-175, orange; LSA-1, purple; SSP2, olive; CelTOS, red; DBL-alpha, blue. Each point represents a cross-sectional survey sampling. White diamonds represent documented clinical episodes of malaria, and black diamonds represent parasitemia at cross-sectional timepoints. The x-axis scale is in days, ranging from 1st June 2003 to 1st June 2007 which includes time points from D0 to M45.

5.5. Experimental Section

5.5.1. Recombinant proteins

Recombinant proteins were either bought or previously produced in a research center:

- BSA: bought from Sigma Aldrich (Tres Cantos, Spain);
- AMA-1 3D7: produced at International Centre for Genetic Engineering and Biotechnology, New Delhi, India (ICGEB);
- AMA-1 FVO: produced at U.S. Military Malaria Vaccine Program, Walter Reed Army Institute of Research, Silver Spring, Maryland, U.S.A. (WRAIR);
- MSP-1$_{42}$ 3D7 and FVO: produced at WRAIR;
- EBA-175 and DBL-alpha: produced at ICGEB;
- SSP2, LSA-1, and CelTOS: produced at Protein Potential, LLC, Rockville, Maryland, U.S.A..

5.5.2. Microsphere Coupling

Microsphere coupling was carried out by a methodology previously described.[40] Briefly, a SAT panel was prepared to detect the IgG response to a total of 9 pre-erythrocytic and erythrocytic *Pf* antigens and the negative control BSA antigen using Luminex xMAP[TMP] and the Bio-Plex 100 Platform. xMAP regions (35-38, 42-44, 46-47, and 51) were selected for each antigen. Microsphere activation was done using 50mg/mL Sulfo-NHS (N-hydroxysulfosuccinimide) and 50 mg/mL of EDC (1-Ethyl-3-[3-dimethylaminopropyl]carbodiimide hydrochloride) in 80 μL 100 mM of bead activation buffer at room temperature for 20 min in reaction tubes protected from light. Subsequently, 1 to 5 μg of the corresponding recombinant proteins per million microspheres were added and the volume of the resulted solution was increased to 250 μL using the respective buffer (table 20). Following, the reaction tubes were incubated at 4°C in a shaker overnight. Finally, microspheres were blocked using 250 μL of 1% BSA (w/v) in phosphate-buffered saline (PBS) for 30 min in a shaker. The reaction tubes were place into a magnetic separator for 60 sec and the supernatant was removed and the microsphere were re-suspended in 500μL of a PBS with 0.05% (w/v) sodium azide (PBS-BN), filtered buffer. A Guava PCA desktop cytometer was used to quantify the microspheres coupled, and equal amount of each analyte were combined in multiplex tubes and stored at 1,000 microspheres/μL at 4°C protected from light.

.

Table 20. Microsphere coupling.

Antigen	Antigen μg/10^6 beads	Protein stock concentration (mg/mL)	Antigen (μL)	Buffer (μL)	Region
AMA-1 3D7	2	0.63	7.94	MES (242)	36
AMA-1 FVO	2	0.235	21.28	MES (229)	37
MSP-1$_{42}$ 3D7	2	0.58	8.62	MES (241)	38
MSP-1$_{42}$ FVO	2	0.25	20	MES (230)	42
EBA-175	2	0.6	8.33	MES (241)	43
DBL-alpha	2	0.4	12.5	PBS (238)	47
SPP2	1	2.56	1	PBS (249)	46
LSA-1	2	1.07	4.7	PBS (245)	44
CelTOS	5	1.23	10.16	PBS (240)	51

Each region tube contains 1mL of 2.5x10^6 beads/tube. BSA was coupled to region 35 using a solution of 1%BSA in 250μL of PBS.

5.5.3. Luminex Assay

The assay consisted on adding 50 μL of a solution of 1,000 microspheres of the SAT previously prepared in PBS-BN to a 96-well plate per well. Following 50 μL of test plasmas (1:500 and 1:20000 in PBS-BN) were respectively added to the wells and incubated for 1 h with agitation and protected from light. The plates were later washed using 0.05% Tween 20 (v/v) in PBS buffer (PBS-T) three times on a Bio-Plex Pro II Wash Station and later re-suspended. 100 μL of biotinylated anti-human IgG diluted at 1:2500 in PBS-BN was applied to all wells and incubated at room temperature for 45 min with agitation and protection from light. Subsequently, the plates were washed as before, and 100 μL of streptavidin-conjugated R-phycoerythrin diluted 1:1000 in PBS-BN was added to each well and incubated for 25 min with agitation and protection from light. After plated were washed as explained before, 100 μL of PBS-BN was added to each well and the plates were immediately read on the Bio-Plex 100 Luminex machine using Bio-Plex Manager software, version 4.0. The panel was designed to include all time points (D0, M3, M8.5, M21, M33, M45, M63) for a child, positive hyperimmune control (1:500 and 1:15,000), two dilutions 1/500 and 1/20,000 of negative control European adults, and duplicate reading for each dilution.

5.6. References

1.   Winstanley, P.; Ward, S. Malaria chemotherapy. *Adv Parasitol* **2006,** 61, 47-76.

2.   Nussenzweig, R. S.; Long, C. A. Malaria vaccines: multiple targets. *Science* **1994,** 265, 1381-3.

3.   Doolan, D. L.; Dobaño, C.; Baird, J. K. Acquired immunity to malaria. *Clin Microbiol Rev* **2009,** 22, 13-36, Table of Contents.

4.   Snow, R. W.; Omumbo, J. A.; Lowe, B.; Molyneux, C. S.; Obiero, J.-O.; Palmer, A.; Weber, M. W.; Pinder, M.; Nahlen, B.; Obonyo, C.; Newbold, C.; Gupta, S.; Marsh, K. Relation between severe malaria morbidity in children and level of Plasmodium falciparum transmission in Africa. *Lancet* **1997,** 349, 1650-1654.

5.   Beeson, J. G.; Amin, N.; Kanjala, M.; Rogerson, S. J. Selective accumulation of mature asexual stages of Plasmodium falciparum-infected erythrocytes in the placenta. *Infect Immun* **2002,** 70, 5412-5.

6.   Hill, A. V. Vaccines against malaria. *Philos Trans R Soc Lond B Biol Sci* **2011,** 366, 2806-14.

7.   A Phase 3 Trial of RTS,S/AS01 Malaria Vaccine in African Infants. *New Engl J Med* **2012,** 367, 2284-2295.

8.   Matuschewski, K. Vaccine development against malaria. *Curr Opin Immunol* **2006,** 18, 449-457.

9.   Trieu, A.; Kayala, M. A.; Burk, C.; Molina, D. M.; Freilich, D. A.; Richie, T. L.; Baldi, P.; Felgner, P. L.; Doolan, D. L. Sterile protective immunity to malaria is associated with a panel of novel P. falciparum antigens. *Mol Cell Proteomics* **2011,** 10, M111 007948.

10.   Baird, J. K.; Purnomo; Basri, H.; Bangs, M. J.; Andersen, E. M.; Jones, T. R.; Masbar, S.; Harjosuwarno, S.; Subianto, B.; Arbani, P. R. Age-specific prevalence of Plasmodium falciparum among six populations with limited histories of exposure to endemic malaria. *Am J Trop Med Hyg* **1993,** 49, 707-19.

11.   Clyde, D. F.; Most, H.; McCarthy, V. C.; Vanderberg, J. P. Immunization of man against sporozite-induced falciparum malaria. *Am J Med Sci* **1973,** 266, 169-77.

12.   Nussenzweig, R. S.; Vanderberg, J.; Most, H.; Orton, C. Protective immunity produced by the injection of x-irradiated sporozoites of plasmodium berghei. *Nature* **1967,** 216, 160-2.

13.   Hoffman, S. L.; Goh, L. M. L.; Luke, T. C.; Schneider, I.; Le, T. P.; Doolan, D. L.; Sacci, J.; de la Vega, P.; Dowler, M.; Paul, C.; Gordon, D. M.; Stoute, J. A.; Church, L. W. P.; Sedegah, M.; Heppner, D. G.; Ballou, W. R.; Richie, T. L.

Protection of Humans against Malaria by Immunization with Radiation-Attenuated Plasmodium falciparum Sporozoites. *J Infect Dis* **2002,** 185, 1155-1164.

14.   Beaudoin, R. L.; Strome, C. P. A.; Mitchell, F.; Tubergen, T. A. Plasmodium berghei: Immunization of mice against the ANKA strain using the unaltered sporozoite as an antigen. *Exp Parasitol* **1977,** 42, 1-5.

15.   Yayon, A.; Vande Waa, J. A.; Yayon, M.; Geary, T. G.; Jensen, J. B. Stage-dependent effects of chloroquine on Plasmodium falciparum in vitro. *J Protozool* **1983,** 30, 642-7.

16.   Roestenberg, M.; McCall, M.; Hopman, J.; Wiersma, J.; Luty, A. J. F.; van Gemert, G. J.; van de Vegte-Bolmer, M.; van Schaijk, B.; Teelen, K.; Arens, T.; Spaarman, L.; de Mast, Q.; Roeffen, W.; Snounou, G.; Rénia, L.; van der Ven, A.; Hermsen, C. C.; Sauerwein, R. Protection against a Malaria Challenge by Sporozoite Inoculation. *New Engl J Med* **2009,** 361, 468-477.

17.   Hoffman, S. L.; Billingsley, P. F.; James, E.; Richman, A.; Loyevsky, M.; Li, T.; Chakravarty, S.; Gunasekera, A.; Chattopadhyay, R.; Li, M.; Stafford, R.; Ahumada, A.; Epstein, J. E.; Sedegah, M.; Reyes, S.; Richie, T. L.; Lyke, K. E.; Edelman, R.; Laurens, M.; Plowe, C. V.; Sim, B. K. L. Development of a metabolically active, non-replicating sporozoite vaccine to prevent Plasmodium falciparum malaria. *Hum Vaccines* **2010,** 6, 97-106.

18.   Kinyanjui, S. M.; Bejon, P.; Osier, F. H.; Bull, P. C.; Marsh, K. What you see is not what you get: implications of the brevity of antibody responses to malaria antigens and transmission heterogeneity in longitudinal studies of malaria immunity. *Malaria J* **2009,** 8, 242.

19.   Kinyanjui, S. M.; Conway, D. J.; Lanar, D. E.; Marsh, K. IgG antibody responses to Plasmodium falciparum merozoite antigens in Kenyan children have a short half-life. *Malaria J* **2007,** 6, 82.

20.   Greenhouse, B.; Ho, B.; Hubbard, A.; Njama-Meya, D.; Narum, D. L.; Lanar, D. E.; Dutta, S.; Rosenthal, P. J.; Dorsey, G.; John, C. C. Antibodies to Plasmodium falciparum antigens predict a higher risk of malaria but protection from symptoms once parasitemic. *J Infect Dis* **2011,** 204, 19-26.

21.   Thera, M. A.; Doumbo, O. K.; Coulibaly, D.; Laurens, M. B.; Kone, A. K.; Guindo, A. B.; Traore, K.; Sissoko, M.; Diallo, D. A.; Diarra, I.; Kouriba, B.; Daou, M.; Dolo, A.; Baby, M.; Sissoko, M. S.; Sagara, I.; Niangaly, A.; Traore, I.; Olotu, A.; Godeaux, O.; Leach, A.; Dubois, M.-C.; Ballou, W. R.; Cohen, J.; Thompson, D.; Dube, T.; Soisson, L.; Diggs, C. L.; Takala, S. L.; Lyke, K. E.; House, B.; Lanar, D. E.; Dutta, S.; Heppner, D. G.; Plowe, C. V. Safety and Immunogenicity of an

AMA1 Malaria Vaccine in Malian Children: Results of a Phase 1 Randomized Controlled Trial. *PLoS ONE* **2010,** 5, e9041.

22. Bergmann-Leitner, E. S.; Mease, R. M.; De La Vega, P.; Savranskaya, T.; Polhemus, M.; Ockenhouse, C.; Angov, E. Immunization with Pre-Erythrocytic Antigen CelTOS from *Plasmodium falciparum* Elicits Cross-Species Protection against Heterologous Challenge with *Plasmodium berghei*. *PLoS ONE* **2010,** 5, e12294.

23. El Sahly, H. M.; Patel, S. M.; Atmar, R. L.; Lanford, T. A.; Dube, T.; Thompson, D.; Sim, B. K. L.; Long, C.; Keitel, W. A. Safety and Immunogenicity of a Recombinant Nonglycosylated Erythrocyte Binding Antigen 175 Region II Malaria Vaccine in Healthy Adults Living in an Area Where Malaria Is Not Endemic. *Clin Vaccine Immunol* **2010,** 17, 1552-1559.

24. Cummings, J. F.; Spring, M. D.; Schwenk, R. J.; Ockenhouse, C. F.; Kester, K. E.; Polhemus, M. E.; Walsh, D. S.; Yoon, I. K.; Prosperi, C.; Juompan, L. Y.; Lanar, D. E.; Krzych, U.; Hall, B. T.; Ware, L. A.; Stewart, V. A.; Williams, J.; Dowler, M.; Nielsen, R. K.; Hillier, C. J.; Giersing, B. K.; Dubovsky, F.; Malkin, E.; Tucker, K.; Dubois, M. C.; Cohen, J. D.; Ballou, W. R.; Heppner, D. G., Jr. Recombinant Liver Stage Antigen-1 (LSA-1) formulated with AS01 or AS02 is safe, elicits high titer antibody and induces IFN-gamma/IL-2 CD4+ T cells but does not protect against experimental Plasmodium falciparum infection. *Vaccine* **2010,** 28, 5135-44.

25. Avril, M.; Hathaway, M. J.; Cartwright, M. M.; Gose, S. O.; Narum, D. L.; Smith, J. D. Optimizing expression of the pregnancy malaria vaccine candidate, VAR2CSA in Pichia pastoris. *Malaria J* **2009,** 8, 143.

26. Epstein, J. E.; Giersing, B.; Mullen, G.; Moorthy, V.; Richie, T. L. Malaria vaccines: are we getting closer? *Curr Opin Mol Ther* **2007,** 9, 12-24.

27. Casares, S.; Brumeanu, T. D.; Richie, T. L. The RTS,S malaria vaccine. *Vaccine* **2010,** 28, 4880-94.

28. Nardin, E. H.; Nussenzweig, R. S. T cell responses to pre-erythrocytic stages of malaria: role in protection and vaccine development against pre-erythrocytic stages. *Annu Rev Immunol* **1993,** 11, 687-727.

29. Sultan, A. A. Molecular mechanisms of malaria sporozoite motility and invasion of host cells. *Int Microbiol* **1999,** 2, 155-60.

30. Schwenk, R. J.; Richie, T. L. Protective immunity to pre-erythrocytic stage malaria. *Trends Parasitol* **2011,** 27, 306-314.

31. Regules, J. A.; Cummings, J. F.; Ockenhouse, C. F. The RTS,S vaccine candidate for malaria. *Expert Rev Vaccines* **2011,** 10, 589-99.

32.   Alloueche, A.; Milligan, P.; Conway, D. J.; Pinder, M.; Bojang, K.; Doherty, T.; Tornieporth, N.; Cohen, J.; Greenwood, B. M. Protective efficacy of the RTS,S/AS02 Plasmodium falciparum malaria vaccine is not strain specific. *Am J Trop Med Hyg* **2003,** 68, 97-101.

33.   Stoute, J. A.; Slaoui, M.; Heppner, D. G.; Momin, P.; Kester, K. E.; Desmons, P.; Wellde, B. T.; Garcon, N.; Krzych, U.; Marchand, M. A preliminary evaluation of a recombinant circumsporozoite protein vaccine against Plasmodium falciparum malaria. RTS,S Malaria Vaccine Evaluation Group. *New Engl J Med* **1997,** 336, 86-91.

34.   Doherty, J. F.; Pinder, M.; Tornieporth, N.; Carton, C.; Vigneron, L.; Milligan, P.; Ballou, W. R.; Holland, C. A.; Kester, K. E.; Voss, G.; Momin, P.; Greenwood, B. M.; McAdam, K. P.; Cohen, J. A phase I safety and immunogenicity trial with the candidate malaria vaccine RTS,S/SBAS2 in semi-immune adults in The Gambia. *Am J Trop Med Hyg* **1999,** 61, 865-8.

35.   Kester, K. E.; McKinney, D. A.; Tornieporth, N.; Ockenhouse, C. F.; Heppner, D. G.; Hall, T.; Krzych, U.; Delchambre, M.; Voss, G.; Dowler, M. G.; Palensky, J.; Wittes, J.; Cohen, J.; Ballou, W. R. Efficacy of recombinant circumsporozoite protein vaccine regimens against experimental Plasmodium falciparum malaria. *J Infect Dis* **2001,** 183, 640-7.

36.   Bojang, K. A.; Olodude, F.; Pinder, M.; Ofori-Anyinam, O.; Vigneron, L.; Fitzpatrick, S.; Njie, F.; Kassanga, A.; Leach, A.; Milman, J.; Rabinovich, R.; McAdam, K. P.; Kester, K. E.; Heppner, D. G.; Cohen, J. D.; Tornieporth, N.; Milligan, P. J. Safety and immunogenicty of RTS,S/AS02A candidate malaria vaccine in Gambian children. *Vaccine* **2005,** 23, 4148-57.

37.   Alonso, P. L.; Sacarlal, J.; Aponte, J. J.; Leach, A.; Macete, E.; Milman, J.; Mandomando, I.; Spiessens, B.; Guinovart, C.; Espasa, M.; Bassat, Q.; Aide, P.; Ofori-Anyinam, O.; Navia, M. M.; Corachan, S.; Ceuppens, M.; Dubois, M. C.; Demoitie, M. A.; Dubovsky, F.; Menendez, C.; Tornieporth, N.; Ballou, W. R.; Thompson, R.; Cohen, J. Efficacy of the RTS,S/AS02A vaccine against Plasmodium falciparum infection and disease in young African children: randomised controlled trial. *Lancet* **2004,** 364, 1411-20.

38.   Alonso, P. L.; Sacarlal, J.; Aponte, J. J.; Leach, A.; Macete, E.; Aide, P.; Sigauque, B.; Milman, J.; Mandomando, I.; Bassat, Q.; Guinovart, C.; Espasa, M.; Corachan, S.; Lievens, M.; Navia, M. M.; Dubois, M. C.; Menendez, C.; Dubovsky, F.; Cohen, J.; Thompson, R.; Ballou, W. R. Duration of protection with RTS,S/AS02A malaria vaccine in prevention of Plasmodium falciparum disease in

Mozambican children: single-blind extended follow-up of a randomised controlled trial. *Lancet* **2005,** 366, 2012-8.

39. Sacarlal, J.; Aide, P.; Aponte, J. J.; Renom, M.; Leach, A.; Mandomando, I.; Lievens, M.; Bassat, Q.; Lafuente, S.; Macete, E.; Vekemans, J.; Guinovart, C.; Sigauque, B.; Sillman, M.; Milman, J.; Dubois, M. C.; Demoitie, M. A.; Thonnard, J.; Menendez, C.; Ballou, W. R.; Cohen, J.; Alonso, P. L. Long-term safety and efficacy of the RTS,S/AS02A malaria vaccine in Mozambican children. *J Infect Dis* **2009,** 200, 329-36.

40. Campo, J. J.; Dobaño, C.; Sacarlal, J.; Guinovart, C.; Mayor, A.; Angov, E.; Dutta, S.; Chitnis, C.; Macete, E.; Aponte, J. J.; Alonso, P. L. Impact of the RTS,S malaria vaccine candidate on naturally acquired antibody responses to multiple asexual blood stage antigens. *PLoS One* **2011,** 6, e25779.

41. Bejon, P.; White, M. T.; Olotu, A.; Bojang, K.; Lusingu, J. P.; Salim, N.; Otsyula, N. N.; Agnandji, S. T.; Asante, K. P.; Owusu-Agyei, S.; Abdulla, S.; Ghani, A. C. Efficacy of RTS,S malaria vaccines: individual-participant pooled analysis of phase 2 data. *Lancet Infect Dis* **2013**.

42. First Results of Phase 3 Trial of RTS,S/AS01 Malaria Vaccine in African Children. *New Engl J Med* **2011,** 365, 1863-1875.

43. WHO. World Malaria Report. **2012**.

44. Aponte, J. J.; Aide, P.; Renom, M.; Mandomando, I.; Bassat, Q.; Sacarlal, J.; Manaca, M. N.; Lafuente, S.; Barbosa, A.; Leach, A.; Lievens, M.; Vekemans, J.; Sigauque, B.; Dubois, M. C.; Demoitie, M. A.; Sillman, M.; Savarese, B.; McNeil, J. G.; Macete, E.; Ballou, W. R.; Cohen, J.; Alonso, P. L. Safety of the RTS,S/AS02D candidate malaria vaccine in infants living in a highly endemic area of Mozambique: a double blind randomised controlled phase I/IIb trial. *Lancet* **2007,** 370, 1543-51.

45. Olotu, A.; Fegan, G.; Wambua, J.; Nyangweso, G.; Awuondo, K. O.; Leach, A.; Lievens, M.; Leboulleux, D.; Njuguna, P.; Peshu, N.; Marsh, K.; Bejon, P. Four-Year Efficacy of RTS,S/AS01E and Its Interaction with Malaria Exposure. *New Engl J Med* **2013,** 368, 1111-1120.

46. Valbuena, J.; Rodríguez, L.; Vera, R.; Puentes, A.; Curtidor, H.; Cortés, J.; Rosas, J.; Patarroyo, M. E. Synthetic peptides from Plasmodium falciparum apical membrane antigen 1 (AMA-1) specifically interacting with human hepatocytes. *Biochimie* **2006,** 88, 1447-1455.

47. Epp, C.; Kauth, C. W.; Bujard, H.; Lutz, R. Expression and purification of Plasmodium falciparum MSP-142: A malaria vaccine candidate. *J Chromatogr B* **2003,** 786, 61-72.

48. Gruner, A. C.; Brahimi, K.; Letourneur, F.; Renia, L.; Eling, W.; Snounou, G.; Druilhe, P. Expression of the erythrocyte-binding antigen 175 in sporozoites and in liver stages of Plasmodium falciparum. *J Infect Dis* **2001,** 184, 892-7.

49. Mayor, A.; Rovira-Vallbona, E.; Srivastava, A.; Sharma, S. K.; Pati, S. S.; Puyol, L.; Quinto, L.; Bassat, Q.; Machevo, S.; Mandomando, I.; Chauhan, V. S.; Alonso, P. L.; Chitnis, C. E. Functional and immunological characterization of a Duffy binding-like alpha domain from Plasmodium falciparum erythrocyte membrane protein 1 that mediates rosetting. *Infect Immun* **2009,** 77, 3857-63.

50. Rogers, W. O.; Malik, A.; Mellouk, S.; Nakamura, K.; Rogers, M. D.; Szarfman, A.; Gordon, D. M.; Nussler, A. K.; Aikawa, M.; Hoffman, S. L. Characterization of Plasmodium falciparum sporozoite surface protein 2. *P Natl Acad Sci USA* **1992,** 89, 9176-80.

51. Hillier, C. J.; Ware, L. A.; Barbosa, A.; Angov, E.; Lyon, J. A.; Heppner, D. G.; Lanar, D. E. Process Development and Analysis of Liver-Stage Antigen 1, a Preerythrocyte-Stage Protein-Based Vaccine for Plasmodium falciparum. *Infect Immun* **2005,** 73, 2109-2115.

52. Bergmann-Leitner, E. S.; Mease, R. M.; De La Vega, P.; Savranskaya, T.; Polhemus, M.; Ockenhouse, C.; Angov, E. Immunization with pre-erythrocytic antigen CelTOS from Plasmodium falciparum elicits cross-species protection against heterologous challenge with Plasmodium berghei. *PLoS One* **2010,** 5, e12294.

53. Elshal, M. F.; McCoy, J. P. Multiplex bead array assays: performance evaluation and comparison of sensitivity to ELISA. *Methods* **2006,** 38, 317-23.

54. Bartczak, D.; Kanaras, A. G. Preparation of peptide-functionalized gold nanoparticles using one pot EDC/sulfo-NHS coupling. *Langmuir* **2011,** 27, 10119-23.

55. Bejon, P.; Warimwe, G.; Mackintosh, C. L.; Mackinnon, M. J.; Kinyanjui, S. M.; Musyoki, J. N.; Bull, P. C.; Marsh, K. Analysis of Immunity to Febrile Malaria in Children That Distinguishes Immunity from Lack of Exposure. *Infect Imm* **2009,** 77, 1917-1923.

Chapter 6

Conclusions and Future Perspectives

6.1. Conclusions

This doctoral project mainly involved the design, synthesis, and evaluation of two generations of compounds as inhibitors *Pf* malaria growth. First generation of compounds, *HE[DI]CIN*s, presented activity in the micromolar range against CQ-resistant (W2) strain of *Pf* (IC_{50} = 0.83- > 10 μM). Results suggested that the MOA of *HEDICIN*s was neither inhibition of falcipains' action or hemozoin formation. For instance, the most active compound of the series, **1c,** against the parasite development, which displayed an IC_{50} of 830 nM, did not inhibit falcipain action or hemozoin formation. The *p*-NH$_2$ cinnamoyl derivative **1e**, was the compound which best reached the goal of dual action inhibitors since the latter was very active against β-H formation, presented activity against falcipain (IC_{50} (FP2) = 20.3 μM) and showed antiplasmodial activity (IC_{50} (*Pf* W2) = 3.28 μM). *HE[DI]CIN*s' results demonstrated the essential role of the: i) chloroquinoline core, ii) hydrophobic link, and iii) cinnamoyl moiety in the antiplasmodial activity of the compounds.

In addition, *HE[DI]CIN*s showed to be more efficient inhibitors of babesipain-1 (bbspn-1) from *B. bigemina* than of FP2. *In silico* studies carried in order to understand the interaction of this generation of compounds against bbspn-1 included i) building of a 3D structure of bbspn-1 by homology model, ii) detailed assessment of the model obtained using ProQ, ProSA, QMEAN, and PROCHECK as validation tools, and iii) docking *HEDICIN*s and *HECIN*s against the well validated model built for bbspn-1 to explain the *in vitro* data obtained. Results suggested the chloroquinoline moiety in *HECIN*s establishes stronger hydrophobic interactions with S2 site residues, explaining their higher efficiency as bbspn-1 inhibitors as compared to results presented against FP2. Further *in vitro* assays need to be carried in order to understand whether the activity of *HE[DI]CIN*s against bbspn-1 correlates with the inhibition of the parasite, *B. bigemina,* development. Results in this study could be employed in the development of new leads to inhibit bbspn-1.

Second generation of compounds, *HEFLECIN*s, was designed based on antiplasmodial results previously found for *HE[DI]CIN*s. *HEFLECIN*s resulted dual-stage inhibitors since they presented activity against blood stage parasite and liver stage parasite, higher or comparable to the reference drug, CQ and PQ, respectively. The SAR of the *HEFLECIN*s demonstrated the essential roles of i) the 4-amino-7-chloroquinoline, ii) the chlorine in position seven of the chloroquinoline ring, iii) the butyl link, and iv) the amide bond for the potent antiplasmodial activity of the compounds against both stages. Two of the most active *HEFLECIN*s, namely, the *p*-iPr and the *p*-Cl cinnamoyl derivatives **13c** and **13h** presented *in vitro* activity against CQ-resistant W2 strain (IC_{50} = 11.0-11.6 nM)

comparable to artemisinin (IC_{50} = 9.5 nM), the base compound of ACT. Furthermore, in this series, compound **13h** and the most potent compound, **13d** (IC_{50} = 20 nM), which also complied with Veber, Lipinski, and Leadlikeness filters, displayed activity *in vivo* against *P. berghei* in rodents. However, these compounds did not inhibit falcipains' action and *HEFLECIN*s' antiplasmodial activities did not correlate with the ability of the compounds to inhibit β-H formation. This lack of correlation could be explained by the absence of the tertiary amine at the end of the butyl chain which have been demonstrated to also promote accumulation of CQ in the FV.[1] Nonetheless, in general, compounds displayed higher antiplasmodial activities than their parent drug, CQ. The latter demonstrates the existence of an alternative MOA, yet to be elucidated, through which these derivatives exert their activity. Preliminary results suggest NPP inhibition since compound **13c**, one of the best inhibitors of *Pf* growth, was clearly able to inhibit NPP in *Plasmodium*-infected RBC. Still, alternative mechanisms of action such as CQ-chemosensitizing activity should not be discarded. In addition, the *p*-OMe and *p*-Cl derivatives **13d**, **28d** and **13h** were evaluated *in vivo* against liver stage parasite. However, none of the tested derivatives display *in vivo* activity. This could be explained by the fact that most drugs are generally converted into less active or inactive compounds when they enter the liver.[2]

Since malaria is known to affect mainly low-income/developing countries, significant efforts have been made in order to expand access to ACT by supplying this chemotherapy at an affordable price to the public and private sectors.[3, 4] However, this strategy is an unsustainable approach against malaria, thus the need to develop new inexpensive drugs which target malaria. All synthetic pathways here developed constituted straightforward procedures and involved low cost reagents. Therefore, *HEFLECIN*s are not only active against dual-stage forms of the malaria parasite but are also affordable. Thus *HEFLECIN*s constitute new antimalarial leads.[5] Furthermore, we were able to demonstrate that the cinnamoylation boosting effect is also observed on other heterocyclic antimalarials such as PQ and AQ, as *PRIMACIN*s **28** were highly active against liver stage (IC_{50} = 1.4-2.4 μM) and AQ-based *HEFLECIN*s **29** displayed higher activity against both blood (IC_{50} = 126-842 nM) and liver stage parasite (IC_{50} = 3.2- < 10 μM). Moreover, the second generation of compounds, namely, compounds **13** and **28** also displayed potent activity against *L. infantum*. Furthermore, activity of *HEFLECIN*s as anti-leishmanial agents suggests that these compounds should be evaluated against a broader panel of protozoans. Results obtained so far demonstrated cinnamoyl/quinoline derivatives to be new candidate in medicinal chemistry to develop novel antiprotozoan agents.

This doctoral project further included a longitudinal analysis on the acquisition of IgG response to *P. falciparum* antigens in 401 African children who completed a 60 month follow-up after three doses of RTS,S vaccination. Results demonstrated:

- According to the reverse cumulative distribution of the Ab-responses against the antigens included in this study, there seems to be a difference between the RTS,S vaccine and control groups which drops over the follow up time.

- Data from this study contribute to the understanding of the immune response in association with intensity of exposure to malaria. High Ab levels against blood stage antigens studied could represent markers of malaria exposure.

- Examining time since last parasite exposure, Ab units drop to low values for each evaluated antigen in less than 90 days.

Moreover, the longitudinal study, carried in the area of malaria prevention, contributes to the understanding of the naturally-acquired Ab responses after immunization with the partially efficacious RTS,S vaccine in children younger than 5 years old. However, the mechanism underlying RTS,S protection is yet to be elucidated. Further studies need to be done in order to understand the mode of action of the vaccine and help to develop future attempts to improve the efficacy of RTS,S vaccination. Results obtained in this three and a half months study contributes to gain insight into the complex immune responses against malaria in children under age five vaccinated and exposed to the disease.

6.2. Future Perspectives

Further studies needs to be carried to understand the MOA of the compounds synthesized in this doctoral project. Most heterocyclic-cinnamic conjugates were already sent for their evaluation as inhibitors of NPP in order to assess whether the antiplasmodial SAR presented by the compounds correlated with activities against NPP.

Preclinical studies need to be done to investigate the absorption, distribution, metabolism, and excretion (ADME) properties of the compounds. The latter will determine which of these properties should be improved and taken into account in further structural modifications in order to enhance the *in vivo* activity displayed by the *N*-cinnamoylated derivatives.

The influence on the substitution of the cinnamoyl moiety by other functionalities should also be studied. Preliminary studies suggest that the absence of the cinnamoyl is not detrimental for the antiplasmodial activity of the compounds but the substitution of the cinnamoyl aromatic ring by alkyl functionalities seems to have a negative impact on the stability of the compounds.

Future studies should be conducted to improve the solubility of the compounds in aqueous media. Synthesizing new derivatives with an additional protonable amine, such as compounds displayed in Fig. 64, should increase the water solubility and consequently the *in vivo* activity displayed against blood stage by the cinnamoyl derivatives. Furthermore, such structural modification might promote compound's ability to inhibit β-H, since the additional protonable amine will also improve accumulation of the corresponding compounds in the FV, consequently increasing the antiplasmodial activity displayed by the compounds. In fact, Cornut et al recently demonstrated that introduction of a basic nitrogen in the spacer of CQ analogues significantly improve the antimalarial activity of the respective compounds against CQ-resistant (W2) and CQ-sensitive parasite (3D7).[6]
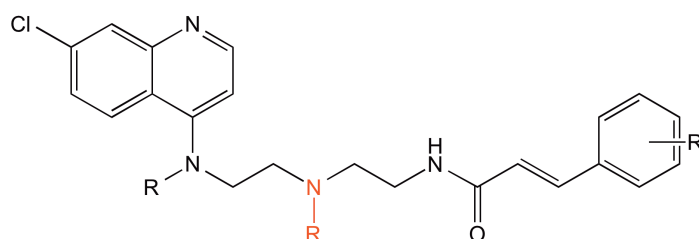

Figure 64. General structure of the cinnamoyl derivatives including an additional protonable amine.

Preliminary cytotoxic studies against human cell (MKN-28, Caco-2, and MCF-7) have been carried. Accordingly, *HEFLECIN*S are only cytotoxic in the micromolar range (IC$_{50}$ =

5.1-59.3 μM). Moreover, compounds demonstrated to be selective for MKN-28, Caco-2, and MCF-7 tumor cells over normal HFF-1 cells (IC$_{50}$ > 100 μM). These results suggest *HEFLECIN*s to be a promising start towards the development of new leads to discover novel affordable antitumor agents.

With regards to the longitudinal analysis carried to measure antibody responses to *P. falciparum* antigens in RTS,S-vaccinated children, further analysis of the data and additional studies need to be performed in order to draw detailed conclusions regarding the influence of RTS,S vaccination on the immune response of children exposed to malaria. Moreover, future work includes analyzing the IgG Ab response for C2 against these antigens to compare both cohorts (C1 and C2) to better understand why C1 maintains RTS,S efficacy for 43 months after vaccination, while C2 efficacy disappears after 6 months. Other types of Ab response such as IgM and IgG subclasses should be also evaluated. Finally, other antigens thought to induce protection should be included in future studies, as well as the evaluation of the effect of IgG levels in malaria risk.

6.3. References

1. Egan, T. J.; Kuter, D. Dual-functioning antimalarials that inhibit the chloroquine-resistance transporter. *Future Microbiol* **2013,** 8, 475-89.

2. Remmer, H. The role of the liver in drug metabolism. *Am J Med* **1970,** 49, 617-629.

3. The Global Fund to fight AIDS, Tuberculosis and Malaria. Affordable Medicines Facility-malaria. http://www.theglobalfund.org/en/amfm/ (May 6th 2013).

4. WHO. Q&A on the Affordable Medicnes Facilty malaria (AMFm). http://www.who.int/malaria/media/affordable_medicines_facility_qa/en/index.html

5. Kouznetsov, V. V.; Gómez-Barrio, A. Recent developments in the design and synthesis of hybrid molecules based on aminoquinoline ring and their antiplasmodial evaluation. *Eur J Med Chem* **2009,** 44, 3091-3113.

6. Cornut, D.; Lemoine, H.; Kanishchev, O.; Okada, E.; Albrieux, F.; Beavogui, A. H.; Bienvenu, A.-L.; Picot, S.; Bouillon, J.-P.; Médebielle, M. Incorporation of a 3-(2,2,2-Trifluoroethyl)-γ-hydroxy-γ-lactam Motif in the Side Chain of 4-Aminoquinolines. Syntheses and Antimalarial Activities. *J Med Chem* **2012,** 56, 73-83.

Appendix